

Geohydrology and numerical simulation of ground-water flow in the central Virgin River basin of Iron and Washington Counties, Utah

Prepared by the U.S. Geological Survey



Technical Publication No. 116
State of Utah
DEPARTMENT OF NATURAL RESOURCES
2000

This report was prepared as a part of the Statewide cooperative water-resource investigation program administered jointly by the Utah Department of Natural Resources, Division of Water Rights and the U.S. Geological Survey. The program is conducted to meet the water administration and water-resource data needs of the State as well as the water information needs of many units of government and the general public.

Ted Stewart
Executive Director
Department of Natural Resources

Robert L. Morgan
State Engineer
Division of Water Rights

Cover photograph by Victor Heilweil, 1998, showing Navajo Sandstone and Pine Valley Mountains.



Copies available at:
Utah Department of Natural Resources
Bookstore
1594 West North Temple
Salt Lake City, Utah 84114

STATE OF UTAH
DEPARTMENT OF NATURAL RESOURCES

Technical Publication No. 116

**GEOHYDROLOGY AND NUMERICAL SIMULATION
OF GROUND-WATER FLOW IN THE
CENTRAL VIRGIN RIVER BASIN OF IRON
AND WASHINGTON COUNTIES, UTAH**

**By V.M. Heilweil, G.W. Freethey, C.D. Wilkowske,
B.J. Stolp, and D.E. Wilberg**

Prepared by the
United States Geological Survey
in cooperation with the
Utah Department of Natural Resources,
Division of Water Rights; and the
Washington County Water Conservancy District

The use of trade, product, industry, or firm names is for descriptive purposes only and does not imply endorsement by the U.S. Government

CONTENTS

Abstract	1
Introduction	2
Description of the study area	4
Previous investigations.....	5
Scope of study.....	6
Purpose and scope of report.....	7
Acknowledgments	7
Geohydrologic framework	7
Upper Ash Creek drainage basin	9
Basin-fill deposits	9
Alluvial-fan deposits	9
Pine Valley monzonite and other formations.....	10
Navajo Sandstone and Kayenta Formation	10
Hydrochemical characteristics	13
Methods and limitations.....	13
Chlorofluorocarbon collection methods	13
Limitations of chlorofluorocarbon age dating	14
Age-dating of ground water with chlorofluorocarbons.....	15
Use of age-dating to investigate sources of recharge to the main part of the Navajo and Kayenta aquifers	17
Comparison of apparent ages calculated from chlorofluorocarbon concentration to radio- isotope age-dating methods.....	20
Use of other geochemical data to investigate sources of ground-water recharge	23
Navajo and Kayenta aquifers.....	23
General chemistry	25
Oxygen and hydrogen isotopes	25
Possible sources of Ash Creek and Toquerville Springs	29
Ground-water hydrology	31
Upper Ash Creek drainage basin ground-water flow system.....	31
Aquifer system geometry and hydrologic boundaries.....	32
Aquifer properties	34
Recharge	35
Precipitation	35
Streams.....	36
Perennial streams.....	38
Ephemeral streams.....	39
Irrigation	39
Ground-water movement.....	40
Discharge.....	40
Wells	40
Evapotranspiration	42
Springs	42
Ash, Sawyer, and Kanarra Creeks	43
Subsurface flow to lower Ash Creek drainage	44
Ground-water budget.....	44
Navajo and Kayenta aquifer system	44
Aquifer system geometry and hydrologic boundaries.....	45
Aquifer properties	48

Ground-water hydrology—Continued	
Navajo and Kayenta aquifer system—Continued	
Navajo aquifer.....	48
Kayenta aquifer.....	50
Recharge.....	51
Precipitation	51
Streams.....	52
Perennial streams.....	52
Ephemeral streams.....	55
Method 1	56
Method 2	61
Overlying and underlying formations.....	65
Irrigation	66
Gunlock Reservoir	66
Ground-water movement.....	67
Discharge.....	67
Wells	67
Springs	70
Streams.....	70
Adjacent and underlying formations.....	70
Evapotranspiration	71
Ground-water budget.....	71
Numerical simulation of ground-water flow	71
Upper Ash Creek drainage basin ground-water system.....	72
Model characteristics and discretization	73
Boundary conditions	73
Recharge boundaries.....	73
Precipitation.....	73
Ephemeral streams.....	73
Ash Creek	78
Irrigation	78
Discharge boundaries.....	78
Evapotranspiration	78
Wells	80
Springs	80
Ash and Kanarra Creeks	80
Subsurface flow to lower Ash Creek drainage.....	80
No-Flow boundaries.....	80
Ground-water divide	82
Faults.....	82
Underlying formations.....	82
Divides	82
Distribution of aquifer characteristics	82
Vertical-head gradients.....	82
Conceptual model and numerical simulations	86
Model applicability	86
Alternative conceptualizations	88
Alternative 1—Flow across the Hurricane Fault	88
Alternative 2—No subsurface outflow to lower Ash Creek drainage.....	88
Alternative 3—Increased transmissivity of the Pine Valley monzonite aquifer ..	88
Alternative 4—Variation in anisotropy of the Pine Valley monzonite aquifer	88

Numerical simulation of ground-water flow—Continued	
Upper Ash Creek drainage basin ground-water system—Continued	
Alternative conceptualizations—Continued	
Model sensitivity.....	93
Need for additional study.....	93
Water-resource management.....	93
Model limitations	95
Navajo and Kayenta aquifer system	95
Main part of the Navajo and Kayenta aquifers.....	97
Model Characteristics and Discretization	97
Boundary conditions	97
Recharge boundaries.....	100
Precipitation	100
Streams.....	101
Underlying formations	104
Irrigation	104
Discharge boundaries.....	104
Wells	104
Springs	104
Virgin River.....	108
Adjacent and underlying formations.....	108
No-flow boundaries.....	108
Distribution of aquifer characteristics.....	108
Conceptual model and numerical simulation.....	109
Model applicability	109
Alternative conceptualizations.....	109
Alternative 1—Effects of faulting.....	113
Alternative 2—Combined effects of faulting and anisotropy	113
Model sensitivity.....	118
Need for additional study.....	118
Water-resource management.....	118
Model limitations	120
Gunlock part of the Navajo aquifer	120
Model characteristics and discretization.....	120
Boundary conditions	121
Recharge boundaries.....	121
Precipitation	121
Santa Clara River	121
Gunlock Reservoir	126
Discharge boundaries.....	126
Wells	126
Santa Clara River	126
No-flow boundaries.....	126
Distribution of aquifer characteristics	126
Conceptual model and numerical simulation	127
Model applicability	127
Alternative simulations	129
Alternative 1—Seepage across the Gunlock Fault	129
Alternative 2—Inflow from underlying formations.....	130
Model sensitivity.....	130
Need for additional study.....	134

Numerical simulation of ground-water flow—Continued	
Navajo and Kayenta aquifer system—Continued	
Model applicability—Continued	
Water-resource management.....	135
Model limitations	135
Summary	135
References	137

Appendices

A. Results of aquifer testing within the study area

Aquifer test analyses	A-2
Hurricane Bench aquifer test	A-2
Anderson Junction aquifer test	A-5
Theory	A-9
Application.....	A-10
Gunlock well field aquifer test.....	A-11
Geology	A-13
Hydrology.....	A-14
Data reduction and analysis.....	A-15
Ground-water flow model.....	A-16
Model calibration	A-18
Summary	A-21
Grapevine Pass aquifer test.....	A-21
New Harmony aquifer test	A-21
Hydrogeology.....	A-23
Data reduction and analysis.....	A-26
Summary	A-29
References	A-30

B. Model Sensitivity Analyses

B1. Sensitivity analysis for model simulating the upper Ash Creek drainage basin aquifers.....	B1-1
B2. Sensitivity analysis for model simulating the main Navajo and Kayenta aquifers.....	B2-1
B3. Sensitivity analysis for model simulating the Gunlock part of the Navajo aquifer	B3-1

Plates

1. Map showing selected geologic units in the central Virgin River basin area, Washington and Iron Counties, Utah
2. Map showing potentiometric surface of the Navajo and Kayenta aquifers in the central Virgin River basin area, Washington and Iron Counties, Utah

Figures

1.	Map showing location of the upper Ash Creek drainage basin and the Navajo Sandstone and Kayenta Formation outcrops within the central Virgin River basin study area, Utah.....	3
2.	Map showing average annual precipitation contours for the central Virgin River basin study area, Utah, 1961-90	5
3.	Graph showing monthly average precipitation at St. George and New Harmony, Utah, based on data from 1980 to 1989	6
4.	Generalized geologic cross sections of the Navajo Sandstone and surrounding formations within the central Virgin River basin study area, Utah	11
5.	Graph showing average CFC-11 and CFC-12 concentration in replicate samples collected with the glass-ampoule method and analyzed at the U.S. Geological Survey versus samples collected with the copper-tube method and analyzed at the University of Utah	12
6.	Map showing location of CFC- and dissolved-gas sampling sites, central Virgin River basin study area, Utah.....	16
7.	Graph showing global atmospheric concentration of CFC-12 as a function of time.....	17
8.	Graph showing apparent ground-water recharge year determined from CFC-12 concentration for selected wells and springs in the main part of the Navajo and Kayenta aquifers within the central Virgin River basin study area, Utah.....	22
9.	Map showing areas of dissolved-solids concentration greater than 500 mg/L and temperatures greater than 20°C from wells and springs in the Navajo and Kayenta aquifers within the central Virgin River basin study area, Utah	24
10.	Diagram showing chemical composition of 73 water samples collected from the Navajo and Kayenta aquifers within the central Virgin River basin study area, Utah	26
11.	Diagram showing relation of Navajo and Kayenta aquifer samples with high dissolved-solids concentration to the chemical composition of samples collected from overlying and underlying formations within the central Virgin River basin study area, Utah	27
12.	Graph showing stable-isotope ratios of hydrogen versus oxygen from ground water in the main part of the Navajo and Kayenta aquifers within the central Virgin River basin study area, Utah	28
13.	Map showing location of general-chemistry sampling sites along the Ash Creek drainage, Utah....	30
14.	Diagram showing chemical composition of ground water and surface water along the Ash Creek drainage, Utah.....	31
15.	Generalized diagram showing sources of recharge to and discharge from the upper Ash Creek basin ground-water system, Utah.....	32
16.	Schematic hydrogeologic section showing subsurface geometry from northwest to southeast near Kanarraville, Utah	33
17-20.	Maps showing:	
17.	Location of streamflow-gaging sites for seepage investigations on Ash, Sawyer, Kanarra, and Taylor Creeks, upper Ash Creek drainage basin, Utah	37
18.	Approximate potentiometric contours in the three aquifers of the upper Ash Creek drainage basin, Utah	41
19.	Areas of phreatophyte growth in the upper Ash Creek drainage basin, Utah.....	43
20.	Location of local and regional springs in the upper Ash Creek drainage basin, Utah.....	44
21.	Generalized diagram showing sources of recharge to and discharge from the Navajo and Kayenta aquifers within the central Virgin River basin study area, Utah	46
22.	Map showing potential sources of recharge to the Navajo and Kayenta aquifers in the central Virgin River basin study area, Utah	53
23.	Diagram showing chemical composition of water from the Santa Clara River and the St. George municipal well field in the Gunlock part of the Navajo aquifer within the central Virgin River basin study area, Utah	56

Figures—Continued

24.	Map showing location of general-chemistry sampling sites and CFC-12 sampling sites in the Gunlock part of the Navajo aquifer, central Virgin River basin study area, Utah.....	57
25.	Graph showing apparent ground-water recharge year determined from CFC-12 concentration at Santa Clara River sites and in water from wells in the Gunlock part of the Navajo aquifer within the central Virgin River basin study area, Utah	58
26.	Map showing approximate potentiometric surface in the Gunlock part of the Navajo aquifer within the central Virgin River basin study area, Utah, February 1996	59
27.	Map showing drainage-basin areas for perennial and ephemeral streams that recharge the Navajo and Kayenta aquifers in the central Virgin River basin study area, Utah	60
28.	Graph showing discharge of Leeds Creek and precipitation at St. George, Utah, from 1965 through 1997	64
29.	Map showing measured and estimated sources of discharge from the Navajo and Kayenta aquifers in the central Virgin River basin study area, Utah.....	68
30.	Graph showing well discharge from St. George municipal wells in the main and Gunlock parts of the Navajo and Kayenta aquifers from 1987 through 1996.....	69
31.	Map showing water levels in three wells in the upper Ash Creek drainage basin, Utah, 1934-95	74
32.	Map and section showing (a) finite-difference model grid and (b) layering scheme for the ground-water flow model of the upper Ash Creek drainage basin, Utah	75
33-40.	Maps showing:	
33.	Boundary conditions and cell assignments for the ground-water flow model of the upper Ash Creek drainage basin, Utah	76
34.	Areal distribution of recharge from infiltration of precipitation in the ground-water flow model of the upper Ash Creek drainage basin, Utah	77
35.	Simulated recharge to and discharge from the aquifers by stream seepage in the ground-water flow model of the upper Ash Creek drainage basin, Utah	79
36.	Location and magnitude of simulated well discharge in the ground-water flow model of the upper Ash Creek drainage basin, Utah	81
37.	Final distribution of transmissivity simulated in the ground-water flow model of the upper Ash Creek drainage basin, Utah	83
38.	Simulated potentiometric contours in (a) layer 1, (b) layer 2, and (c) layer 3 from the baseline simulation of the upper Ash Creek drainage basin, Utah	87
39.	Potentiometric contours in (a) layer 1, (b) layer 2, and (c) layer 3 from alternative simulation depicting flow across the Hurricane Fault, the upper Ash Creek drainage basin, Utah	90
40.	Simulated potentiometric contours in (a) layer 1, (b) layer 2, and (c) layer 3 from alternative simulation depicting no outflow from the basin near Ash Creek reservoir, upper Ash Creek drainage basin, Utah	92
41.	Diagrammatic bar chart showing relative sensitivity of the baseline model representing the upper Ash Creek drainage ground-water flow system to uncertainty in selected properties and flows	95
42-44.	Maps showing:	
42.	Water-level changes in the Navajo and Kayenta aquifers from 1974 to February/March 1996, 1997 in the central Virgin River basin study area, Utah	96
43.	Model grid of the ground-water flow model of the main part of the Navajo and Kayenta aquifers within the central Virgin River basin study area, Utah	98
44.	Altitude of the base level of layer 2, representing the base of the Kayenta Formation, in the ground-water flow model of the main part of the Navajo and Kayenta aquifers within the central Virgin River basin study area, Utah	99

Figures—Continued

45.	Generalized cross section along column 20 of the ground-water flow model of the main part of the Navajo and Kayenta aquifers within the central Virgin River basin study area, Utah	100
46-57.	Maps showing:	
46.	Distribution of recharge from infiltration of precipitation simulated in the ground-water flow model of the main part of the Navajo and Kayenta aquifers within the central Virgin River basin study area, Utah.....	101
47.	Distribution of recharge from streams and infiltration of unconsumed irrigation water simulated for layer 1 of the ground-water flow model of the main part of the Navajo and Kayenta aquifers within the central Virgin River basin study area, Utah.....	102
48.	Location of recharge from ephemeral streams and inflow from underlying formations simulated for layer 2 of the ground-water flow model of the main part of the Navajo and Kayenta aquifers within the central Virgin River basin study area, Utah.....	105
49.	Discharge to wells and to the Virgin River from layer 1 of the ground-water flow model of the main part of the Navajo and Kayenta aquifers within the central Virgin River basin study area, Utah	106
50.	Discharge to wells, springs, and subsurface outflow to adjacent and underlying formations from layer 2 of the ground-water flow model of the main part of the Navajo and Kayenta aquifers in the central Virgin River basin study area, Utah.....	107
51.	Location of observation wells used for comparison of computed and measured water levels for the ground-water flow model of the main part of the Navajo and Kayenta aquifers within the central Virgin River basin study area, Utah	111
52.	Simulated potentiometric contours for (a) layer 1 and (b) layer 2 of the baseline main Navajo aquifer ground-water flow model.....	112
53.	Location of model cells that simulate effects of faulting in the ground-water flow model of the main part of the Navajo and Kayenta aquifers within the central Virgin River basin study area, Utah.....	114
54.	Simulated potentiometric contours for (a) layer 1, and (b) layer 2 of the alternative depicting effects of faulting, main Navajo aquifer ground-water flow model.....	115
55.	Simulated potentiometric contours for (a) layer 1, and (b) layer 2 of the alternative depicting effects of faulting and north-south anisotropy of the main Navajo aquifer ground-water flow model.....	117
56.	Simulated potentiometric contours for (a) layer 1, and (b) layer 2 of the alternative depicting effects of faulting and east-west anisotropy of the main Navajo aquifer ground-water flow model.....	119
57.	Diagrammatic bar chart showing relative sensitivity of the baseline model representing the main part of the Navajo and Kayenta aquifers to uncertainty in selected properties and flows	120
58.	Map showing model grid of the Gunlock part of the Navajo and Kayenta aquifers within the central Virgin River basin study area, Utah.....	122
59.	Generalized cross section along column 45 of the ground-water flow model of the Gunlock part of the Navajo and Kayenta aquifers within the central Virgin River basin study area, Utah.....	123
60-64.	Maps showing:	
60.	Distribution of recharge from infiltration of precipitation and reservoir leakage simulated in the ground-water flow model of the Gunlock part of the Navajo and Kayenta aquifers within the central Virgin River basin study area, Utah	124
61.	Distribution of streambed hydraulic conductivity that simulates seepage from the Santa Clara River in the ground-water flow model of the Gunlock part of the Navajo and Kayenta aquifers within the central Virgin River basin study area, Utah.....	125
62.	Simulated potentiometric contours for (a) layer 1 and (b) layer 2 of the baseline simulation of the Gunlock ground-water flow model.....	129

Figures—Continued

63.	Simulated potentiometric contours for (a) layer 1 and (b) layer 2 of the alternative simulation depicting flow across the Gunlock fault, Gunlock ground-water flow model	131
64.	Simulated potentiometric contours for (a) layer 1 and (b) layer 2 of the alternative simulation depicting inflow from underlying formations, Gunlock ground-water flow model	134
65.	Diagrammatic bar chart showing relative sensitivity of the baseline model of the Gunlock part of the Navajo and Kayenta aquifers to uncertainty in selected properties and flows	135
A-1.	Map showing location of aquifer-test sites within the central Virgin River basin study area, Washington County, Utah, 1996	A-2
A-2.	Map showing location of wells in the Hurricane Bench aquifer test, Washington County, Utah, January and February 1996	A-3
A-3.	Graph showing recovery data from wells during the Hurricane Bench aquifer test, Washington County, Utah, January and February 1996 (modified Hantush Solution)	A-6
A-4.	Map showing location of wells in the Anderson Junction aquifer test, Washington County, Utah, March and April 1996	A-7
A-5	Diagram showing well-location geometry needed for applying modified version of Papadopoulos solution (1965)	A-9
A-6.	Diagram showing idealized data set for an anisotropic and homogeneous aquifer	A-10
A-7.	Graph showing recovery data from wells during the Anderson Junction aquifer test, Washington County, Utah, March and April 1996	A-10
A-8.	Graph showing recovery data for wells during the Anderson Junction aquifer test showing range of possible slope, Washington County, Utah, March and April 1996	A-11
A-9.	Map showing location of wells in the Gunlock aquifer test, Washington County, Utah, February 1996	A-12
A-10.	Generalized geologic cross section in the vicinity of the pumped well in the Gunlock aquifer test, Washington County, Utah, February 1996	A-14
A-11.	Graph showing recovery data from two observation wells during the Gunlock aquifer test, Washington County, Utah, February 1996 (Theis solution, 1935)	A-16
A-12.	Graph showing recovery data from wells during the Gunlock aquifer test, Washington County, Utah, February 1996 (Neuman solution, 1974)	A-17
A-13.	Graph of recovery data showing different late-time slopes for wells during the Gunlock aquifer test, Washington County, Utah, February 1996	A-18
A-14.	Map showing (a) boundary, (b) finite-difference grid, and (c) detail of finite-difference grid for the ground-water flow model of the Gunlock aquifer test, Washington County, Utah, February 1996	A-19
A-15.	Graph showing measured recovery and computed drawdown for wells during the Gunlock aquifer test, Washington County, Utah, February 1996	A-20
A-16.	Map showing location of well in the Grapevine Pass aquifer test, Washington County, Utah, February 1996	A-22
A-17.	Graph showing recovery data for the Grapevine Pass aquifer test using the Cooper-Jacob straight-line method, Washington County, Utah, February 1996	A-25
A-18.	Map showing location of wells in the New Harmony aquifer test, Washington County, Utah, October and November 1996	A-25
A-19.	Schematic cross section of selected wells and lithology of the New Harmony aquifer-test site, Washington County, Utah, October and November 1996	A-27
A-20.	Graph showing drawdown data from the recorder well during the New Harmony aquifer test, Washington County, Utah, October and November 1996 (Unconfined Theis solution)	A-28
A-21	Graph showing drawdown data from the recorder well during the New Harmony aquifer test, Washington County, Utah, October and November 1996 (Jenkins and Prentice solution)	A-29

Figures—Continued

- A-22. Diagram showing the conceptual model of a homogeneous aquifer bisected by a single fracture (Jenkins and Prentice, 1982).....	A-30
B1-16. Graphs showing:	
B1-1. Sensitivity of water level to variations in horizontal hydraulic conductivity of the basin-fill aquifer in the ground-water flow model of the upper Ash Creek drainage basin, Utah	B1-2
B1-2. Sensitivity of water level to variations in horizontal hydraulic conductivity of the alluvial-fan aquifer in the ground-water flow model of the upper Ash Creek drainage basin, Utah.....	B1-2
B1-3. Sensitivity of water level to variations in horizontal hydraulic conductivity of the Pine Valley monzonite aquifer in the ground-water flow model of the upper Ash Creek drainage basin, Utah	B1-2
B1-4. Sensitivity of discharge boundaries to variations in horizontal hydraulic conductivity of the basin-fill aquifer in the ground-water flow model of the upper Ash Creek drainage basin, Utah	B1-2
B1-5. Sensitivity of discharge boundaries to variations in horizontal hydraulic conductivity of the alluvial-fan aquifer in the ground-water flow model of the upper Ash Creek drainage basin, Utah	B1-2
B1-6. Sensitivity of discharge boundaries to variations in horizontal hydraulic conductivity of the Pine Valley monzonite aquifer in the ground-water flow model of the upper Ash Creek drainage basin, Utah.....	B1-2
B1-7. Sensitivity of water level to variations in vertical conductance between the basin-fill and alluvial-fan aquifers in the ground-water flow model of the upper Ash Creek drainage basin, Utah.....	B1-3
B1-8. Sensitivity of water level to variations in vertical conductance between the alluvial-fan and Pine Valley monzonite aquifers in the ground-water flow model of the upper Ash Creek drainage basin, Utah	B1-3
B1-9. Sensitivity of discharge boundaries to variations in vertical conductance between the basin-fill and alluvial-fan aquifers in the ground-water flow model of the upper Ash Creek drainage basin, Utah.....	B1-3
B1-10. Sensitivity of discharge boundaries to variations in vertical conductance between the alluvial-fan and Pine Valley monzonite aquifers in the ground-water flow model of the upper Ash Creek drainage basin, Utah	B1-3
B1-11. Sensitivity of water level to variations in streambed conductance in the ground-water flow model of the upper Ash Creek drainage basin, Utah.....	B1-3
B1-12. Sensitivity of discharge boundaries to variations in streambed conductance in the ground-water flow model of the upper Ash Creek drainage basin, Utah.....	B1-3
B1-13. Sensitivity of water level to variations in the depth at which evapotranspiration ceases in the ground-water flow model of the upper Ash Creek drainage basin, Utah.....	B1-4
B1-14. Sensitivity of discharge boundaries to variations in the depth at which evapotranspiration ceases in the ground-water flow model of the upper Ash Creek drainage basin, Utah	B1-4
B1-15. Sensitivity of water level to variations in maximum evapotranspiration rate in the ground-water flow model of the upper Ash Creek drainage basin, Utah.....	B1-4
B1-16. Sensitivity of discharge boundaries to variations in the maximum evapotranspiration rate in the ground-water flow model of the upper Ash Creek drainage basin, Utah.....	B1-4
B2-1. Sensitivity of water level to variations in horizontal hydraulic conductivity of the Navajo aquifer in the ground-water flow model of the main part of the Navajo and Kayenta aquifers within the central Virgin River basin study area, Utah	B2-2

Figures—Continued

- B2-2. Sensitivity of simulated flux to variations in horizontal hydraulic conductivity of the Navajo aquifer in the ground-water flow model of the main part of the Navajo and Kayenta aquifers within the central Virgin River basin study area, Utah B2-2
- B2-3. Sensitivity of water level to variations in horizontal hydraulic conductivity of the Kayenta aquifer in the ground-water flow model of the main part of the Navajo and Kayenta aquifers within the central Virgin River basin study area, Utah B2-2
- B2-4. Sensitivity of simulated flux to variations in horizontal hydraulic conductivity of the Kayenta aquifer in the ground-water flow model of the main part of the Navajo and Kayenta aquifers within the central Virgin River basin study area, Utah B2-2
- B2-5. Sensitivity of water level to variations in vertical conductance between the Navajo and Kayenta aquifers in the ground-water flow model of the main part of the Navajo and Kayenta aquifers within the central Virgin River basin study area, Utah B2-2
- B2-6. Sensitivity of simulated flux to variations in vertical conductance between the Navajo and Kayenta aquifers in the ground-water flow model of the main part of the Navajo and Kayenta aquifers within the central Virgin River basin study area, Utah B2-2
- B2-7. Sensitivity of water level to variations in streambed conductance in the ground-water flow model of the main part of the Navajo and Kayenta aquifers within the central Virgin River basin study area, Utah B2-3
- B2-8. Sensitivity of simulated flux to variations in streambed conductance in the ground-water flow model of the main part of the Navajo and Kayenta aquifers within the central Virgin River basin study area, Utah B2-3
- B2-9. Sensitivity of water level to variations in general-head boundary conductance, representing inflow from underlying formations, in the ground-water flow model of the main part of the Navajo and Kayenta aquifers within the central Virgin River basin study area, Utah B2-3
- B2-10. Sensitivity of simulated flux to variations in general-head boundary conductance, representing inflow from underlying formations, in the ground-water flow model of the main part of the Navajo and Kayenta aquifers within the central Virgin River basin study area, Utah B2-3
- B2-11. Sensitivity of water level to variations in drain conductance, representing spring discharge, in the ground-water flow model of the main part of the Navajo and Kayenta aquifers within the central Virgin River basin study area, Utah B2-3
- B2-12. Sensitivity of water-budget flux to variations in drain conductance, representing spring discharge, in the ground-water flow model of the main part of the Navajo and Kayenta aquifers within the central Virgin River basin study area, Utah B2-3
- B2-13. Sensitivity of water level to variations in recharge from precipitation and unconsumed irrigation water in the ground-water flow model of the main part of the Navajo and Kayenta aquifers within the central Virgin River basin study area, Utah B2-4
- B2-14. Sensitivity of simulated flux to variations in recharge from precipitation and unconsumed irrigation water in the ground-water flow model of the main part of the Navajo and Kayenta aquifers within the central Virgin River basin study area, Utah B2-4
- B3-1. Sensitivity of water level to variations in horizontal hydraulic conductivity of the Navajo aquifer in the ground-water flow model of the Gunlock part of the Navajo and Kayenta aquifers within the central Virgin River basin study area, Utah B3-2
- B3-2. Sensitivity of simulated flux to and from the Santa Clara River to variations in horizontal hydraulic conductivity of the Navajo Sandstone aquifer in the ground-water flow model of the Gunlock part of the Navajo and Kayenta aquifers within the central Virgin River basin study area, Utah B3-2

Figures—Continued

B3-3.	Sensitivity of water level to variations in the horizontal hydraulic conductivity of the Kayenta aquifer in the ground-water flow model of the Gunlock part of the Navajo and Kayenta aquifers within the central Virgin River basin study area, Utah	B3-3
B3-4.	Sensitivity of simulated flux to and from the Santa Clara River to variations in horizontal hydraulic conductivity of the Kayenta aquifer in the ground-water flow model of the Gunlock part of the Navajo and Kayenta aquifers within the central Virgin River basin study area, Utah	B3-3
B3-5.	Sensitivity of water level to variations in vertical conductance between the Navajo and Kayenta aquifers in the ground-water flow model of the Gunlock part of the Navajo and Kayenta aquifers within the central Virgin River basin study area, Utah.....	B3-4
B3-6.	Sensitivity of simulated flux to and from the Santa Clara River to variations in vertical conductance between the Navajo and Kayenta aquifers in the ground-water flow model of the Gunlock part of the Navajo and Kayenta aquifers within the central Virgin River basin study area, Utah.....	B3-4
B3-7.	Sensitivity of water level to variations in streambed conductance in the ground-water flow model of the Gunlock part of the Navajo and Kayenta aquifers within the central Virgin River basin study area, Utah.....	B3-5
B3-8.	Sensitivity of simulated flux to and from the Santa Clara River to variations in streambed conductance in the ground-water flow model of the Gunlock part of the Navajo and Kayenta aquifers within the central Virgin River basin study area, Utah.....	B3-5
B3-9.	Sensitivity of water level to variations in anisotropy in the ground-water flow model of the Gunlock part of the Navajo and Kayenta aquifers within the central Virgin River basin study area, Utah.....	B3-6
B3-10.	Sensitivity of simulated flux to and from the Santa Clara River to variations in anisotropy in the ground-water flow model of the Gunlock part of the Navajo and Kayenta aquifers within the central Virgin River basin study area, Utah.....	B3-6
B3-11.	Sensitivity of water level to variations in recharge from precipitation in the ground-water flow model of the Gunlock part of the Navajo and Kayenta aquifers within the central Virgin River basin study area, Utah	B3-6
B3-12.	Sensitivity of simulated flux to and from the Santa Clara River to variations in recharge from precipitation in the ground-water flow model of the Gunlock part of the Navajo and Kayenta aquifers within the central Virgin River basin study area, Utah.....	B3-7
B3-13.	Sensitivity of water level to variations in recharge from the Gunlock Reservoir in the ground-water flow model of the Gunlock part of the Navajo and Kayenta aquifers within the central Virgin River basin study area, Utah	B3-7
B3-14.	Sensitivity of simulated flux to and from the Santa Clara River to variations in recharge from the Gunlock Reservoir in the ground-water flow model of the Gunlock part of the Navajo and Kayenta aquifers within the central Virgin River basin study area, Utah.....	B3-7

Tables

1.	Hydrostratigraphic section of selected water-bearing formations within the central Virgin River basin study area, Utah	8
2.	Hydrostratigraphic section of the upper Ash Creek drainage basin area, Utah	9
3.	Chlorofluorocarbon concentration measured from samples from the central Virgin River basin collected by copper-tube versus glass-ampoule method	14
4.	Average chlorofluorocarbon-12 concentration and estimated recharge year for selected springs, surface-water sites, and wells within the central Virgin River basin study area, Utah	18
5.	Transmissivity of three aquifers in the upper Ash Creek drainage basin, Utah	34
6.	Precipitation and recharge in subbasins of the upper Ash Creek drainage basin, Utah	36
7.	Measurements of discharge, temperature, and specific conductance and analysis of seepage losses and gains at selected sites on Ash, Kanarra, and Sawyer Creeks, upper Ash Creek drainage basin, Utah.....	38
8.	Miscellaneous discharge measurements at selected sites along Kanarra Creek and its tributaries, upper Ash Creek drainage basin, Utah.....	39
9.	Estimated ground-water budget for the upper Ash Creek drainage basin, Utah.....	45
10.	Aquifer-test results from the Navajo aquifer, central Virgin River basin study area, Utah.....	49
11.	Seepage measurements and estimated recharge from perennial streams to the Navajo aquifer in the central Virgin River basin, Utah	54
12.	Drainage-basin parameters for perennial and ephemeral streams that recharge the Navajo aquifer in the central Virgin River basin, Utah.....	61
13.	Estimated annual recharge from ephemeral streams to the Navajo aquifer based on estimated annual stream discharge, central Virgin River basin, Utah	62
14.	Estimated recharge from ephemeral streams to the Navajo aquifer based on the City Creek infiltration experiment, February to March 1997, central Virgin River basin, Utah	63
15.	Estimated ground-water budget for the main part of the Navajo and Kayenta aquifers, central Virgin River basin, Utah.....	72
16.	Estimated ground-water budget for the Gunlock part of the Navajo and Kayenta aquifers central Virgin River basin, Utah.....	72
17.	(a) Conceptual and simulated ground-water budgets and (b) simulated versus measured water-level differences for the upper Ash Creek drainage basin ground-water system, Utah	86
18.	(a) Conceptual and simulated ground-water budgets and (b) simulated versus measured water-level differences for the baseline simulation and the simulation testing flow across the Hurricane Fault in the upper Ash Creek drainage basin ground-water system, Utah	89
19.	(a) Conceptual and simulated ground-water budgets and (b) simulated versus measured water-level differences for the baseline simulation and the simulation of no subsurface outflow to the lower Ash Creek drainage basin, Utah	91
20.	(a) Conceptual and simulated ground-water budgets and (b) simulated versus measured water-level differences for the baseline simulation and the simulation testing anisotropy in the Pine Valley monzonite aquifer in the upper Ash Creek drainage basin ground-water system, Utah.....	94
21.	Measured, estimated, and simulated hydraulic-conductivity values for the main part of the Navajo and Kayenta aquifers, central Virgin River basin, Utah.....	109
22.	(a) Conceptual and simulated ground-water budgets and (b) simulated versus measured water-level differences for the main part of the Navajo and Kayenta aquifers, central Virgin River basin, Utah	110
23.	(a) Conceptual and simulated ground-water budgets and (b) simulated versus measured water-level differences for the baseline simulation and simulations testing faulting and anisotropy in the main part of the Navajo and Kayenta aquifers, central Virgin River basin, Utah	116

Tables—Continued

24.	Hydraulic-conductivity values used in the baseline simulation of the Gunlock part of the Navajo and Kayenta aquifers, central Virgin River basin, Utah	127
25.	(a) Conceptual and simulated ground-water budgets and (b) simulated versus measured water-level differences in the Gunlock part of the Navajo and Kayenta aquifers, central Virgin River basin, Utah	128
26.	(a) Conceptual and simulated ground-water budgets and (b) simulated versus measured water-level differences for the baseline simulation and the simulation testing flow across the Gunlock Fault in the Gunlock part of the Navajo and Kayenta aquifers, central Virgin River basin, Utah	132
27.	(a) Conceptual and simulated ground-water budgets and (b) simulated versus measured water-level differences for the baseline simulation and the simulation testing inflow from underlying formations in the Gunlock part of the Navajo and Kayenta aquifers, central Virgin River basin, Utah	133
A-1	Construction data for the wells used in the Hurricane Bench aquifer test, Washington County, Utah	A-4
A-2.	Construction data for the wells used in the Anderson Junction aquifer test, Washington County, Utah	A-8
A-3.	Construction data for wells used in the Gunlock aquifer test, Washington County, Utah, February 1996.....	A-13
A-4.	Construction data for wells observed during the New Harmony aquifer test, Washington County, Utah, October and November 1996	A-26

CONVERSION FACTORS, VERTICAL DATUM, AND ABBREVIATED WATER-QUALITY UNITS

Multiply	By	To obtain
Length		
inch (in.)	2.54	centimeter
inch (in.)	25.4	millimeter
foot (ft)	0.3048	meter
mile (mi)	1.609	kilometer
Area		
acre	4,047	square meter
acre	0.4047	hectare
acre	0.4047	square hectometer
acre	0.004047	square kilometer
square foot (ft ²)	929.0	square centimeter
square foot (ft ²)	0.09290	square meter
square mile (mi ²)	259.0	hectare
square mile (mi ²)	2.590	square kilometer
Volume		
acre-foot (acre-ft)	1,233	cubic meter
acre-foot (acre-ft)	0.001233	cubic hectometer
Flow rate		
acre-foot per day (acre-ft/d)	0.01427	cubic meter per second
acre-foot per year (acre-ft/yr)	1,233	cubic meter per year
acre-foot per year (acre-ft/yr)	0.001233	cubic hectometer per year
foot per second (ft/s)	0.3048	meter per second
foot per year (ft/yr)	0.3048	meter per year
square foot per second (ft ² /s)	0.02832	cubic meter per second
cubic foot per second (ft ³ /s)	0.06309	liter per second
gallon per minute (gal/min)	0.06791	liter per second per meter squared
gallons per minute per square foot [(gal/min)/ft ²]	25.4	millimeter per year
Specific capacity		
gallon per minute per foot [(gal/min)/ft]	0.2070	liter per second per meter
Hydraulic conductivity		
foot per day (ft/d)	0.3048	meter per day
Hydraulic gradient		
foot per foot (ft/ft)	1	meter per meter
foot per mile (ft/mi)	0.1894	meter per kilometer
Transmissivity¹ and Conductance		
foot squared per day (ft ² /d)	0.09290	meter squared per day
Leakance		
acre-foot per day per mile [(acre-ft/d)/mi]	1	cubic meter per second per kilometer

Temperature in degrees Celsius (°C) may be converted to degrees Fahrenheit (°F) as follows:

$$^{\circ}\text{F} = (1.8 \times ^{\circ}\text{C}) + 32$$

Sea level: In this report, “sea level” refers to the National Geodetic Vertical Datum of 1929—a geodetic datum derived from a general adjustment of the first-order level nets of both the United States and Canada, formerly called Sea Level Datum of 1929.

Altitude, as used in this report, refers to distance above or below sea level.

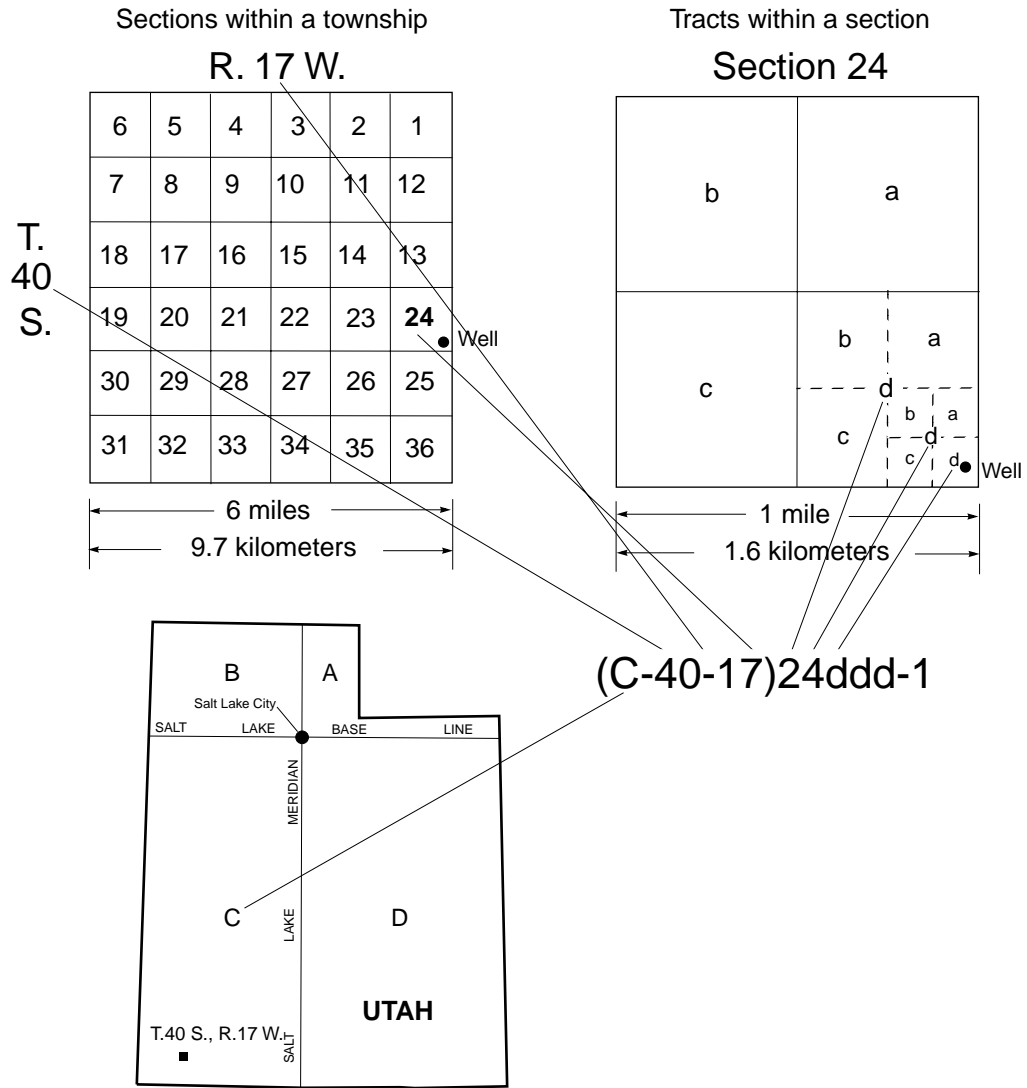
¹Transmissivity: The standard unit for transmissivity is cubic foot per day per square foot times foot of aquifer thickness [$(\text{ft}^3/\text{d})/\text{ft}^2$]ft. In this report, the mathematically reduced form, foot squared per day (ft^2/d), is used for convenience.

Specific conductance is recorded in microsiemens per centimeter at 25 degrees Celsius ($\mu\text{S}/\text{cm}$).

Chemical concentration and water temperature are reported only in International System (SI) units. Chemical concentration in water is reported in either in milligrams per liter (mg/L) or micrograms per liter ($\mu\text{g}/\text{L}$). The chlorofluorocarbon concentration in water is reported in picomoles per kilogram (pmole/kg) or parts per trillion (ppt). These units express the solute weight per unit volume (liter) or unit mass (kilogram) of water. A liter of water is assumed to weigh 1 kilogram. The numerical value in milligrams per liter is about the same as for concentrations in parts per million. One thousand micrograms per liter is equivalent to 1 milligram per liter, one million picomoles per kilogram is equivalent to 1 mole per liter, and one million parts per trillion is equivalent to 1 part per million. A mole of substance is its atomic or formula weight in grams. Concentration in moles per liter can be determined from milligrams per liter by dividing by the atomic or formula weight of the constituent, in milligrams. Stable isotope concentration is reported as per mil, which is equivalent to parts per thousand.

Tritium units (TU) are used to report tritium concentration. One TU equals tritium concentration in pico-Curies per liter divided by 3.22.

The system of numbering wells and springs in Utah is based on the cadastral land-survey system of the U.S. Government. The number, in addition to designating the well or spring, describes its position in the land net. The land-survey system divides the State into four quadrants separated by the Salt Lake Base Line and the Salt Lake Meridian. These quadrants are designated by the uppercase letters A, B, C, and D, indicating the northeast, northwest, southwest, and southeast quadrants, respectively. Numbers designating the township and range, in that order, follow the quadrant letter, and all three are enclosed in parentheses. The number after the parentheses indicates the section and is followed by three letters indicating the quarter section, the quarter-quarter section, and the quarter-quarter-quarter section—generally 10 acres for a regular section¹. The lowercase letters a, b, c, and d indicate, respectively, the northeast, northwest, southwest, and southeast quarters of each subdivision. The number after the letters is the serial number of the well or spring within the 10-acre tract. When the serial number is not preceded by a letter, the number designates a well. When the serial number is preceded by an “S,” the number designates a spring. A number having all three quarter designations but no serial number indicates a miscellaneous data site other than a well or spring, such as a location for a surface-water measurement site or tunnel portal. Thus, (C-40-17)24ddd-1 designates the first well constructed or visited in the southeast 1/4 of the southeast 1/4 of section 24, T. 40 S., R. 17 W.



¹. Although the basic land unit, the section, is theoretically 1 square mile, many sections are irregular in size and shape. Such sections are subdivided into 10-acre tracts, generally beginning at the southeast corner, and the surplus or shortage is taken up in the tracts along the north and west sides of the section.

Numbering system used for hydrologic-data sites in Utah.

GEOHYDROLOGY AND NUMERICAL SIMULATION OF GROUND-WATER FLOW IN THE CENTRAL VIRGIN RIVER BASIN OF IRON AND WASHINGTON COUNTIES, UTAH

By V.M. Heilweil, G.W. Freethey, C.D. Wilkowske, B.J. Stolp, and D.E. Wilberg

ABSTRACT

Because rapid growth of communities in Washington and Iron Counties, Utah, is expected to cause an increase in the future demand for water resources, a hydrologic investigation was done to better understand ground-water resources within the central Virgin River basin. This study focused on two of the principal ground-water reservoirs within the basin: the upper Ash Creek basin ground-water system and the Navajo and Kayenta aquifer system.

The ground-water system of the upper Ash Creek drainage basin consists of three aquifers: the uppermost Quaternary basin-fill aquifer, the Tertiary alluvial-fan aquifer, and the Tertiary Pine Valley monzonite aquifer. These aquifers are naturally bounded by the Hurricane Fault and by drainage divides. On the basis of measurements, estimates, and numerical simulations of reasonable values for all inflow and outflow components, total water moving through the upper Ash Creek drainage basin ground-water system is estimated to be about 14,000 acre-feet per year. Recharge to the upper Ash Creek drainage basin ground-water system is mostly from infiltration of precipitation and seepage from ephemeral and perennial streams. The primary source of discharge is assumed to be evapotranspiration; however, subsurface discharge near Ash Creek Reservoir also may be important.

The character of two of the hydrologic boundaries of the upper Ash Creek drainage basin ground-water system is speculative. The eastern boundary provided by the Hurricane Fault is assumed to be a no-flow boundary, and a substan-

tial part of the ground-water discharge from the system is assumed to be subsurface outflow beneath Ash Creek Reservoir along the southern boundary. However, these assumptions might be incorrect because alternative numerical simulations that used different boundary conditions also proved to be feasible. The hydrogeologic character of the aquifers is uncertain because of limited data. Differences in well yield indicate that there is considerable variability in the transmissivity of the basin-fill aquifer. Field data also indicate that the basin-fill aquifer is more transmissive than the underlying alluvial-fan aquifer. Data from the Pine Valley monzonite aquifer indicate that its transmissivity may be highly variable and that it is strongly influenced by the connection of fractures.

The Navajo and Kayenta aquifers provide most of the potable water to the municipalities of Washington County. Because of large outcrop exposures, uniform grain size, and large stratigraphic thickness, these formations are able to receive and store large amounts of water. In addition, structural forces have resulted in extensive fracture zones that enhance ground-water recharge and movement within these aquifers. Aquifer testing of the Navajo aquifer indicates that horizontal hydraulic-conductivity values range from 0.2 to 32 feet per day at different locations and may be primarily dependent on the extent of fracturing. Limited data indicate that the Kayenta aquifer generally is less transmissive than the Navajo aquifer. The aquifers are bounded to the south and west by the erosional extent of the formations and to the east by the Hurricane Fault, which completely offsets these formations and is assumed to be a lateral

no-flow boundary. Like the Hurricane Fault, the Gunlock Fault is assumed to be a lateral no-flow boundary that divides the Navajo and Kayenta aquifers within the study area into two parts: the main part, between the Hurricane and Gunlock Faults; and the Gunlock part, west of the Gunlock Fault.

Generally, the water in the Navajo and Kayenta aquifers contains few dissolved minerals. However, two distinct areas contain water with dissolved-solids concentrations greater than 500 milligrams per liter: a larger area north of the city of St. George and a smaller area a few miles west of the town of Hurricane. Mass-balance calculations indicate that in the higher-dissolved-solids area north of St. George, as much as 2.7 cubic feet per second may be entering the aquifer from underlying formations. For the area west of Hurricane, as much as 1.5 cubic feet per second may be entering the aquifer from underlying formations.

On the basis of measurements, estimates, and numerical simulations, total water moving through the Navajo and Kayenta aquifers is estimated to be about 25,000 acre-feet per year for the main part and 5,000 acre-feet per year for the Gunlock part. The primary source of recharge is assumed to be infiltration of precipitation in the main part and seepage from the Santa Clara River in the Gunlock part. The primary source of discharge is assumed to be well discharge for both the main and Gunlock parts of the aquifers. Numerical simulations indicate that faults with major offset, such as the Washington Hollow Fault and an unnamed fault near Anderson Junction, may impede horizontal ground-water flow. Also, increased horizontal hydraulic conductivity along the orientation of predominant surface fracturing may be an important factor in regional ground-water flow. Simulations with increased north-south hydraulic conductivity substantially improved the match to measured water levels in the central area of the model between Snow Canyon and Mill Creek. Numerical simulation of the Gunlock part, using aquifer properties determined for the city of St. George municipal well field, resulted in a reasonable representation of regional water levels and estimated seepage from and to the Santa Clara

River. To further quantify the Gunlock part of the Navajo and Kayenta aquifers, a better understanding of ground-water flow at the Gunlock Fault is needed.

INTRODUCTION

Ground-water resources in the central Virgin River basin of Washington and Iron Counties, Utah, were studied at the request of the State of Utah Division of Water Rights and the Washington County Water Conservancy District. The central Virgin River basin study area (fig. 1) encompasses the part of the Virgin River drainage west of the Hurricane Fault up to and including the Santa Clara River. Although the study area is contiguous with respect to surface water flow, two distinct types of aquifer systems provide most of the available ground water in the region: alluvial-basin sediments and consolidated-rock formations. The main alluvial-basin aquifer is located in the upper Ash Creek drainage basin. The main consolidated-rock aquifers in the study area are within the Navajo Sandstone and the Kayenta Formation. Alluvial deposits along the Virgin River Valley and the Santa Clara Valley also yield substantial amounts of ground water to wells but generally do not provide water of sufficient quality for potable uses. The primary objective of this study is to investigate the amount and quality of ground water within the upper Ash Creek drainage basin and the Navajo Sandstone and Kayenta Formation.

The population of southwestern Utah is increasing rapidly. In 1980 the population of Washington County was 26,000, whereas in 1997, the population was estimated to be 76,350 (Utah State Data Center, written commun., 1998) and is expected to continue increasing in the future. This growth is driving the need for further development of existing water resources and the search for additional potential ground-water sources. To meet the growing demand for water, the Utah State Department of Natural Resources, Division of Water Rights, and the Washington County Water Conservancy District provided funding for the U.S. Geological Survey (USGS) to conduct a hydrogeologic study to determine the amount and quality of ground water moving through the study area and to assess the hydrologic character of the aquifers. The information will be used to assess the potential effects of increased development on ground-water resources and to aid in the search for additional ground-water reserves.

A better understanding of the ground-water systems is critical for the further development of ground-

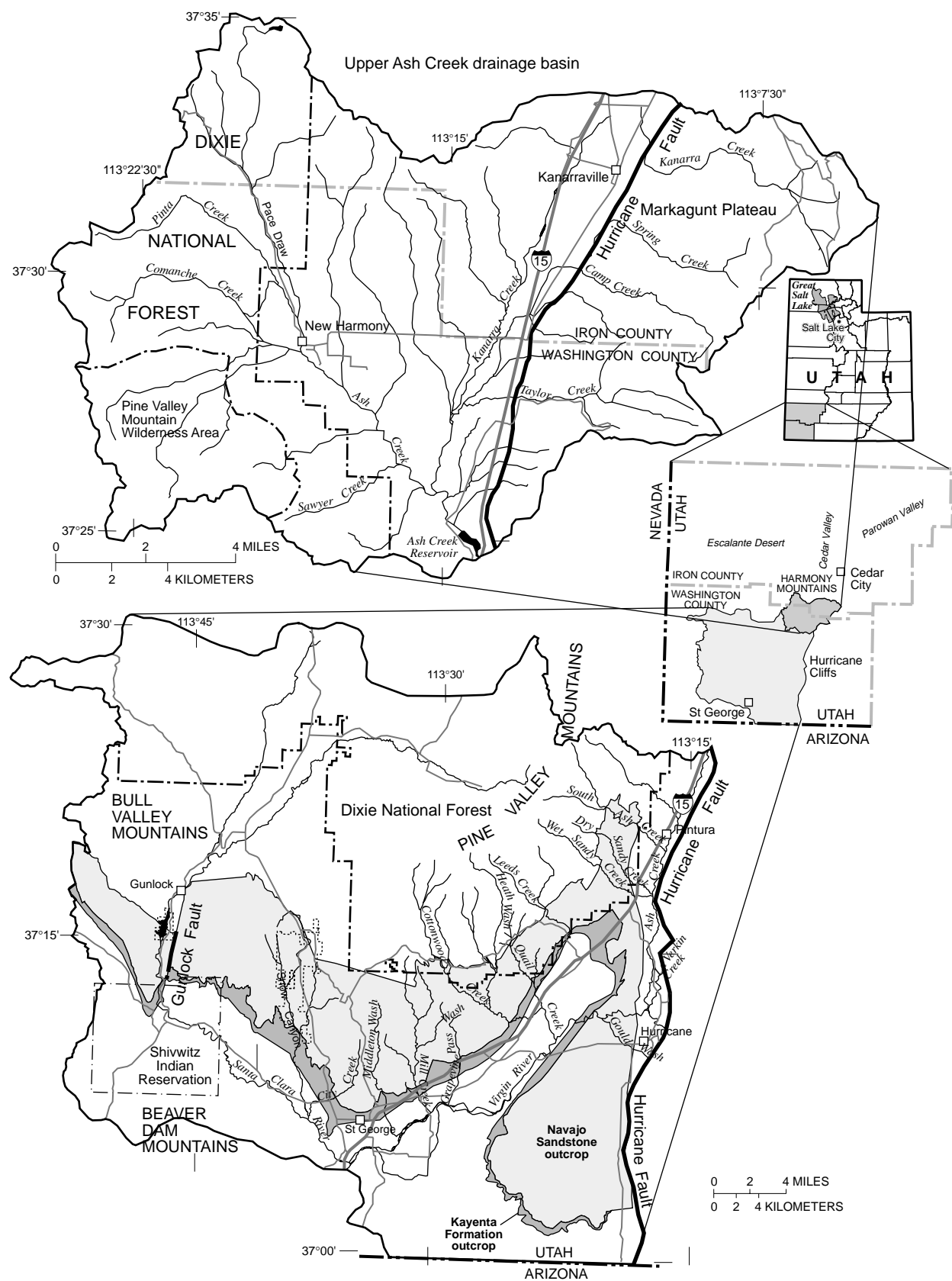


Figure 1. Location of the upper Ash Creek drainage basin and the Navajo Sandstone and Kayenta Formation outcrops within the central Virgin River basin study area, Utah.

water resources, and the scarcity of hydrologic information is a problem. The small amount of hydrologic information available for the upper Ash Creek drainage basin results in a hydrologic conceptualization that is irresolute. Existing wells, which mostly tap the basin-fill deposits, vary widely in yield, presumably because of the variability in the hydraulic conductivity of the saturated deposits. A group of more recently drilled wells on the southwest side of the drainage basin is finished in igneous rocks commonly exposed in the Pine Valley Mountains. A few of these wells can be pumped at several thousand gal/min with only a small decline in water level. Other wells finished in the same igneous rocks have low yields. These differences are thought to be caused by heterogeneity and anisotropy from the varying density and connectivity of fractures. Both properties are difficult to quantify and to map.

Ground water from the Navajo Sandstone and the Kayenta Formation has been extensively developed in certain areas along the formation outcrops; however, hydrologic data are not available for many other parts of the outcrops, or where the formations are buried in the north part of the study area. Also, fracturing within these formations, which is extremely variable throughout the study area and strongly affects the movement of ground water, is not well defined. Therefore, the conceptualization of how the hydrologic system functions is not well understood.

Development of an accurate ground-water budget is needed to improve the understanding of the ground-water systems. Ground-water recharge from precipitation, from infiltration beneath streams, from irrigated fields, and possibly from overlying or underlying formations, make up the inflow components of a ground-water budget. However, these components are not well understood or quantified for the upper Ash Creek drainage basin ground-water system for the aquifers of the Navajo Sandstone and Kayenta Formation. Some components of ground-water discharge, such as well pumping, spring discharge, and discharge to streams can be fairly accurately quantified. However, other discharge components, including evapotranspiration and subsurface outflow to adjacent aquifers, cannot be accurately determined.

Description of the Study Area

The central Virgin River basin study area is in the southwestern corner of Utah, generally west of the Hurricane Fault (fig. 1). The area encompasses about 1,070 mi² along the transition between the complexly faulted

and folded formations of the Basin and Range Physiographic Province and the gently dipping formations of the Colorado Plateau Physiographic Province, as described by Fenneman (1931). The study area is defined on the west and north sides by the drainage divide between the Virgin and Santa Clara River basins and adjacent drainage basins along the Beaver Dam Mountains, Bull Valley Mountains, Pine Valley Mountains, and Harmony Mountains; the boundary on the east is generally the Hurricane Cliffs, except for a small part of the Markagunt Plateau farther east; the boundary on the south is the Utah-Arizona State line (Cordova and others, 1972). Most of the study area is characterized by sedimentary formations of Mesozoic age, igneous rocks of Tertiary age, and alluvial and basalt-flow deposits of Quaternary age (pl. 1).

The 134 mi² upper Ash Creek drainage basin is defined as the surface-water drainage basin that drains into Ash Creek Reservoir, which is located 21 mi south of Cedar City and just west of Interstate 15 (fig. 1). The northern study area boundary divides the internal drainage of the Great Basin from the Virgin River part of the Colorado River drainage basin. The position of the surface-water divide is about 1.5 mi north of Kanarraville, Utah. The ground-water divide in the unconsolidated alluvium, which is roughly coincident with the surface-water divide, can shift slightly with variations in the location and amount of both recharge and pumpage. Topographically, the upper Ash Creek drainage basin consists of gently sloping lowland valley areas that are nearly encircled by the Harmony Mountains to the north, the Pine Valley Mountains to the southwest, and the Markagunt Plateau to the east. The Hurricane Fault zone trends north-northeast near the eastern edge of the upper Ash Creek basin, just east of Interstate 15. A narrow but thick deposit of unconsolidated alluvium has accumulated along the trace of the Hurricane Fault and connects the upper Ash Creek drainage basin northward with the southern end of Cedar Valley (pl. 1).

Within the study area, the Navajo Sandstone has an outcrop area of about 220 mi². The Kayenta Formation has an outcrop area of about 35 mi². Both formations are buried toward the north by overlying formations for an additional 500 mi² within the study area. The formations are absent in the southern part of the study area because of erosion. The outcrops extend from the Hurricane Fault on the east to the Bull Valley Mountains on the west (fig. 1) and vary in altitude from about 2,900 ft to 5,300 ft. In the western part of the study area is the Gunlock Fault, across which the Navajo Sandstone and Kayenta Formation are verti-

cally offset from their southernmost erosional extents to where these formations become buried adjacent to Gunlock Reservoir (pl. 1).

At the latitude of the study area (about 37°15' N), the effects of both the subtropical and polar jet streams influence the local climate. Also, a large variation in precipitation within the study area results from the large variation in altitude. During 1947-97, precipitation at St. George (altitude 2,820 ft) averaged about 8 in/yr, while the precipitation at New Harmony (altitude 5,290 ft) averaged about 17.8 in/yr. Average precipitation (1961-90) was about 23 in/yr at the highest altitude in the Harmony Mountains (about 8,400 ft), about 30 in/yr at the highest altitude of the Pine Valley Mountains (about 10,400 ft), and about 33 in/yr at the highest altitude of the Markagunt Plateau (about 8,000 ft) (fig. 2). Most of the precipitation in the study area occurs from

December through March, although substantial precipitation also can occur from August through November and is related to a monsoonal weather pattern that brings warm, moist air northward from the Gulf of Mexico. The monthly distribution of precipitation at St. George and New Harmony is shown in figure 3.

Previous Investigations

Several reports have been written describing the geology and hydrology of the central Virgin River basin study area. Most recently, Hurlow (1998) did an extensive geologic compilation, as well as field work, to delineate the structure, lithology, and fractures of the Navajo Sandstone, as well as the structure and lithology of basin fill and older consolidated-rock formations along the Ash Creek drainage basin. Cordova, Sand-

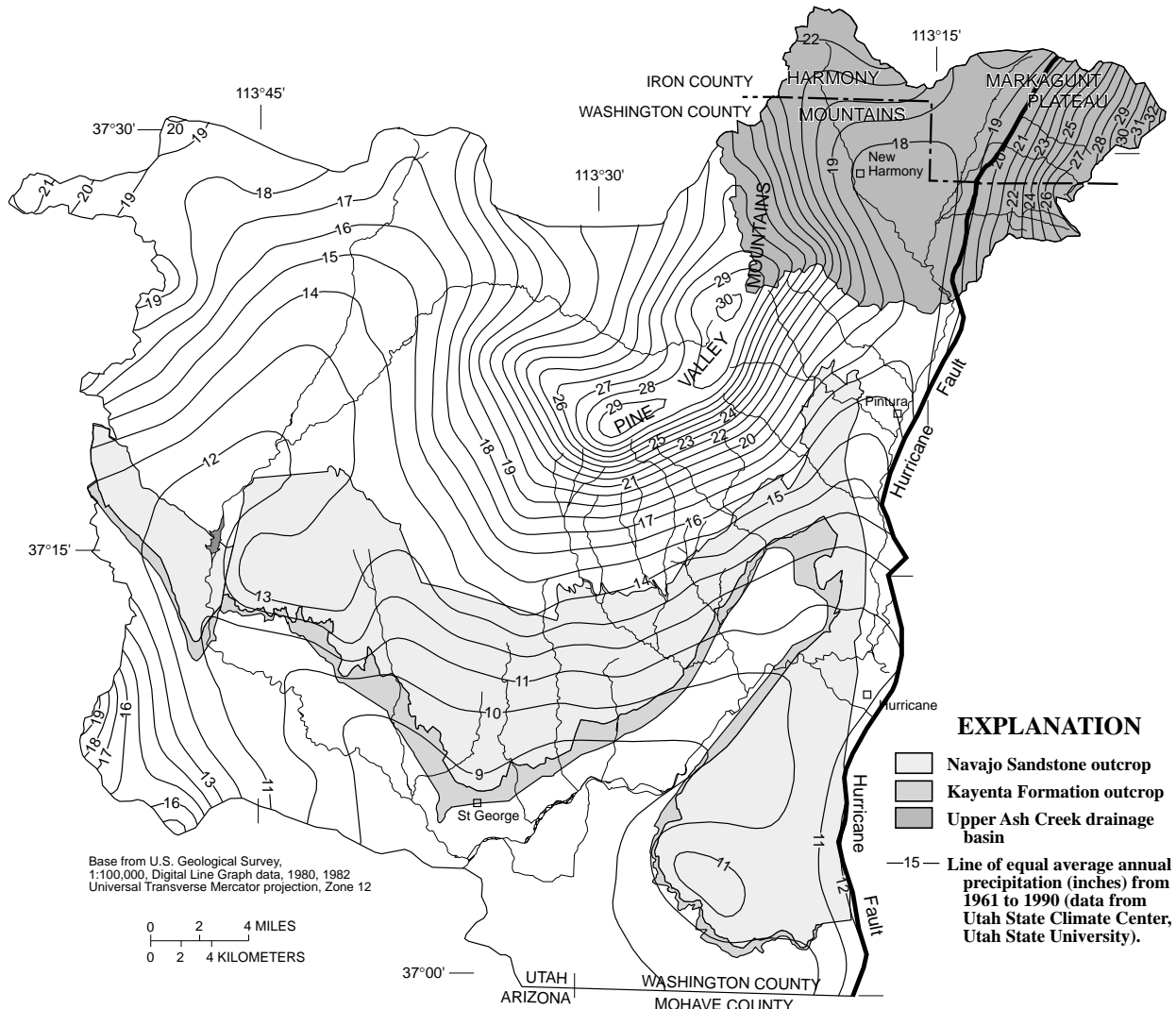


Figure 2. Average annual precipitation contours for the central Virgin River basin study area, Utah, 1961-90.

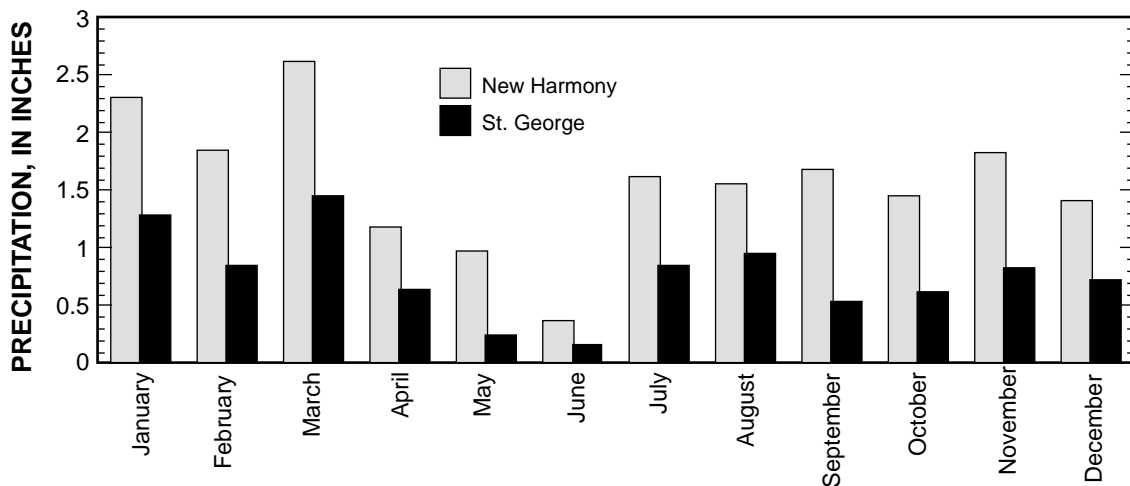


Figure 3. Monthly average precipitation at St. George and New Harmony, Utah, based on data from 1980 to 1989.

berg, and McConkie (1972) described the hydrogeology of both the unconsolidated and consolidated-rock aquifers, including aquifer properties and ground-water budgets. A follow-up study by Cordova (1978) provides a more detailed investigation of ground-water conditions in the Navajo Sandstone within the study area, including aquifer testing and the compilation of a hydrologic budget. A report by Budding and Sommer (1986) describes an assessment of the low-temperature geothermal potential of the Santa Clara River and Virgin River Valleys in Washington County, including extensive water-chemistry data. Clyde (1987) compiled and summarized hydrologic information for both the central Virgin River and upper Virgin River drainage basins. Herbert (1995) described a seepage study of a section of the Virgin River within Washington County. Jenson, Lowe, and Wireman (1997) provided a detailed hydrologic analysis of Sheep Spring near Santa Clara. Cook (1960) presented an overview of the geology of Washington County and a more-detailed description (Cook, 1957) of the geology of the Pine Valley Mountains. Spencer Reber (written commun., 1994) wrote a number of unpublished reports for the municipalities of St. George, Washington, and Leeds, including detailed geologic maps and cross sections. With regard to geo-hydrology of the upper Ash Creek drainage basin, Thomas and Taylor (1946) and Bjorklund, Sumsion, and Sandberg (1978), as part of their overall hydrologic study of the more populated Cedar City and Parowan Valleys, briefly described ground-water occurrence and use near Kanarraville, Utah.

Scope of study

The purpose of the study was to assess the quantity of ground water in the central Virgin River basin and to document, to the closest extent possible, direction and rate of movement of ground water through the aquifer systems. In general, the approach of this study was to (1) compile available geologic information on the various aquifer formations; (2) collect additional hydrologic, geologic, and chemical data, where possible and practical; (3) formulate hydrologic conceptualizations of ground-water movement through the principal aquifers; (4) develop computer simulations representing the aquifers to test various alternative hydrologic conceptualizations; (5) compare model-computed results with measured hydrologic data to determine how confidently the models can be used as tools for the management of ground-water resources; and (6) determine which additional data collection would be most helpful in refining present hydrologic conceptualizations. Water chemistry was also investigated when it could be used to aid in the analysis of recharge, ground-water movement, and discharge. Generally, well and spring locations within the study area were selected on the basis of proximity to municipalities, depth to water, quality of water, and natural factors such as topography and surface recharge. Thus, more information is available for certain parts of the aquifers, which allows for more detailed hydrologic analyses in those areas. Conversely, only a small amount of information is available regarding ground-water conditions in many parts of the upper Ash Creek drainage basin ground-water system and the Navajo and Kayenta aquifers.

Purpose and Scope of Report

The purpose of the report is to document the findings of the study, which include descriptions of the geo-hydrologic framework, analyses of the chemical and isotopic character of the ground water, and conceptual and mathematical representation of three separate aquifer systems in the study area. This report describes the geohydrology of the upper Ash Creek drainage basin ground-water system and the aquifers within the central Virgin River basin formed by the Navajo Sandstone and the Kayenta Formation. The Navajo Sandstone and the Kayenta Formation are two of the formations that make up the principal regional aquifer of the Colorado Plateau, the Glen Canyon aquifer. For this report they will be referred to individually as the Navajo aquifer and the Kayenta aquifer. Information was compiled and analyzed regarding their lateral and vertical extents, hydraulic properties, ground-water budgets, and directions of ground-water flow.

In addition to the data provided by previous investigations, hydrologic data collected for this study included water level measurements in wells, discharge measurements from pumping wells and springs, discharge measurements in streams, aquifer testing, and the collection of water samples for the analysis of general chemistry, stable and radioactive isotopes, dissolved gases, and chlorofluorocarbons (Wilkowske and others, 1998). Water levels were measured in about 30 wells in the upper Ash Creek drainage basin and in about 80 wells in the Navajo and Kayenta aquifers to determine the configuration of water-level contours (Wilkowske and others, 1998, tables 1 and 2). Most of the municipal well pumpage information was available from the Utah Division of Water Rights and private well owners; however, power consumption and discharge were measured at 14 irrigation wells in the Navajo and Kayenta aquifers southwest of Hurricane and at 8 irrigation wells in the upper Ash Creek drainage basin to estimate annual average rates of ground-water discharge (Wilkowske and others, 1998, table 1). Surface-water discharge was measured at 58 sites in the study area to determine the relative amount of stream loss and gain and the locations where these losses and gains occur (Wilkowske and others, 1998, table 6). Four aquifer tests were conducted at wells that pump water from the Navajo Sandstone and one aquifer test was conducted at a well that pumps water from the igneous rocks in the upper Ash Creek drainage basin.

Field and laboratory analyses were done on ground- and surface-water samples, not to characterize

water quality, but to evaluate surface- and ground-water relations and to get a sense of how water enters, moves through, and leaves the ground-water systems of interest. Specific conductance, water temperature, and pH were measured at many of the surface water and ground-water sites inventoried to determine the range and the areal and temporal trends of the values (Wilkowske and others, 1998, tables 3, 4, 5, 6). Water samples for general chemistry were collected at 7 wells, in addition to a compilation of 113 previously reported analyses (Wilkowske and others, 1998, table 4). Thirty-four samples were analyzed for the stable isotopes of oxygen and hydrogen; 25 water samples and 2 rock samples were analyzed for strontium isotopes; and 2 water samples were analyzed for the radioactive isotope of hydrogen (tritium) (Wilkowske and others, 1998, table 5). Water samples from 36 sites were analyzed for chlorofluorocarbons and 6 samples were analyzed for dissolved gases (Wilkowske and others, 1998, table 5).

Acknowledgments

The authors thank the many individuals who assisted with this study. Jerry Olds of the Utah Division of Water Rights provided a variety of information including well pumpage and water-rights data. Ronald Thompson, Morgan Jenson, Chuck Carney, and Lloyd Jessup of the Washington County Water Conservancy District provided much assistance in data collection, such as drilling observation wells for aquifer testing and taking monthly water-level measurements. Phillip Solomon and Frank Kell of the city of St. George and Grand Henline of the city of Washington were very helpful in assisting with aquifer testing, water-level measurements, and water-chemistry sampling of wells and springs. Other municipalities, including the towns of Gunlock, Hurricane, Leeds, and Santa Clara assisted with data collection at their wells and springs. Arwin Stratton of the Winding Rivers Corporation and Elliot Christensen of the Property Division of the Church of Jesus Christ of Latter Day Saints assisted with aquifer testing conducted on their properties. Dr. D. Kip Solomon of the University of Utah generously provided the use of his laboratory for the analysis of chlorofluorocarbons and assistance with data interpretation.

GEOHYDROLOGIC FRAMEWORK

The central Virgin River basin study area is located at the transition zone between the Basin and Range and the Colorado Plateau Physiographic Prov-

inces (Fenneman, 1931). This area contains a variety of geologic structures and outcropping formations, many with proven or potential ground-water reserves. Generally northward-dipping sedimentary rock formations of Permian through Tertiary age cover most of the study area and include water-bearing sandstones, siltstones, conglomerates, and limestones (table 1). In addition, the cores of the Pine Valley and Harmony mountain ranges are composed of fractured igneous rocks which can yield from small to large amounts of water.

The Navajo Sandstone and Kayenta Formation provide most of the potable water in the region. Normal faulting along the Hurricane and Gunlock Faults has resulted in offset of most of the outcropping sedimentary formations, including the Navajo Sandstone and the Kayenta Formation, likely resulting in lateral

boundaries to the flow of ground water in these formations (pl. 1). Fracturing, commonly observed in the Navajo Sandstone and the Kayenta Formation, can greatly enhance the movement of ground water. In addition, unconsolidated alluvial deposits line the valley bottoms along Ash Creek, the Virgin River, and the Santa Clara River and generally consist of coarse-to-fine-grained, unconsolidated sediments that generally have been developed as a source of irrigation water (pl. 1). Recent Quaternary volcanic eruptions have left a veneer of basalt along large parts of the Ash Creek and Santa Clara River Valleys, as well as on top of the Navajo Sandstone outcrop east of Hurricane and north of St. George (pl. 1). Some of the fractured basalt acts as shallow, highly permeable aquifers, and provides conduits for rapid recharge to underlying formations.

Table 1. Hydrostratigraphic section of selected water-bearing formations within the central Virgin River basin study area, Utah

[Adapted from Hurlow, 1998]

Age	Geologic unit	Abbreviation	Thickness (feet)	Lithologic character	Aquifer
Quaternary	Sediments and basalt	Qs	0-1,200	Boulders, gravel, sand, and silt	Quaternary basin-fill, alluvial-fan, and basalt aquifers
Quaternary—Tertiary	Basalt	QTb	0-550	Fractured, broken basalt	
	Alluvial-fan deposits	QTaf	0-350	Poorly sorted boulder conglomerate	
Tertiary	Undifferentiated igneous and sedimentary deposits	Tsi	0-9,500	Fractured monzonite, volcanic ash-flow tuff, andesite, volcanic breccia, sandstone, conglomerate, and limestone	Pine Valley monzonite aquifer
Cretaceous	Undifferentiated	Ks	3,800-4,000	Sandstone, siltstone, mudstone, and conglomerate	
Jurassic	Carmel Formation	Jc	700	Limestone, shale, and gypsum	
	Navajo Sandstone	Jn	2,000-2,800	Fractured, cross-bedded sandstone	Navajo aquifer
	Kayenta Formation	Jk	800-900	Sandstone, siltstone, and silty mudstone	Kayenta aquifer
	Moenave Formation	Jm	450	Siltstone	
Triassic	Petrified Forest Member of Chinle Formation	Trcp	400	Shale, claystone, and siltstone	
	Shinarump Member of Chinle Formation	Trcs	80-150	Medium-to-course grained sandstone and chert pebble conglomerate	
	Moenkopi	Trm	1,550-2,500	siltstone, mudstone, and shale	
Permian	Undifferentiated	Pu	3,350-3,550	Limestone, shale, sandstone, dolomite	

Upper Ash Creek Drainage Basin

Hurlow (1998) describes 13 different formations of varying lithology represented within the upper Ash Creek drainage basin. Eleven of those formations have been consolidated into three aquifers for this report (table 2). The aquifers were named for use in this report on the basis of the lithologic unit that was deemed of greatest importance to ground-water movement in that formation. The principal aquifers that are thought to form the ground-water system in the upper Ash Creek drainage basin are the Quaternary basin-fill aquifer, the Tertiary alluvial-fan aquifer, and the Tertiary Pine Valley monzonite aquifer. The Quaternary basin-fill aquifer consists of Quaternary sediments, Quaternary basalt, and Quaternary-Tertiary alluvial-fan deposits. The Tertiary alluvial-fan aquifer consists of the upper, middle, and lower members of the Pliocene-Miocene alluvial-fan deposits. The Tertiary Pine Valley monzonite aquifer consists of the Racer Canyon Tuff, the Pine Valley monzonite and latite, the Stoddard Mountain Intrusion, the Quichapa Group, the Claron Formation, and the Iron Springs Formation as shown in Hurlow (1998, p. 42).

Basin-Fill Deposits

Sedimentary deposits included in the Quaternary basin-fill aquifer originated from alluvial and fluvial erosion from surrounding mountains and plateaus. The deposits are interbedded with basalt from a local eruptive center. The deposits contain material that ranges in size from boulders to silt. Thickness of the deposits in the upper Ash Creek drainage basin is generally about 100-500 ft in the western part of the basin near New Harmony, but increases to about 1,000-1,500 ft near the Hurricane Fault.

Alluvial-Fan Deposits

As described in Hurlow (1998), erosion of the volcanic material to the west of the study area is preserved in the upper Ash Creek drainage basin as alluvial-fan and debris-flow deposits. The Tertiary alluvial-fan deposits underlie the Quaternary basin fill in the upper Ash Creek drainage basin. Only a few wells in the area are completed in the alluvial-fan deposits. Maximum thickness for the deposits could be as much as 1,500 ft along the presumed east-west axis of the

Table 2. Hydrostratigraphic section of the upper Ash Creek drainage basin area, Utah

[Adapted from Hurlow, 1998]

Age	Geologic unit	Thickness (feet)	Lithologic character	Aquifer
Quaternary	Quaternary sediments	0-1,500	Boulder gravel, sand, and silt	Basin fill
	Quaternary basalt	0-500	Fractured, broken basalt	
	Alluvial-fan deposits	0-150	Poorly sorted boulder conglomerate	
Tertiary	Alluvial-fan deposits	Upper	Unconsolidated boulder gravel	Alluvial fan
		Middle	Siltstone with conglomerate beds	
		Lower	Cemented breccia, sandstone, and siltstone	
	Racer Canyon Tuff	1,000		
	Pine Valley monzonite & latite		Fractured monzonite and latite	Pine Valley monzonite
	Stoddard Mountain Intrusion			
	Quichapa Group	1,000	Cemented to partially cemented volcanic ash	
	Claron Formation	700-1,000	Sandstone, limestone, shale, and conglomerate	
Cretaceous	Iron Springs Formation	3,800	Sandstone, shale, and conglomerate	

inferred New Harmony structural basin. Hurlow (1998) indicated that the deposits consist of three members; lower, middle, and upper. The lower and middle members are consolidated to semiconsolidated where they crop out, and are considered to be poorly permeable because of poor sorting, fine grain size, and substantial cementation. The upper member is poorly sorted, but also unconsolidated and coarse grained, and is known to yield water to a few domestic wells on the flanks of the Harmony Mountains.

Pine Valley Monzonite and Other Formations

The igneous and sedimentary formations that underlie and laterally bound the alluvial-fan and basin-fill deposits are designated the Pine Valley monzonite aquifer in this report. Igneous plutonic and volcanic rocks associated with the mid-Miocene Pine Valley Mountain igneous center (Cook, 1957) are exposed south and southeast of New Harmony, including basalt flows, rhyolitic ash-flow tuff, andesite flows, volcanic breccia, sandstone, conglomerate, siltstone, and mudstone (Hurlow, 1998). Other igneous and sedimentary rocks are exposed to the north and west of New Harmony in the Harmony Mountains. These rocks are faulted and folded in the Harmony Mountains and faulted beneath the alluvial-fan deposits under New Harmony. The subsurface geometry is not well known. Hurlow (1998), on the basis of his and previous work on the structure and stratigraphy of the area, put the thickness of the Pine Valley monzonite at about 1,000 ft. Other Tertiary intrusions and volcanics are thought to be about 1,000 ft thick. The Claron Formation is from 700 to 1,000 ft thick. Thus, the transition from the Pine Valley monzonite aquifer to deeper formations probably happens at about 1,000 to 3,000 ft below land surface. The hydrologic nature of this transition is not known.

Navajo Sandstone and Kayenta Formation

The Navajo Sandstone and underlying Kayenta Formation are of Jurassic age and are stratigraphically near the center of a suite of Permian to Quaternary sedimentary formations found within the study area (table 2). In general, the Navajo Sandstone is well sorted, consisting primarily of fine-to-medium sand-size quartz grains (Cordova, 1978, table 1). Petrographic analysis of borehole cuttings indicates that the cementation between sand grains includes varying amounts of calcite, silica, and hematite (J. Wallace, Utah Geological

Survey, written commun., 1997). Because the Navajo Sandstone was deposited under eolian conditions, bedding and cross-bedding features are prominent throughout the formation. A detailed lithologic description of the Navajo Sandstone is given by Hurlow (1998). The Navajo Sandstone, where buried by overlying formations, is about 2,400 ft thick; individual measurements include 2,800 ft west of the Gunlock Fault, about 2,300 ft at Harrisburg Junction, and about 2,000 ft at Sandstone Mountain. The lowest 100 to 150 ft of the Navajo Sandstone is defined by Hurlow (1998) as a transition zone containing siltstone and fine-grained sandstone typical of the Kayenta Formation interbedded with cross-bedded sandstone typical of the Navajo Sandstone. The Kayenta Formation consists of laminar beds of sandstone, siltstone, and silty mudstone. Where buried by overlying formations, thickness of the Kayenta Formation ranges from about 380 to 930 ft but is estimated to be about 850 ft through most of the study area (Hugh Hurlow, Utah Geological Survey, oral commun., 1998). The vertical thickness of the Navajo Sandstone and Kayenta Formation generally decreases to the south are due to erosion (fig. 4).

Tectonic forces have folded and faulted the Navajo Sandstone and Kayenta Formation. The major folds within the study area (fig. 5), from east to west, are (1) the Hurricane Bench syncline, (2) the Virgin anticline, (3) the St. George syncline, and (4) the Gunlock (or Shivwits) syncline (Cordova, 1978, p. 11; Hurlow, 1998). Because of a generally northward dip, the Navajo Sandstone and Kayenta Formation become deeply buried toward the northern boundary of the study area. The ARCO Three Peaks #1 oil exploration drill hole 10 miles northwest of Cedar City (about 50 mi northeast of St. George) reached the top of the Navajo Sandstone at a depth of 6,286 ft beneath land surface, or about 900 ft below sea level (Van Kooten, 1988). Tilting associated with the Hurricane Fault causes the Navajo Sandstone and Kayenta Formation in the northeast part of the study area to dip steeply; the top of the Navajo Sandstone is estimated to be buried as deep as 2,000 ft below sea level (Hurlow, 1998, pl. 5B). The Hurricane Fault completely offsets the Navajo Sandstone and Kayenta Formation along its entire trace. The Gunlock Fault offsets the Navajo Sandstone and the Kayenta Formation to some point north of Gunlock Reservoir (Hintze and Hammond, 1994). West of the Gunlock fault, the Navajo Sandstone and Kayenta Formation dip northeast more steeply than the gently dipping synclines east of the fault (fig. 5; Hurlow, 1998, pl. 5b). Other faults that partly offset the Navajo Sand-

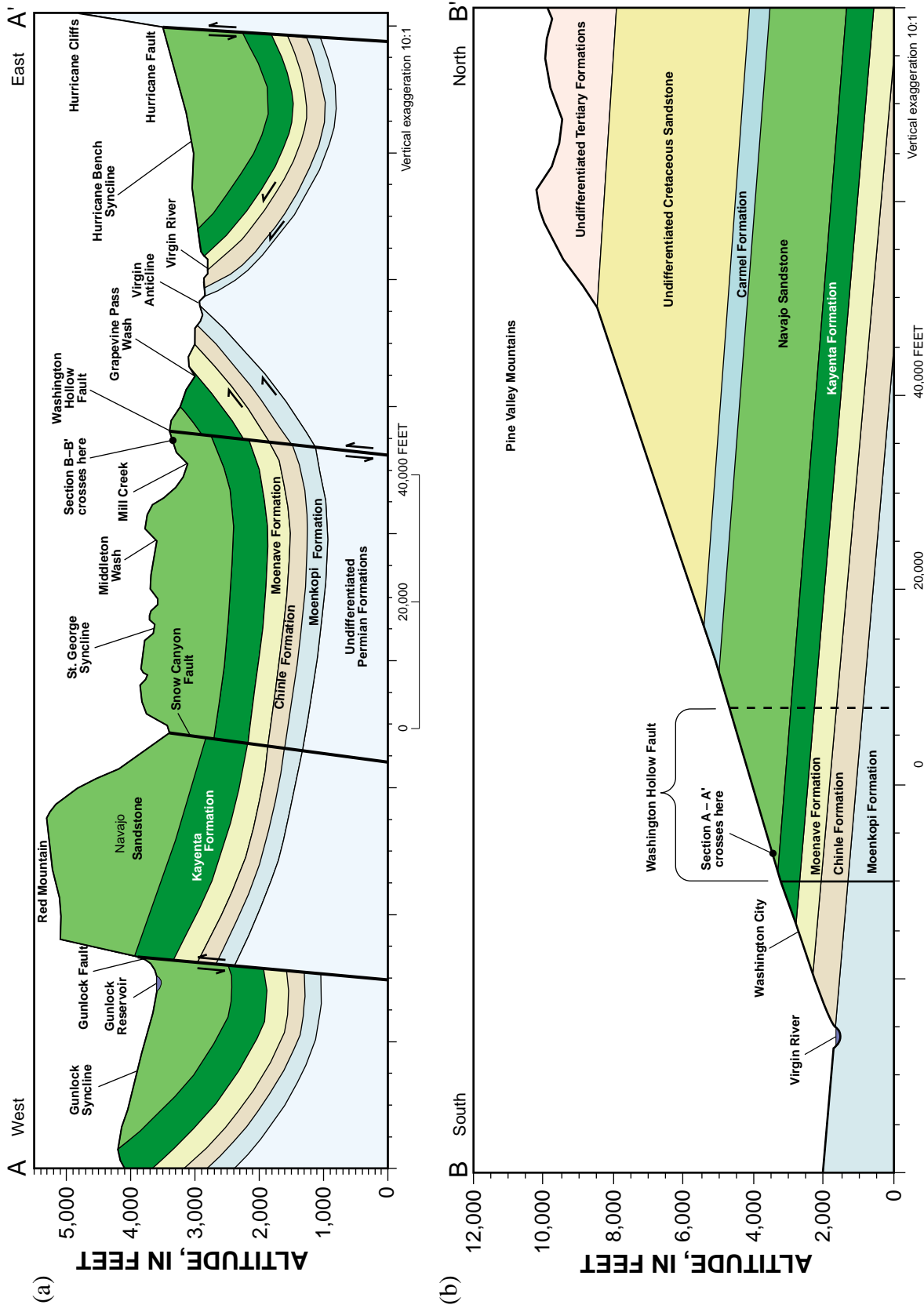


Figure 4. Generalized geologic cross sections of the Navajo Sandstone and surrounding formations within the central Virgin River basin study area, Utah. Location of cross section (a) shown by line A-A' on plate 1. Location of cross section (b) shown by line B-B' on plate 1.

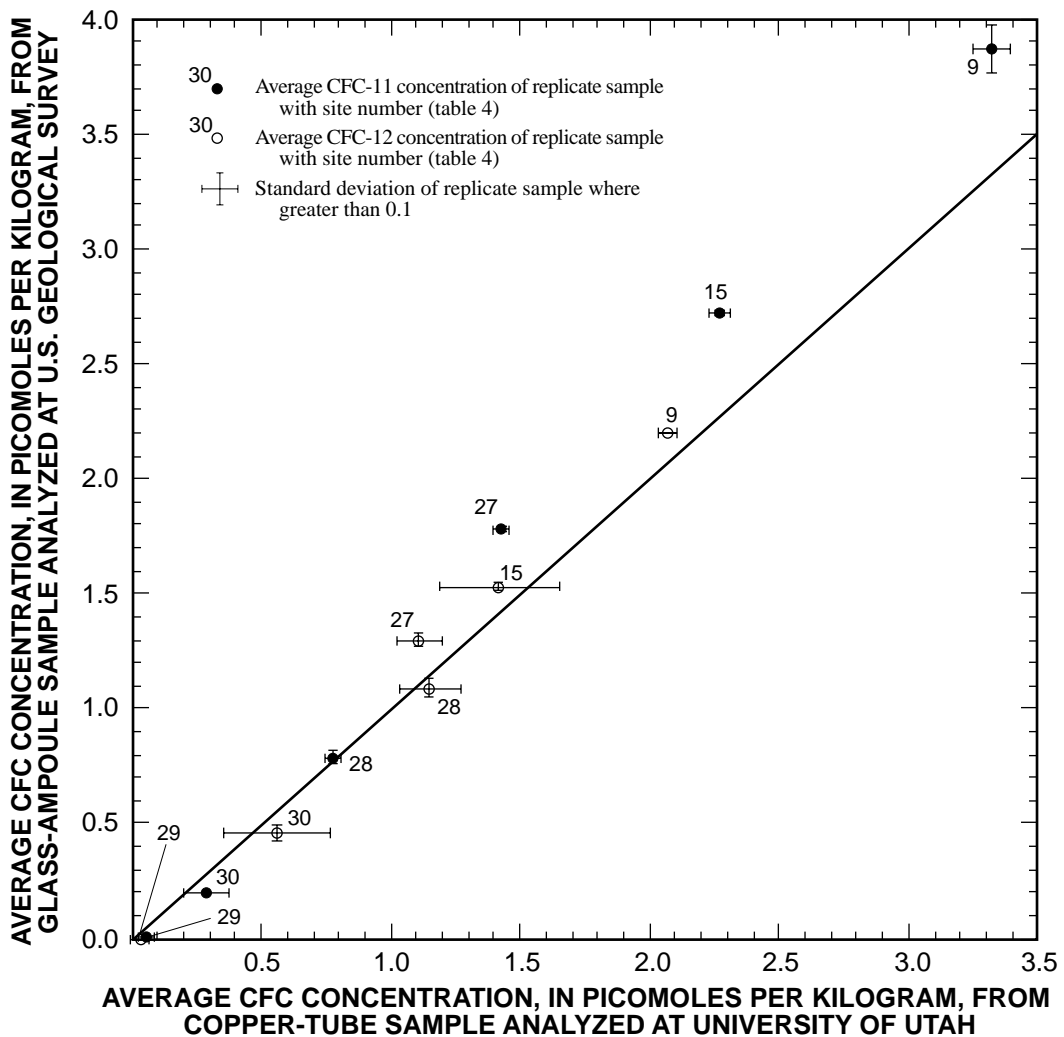


Figure 5. Average CFC-11 and CFC-12 concentration in replicate samples collected with the glass-ampoule method and analyzed at the U.S. Geological Survey versus samples collected with the copper-tube method and analyzed at the University of Utah.

stone and Kayenta Formation within the study area include the Washington Hollow Fault north of Washington and an unnamed series of faults between Anderson Junction and Toquerville (pl. 1). These faults, along with other numerous faults whose actual offset is difficult to measure, such as the Snow Canyon Fault and the Washington Hollow Fault, likely act as barriers to ground-water flow perpendicular to the fault plane, yet may act as conduits parallel to the fault plane. Low transverse permeability is expected perpendicular to the fault because of poorly-sorted breccia and finer clay-rich materials generally found along the plane of the fault, such as cataclasite, gouge, and secondary calcite cementation (Hurlow, 1998, p. 20).

Extensive joints and joint zones are found in the Navajo Sandstone and Kayenta Formation outcrops.

Unlike faults, there was no movement along the fracture plane of joints during their formation, so they do not contain low-permeability gouge or breccia zones and thus allow ground water to move perpendicular to the joint plane. Similar to fault zones, joints probably act as conduits parallel to the joint plane. Joints within the study area are essentially vertical, dipping at angles generally greater than 70 degrees. Surface fracture mapping indicates that individual joints have surface traces of as much as 600 ft in length, and interconnected joint networks may extend thousands of feet laterally (Hurlow, 1998).

Aerial photographs published by Cordova (1978) generally show a prominent north-south fracture trend in the central part of the study area. However, a more detailed fracture analysis of the Navajo Sandstone in

the study area based on both aerial photographs and outcrop data shows large variation in both the orientation of prominent fractures and the fracture density (Hurlow, 1998, pl. 6). In general, the aerial photograph data and the outcrop data indicate prominent fracturing in the north-south orientation between Anderson Junction and the Gunlock Fault (Hurlow, 1998, p. 27). However, some rose-diagram plots of data from Anderson Junction, Sandstone Mountain, Washington Hollow, and the Red Mountains show an additional east-west to northwest trending set of fractures (Hurlow, 1998, pl. 6). Rose diagrams from aerial photographs depicting joint frequency weighted by fracture length emphasize the orientation of the longer joints and joint zones. Rose diagrams from outcrop data are not weighted toward the longer joints and thus may be less meaningful with regard to the regional movement of ground water. In addition, the outcrop data contain an inherent sampling bias because more resistant, less fractured outcrop locations provide the best surfaces for conducting the surveys. This is likely a problem along the Santa Clara River west of the Gunlock Fault, where outcrop data show the main fracture orientation to be east-northeast, whereas aerial photographs (Cordova, 1978) and field observations indicate predominant north-south trending fractures. The recent study by Hurlow (1998) suggests that no correlation exists between outcrop fracture density and aerial-photograph-determined fracture density. Generalized conclusions based on aerial photograph data indicate that fracture density generally is high at Snow Canyon, Anderson Junction, Sandstone Mountain, and near the Gunlock Fault zone; contrarily, fracture density from aerial photographs is relatively low near Mill Creek and Sand Mountain (Hurlow, 1998).

About 25 percent of the outcrop surface of the Navajo Sandstone and Kayenta Formation is covered by sand dunes, alluvial deposits, and basalt flows (pl. 1). Sand dunes and alluvial deposits generally are less than 150 ft thick (Hurlow, 1998, pl. 4). However, two areas of the Navajo Sandstone outcrop are overlain by thicker wedges of alluvial deposits at Anderson Junction (more than 350 ft thick) and south of Hurricane near Gould Wash and Frog Hollow Wash (pl. 1). The thickness of basalt covering the Navajo Sandstone outcrop generally is less than 100 ft (Hugh Hurlow, Utah Geological Survey, oral commun., 1998).

HYDROCHEMICAL CHARACTERISTICS

Knowledge of the role of ground water in the hydrochemical framework of a ground-water system is as important as knowledge of how aquifers fit into the geologic framework of an area. To investigate ground-water direction and rate of movement within the Navajo and Kayenta aquifers and the Ash Creek drainage basin, chemical and isotopic data from water samples were collected or compiled from previous investigations (Wilkowske and others, 1998, tables 4 and 5). CFC, dissolved gas, general chemistry, and stable isotope data were used to evaluate potential sources of recharge to the aquifers and average residence times within the aquifers, both of which aid in determining possible ground-water flow directions.

Methods and Limitations

Chlorofluorocarbon Collection Methods

Concentrations of chlorofluorocarbons (CFCs) in the modern atmosphere are greater than in older ground water that entered the water table in the past, so care must be taken to avoid sample contamination via contact with modern air. Two methods have been developed to collect water samples for CFC analysis that prevent atmospheric contamination—the copper-tube method and the glass-ampoule method.

The copper-tube collection method requires that CFC samples be collected in sealed 3/8-in.-diameter copper tubes approximately 30 in. long (about a 30-mL sample). Prior to sampling, the tubes were annealed in an argon atmosphere at 600 °C, which cleaned the tubes and made them easier to seal. Rubber and plastic gaskets can absorb CFCs and be a source of contamination; therefore, the tubes were connected directly to well heads using all metal connections. For the collection of spring and surface-water samples, the copper tubes were placed directly in a flowing spring or stream. A 2-ft piece of Tygon tubing with a plastic pinch valve was connected to the downstream end of the tube to prevent any back diffusion of atmospheric CFCs into the sampler. The tubes were then flushed with at least 10 sample volumes of ambient water. While water was flowing through the sampler, the copper tube was crimped off using a hand-held crimping tool. This seal holds best under a vacuum, so prior to sampling, a 1-to 2-in. section of the copper tube was flattened using pliers to reduce the volume of the sampler. After crimping the

ends of the tube, the flattened part was re-rounded, creating a negative pressure inside the tube. If a good seal is made, a water hammer will make a clicking noise when the tube is moved in a rapid up and down motion. Copper-tube samples were analyzed for CFCs at the University of Utah with a gas chromatograph within 1 month after collection to ensure sample integrity. Sample blanks were run with each batch of copper-tube samples to ensure that no CFC contamination was introduced by the copper tubing or the hand-crimping tool.

The glass-ampoule method for collecting CFC samples is described by Busenberg and Plummer (1992). Replicate samples were collected in sealed borosilicate glass ampoules for comparison with samples collected in copper tubes. These samples were analyzed by both the University of Utah Department of Geology and Geophysics and the U.S. Geological Survey (USGS), Eastern Region Office of Hydrologic Research in Reston, Virginia. Because the University of Utah lab primarily analyzes water collected in copper tubes and the USGS primarily analyzes water collected in glass ampoules, a comparison was made between CFC-11 and CFC-12 concentrations from water collected in copper tubes and analyzed at the University of Utah versus water collected in glass ampoules and analyzed at the USGS (fig. 4) (table 3). Mean apparent recharge ages of water calculated from CFC-12 samples collected in copper tubes and analyzed at the University of Utah were within about 2 years of ages calculated from samples collected in glass ampoules and analyzed at the USGS. Comparison of CFC-11-determined ages did not correlate as closely. Mean apparent ages calculated from CFC-11 samples collected in copper tubes and analyzed at the University of Utah were about 4 years different than ages calculated from samples collected in glass ampoules and analyzed at the USGS. On the basis of this comparison and other published information, only CFC-12 concentration was used for determination of apparent ages reported in this study.

Limitations of Chlorofluorocarbon Age Dating

The calculated equivalent-air concentration of CFCs assumes that concentrations in the unsaturated zone are the same as those in the atmosphere. Generally, this is the case in aquifers with shallow unsaturated zones (Cook and Solomon, 1995). However, depth to the water table in the central Virgin River basin varies from just below land surface to more than 800 ft

Table 3. Chlorofluorocarbon concentration measured from samples from the central Virgin River basin collected by copper-tube versus glass-ampoule method

Location	Sample type	Sample number ¹	Sample date	CFC-11		CFC-12	
				U of U glass-ampoule method average concentration and standard deviation (pmole/kg)	U of U copper-tube method average concentration and standard deviation (pmole/kg)	USGS glass-ampoule method average concentration and standard deviation (pmole/kg)	U of U copper-tube method average concentration and standard deviation (pmole/kg)
(C-41-17)8abc	Stream	9	6-04-97	2.85 ± 0.31	3.32 ± 0.07	3.87 ± 0.10	2.21 ± 0.22
(C-38-13)35aba	Well	15	6-05-97	2.03 ± .01	2.27 ± .04	2.72 ± .01	1.37 ± .04
(C-41-17)8bad-1	Well	27	6-05-97	1.34 ± .04	1.43 ± .03	1.78 ± .01	1.23 ± .08
(C-41-17)8cda-2	Well	28	6-05-97	.65 ± .06	.78 ± .03	.79 ± .03	1.11 ± .08
(C-41-17)8dba-1	Well	29	6-06-97	.01 ± .0003	.06 ± .03	.01 ± .0004	.00 ± 0
(C-41-17)17bdb-1	Well	30	6-06-97	.19 ± .02	.29±.09	.20±.01	.47 ± .08

¹Sample numbers correspond to CFC data in table 4.

(Wilkowske and others, 1998, table 1). Where depth to the water table is more than a few tens of feet, the movement of water through the unsaturated zone could effectively lower or raise its CFC concentration as a result of interaction with unsaturated zone pore air not in equilibrium with the atmosphere. Cook and Solomon (1995) indicated that unsaturated-zone pore air is typically lower in CFCs than recharging pore water. However, in some geologic environments such as fractured basalt, pore air may move more quickly to depth and be a source of higher CFC concentration for water moving through the unsaturated zone (D.K. Solomon, University of Utah, oral commun., 1998). Other factors, such as anaerobic microbial degradation, contamination by the atmosphere during sampling, contamination from sampling equipment such as submersible pumps containing plastic or rubber, CFC enrichment from dry organic matter in the vadose zone, or incorporation of excess air in the recharge water also can affect the measured CFC concentrations in ground water and result in an inaccurate age determination (Plummer and others, 1993; Russell and Thompson, 1983). Additionally, ground water often is stratified with depth, so that younger ground water is found at shallower depths. In this study, most of the wells are constructed with open intervals over hundreds of vertical feet. Because horizontally stratified flow paths converge at the well bore, the apparent CFC age may be an average of ground waters with varying ages. Similarly, springs may be points of convergence for ground-water flow paths with different aquifer residence times (D.K. Solomon, University of Utah, oral commun., 1998). Because ages determined for a particular site may not represent the actual recharge age of the water sampled, ages in this report are shown as apparent rather than actual. Although aquifer residence times based on these CFC data should be considered approximate, the presence of CFCs in wells and springs indicates that some fraction of recently recharged water is traveling to these discharge points, showing the importance of protecting recharge zones.

Age-Dating of Ground Water with Chlorofluorocarbons

CFC samples were collected at 36 ground- and surface-water sites to investigate sources of recharge and ground-water residence times (fig. 6; table 4). CFCs are anthropogenic compounds that were first released into the atmosphere in the 1930s (Lovelock, 1971). They have since been used as refrigerants, blow-

ing agents for expanded foams, and propellants in spray cans. Because CFCs are man-made substances, their concentration in the atmosphere is a function of their rate of production (Rowland and Molina, 1975). The steady growth of CFC-12 (CCl_2F_2) in the atmosphere during the last 50 years (Busenberg and Plummer, 1992; Elkins and others, 1993) is shown in figure 7. CFCs are water soluble and can therefore enter ground water by dissolving in rainwater that enters the water table as recharge. Because the total concentration of CFCs released to the atmosphere is a function of time, the amount of CFCs dissolved in ground water at equilibrium conditions is a function of age and solubility. Therefore, by measuring the CFC concentration in water, an equivalent air concentration of CFCs can be calculated by assuming a temperature and elevation of water recharging the aquifer. This concentration is then compared to the atmospheric CFC concentration (fig. 7) to estimate the recharge age of the ground water.

Because CFC solubility in water is temperature dependent, the age of ground water determined from CFC concentration depends on the water temperature as it enters the water table, known as the recharge temperature. In areas where the water table is more than 10 ft below land surface, including most of the CFC-sampling sites in the study area, the recharge temperature generally corresponds to the mean annual temperature of the recharge location (Plummer and others, 1993, p. 271). The recharge temperature, however, can be lower than the mean annual temperature in late winter and early spring when most recharge is likely to occur.

To determine recharge temperature, six samples (fig. 6; table 4) were collected for analysis of a suite of dissolved gases including nitrogen and argon (Wilkowske and others, 1998, table 5). Dissolved concentrations of these gases is a function of the air temperature at the point where the ground water enters the water table. Therefore, by measuring the dissolved concentration of these gases in ground water and knowing their solubilities, the recharge temperature can be calculated. Calculated recharge temperatures for the six dissolved-gas samples range from 6.1 to 12.6°C (table 4). Dissolved-gas samples from LDS Church Well B ((C-38-13)35aba-1) had the lowest calculated recharge temperature of 6.1°C, probably because it receives most of its recharge from higher (thus colder) altitudes in the Pine Valley Mountains. Dissolved-gas samples from Newell Matheson's well ((C-40-13)22dcd-1) had the highest calculated recharge temperature of 12.6°C, consistent with the oxygen and hydrogen isotope data

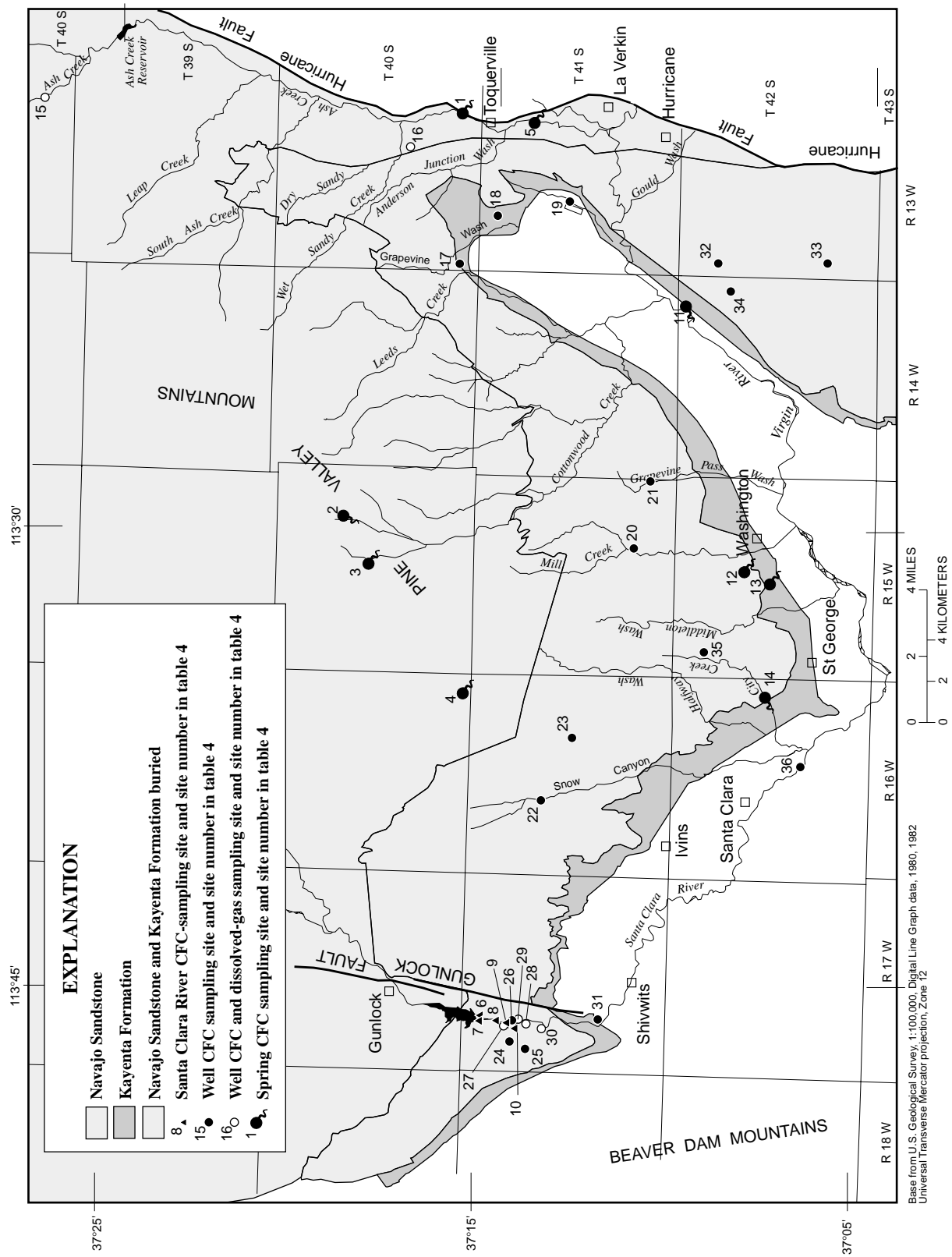


Figure 6. Location of CFC- and dissolved-gas sampling sites, central Virgin River basin study area, Utah.
(Data are contained in table 4.)

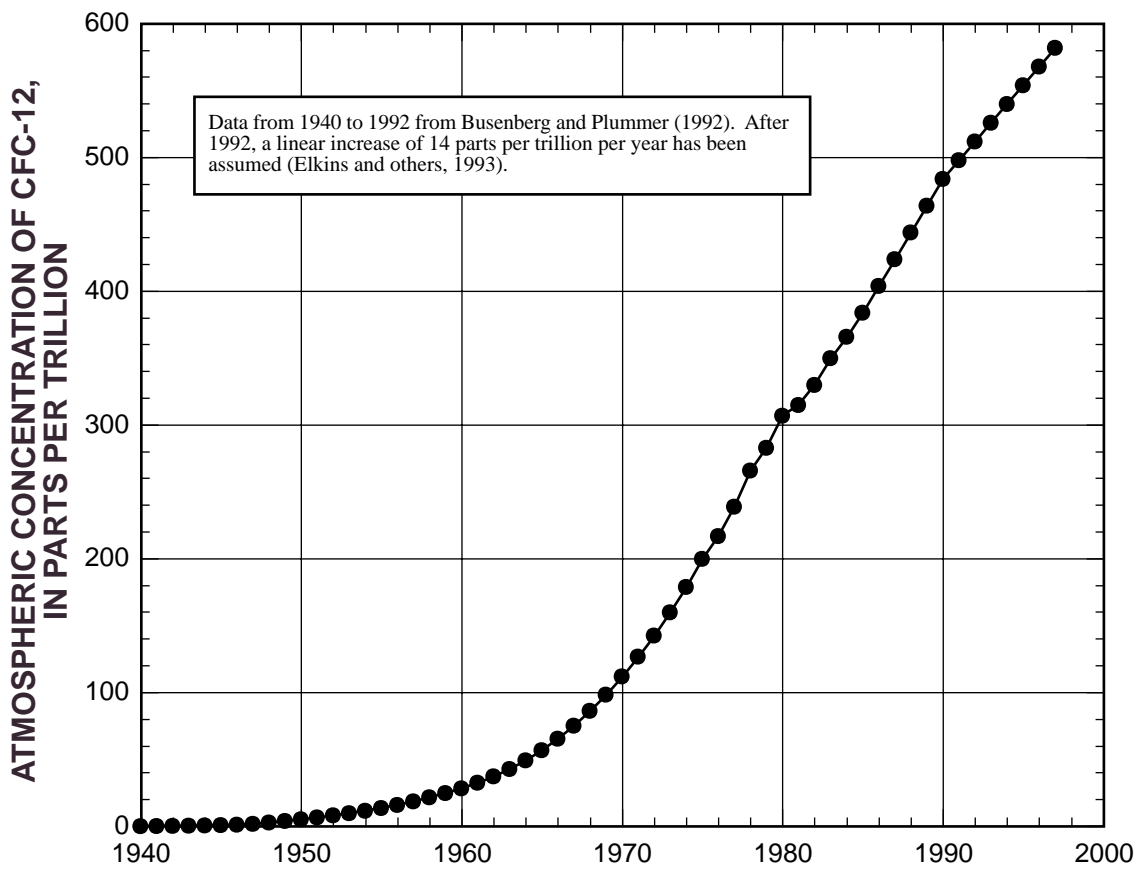


Figure 7. Global atmospheric concentration of CFC-12 as a function of time.

that indicated lower-altitude recharge. The recharge temperatures for the other ground-water sites were estimated on the basis of their proximity to the six dissolved-gas sample sites and to St. George, where the average annual air temperature is 16 °C.

Use of Age-Dating to Investigate Sources of Recharge to the Main Part of the Navajo and Kayenta Aquifers

Ten wells and 4 springs in the main part (between the Gunlock and Hurricane Faults) of the Navajo and Kayenta aquifers were sampled for CFCs (fig. 8, wells and springs with formation type "Jn" or "Jk" in table 4). Apparent ground-water recharge years range from pre-1950 to the late 1970s (fig. 8).

Water discharging from wells and springs with a ground-water recharge year in or prior to the 1950s had a very low or no CFC concentration, generally indicating long, deep flow paths with little local recharge or a very thick unsaturated zone. The oldest water sample

collected from the main part of the Navajo and Kayenta aquifers was from Winchester Hills Well 1 ((C-41-16)23bba-2), where the water table is more than 700 ft deep (Wilkowske and others, 1998, table 1). The low CFC concentrations from this well are within the error of analysis, indicating an apparent ground-water recharge age during or prior to the 1950s. The St. George City Mill Creek Well 2 ((C-41-15)27dda-1), the St. George City Creek Well 2 ((C-42-15)6dcd-1), West City Spring ((C-42-16)13dcb-S1), and the Washington City Grapevine Pass Well ((C-41-15)36aad-1), all had apparent recharge ages in the mid-to-late 1950s. Their CFC concentrations are just above the error of analysis and may indicate mixing of older, deeper ground water with a small amount of younger, shallower water. These wells and springs are mostly in the central part of the Navajo and Kayenta aquifers north of St. George and Washington, and may receive recharge from higher-altitude parts of the outcrop near the base of the Pine Valley mountains (table 4, fig. 6).

Table 4. Average chlorofluorocarbon-12 concentration and estimated recharge year for selected springs, surface-water sites,

[NA, not applicable; vmoles/kg, picomoles per kilogram]

Site no.: See figure 8 for map location

Location: See “numbering system” at beginning of report for an explanation of the numbering system used for hydrologic data sites in Utah.

Owner (Well name): WCWCD, Washington County Water Conservancy District; Well name given in parentheses.

Formation: Qtb, Quaternary and Tertiary basalt; Tvip, Pine Valley quartz monzonite; Ks, undifferentiated Cretaceous sedimentary
the Moenave Formation; Trcs, Shinarump Member of the Chinle Formation.

Casing Finish: P, perforated; X, open hole; S, screened; —, no information.

Recharge temperature: Estimated temperature of water as it entered the aquifer as recharge; e, estimated recharge temperature; m, measured

Average CFC concentration, water: Average concentration of CFC-12 in water in replicate samples measured at the University of

Standard deviation: Standard deviation of replicate samples.

CFC concentration, air equivalent: ppt, parts per trillion; Calculated atmospheric concentration of CFC-12 in equilibrium with sample

Apparent recharge year: Apparent year that water entered the ground-water flow system as recharge based on CFC-12

Site no.	Location	Owner (Well name)	Formation	Altitude of land surface (feet)	Approximate depth to water below land surface (feet)	Casing finish below land surface (feet)
Springs and surface-water sites						
1	(C-40-13)35acd-S1	Toquerville Spring	QTb	3,440	NA	NA
2	(C-40-15)14bab-S1	Cottonwood (Main) Spring	Tvip	7,800	NA	NA
3	(C-40-15)15cbd-S1	West Fork Spring	Tvip	6,900	NA	NA
4	(C-40-16)36cda-S1	Diamond Valley Spring	Ks	4,780	NA	NA
5	(C-41-13)11cad-S1	Ash Creek Spring	QTb	3,200	NA	NA
6	(C-41-17) 5acd	Santa Clara River at hydro plant	NA	3,540	NA	NA
7	(C-41-17) 5acd-S1	Seep below Gunlock dam	NA	3,540	NA	NA
8	(C-41-17) 5dcc	Santa Clara River (1,500 feet from dam)	NA	3,520	NA	NA
9	(C-41-17) 8abc	Santa Clara River (2,250 feet from dam)	NA	3,510	NA	NA
10	(C-41-17) 8bdc	Santa Clara River (3,000 feet from dam)	NA	3,500	NA	NA
11	(C-42-14) 1bcb-S1	Berry Springs	QTb/Jn	2,860	NA	NA
12	(C-42-15)15bbd-S1	Green Spring	Jn	2,880	NA	NA
13	(C-42-15)16ddd-S1	Huntington Spring	Jk	2,880	NA	NA
14	(C-42-16)13dcb-S1	West City Spring	Jn	2,960	NA	NA
Wells						
15	(C-38-13)35aba- 1	LDS Church (Well B)	Tvip	5,010	59	P 220-620
16	(C-40-13)22dcd- 1	Newell Matheson	Qs	3,830	220	P 320-340
17	(C-40-13)31bcc- 1	Leeds Domestic (Well #1)	Jk	3,980	204	X 69-400
18	(C-41-13) 5dba- 2	Alan Howard	Jn/Jk	3,600	21	X 83-97
19	(C-41-13)16bcd- 1	Sullivan Flowing Well	Jmss	3,240	—	—
20	(C-41-15)27dda- 1	St. George (Mill Creek Well #2)	Jn	3,325	249	P, S 330-768
21	(C-41-15)36aad- 1	Washington (Grapevine Pass Well)	Jn	3,490	347	S 496-900
22	(C-41-16)16bbd- 1	St. George (Snow Canyon Well #2)	Jn	3,460	301	S 350-830
23	(C-41-16)23bba- 2	Winchester Hills (Well #1)	Jn	3,840	722	P 740-940
24	(C-41-17) 7ada-2	St. George (Gunlock Well #6)	Jn	3,598	246	S 123-573
25	(C-41-17) 7ddb-1	St. George (Gunlock Well #2)	Jn	3,570	227	P 176-466
26	(C-41-17) 8acc-1	St. George (Gunlock Well #7)	Jn	3,485	74	S 200-800
27	(C-41-17) 8bad-1	St. George (Gunlock Well #5)	Jn	3,443	24	P 100-384

and wells within the central Virgin River basin study area, Utah

rocks; Jn, Navajo Sandstone; Jk, Kayenta Formation; Qs, Quaternary sediments; Jmss, Springdale Sandstone Member of

temperature of the water sample; c, recharge temperature calculated from dissolved gas concentrations; °C, degrees Celsius. Utah; pmoles/kg, picomoles per kilogram.

water at recharge temperature.

concentration.

Site no.	Location	Re-charge temperature (°C)	Sam-ping date	Number of rep-licates	Average CFC concen-tration, water (pmoles/kg)	Stand ard devia-tion (pmoles/kg)	CFC concen-tration, air equivalent (ppt)	Stand ard devia-tion (ppt)	Esti-mated re-charge year	Stand ard devia-tion (years)
Springs and surface-water sites										
1	(C-40-13)35acd-S1	12.0 e	10-27-96	3	1.39	0.18	331	43.4	1982	3
		12.0 e	06-04-97	4	1.43	.15	339	36.0	1982	2
2	(C-40-15)14bab-S1	6.0 e	10-23-96	3	2.42	.22	426	39.4	1987	2
3	(C-40-15)15cbd-S1	6.0 e	10-23-96	3	1.70	.18	299	32.2	1980	2
4	(C-40-16)36cda-S1	8.0 e	10-26-96	2	.00	NA	0	NA	pre-1950	NA
5	(C-41-13)11cad-S1	12.0 e	10-25-96	3	1.84	.45	436	107	1987	5
6	(C-41-17) 5acd	19.0 m	10-07-97	3	1.57	.08	354	26.3	1983	2
7	(C-41-17) 5acd-S1	12.5 m	06-04-97	4	.310	.02	74.6	5.29	1967	1
8	(C-41-17) 5dcc	19.0 m	10-07-97	3	1.41	.26	393	22.7	1985	1
9	(C-41-17) 8abc	12.5 m	06-04-97	4	2.07	.04	497	8.75	1991	1
		19.0 m	10-07-97	3	1.25	.04	389	11.2	1985	1
10	(C-41-17) 8bdc	19.0 m	10-07-97	3	1.19	.06	368	17.8	1984	1
11	(C-42-14) 1bcb-S1	12.0 e	10-26-96	3	1.42	.32	338	76.6	1982	4
12	(C-42-15)15bbd-S1	12.0 e	10-22-96	3	.34	.16	79.9	37.2	1966	4
13	(C-42-15)16ddd-S1	12.0 e	10-25-96	2	.93	.13	222	31.7	1976	2
14	(C-42-16)13dcb-S1	12.0 e	10-25-96	3	.04	.04	10.3	8.94	1953	5
Wells										
15	(C-38-13)35aba- 1	6.1 c	10-28-96	4	1.82	.22	321	39.2	1981	3
		6.1 e	06-05-97	4	1.42	.23	250	41.2	1977	2
16	(C-40-13)22ddc- 1	12.6 c	10-30-96	3	1.12	.22	273	54.1	1979	3
17	(C-40-13)31bcc- 1	12.0 e	10-26-96	2	.23	.22	52.8	51.6	1962	8
18	(C-41-13) 5dba- 2	12.0 e	10-30-96	3	.67	.24	158	57.8	1972	3
19	(C-41-13)16bcd- 1	12.0 e	10-26-96	3	.72	.22	170.7	52.2	1973	3
20	(C-41-15)27dda- 1	12.0 e	10-23-96	3	.07	.08	15.9	18.2	1953	7
21	(C-41-15)36aad- 1	12.0 e	10-26-96	1	.09	NA	21.1	NA	1957	NA
22	(C-41-16)16bbd- 1	11.0 e	10-24-96	2	.52	.11	119	24.7	1970	1
23	(C-41-16)23bba- 2	10.0 e	10-24-96	3	0	NA	0	NA	pre-1950	NA
24	(C-41-17) 7ada-2	10.0 e	02-24-97	3	.04	.00	8.99	0.520	1952	0
25	(C-41-17) 7ddb-1	10.0 e	02-24-97	3	.42	.21	87.7	43.6	1967	5
26	(C-41-17) 8acc-1	10.0 e	02-24-97	3	.11	.07	24.2	14.9	1957	4
27	(C-41-17) 8bad-1	10.8 c	02-28-97	3	1.14	.29	246	62.3	1977	3
		10.8 e	06-05-97	4	1.11	.09	239	20.2	1977	1

Table 4. Average chlorofluorocarbon-12 concentration and estimated recharge year for selected springs, surface-water sites,

Site no.	Location	Owner (Well name)	Formation	Altitude of land surface (feet)	Approximate depth to water below land surface (feet)	Casing finish below land surface (feet)
Wells—Continued						
28	(C-41-17) 8cda-2	St. George (Gunlock New Well #4)	Jn	3,445	94	S 123-573
29	(C-41-17) 8dba-1	St. George (Gunlock Well #8)	Jn	3,454	47	S 200-800
30	(C-41-17)17bdb-1	St. George (Gunlock Original Well #3)	Jn	3,444	115	X 9-626
31	(C-41-17)29aba-1	BIA (Shivwits Flowing Well)	Trcs	3,240	—	P 100-700
32	(C-42-13) 7bba-3	Winding Rivers	Jn	2,960	51	X 50-705
33	(C-42-13)30bdc-1	WCWCD (Sky Ranch Well)	Jn	3,040	131	X 52-590
34	(C-42-14)12ddb-3	Winding Rivers	Jn	2,920	60	S 140-503
35	(C-42-15) 6dcld-1	St. George (City Creek Well #2)	Jn	3,308	279	P 260-660
36	(C-42-16)22cdd-1	St. George (Sunbrook Golf Course Well)	Trcs	2,660	130	P 260-580

Wells and springs with apparent recharge ages in the 1960s and 1970s probably receive a greater component of younger recharge than those in the central part of the aquifers. These apparent recharge ages indicate younger, more localized recharge which may be entering the water table more rapidly through fracture zones or along ephemeral stream channels. Two Winding Rivers wells ((C-42-13)7bba-3 and (C-42-14)12ddb-3), Leeds Domestic Well (C-40-13)31bcc-1, along with Green Spring ((C-42-15)15bba-S1), have apparent ages in the 1960s. Alan Howard's Well ((C-41-13)5dba-2), St. George City Snow Canyon Well 2 ((C-41-16)16bbd-1), the Sky Ranch Well ((C-42-13)30bdc-1), and Huntington Spring ((C-42-15)16ddd-S1), all have apparent ages in the early-to-mid-1970s (table 4).

The highest measured CFC concentrations from the Navajo and Kayenta aquifers are from Berry Springs ((C-42-14)1bcb-S1), indicating an apparent recharge age of early 1980s. Berry Springs emerge at the contact of basalt with the underlying Kayenta Formation. Ground water moving through basalt aquifers within the study area typically has relatively high (36–44 mg/L) silica concentrations. Berry Springs, however, had a silica concentration of 26 mg/L on February 24, 1986 (Wilkowske and others, 1998, table 4), similar to the lower silica concentrations found in the Navajo and Kayenta aquifers. Thus the young apparent recharge age, in combination with the lower silica concentration, may indicate a mixing of waters from both the basalt and Kayenta aquifers.

In summary, age-dating with CFCs indicate that residence times for the main part of the Navajo and Kayenta aquifers range from more than 50 years to less than 20 years. These ages are likely dependent on both the lateral length of the flow path from point of recharge to point of discharge, as well as vertical stratification of the aquifer such that shallower ground water has been recharged more recently from local infiltration than deeper ground water. However, the relatively small number of sampling sites (14), the vertical averaging because of large perforated borehole intervals, and the inability of CFC techniques to age date water older than the 1950s all indicate the need for a more comprehensive age-dating study, in combination with particle-tracking computer analysis, before this information can be readily incorporated into the hydrologic conceptualization of ground-water flow within the main part of the Navajo and Kayenta aquifers.

Comparison of Apparent Ages Calculated from Chlorofluorocarbon Concentration to Radio-Isotope Age-Dating Methods

Tritium (^3H) is a radioactive or unstable isotope of hydrogen that decays with a half-life of about 12.3 years. Tritium occurs naturally in the atmosphere, but the largest source has been atmospheric nuclear testing between 1952 and 1969. The natural level for tritium prior to atmospheric nuclear testing ranged from 2 to 8 tritium units (TU). Large scale testing during 1962–63 raised tritium levels to more than three orders of magnitude larger than natural concentrations (Plummer and

and wells within the central Virgin River basin study area, Utah—Continued

Site no.	Location	Re-charge temperature (°C)	Sampling date	Number of replicates	Average CFC concentration, water (pmoles/kg)	Standard deviation (pmoles/kg)	CFC concentration, air equivalent (ppt)	Standard deviation (ppt)	Estimated recharge year	Standard deviation (years)
Wells—Continued										
28	(C-41-17) 8cda-2	10.4 c	02-24-97	3	.42	.08	89.5	16.1	1968	1
		10.4 e	06-05-97	4	1.15	.12	242	25.0	1976	1
29	(C-41-17) 8dba-1	9.9 c	10-24-96	3	0	NA	0	NA	pre-1950	NA
		9.9 e	06-06-97	4	.2	.03	5.08	7.05	pre-1950	NA
30	(C-41-17)17bdb-1	9.7 c	02-28-97	2	.35	.31	73.0	64.2	1965	8
		10.2 e	06-06-97	4	.56	.21	118	44	1970	3
31	(C-41-17)29aba-1	10.0 e	10-23-96	3	0	NA	0	NA	pre-1950	NA
32	(C-42-13) 7bba-3	12.0 e	10-24-96	3	.17	.03	39.2	6.30	1962	1
33	(C-42-13)30bdc-1	12.0 e	10-30-96	2	.56	.01	133.2	3.47	1971	0
34	(C-42-14)12ddb-3	12.0 e	10-25-96	3	.37	.12	87.0	27.4	1967	3
35	(C-42-15) 6dcd-1	12.0 e	10-25-96	3	.10	.06	22.8	14.4	1957	4
36	(C-42-16)22cdd-1	12.0 e	10-24-96	4	.03	.03	6.06	7.07	1950	5

others, 1993, p. 258). In 1998, while still above pre-nuclear testing values, atmospheric tritium concentrations have decreased back down to a range of about 10 to 30 TU as a result of radioactive decay and the cessation of most atmospheric testing (D.K. Solomon, Univ. of Utah, oral commun., 1999).

Two wells were sampled for tritium analysis (Wilkowske and others, 1998, table 5) to compare estimated recharge ages with those determined by CFC sampling. Tritium concentrations were less than the detection limit at both the St. George City Gunlock Well #8 ((C-41-17)8dba-1) and the Sky Ranch well ((C-42-13)30bdc-1) (Wilkowske and others, 1998, table 5), indicating that water recharging these wells entered the aquifers prior to 1953. This is consistent with the pre-1950s apparent recharge age estimates at the St. George Gunlock Well #8 (water table at 47 ft), which are based on CFC sampling (table 4). Apparent recharge age is the estimated year when water enters the water table. However, apparent recharge age estimated on the basis of CFC sampling at Sky Ranch well #1 (water table at 131 ft), indicated that water recharging this well entered the aquifer in the early 1970s. One possibility for this discrepancy is that CFC enrichment may occur by exchange with unsaturated-zone pore air above the water table. Vertical sampling done at other study sites with thick unsaturated zones has determined the tritium peak to be in the unsaturated zone; samples at the water table have had detectable CFC concentrations.

Differences in apparent recharge ages between the tritium and CFC samples may be explained by differences in the way the two are transported through the unsaturated zone. Transport of tritium is primarily by water, whereas CFCs diffuse between air and water and can be transported to the water table by both phases (D.K. Solomon, oral commun., 1998). Thus, as discussed in the “Methods and Limitations” section, the presence of CFCs in ground water beneath thick unsaturated zones may falsely give a more recent apparent recharge age where pore-gas transport of CFCs reaches the water table sooner than pore water transport of CFCs. However, other wells with similar depths to water (St. George City Sunbrook Golf Course well), or shallower depths to water (St. George City Gunlock well 8) had no detectable CFC-12, arguing against the mechanism of pore-gas transport of CFCs (table 4).

Another possible reason for the discrepancy in apparent recharge year at the Sky Ranch well is that the CFC sampling method had a higher level of accuracy than the selected tritium analysis method, which had a detection limit of 2.5 TU. The apparent CFC recharge year of 1971 could result from the mixing of a small fraction of younger, shallow ground water with a large fraction of older, deep ground water. If one assumes a two-member mixing model with young and old waters such that 30 percent of the water is young (1984) water with a CFC-12 concentration of 1.5 pmoles/kg and 15.0 TU initial tritium concentration. The 1997 tritium concentration after one half life (10.7 yr) of decay would be

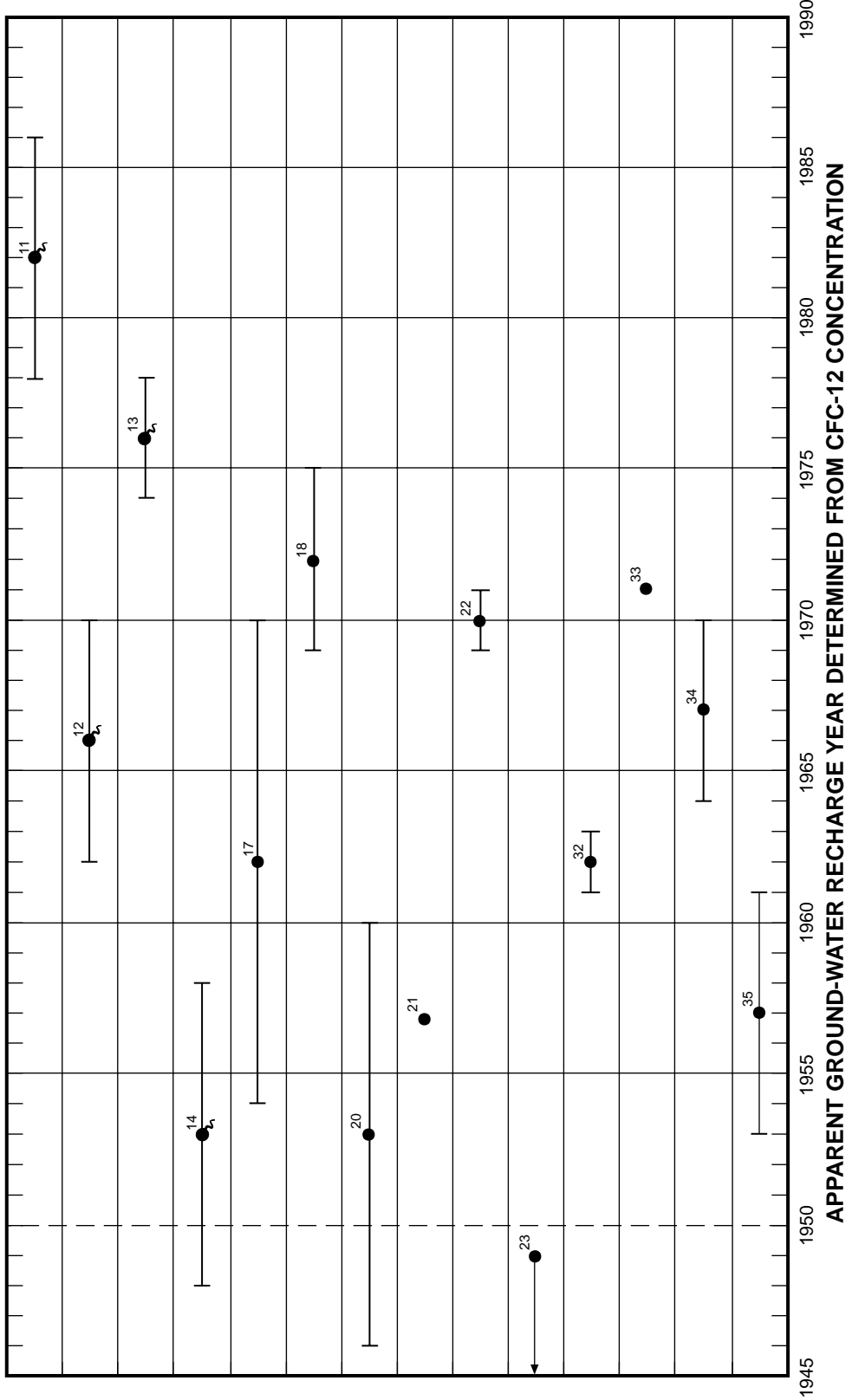


Figure 8. Apparent ground-water recharge year determined from CFC-12 concentration for selected wells and springs in the main part of the Navajo and Kayenta aquifers within the central Virgin River basin study area, Utah.

7.5 TU's. The other 70 percent is old (pre-1950) water with a CFC concentration of 0 pmole/kg and 0 TU's. The resulting CFC-12 and tritium concentrations would be about 0.5 pmoles/kg and 2.5 TU's, respectively. The 0.5 pmole/kg CFC-12 concentration (the value measured at Sky Ranch Well #1) is within detection limits, but the tritium concentration is right at the detection limit. Similar to Sky Ranch Well #1, most of the wells sampled for CFCs had large screened intervals. Thus, it is likely that many of the 1960s through 1980s apparent CFC recharge ages reflect a mixture of a large fraction of old (pre-1950s) water with a small fraction of younger water. The possibility of young, recent precipitation rapidly reaching the aquifer highlights the need for adequate protection of the aquifer's recharge zones.

Four wells and one spring also were sampled for chlorine-36 (^{36}Cl) as part of a broad regional study of its distribution in ground water across the United States (S. Davis, written commun., 1997). Low concentrations of chlorine-36 are produced naturally in the atmosphere by cosmic radiation interacting with argon, but the largest source has been testing of thermonuclear devices from 1952 to 1958. These tests produced atmospheric ^{36}Cl concentrations that remain 100 times higher than pre-bomb concentrations (Lehmann and others, 1993). Three St. George wells finished in the Navajo Sandstone (Gunlock Well #6, Gunlock Well #8, and Mill Creek Well #2) and the Bureau of Indian Affairs Shivwits flowing well finished in the Shinarump conglomerate of the Chinle Formation ((C-41-17)29aba-1) all had reported $(^{36}\text{Cl})/(^{35}\text{Cl} \times 10^{15})$ ratios of less than 400, indicating apparent recharge ages of pre-1952 (S. Davis, written commun., 1997). These ages generally are consistent with ages determined from CFC sampling (table 4). A higher $(^{36}\text{Cl})/(^{35}\text{Cl} \times 10^{15})$ ratio of about 780 from water sampled at Toquerville Springs ((C-40-13)35acd-S1), which emanates from an outcrop of Quaternary-Tertiary fractured basalt along Ash Creek, indicates more recent recharge. This is consistent with an early 1980s apparent recharge age determined from CFC-12 data (table 4). In summary, CFC age dating from four of the five ground-water sites, which were compared with other age-dating methods, yielded similar ages. Although the apparent recharge year determined by both the CFC method and the tritium method were not the same for the fifth site (Sky Ranch Well #1), this can be explained by the lack of accuracy in the chosen tritium age-dating method.

Use of Other Geochemical Data to Investigate Sources of Ground-Water Recharge

The chemistry of water changes as it moves from land surface, through the unsaturated zone, into and through an aquifer, and finally back to land surface. Water dissolves some minerals that it contacts and retains certain isotopic species during its journey. Dissolved chemicals in the ground water also may react with minerals in the aquifer material, further altering water chemistry. Knowledge of water chemistry at various points along a flow path can be a valuable aid to understanding the workings of an entire hydrologic system.

Navajo and Kayenta Aquifers

Dissolved-solids concentration of ground-water samples from wells and springs in the Navajo and Kayenta aquifers ranged from 110 to 1,310 mg/L (Wilkowske and others, 1998) at 73 sample sites. Ground water from most of the Navajo and Kayenta aquifers was low in dissolved minerals, with an average dissolved-solids concentration of about 300 mg/L in water from 54 well and spring samples. However, there were two distinct areas with dissolved-solids concentrations greater than 500 mg/L: a large area north of St. George and a smaller area a few miles west of Hurricane (fig. 9). Nineteen wells and springs from these areas had an average dissolved-solids concentration of about 1,020 mg/l.

Cordova (1978, p. 38) stated that the "Navajo Sandstone is mineralogically a relatively pure lithologic unit composed mostly of silica and other low-solubility substances. The water that flows through such a lithologic medium would expectably dissolve relatively small amounts of minerals even if the water was in contact with them for a long time." The Kayenta Formation is finer grained and contains more clays and feldspar than the Navajo Sandstone, but also generally consists of minerals that do not dissolve easily. Therefore, there is likely an external source for the higher salinity water moving into the Navajo and Kayenta aquifers at the two higher salinity zones, either from overlying or underlying formations.

Both overlying Upper Jurassic and Cretaceous and underlying Lower Jurassic, Triassic, and Permian formations contain alternating layers of conglomerate, sandstone, siltstone, shale, limestone, and evaporite beds that contain gypsum, mirabilite, and other easily

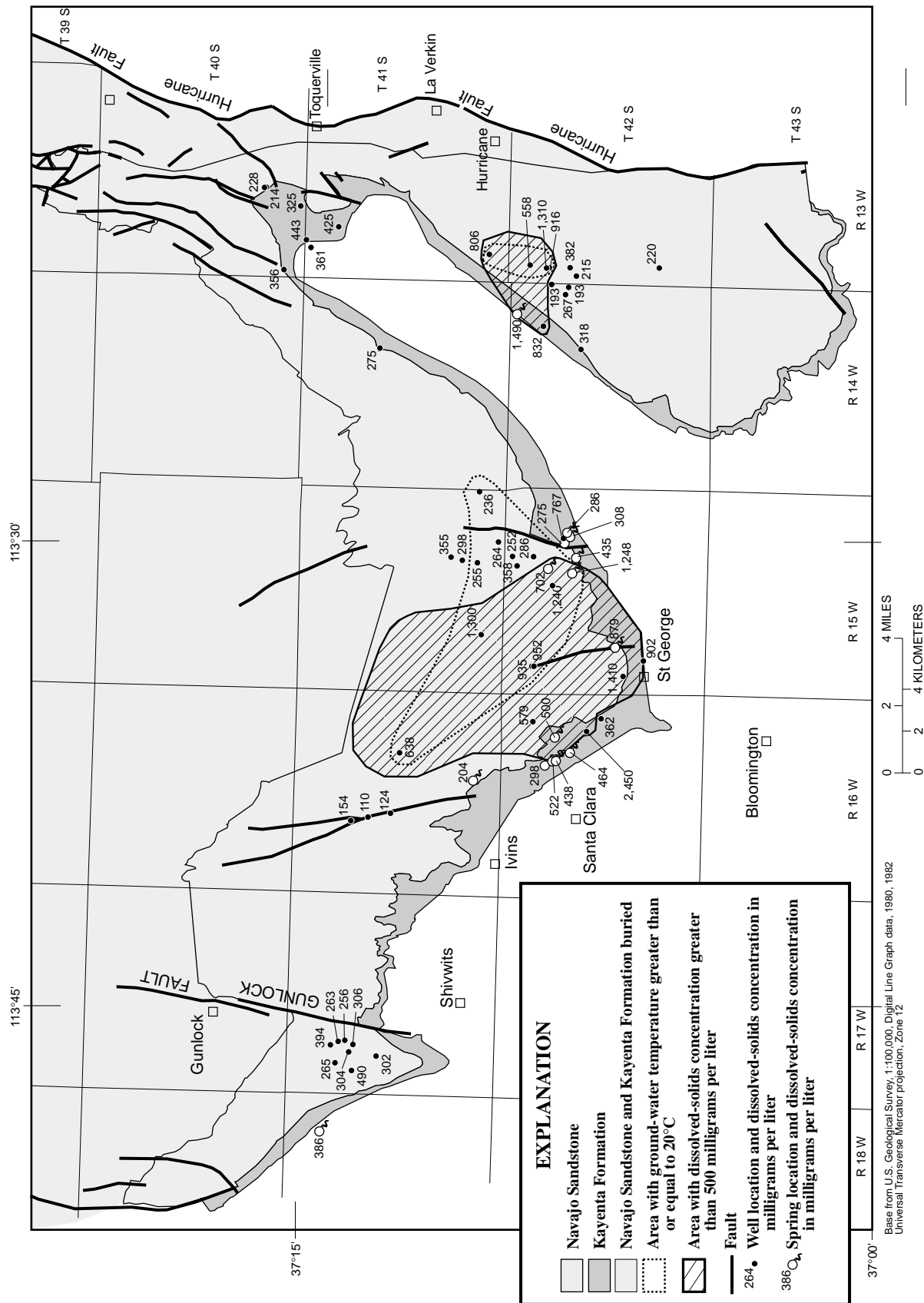


Figure 9. Areas of dissolved-solids concentration greater than 500 mg/L and temperatures greater than 20°C from wells and springs in the Navajo and Kayenta aquifers within the central Virgin River basin study area, Utah.

dissolved minerals (Cook, 1957). Therefore, no conclusive determination about the source of higher salinity water can be made on the basis of lithology of overlying versus underlying formations. Thus, further geochemical investigation was necessary to determine the probable source.

One relation that can be seen in figure 9 is that two zones of warmer water (20.0 to 35.5°C) partially overlap the higher salinity zones. This indicates that the source of higher salinity water entering the Navajo aquifer is the underlying formations, possibly from the hydrothermally induced upward vertical flow along fractures. The zone north of St. George corresponds with a low-temperature geothermal area identified by the Utah Geological Survey (UGS) as the “central St. George Basin”; the zone west of Hurricane corresponds to the “southeast St. George Basin” (Budding and Sommer, 1986, fig. 3). The larger area north of St. George is considered by the UGS to have geothermal development potential. Budding and Sumner (1986) stated that the location of several low-temperature geothermal areas in the St. George basin probably are related to three major fault zones: the Hurricane, Gunlock, and Washington Faults. The UGS report indicates that fault zones provide conduits for the upward movement of geothermal waters. The low-temperature geothermal area north of St. George is located as much as 3 mi west of the Washington Fault; the area west of Hurricane City is located up to 5 mi west of the Hurricane Fault (Budding & Sommer, 1986, p. 15-16, fig. 3). Budding and Sumner (1986) suggested that lateral movement of ground water away from the faults may be responsible for the higher temperature zones; however, an alternative is that the zones correspond to increased vertical permeability associated with fracturing adjacent to the faults.

General Chemistry

The samples with low dissolved-solids concentration (less than 500 mg/L) and high dissolved-solids concentration (greater than 500 mg/L) from the Navajo aquifer have distinctive geochemical signatures when displayed on a trilinear diagram (fig. 10). The low dissolved-solids waters generally are a calcium-carbonate type; the higher dissolved-solids ground waters generally are a calcium-sodium-sulfate type.

The relation of samples with higher dissolved-solids concentration from the Navajo and Kayenta aquifers to the chemical composition of water samples from overlying and underlying formations is shown in figure

11. The samples with higher dissolved-solids concentration are geochemically more similar to water from the underlying formations than they are to the overlying formations.

Oxygen and Hydrogen Isotopes

The stable isotopes of oxygen (^{18}O and ^{16}O) and hydrogen (^2H , or deuterium, and ^1H) in water provide a useful geochemical tool to determine sources of recharge to an aquifer. The ratios of these isotopes vary in precipitation primarily from changes in topography, air temperature, and distance from water bodies (Mazor, 1991). Because these stable isotopes generally are conservative in ground-water systems, water recharging the aquifer has an isotopic signature that indicates the relative altitude at which it fell as precipitation. The oxygen isotopic ratio ($^{18}\text{O}/^{16}\text{O}$) and the hydrogen isotopic ratio ($^2\text{H}/^1\text{H}$) in a water sample are reported in delta (d) units per mil (parts per thousand) deviation from a reference standard called Standard Mean Ocean Water (SMOW) (Craig, 1961). These delta values are determined from the following equation:

$$\delta R = \left[\frac{(R_{sample} - R_{standard})}{R_{standard}} \right] \times 1,000 \quad (1)$$

where

$\delta R = \delta^2\text{H}$ or $\delta^{18}\text{O}$ in the water sample,

R_{sample} = ratio of $^{18}\text{O}/^{16}\text{O}$ or $^2\text{H}/^1\text{H}$ in the water sample, and

$R_{standard}$ = ratio of $^{18}\text{O}/^{16}\text{O}$ or $^2\text{H}/^1\text{H}$ in the reference standard.

Waters that have not undergone evaporation generally plot along a meteoric water line (fig. 12) where the heavier isotopes of oxygen and hydrogen condense first and fall as precipitation at lower altitudes. Subsequent precipitation at higher altitudes is depleted in the heavier isotopic species. The isotopic composition of 17 ground-water samples from the main part of the Navajo and Kayenta aquifers (between the Gunlock and Hurricane Faults) was compared with the North American (Craig, 1961) and arid-zone (Welch and Preissler, 1986) meteoric water lines (fig. 12). All of the Navajo and Kayenta aquifer water samples plot between the two meteoric water lines, indicating that little or no evaporation occurs before infiltration and recharge. Although no precipitation samples were collected during this study, two composite snow samples from the Abajo Mountains about 200 mi to the east of the study area in Utah and an average of eight snow samples from

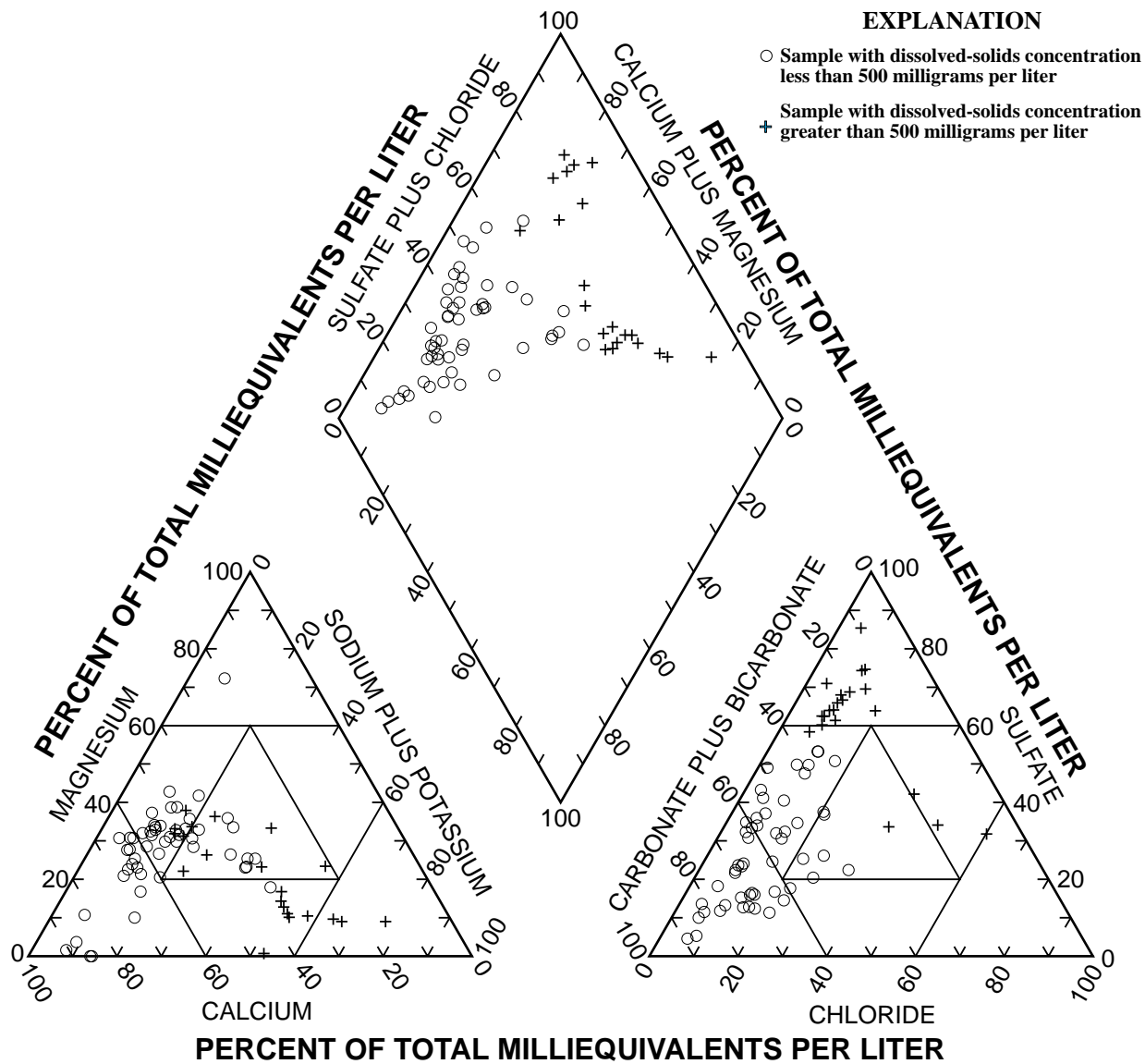


Figure 10. Chemical composition of 73 water samples collected from the Navajo and Kayenta aquifers within the central Virgin River basin study area, Utah.

the Spring Mountains near Las Vegas, Nevada, are plotted to show nearby isotopic signatures of high-altitude precipitation.

The data plotted in figure 12 indicate that groundwater samples from the main part of the Navajo and Kayenta aquifers with heavier isotopic signatures (less negative values) also had dissolved-solids concentrations less than 500 mg/L. In contrast, samples with lighter isotopic signatures generally have elevated dissolved-solids concentrations. One possible explanation for this is that recharge along the outcrop from local lower-elevation precipitation (either diffuse or along stream channels) is only in contact with the Navajo Sandstone (fairly clean quartz sand). Conversely,

streams originating higher in the Pine Valley Mountains from higher-elevation precipitation must first cross the highly soluble evaporite deposits of the Carmel and other overlying formations. During low-flow conditions, the dissolved-solids concentrations of this surface water may be elevated by dissolution of these minerals, as was found at site (C-41-15)12baa along Bitter Creek (Wilkske and others, 1994, table 4) just upstream of the Navajo Sandstone outcrop. Thus, recharge from streams carrying this isotopically light precipitation could also have an elevated dissolved-solids concentration.

Another possible explanation for the relation between lighter isotopic species and higher dissolved-

EXPLANATION

+

Sample from the Navajo and/or Kayenta aquifers with dissolved-solids concentration greater than 500 milligrams per liter

Formations overlying the Navajo and Kayenta aquifers

- Samples from Quarternary sediment and Quarternary-Tertiary alluvial formations
- + Samples from Quarternary-Tertiary basalt
- △ Samples from Tertiary Pine Valley Monzonite
- Samples from Cretaceous sedimentary formations

Formations underlying the Navajo and Kayenta aquifers

- ◊ Samples from Jurassic Moenave Formation
- Samples from Triassic Chinle Formation
- Samples from Triassic Moenkopi Formation
- × Samples from Permian Kaibab Formation

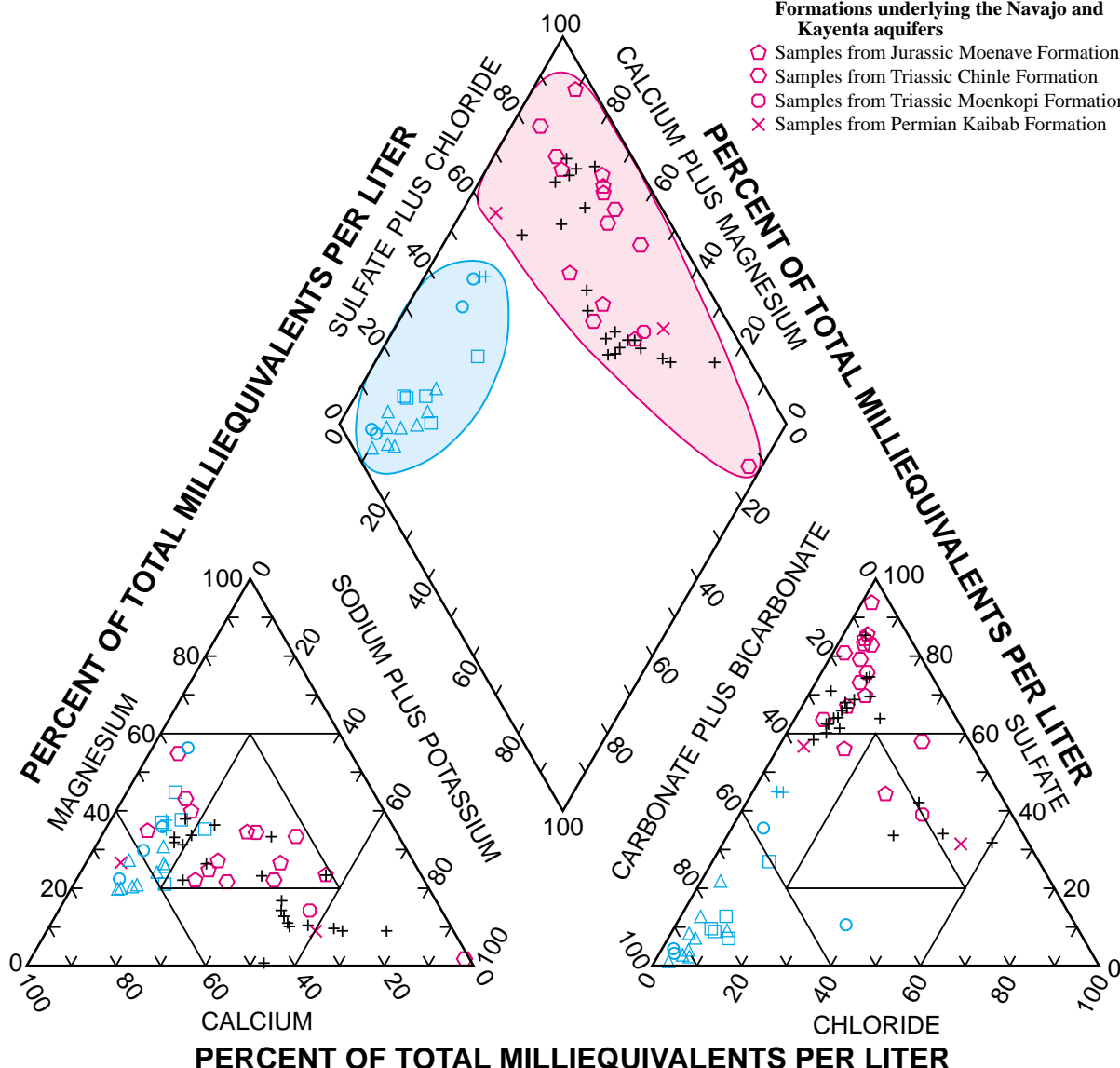


Figure 11. Relation of Navajo and Kayenta aquifer samples with high dissolved-solids concentration to the chemical composition of samples collected from overlying and underlying formations within the central Virgin River basin study area, Utah.

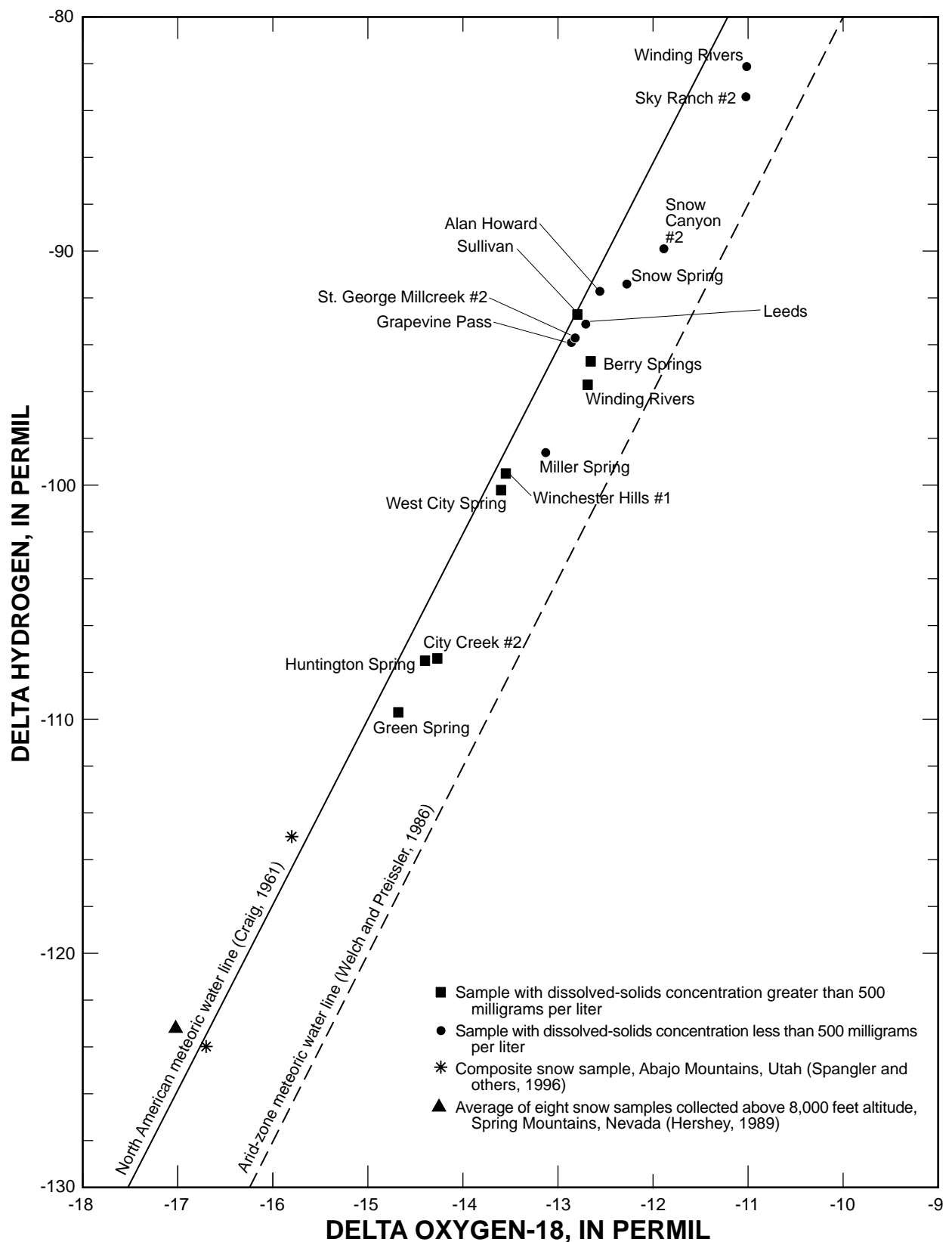


Figure 12. Stable-isotope ratios of hydrogen versus oxygen from ground water in the main part of the Navajo and Kayenta aquifers within the central Virgin River basin study area, Utah.

solids concentrations is mixing of recharge from precipitation from the higher-elevation Pine Valley Mountains with higher dissolved-solids hydrothermal water migrating upward along fractures into the Navajo and Kayenta aquifers (discussed in more detail in the “Recharge from overlying and underlying formations” section). This hypothesis requires that recharge from streams carrying isotopically light precipitation generally occurs higher along the outcrop, creating deeper and longer flow paths that would mix more with upwardly migrating hydrothermal water deeper in the aquifer than the shallow and shorter flow paths associated with precipitation that falls locally on the outcrop. One advantage of this explanation is that it also explains the elevated temperatures (greater than 20°C) related to the higher dissolved-solids concentrations. Further investigation, including the determination of ground-water recharge temperatures from dissolved noble gases to augment the stable-isotope and general-chemistry data of sampling sites shown in figure 12, is necessary to more conclusively determine ground-water flow paths within the Navajo and Kayenta aquifers.

Possible Sources of Ash Creek and Toquerville Springs

The hydrology of the Ash Creek drainage below Ash Creek Reservoir is of particular interest to local water management agencies in Washington County, especially with respect to possible sources for Toquerville and Ash Creek Springs. These springs, with a combined flow of about 28 ft³/s (Wilkowske and others, 1998, table 3), are likely the principal source of discharge from the lower Ash Creek drainage ground-water system. Wells along the Ash Creek drainage below the reservoir also discharge small amounts of water from the aquifer. Ground water also may migrate from the lower Ash Creek drainage ground-water system into the Navajo aquifer where it is buried between Pintura and Toquerville.

Ash Creek is ephemeral just upstream of the reservoir, which is often empty. However, when the reservoir is full, water rapidly flows out through fractures in the basalt outcrop near the dam abutment. Although the amount and fate of this water is unknown, it is likely only a small component of overall recharge to the lower Ash Creek drainage ground-water system. Several other potential sources recharge the ground-water system. One possible source is seepage of surface water from Kanarra, Spring, Camp, and Taylor Creeks (pl. 1).

These creeks generally dry up as they flow west across the Hurricane Fault, indicating recharge to the alluvial deposits north of Ash Creek Reservoir. A part of this ground water likely migrates southward through boulder conglomerate and fractured basalt along the Ash Creek drainage (Hurlow, 1998). The Pine Valley monzonite aquifer, part of the undifferentiated Tertiary igneous and sedimentary rocks (labeled “Ts” on fig. 13), also may provide a source of recharge where it contacts the fractured basalt between Ash Creek Reservoir and Pintura. Similarly, the Navajo Sandstone (labeled “Jn” on fig. 13) may provide recharge where it contacts with the basalt between Anderson Junction and Ash Creek Springs. Finally, seepage studies along South Ash Creek indicate that water seeps from the stream into coarse boulder conglomerate (labeled “Qs” on fig. 13) that overlies the fractured basalt of the Ash Creek drainage (Dale Wilberg, U.S. Geological Survey, oral commun., 1998) and is likely an additional source of recharge to the lower Ash Creek drainage ground-water system.

Water-chemistry data from Toquerville and Ash Creek Springs, along with nine other ground- and surface-water sampling sites along the Ash Creek drainage, were compiled and analyzed to investigate possible sources to the springs. The chemical composition of water from these sites is shown in figure 14. Dissolved-solids concentrations ranged from 56 to 1,028 mg/L. The most obvious geochemical trend is an increase in the percent sulfate and a decrease in the percent bicarbonate with increased dissolved solids. Water samples from Toquerville and Ash Creek Springs are at the median of the range of dissolved-solids concentration and have about equal fractions of sulfate and bicarbonate. The geochemical signatures of surface-water samples from upper Ash Creek and LaVerkin Creek generally show higher sulfate and lower bicarbonate percentages than Toquerville and Ash Creek Springs (fig. 14). Water samples from New Harmony LDS Well B, Sawyer Spring, the WCWCD well, and South Ash Creek, all have very low sulfate and dissolved-solids concentrations. Therefore, water lost from Ash Creek Reservoir may be mixing with other lower sulfate ground water from the Pine Valley Monzonite aquifer, the Navajo aquifer, or upper Ash Creek drainage before being discharged at Toquerville and Ash Creek Springs. Several other sources for the springs are possible, however, which also would be consistent with the scarce available geochemical data. Therefore, more water-quality data from wells, springs, and streams are needed to better determine recharge to the ground-

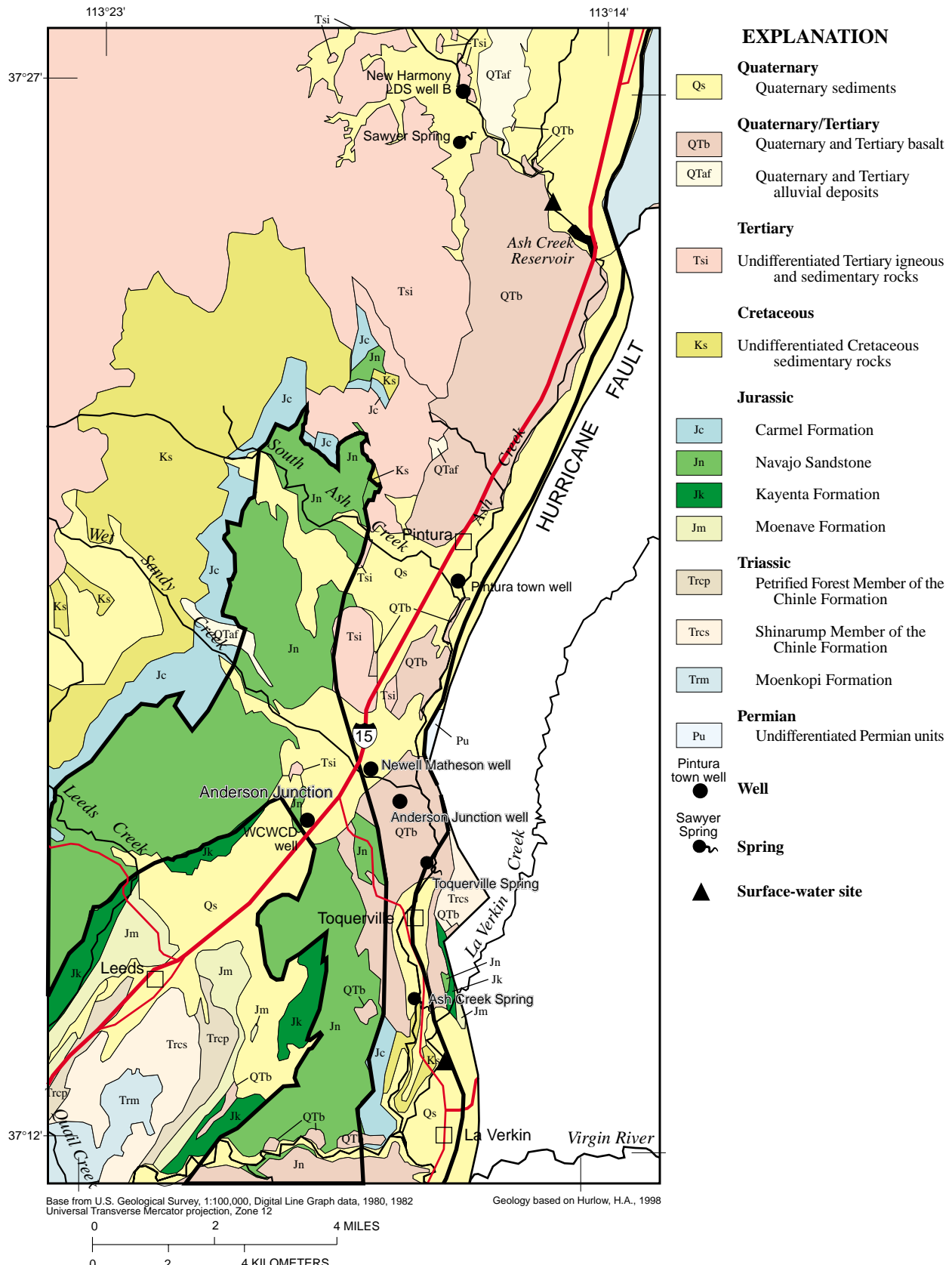


Figure 13. Location of general-chemistry sampling sites along the Ash Creek drainage, Utah.

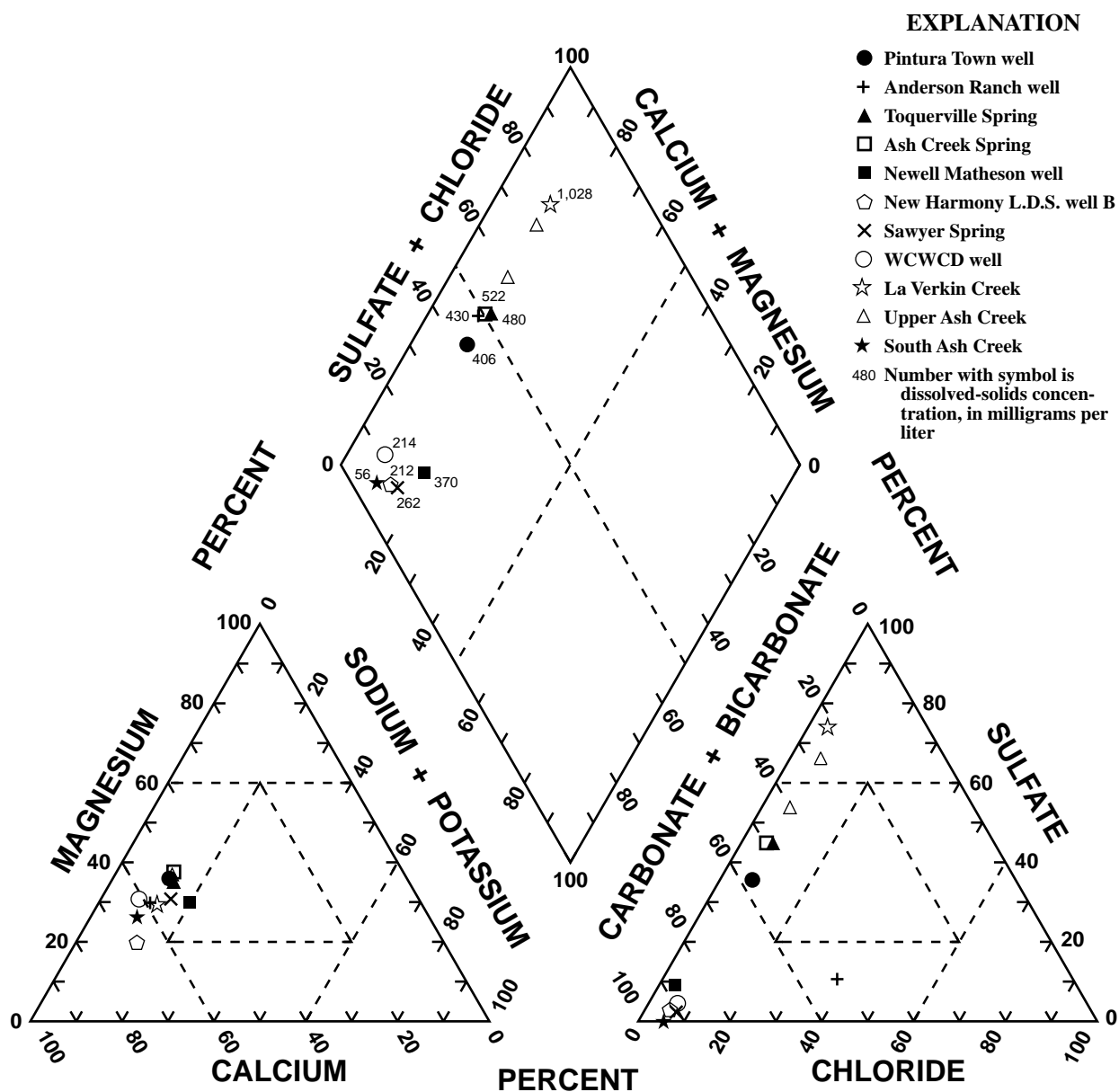


Figure 14. Chemical composition of ground water and surface water along the Ash Creek drainage, Utah.

water system. Additionally, the recharge could be better defined by measuring seepage losses (1) along creeks entering the lower Ash Creek drainage, (2) from Ash Creek Reservoir, and (3) along Ash Creek between Toquerville Springs and the confluence with the Virgin River. Such information would be helpful in more accurately identifying possible sources of water for Toquerville and Ash Creek Springs.

GROUND-WATER HYDROLOGY

Upper Ash Creek Drainage Basin Ground-Water Flow System

The 134-mi² drainage basin for Ash Creek Reservoir includes several geographic features that affect the ground-water system in distinctive ways. The basin floor is where most of the irrigation, evapotranspiration, ground-water discharge, and stream-aquifer interaction

occur. The Hurricane Fault is a hydrologic boundary along the eastern edge of the basin floor and likely precludes subsurface flow into the system from the Markagunt Plateau. The high plateau east of the Hurricane Fault is where precipitation is greatest, but recharge to the principal alluvial aquifers is only through ephemeral streams that flow across the Hurricane Fault.

Because of the large amount of precipitation along the north slope of the Pine Valley Mountains, recharge from infiltration of precipitation to the upper Ash Creek drainage basin ground-water system is assumed to be substantial. Along the low hills to the west and north, precipitation and recharge from infiltration of precipitation are assumed to be moderate. Lastly, the fractured basalt flows at the south end of the basin likely act as a

drain for subsurface outflow from the ground-water system. A generalized conceptualization of how water recharges to and discharges from the upper Ash Creek drainage basin ground-water system is shown in figure 15.

Aquifer System Geometry and Hydrologic Boundaries

The upper Ash Creek drainage basin includes numerous igneous and sedimentary rocks, and unconsolidated deposits that contain ground water (pl. 1). The aquifer system of the upper Ash Creek drainage basin consists of three aquifers, all on the west side of the Hurricane Fault. The uppermost Quaternary basin-fill

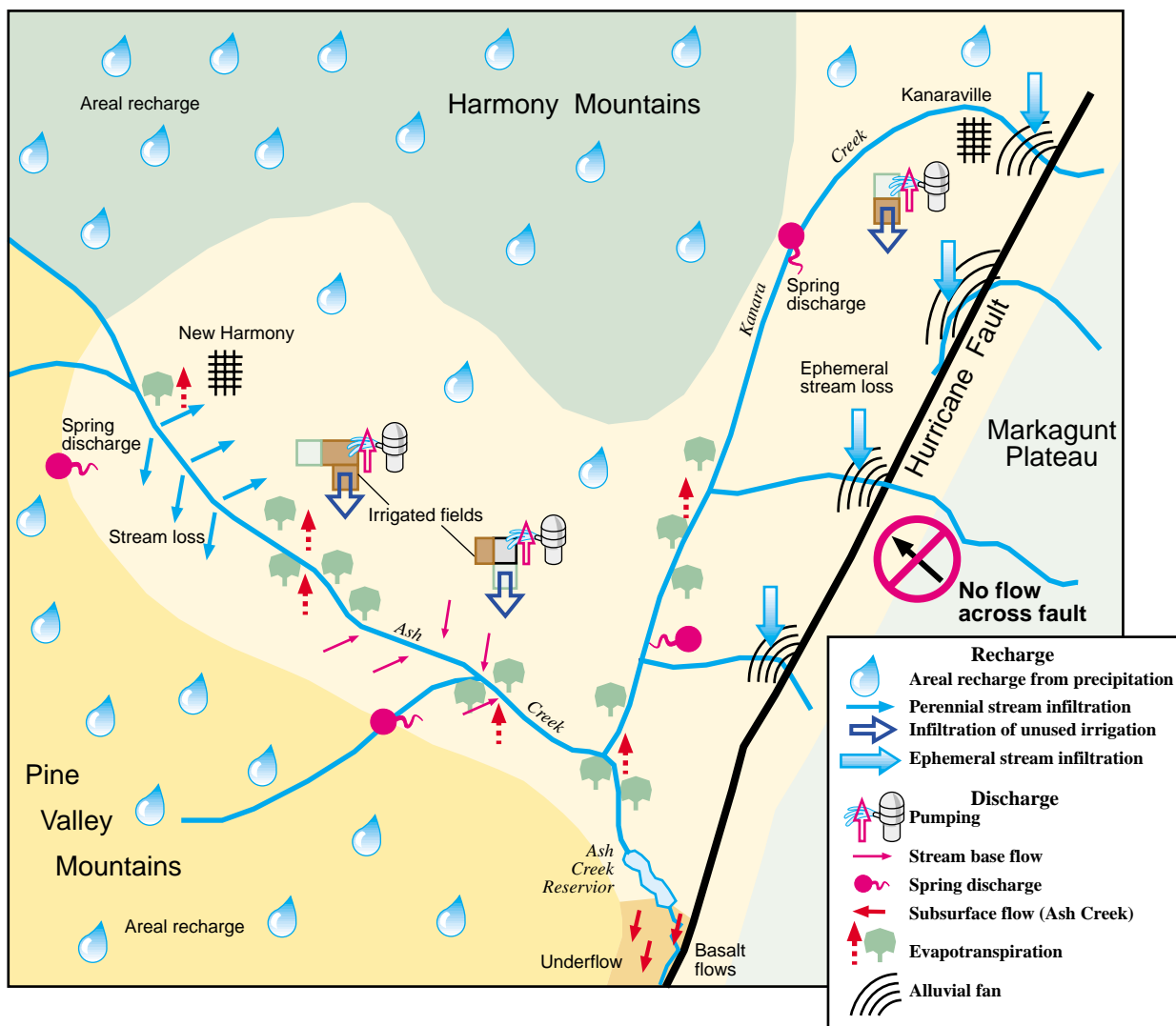


Figure 15. Generalized diagram showing sources of recharge to and discharge from the upper Ash Creek basin ground-water system, Utah.

aquifer has the smallest areal extent. It is confined between the Hurricane Fault and the beginning edge of the Harmony and Pine Valley Mountains (fig. 16). From west to east it is about 2 to 3 mi wide near Kanarraville where the edge of the Harmony Mountains are closest to the Hurricane Fault, and about 6 mi wide at the latitude of the town of New Harmony. The Tertiary alluvial-fan aquifer, which is thought to underlie the basin-fill aquifer in the vicinity of Kanarraville, extends about 5 mi west from the Hurricane Fault where it ends at the lower slopes of the Harmony Mountains. The alluvial-fan aquifer is about 6.5 mi wide at the latitude of the town of New Harmony. The Tertiary Pine Valley monzonite aquifer and other consolidated rock aquifers of the Harmony Mountains extend throughout the rest of the drainage basin and underlie the alluvial-fan aquifer at the southwest end of the Ash Creek valley. The existence of this aquifer at depth under the alluvial-fan deposits in the middle and northern parts of the valley has not been confirmed.

The basin-fill aquifer is thickest (1,500 ft) (Hurlow, 1998) near the Hurricane Fault, about 200 to 500 ft thick east of New Harmony, and less than 100 ft thick under most of the Ash Creek stream channel. The aquifer thins to less than 200 ft on the west as it merges with the alluvial-fan aquifer near the base of the Harmony Mountains. The alluvial-fan aquifer is thought to be about 1,200 to 1,400 ft thick throughout the upper Ash Creek drainage basin (Hurlow, 1998, pl. 2). The thickness of the Pine Valley monzonite aquifer is unknown, but it is thought to be in excess of 2,000 ft.

The hydrologic boundaries of the system are thought to correlate closely with structural and watershed boundaries. The eastern boundary is presumed to

be the Hurricane Fault, which, because of the large offset and associated fine-grained fault gouge (Hurlow, 1998), would likely be a barrier to ground-water flow from the east. The northern boundary is a ground-water divide north of Kanarraville, as defined in Thomas and Taylor (1946). Water-level measurements from 1995 indicate that the location of this divide has apparently moved about 2 mi farther south than the reported location in 1946, probably because of increased well discharge in Cedar Valley to the north. The northern, western, and southern lateral boundaries of the basin-fill and alluvial-fan aquifers are defined by their areal extent. The boundaries for the Pine Valley monzonite aquifer are defined by the watershed boundary (surface-water divide) of Ash Creek basin. The southern discharge boundary of all three aquifers is presumed to be the fractured basalt flows near Ash Creek Reservoir in the narrow part of the Ash Creek Valley. Ground water can move through fractures in this basalt or through interbedded and underlying coarse-grained, unconsolidated deposits reported by Hurlow (1998). All three aquifers are assumed to be present in this area, although the existence of the alluvial-fan and Pine Valley monzonite aquifers is not a certainty because no wells have been drilled to that depth. The depth of the lower boundary for the system, the contact between the fractured igneous rocks and underlying formations, is not known. It is assumed that no ground water moves across this contact. The upper boundary of the system is the transition between the saturated and unsaturated material regardless of which aquifer is uppermost, and is the main avenue for recharge to and discharge from all aquifers.

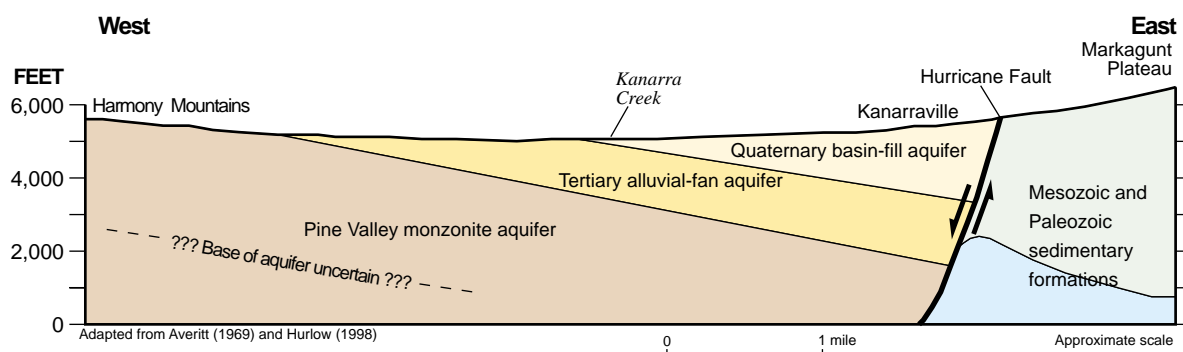


Figure 16. Schematic hydrogeologic section showing subsurface geometry from northwest to southeast near Kanarraville, Utah.

Table 5. Transmissivity of three aquifers in the upper Ash Creek drainage basin, Utah

Aquifer	Transmissivity range from aquifer testing (feet squared per /day)	Hydraulic conductivity from (Cordova, Sandberg, and McConkie, 1972) (feet per day)	Average specific capacity	Minimum specific capacity	Maximum specific capacity	Number of specific-capacity values available
			(gallons per minute per foot of drawdown)			
Basin fill	1,2540 -16,000	35 to 200	9.7	0.1	47	16
Alluvial fan	—	—	1.5	.05	2.5	9
Pine Valley monzonite	—	—	12.2	.5	73	11

¹Range based on four aquifer tests.

Aquifer Properties

The three aquifers defined for the upper Ash Creek drainage basin have variable transmissivity and storage capacity. On the basis of specific-capacity values from wells, aquifer testing, and previously reported transmissivity values, the Pine Valley monzonite aquifer is the most transmissive and the alluvial-fan aquifer is the least transmissive (table 5). The basin-fill aquifer is moderately permeable around Kanarraville, but poorly permeable near the Hurricane Fault directly east of New Harmony. Cordova, Sandberg, and McKonkie (1972) reported that the hydraulic conductivity of the basin fill near Kanarraville was about six times higher than it was 5 mi farther south. The reasons for this difference are unknown but are probably related to depositional history. Specific capacity of the alluvial-fan aquifer indicates that it may be a poor aquifer. Specific-capacity values are about 10 times smaller than values for the other two aquifers. The Pine Valley monzonite aquifer is transmissive where wells penetrate fractures in the rock. Analysis of water-level data after 6 days of constant-rate pumping from an irrigation well and an observation well south of Ash Creek indicates that horizontal anisotropy is substantial and that the aquifer properties cannot be analyzed by using flow equations for porous media. The observation well and pumped well were about 500 ft apart and apparently open to the same fracture, which was highly conductive. Drawdown in the pumped well pumping at 1,100 gal/min was only 15 ft after 6 days of pumping. The specific capacity of the well was 73 gal/min/ft of drawdown, the highest measured value for the basin. However, without additional observation wells located off of the fracture zone connecting the two wells, the long-term production capability of the aquifer cannot be determined with

confidence (Victor Heilweil, U.S. Geological Survey, 1998, written commun., Aquifer test at well C-38-13-35aba.).

The presence of a proposed fault (Hurlow, 1998) that runs approximately north-to-south beneath New Harmony and then southwest into the Pine Valley Mountains (pl. 1) may have some effect on the hydraulic conductivity of the Pine Valley monzonite aquifer. Differences in water levels between wells drilled on the west and east sides of this fault zone indicate a relatively steep hydraulic gradient (about 0.035), whereas hydraulic gradients to the east are less steep (0.014 to 0.019). This indicates that the fault zone may have a lower transmissivity (and hydraulic conductivity) perpendicular to the fault direction than there is in areas that are not faulted. Hugh Hurlow (Utah Geological Survey, oral commun., 1998) has also observed northeast-southwest fractures at outcrops of the Pine Valley monzonite. This could cause anisotropic conditions in this part of the Pine Valley monzonite aquifer.

The storage capacity of aquifers is often assumed to be the percentage of interconnected pore space in the aquifer, or effective porosity. This is true in theory but not in practice. All water in pore spaces cannot be removed because of the molecular attraction of water to the aquifer materials. The actual storage capacity is better measured through hydraulic testing which allows for the estimation of the aquifer's storage properties; storage coefficient for confined aquifers and specific yield for unconfined aquifers. Both confined and unconfined conditions likely occur in various places throughout the study area in the aquifers described. Confined conditions result when fine-grained layers overlie and confine coarse-grained layers that are more transmissive. This confinement allows hydraulic heads

to increase to greater than atmospheric pressure, and water removed comes from a release in that pressure and subsequent compaction of the aquifer skeleton and expansion of water. Water released from an unconfined aquifer is from dewatering the pore space in the aquifer (Freeze and Cherry, 1979). On the basis of aquifer tests and observation of sediments penetrated in drill holes, Cordova, Sandberg, and McConkie (1972) estimated the storage coefficient of the basin-fill aquifer to range from 0.0001 to 0.0004, and specific yield to be about 0.30. Storage properties of the alluvial-fan and Pine Valley monzonite aquifers are not available from aquifer testing. Although the transmissivity and hydraulic conductivity in the alluvial-fan aquifer are probably an order-of-magnitude lower than those of the basin-fill aquifer, it cannot be assumed that the storage coefficient in that aquifer is similarly low. However, specific yield would likely be somewhat less than that of the basin-fill aquifer because of the greater degree of cementation, tighter packing of grains, and poorer sorting of grain sizes, which would tend to decrease effective porosity, increase specific retention of ground water, and decrease specific yield. The storage capacity of a fractured crystalline rock such as the Pine Valley monzonite will be substantially smaller than either of the aquifers composed of unconsolidated deposits. Primary porosity, the principal factor that determines the amount of ground water stored, is typically only a fraction of 1 percent in crystalline rocks and rarely exceeds 2 percent (Freeze and Cherry, 1979). Secondary porosity from fracture openings, although responsible for large ground-water velocities, is not large enough to create substantial storage capacity. Bulk fracture porosity generally accounts for only a few percent of effective porosity in consolidated rocks, and even then is usually only present in the first 300 ft below land surface.

Recharge

The Upper Ash Creek drainage basin ground-water system is recharged by rain and melting snow that infiltrates until reaching the uppermost saturated zone. This process includes seepage losses from perennial streams, by periodic seepage losses from ephemeral streams, and possibly by infiltration of unconsumed irrigation water. The amount of recharge by these mechanisms is estimated to range from 6,100 to 18,800 acre-ft/yr.

Precipitation

Precipitation is the principal means by which the ground-water system of the upper Ash Creek drainage basin is recharged; however, it is believed that only precipitation falling west of the Hurricane Fault recharges the system through direct infiltration. Several things typically happen to precipitation as it falls or after it falls. It can evaporate as it is falling, after it reaches land surface, or after it enters the subsurface. It can be intercepted by plants above ground or used by plant roots below land surface. It can run off into drainage channels and eventually flow into stream channels. It can infiltrate into the unsaturated zone below the plant root zone and remain there until subsequent infiltration pushes it deeper into the uppermost saturated zone. Estimated total annual precipitation for the Ash Creek drainage basin is about 153,000 acre-ft (table 6). About 109,000 acre-ft falls on the west side of the Hurricane Fault and the remainder falls on the Markagunt Plateau east of the fault. Only a small amount of the total precipitation typically recharges a ground-water system through direct infiltration.

Average annual recharge from precipitation was estimated using precipitation-recharge relations developed in previous studies. On the basis of budget calculations and change in storage, Bjorklund, Sumsion, and Sandberg (1978) estimated that about 8.5 percent of total precipitation recharges the ground-water systems in Cedar and Parowan Valleys, north of the upper Ash Creek drainage basin. If this percentage is assumed, total average annual recharge to the Ash Creek aquifer system is estimated to be 9,200 acre-ft (table 6). Harrill and Prudic (1998) and Anderson (1995) developed precipitation-recharge relations for alluvial basins of Nevada and Arizona. These relations were developed by correlating known or estimated recharge with the amount of precipitation in excess of 8 in. falling on a basin. The recharge estimates were obtained from several sources including ground-water flow modeling, water-budget analyses, chloride-balance (Dettinger, 1989), and the Maxey-Eakin method (Maxey and Eakin, 1949). Precipitation in excess of 8 in. for the upper Ash Creek drainage basin west of the Hurricane Fault is about 66,000 acre-ft/yr. Recharge from infiltration of precipitation west of the Hurricane Fault using Harrill and Prudic's relation was 3,600 acre-ft/yr. Recharge using Anderson's relation was 2,600 acre-ft/yr. The percentage of recharge derived from precipitation is areally variable and depends on a host of climatic factors such as the amount and duration of

Table 6. Precipitation and recharge in subbasins of the upper Ash Creek drainage basin, Utah

Name of subbasin	Range of normal annual precipitation 1961-90 (feet)	Area of basin (acres)	Annual volume of precipitation (acre-feet)	Volume of precipitation greater than 8 inches (acre-feet per year)	Recharge using Anderson (1995) (acre-feet per year)	Recharge using Harrill and Prudic (1998) (acre-feet per year)	Recharge using Bjorklund, Sumsion, and Sandberg (1978) (acre-feet per year)	Area (square miles)
Subbasins west of the Hurricane Fault								
Upper Ash Creek Valley floor	1.46-1.96	22,000	33,240	18,580	600	900	2,800	34.3
Harmony Mountains	1.46-1.88	16,710	27,850	16,720	500	800	2,400	26.1
Pine Valley Mountains	1.46-2.46	25,140	47,440	30,680	1,000	1,600	4,000	39.3
Subtotal	1.46-2.46	63,850	108,530	65,980	2,100	3,300	9,200	99.7
Subbasins east of the Hurricane Fault								
Kanarra Creek	1.71-2.54	6,410	14,040	9,760	No recharge to upper Ash Creek drainage basin by direct infiltration east of fault			10
Spring Creek	1.71-2.46	3,620	7,640	5,230				5.7
Camp Creek	1.71-2.38	2,900	6,030	4,100				4.5
Taylor Creek	1.63-2.29	4,400	8,600	5,670				6.9
Other	1.54-2.04	4,620	7,840	4,760				7.2
Subtotal	1.54-2.54	21,950	44,150	29,520				34.3
Total	1.46-2.54	85,800	152,680	95,500				134

precipitation, topographic setting, altitude, temperature, aspect, vegetation, latitude, and others. For example, a smaller percentage of the total precipitation near Ash Creek Reservoir (about 17 in. annually) probably recharges the basin-fill aquifer than in the Pine Valley Mountains, where total precipitation is about 29 in. annually. The variability between methods is attributable mostly to climatic factors, particularly temperature. Lower altitudes typically have higher temperatures, which results in more of the precipitation being evaporated and transpired than would occur at a higher altitude.

The estimated precipitation on the upper Ash Creek valley floor is about 33,000 acre-ft/yr. Infiltration of precipitation likely is smallest here because lower altitudes and higher temperatures increase soil-zone evaporation and transpiration. In addition, infiltration of precipitation likely has been decreased in specific valley locations because of human development such as roads, houses, and croplands. The minimum amount of estimated infiltration, determined from precipitation-recharge relation developed by Harrill and Prudic (1998) and Anderson (1995), is about 600 acre-ft/yr. The maximum amount of estimated infiltration, deter-

mined by the Cedar-Parowan basin study (Bjorklund, Sumsion, and Sandberg, 1978) is about 2,800 acre-ft/yr.

The Pine Valley and Harmony Mountains receive about 75,000 acre-ft of precipitation annually, much of it as snow during the colder months when temperatures and evaporation rates are low. The mountains typically have a thinner soil cover than the valley floor, which allows more rapid infiltration. However, steeper slopes promote more rapid runoff than the flat areas in the valley; thus, slowly melting snow provide the optimum recharge source. The minimum amount of estimated infiltration, determined from precipitation-recharge relation developed by Anderson (1995), is about 1,500 acre-ft/yr. The maximum amount of estimated infiltration, determined from the Cedar-Parowan basin study, is about 6,400 acre-ft/yr.

Streams

Discharge measurements along perennial and ephemeral streams indicate that the upper Ash Creek drainage basin ground-water system is partially recharged by stream seepage. Discharge in Ash Creek was measured at eight sites from just south of the town

of New Harmony to the abandoned Highway 91 bridge near Ash Creek Reservoir (fig. 17) as part of a seepage study done in October 1995 (Wilkowske and others, 1998, table 6). The study indicates that seepage to the aquifers may occur in the central and lower reaches of the stream. Streams draining the Markagunt Plateau are ephemeral before they cross the Hurricane Fault but lose all of their flow after crossing the fault. During spring runoff they may flow throughout their entire

length. One-time measurements on four of these streams in 1995 indicated a combined discharge of about 4 ft³/s (2,900 acre-ft/yr). Analysis of base flow for these streams indicates that recharge could be occurring during the winter when vegetation is dormant and during spring runoff. Other ephemeral streams flow for brief periods when snow is melting or intense rainfall occurs. The amount of recharge resulting from these flows is not known.

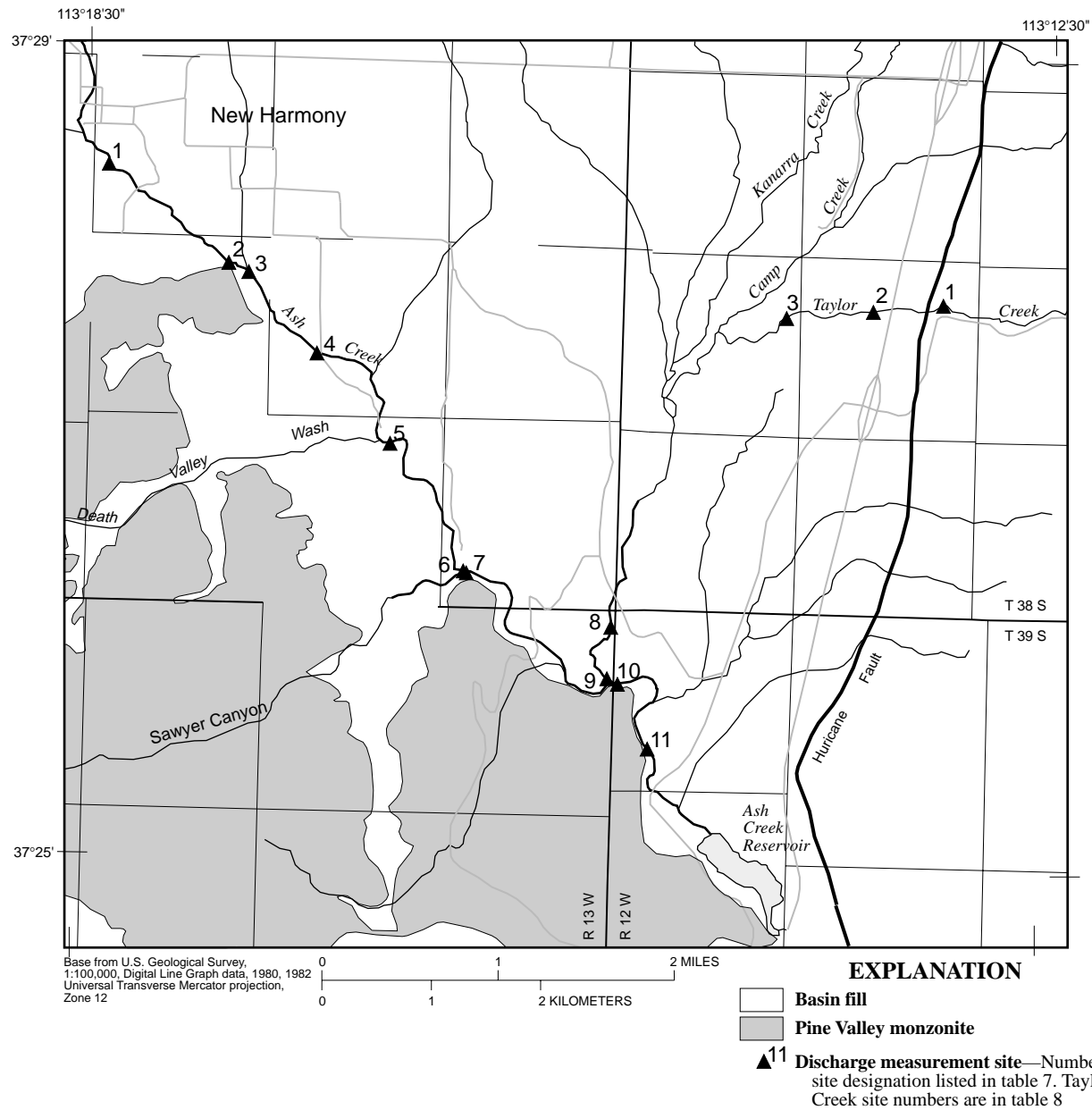


Figure 17. Location of streamflow-gaging sites for seepage investigations on Ash, Sawyer, Kanarra, and Taylor Creeks, upper Ash Creek drainage basin, Utah.

Perennial Streams

Ash Creek is fed from tributaries flowing out of the Pine Valley and Harmony Mountains. It is perennial in certain reaches and ephemeral in others. Average discharge for nine years of streamflow record from a streamflow-gaging station near the present site of Ash Creek Reservoir (1939-47) is 10.6 ft³/s (7,700 acre-ft/yr). Monthly mean discharge averaged for the period of record ranges from 1.1 ft³/s (800 acre-ft/yr) in July to 28.8 ft³/s (20,900 acre-ft/yr) in April. Base flow, the flow attributed only to ground-water inflow, was estimated from monthly mean flows for December and January and probably ranges from 1 to 4 ft³/s (725 to 2,900 acre-ft/yr). Cordova, Sandberg, and McConkie (1972) estimated about 3 ft³/s (2,200 acre-ft/yr) of seepage to Ash Creek in 1970. On the basis of a seepage investigation in October 1995 (fig. 17), some reaches of the stream lose water to the aquifers (table 7). A half-mile

long stream reach starting about 2 mi downstream from New Harmony lost about 0.6 ft³/s (440 acre-ft/yr) to the unconsolidated aquifers. The reach from the Sawyer Creek confluence to about 1 mi upstream of the Ash Creek Reservoir spillway lost about 0.7 ft³/s (500 acre-ft/yr) to the same aquifers. A seepage study in October 1995 (Wilkowske and others, 1998) along the perennial section of Kanarra Creek near the inflow to Ash Creek indicates that the last $\frac{1}{3}$ mi of Kanarra Creek upstream from its confluence with Ash Creek lost about 0.08 ft³/s (60 acre-ft/yr) to the aquifers. Because only one series of seepage investigations has been conducted, it is not known if losses measured in October 1995 were sustained throughout the year, or even if these losses are sustained from year to year. On the basis of the yearly variability in flow in all perennial streams, total recharge from perennial streams is estimated to range from 0.7 to 1.5 ft³/s (500 to 1,100 acre-ft/yr).

Table 7. Measurements of discharge, temperature, and specific conductance and analysis of seepage losses and gains at selected sites on Ash, Kanarra, and Sawyer Creeks, upper Ash Creek drainage basin, Utah

[ft³/s, cubic feet per second, acre-ft/yr, acre-feet per year]; $\mu\text{s}/\text{cm}$, microsiemens per centimeter at 25 degrees Celsius

Measurement site	Date	Discharge ft ³ /s	Losses (Recharge to the aquifer) ft ³ /s (acre-ft/yr)	Gains (Discharge from the aquifer) ft ³ /s (acre-ft/yr)	Temperature, degrees Celsius	Specific conductance, $\mu\text{s}/\text{cm}$ at 25°C
Ash Creek						
Ash Creek #1	10-10-95	0.553			13.0	340
Ash Creek #2	10-10-95	1.52 outflow		.97 (700)	12.0	435
Ash Creek #3	10-10-95	.090				
Ash Creek #4	10-10-95	1.05		.96 (695)	15.0	520
Ash Creek #5	10-10-95	.444	.61 (440)			470
Mountain Spring diversion		.2 estimated outflow				
Ash Creek #6	10-11-95	.238			10.0	510
Sawyer Creek #7	10-11-95	1.56 inflow			12.0	480
Kanarra Creek #9	10-11-95	.280 inflow			16.0	
Ash Creek #10	10-11-95	1.57			11.5	840
Ash Creek #11	10-11-95	1.39	.18 (130)		16.0	830
Total			1.30 (940)	1.93 (1,400)		
Kanarra Creek						
Kanarra Creek start	10-11-95	0				
Kanarra Creek #8	10-11-95	.357		.357 (260)	16.0	2,500
Kanarra Creek #9	10-11-95	.280	.080 (60)		16.0	

Ephemeral Streams

Recharge from ephemeral streams whose source is the Markagunt Plateau depends substantially on the hydrologic character of the Hurricane Fault. Observations indicate that ground-water movement in the sedimentary formations east of the Hurricane Fault is different than ground-water movement west of the fault and that the two ground-water systems may be isolated from one another. Water-level data from wells completed in the basin-fill aquifer near the fault zone indicate that potentiometric contours would be nearly perpendicular to the fault. This is typical of no-flow boundaries. Results from three surface-water discharge measurements in October 1995 along Taylor Creek and single discharge measurements on Camp and Spring Creeks as they traverse the fault indicated that virtually all flow ceased a short distance (less than 0.75 mi) after traversing the fault zone (table 8). October through March is usually when these stream flow because vegetation along the channels is dormant. Thus, if recharge occurs at a similar rate for 6 months, the likely minimum recharge to the basin-fill aquifer from these streams when they flow is assumed to be equal to one-half of base-flow discharge of the streams. Additional recharge could take place during the higher flows of spring runoff, but the amount of this recharge is unknown.

Long-term discharge records exist only for Kanarra Creek; thus, an estimate of average base flow for Spring, Camp, and Taylor Creeks was roughly determined by (1) deriving a mean annual discharge by

using the regression equation from Christensen and others (1985), (2) adjusting the calculated mean annual discharge on the basis of the difference between calculated and measured mean-annual discharge for Kanarra Creek, and (3) estimating base flow for Spring, Camp, and Taylor Creeks by using the ratio (base flow/mean annual discharge) from Kanarra Creek. The result was a minimum annual recharge rate of almost 7 ft³/s during the 6 months while the streams were flowing, or an annual total of 2,500 acre-ft.

Several ephemeral stream washes also begin in the Harmony and Pine Valley Mountains and drain into Kanarra and Ash Creeks. During sporadic runoff, these washes may recharge about 1,000 acre-ft/yr to the Pine Valley monzonite, alluvial-fan, and basin-fill aquifers where they traverse the formations, but the amount is highly speculative.

Irrigation

Recharge to the ground-water system of the upper Ash Creek drainage basin by infiltration of unconsumed irrigation water has not been confirmed by measurements. This recharge mechanism has been observed and documented for other basins of western Utah (Susong, 1995; Thiros and Brothers, 1993; Mower and Sandberg, 1982; and Bjorklund, Sumsion, and Sandberg, 1978) and is primarily a result of flood irrigation or liberal sprinkler-irrigation practices. Estimates of recharge that occur in other areas by this means range from 0 to 50 percent of the water applied.

Table 8. Miscellaneous discharge measurements at selected sites along Kanarra Creek and its tributaries, upper Ash Creek drainage basin, Utah

[ft³/s, cubic feet per second, acre-ft/yr, acre-feet per year; µS/cm, microsiemens per centimeter at 25 degrees Celsius]

Site (see fig. 19 for map location)	Date	Discharge, in ft ³ /s	Losses (recharge to the aquifer), in acre-ft/yr, ft ³ /s		Temperature, in degrees Celsius	Specific conductance in µS/cm at 25°C
Taylor Creek #1	10-12-95	.280			10.5	1,360
Taylor Creek #2	10-12-95	.170	80	(.11)	16.5	—
Taylor Creek #3	10-12-95	.013	115	(.157)	19.0	1,380
Taylor Creek 300 feet west of #3	10-12-95	0	10	(.013)	—	—
Camp Creek at mouth	10-13-95	.057	40	(.057)	6.0	2,150
Spring Creek at mouth	10-13-95	.063	45	(.063)	10.5	780
Kanarra Creek at mouth just above diversions	10-12-95	3.39	2,455	(3.39)	11.5	—

The records of the Utah Division of Water Rights indicate that about 50 wells, 4 springs, and about 20 streams are used primarily for irrigation. The total amount of water allowed for irrigation in 1998 was about 40,000 acre-ft and consisted of about 25,000 acre-ft from streams, 15,000 acre-ft from wells, and 1,500 acre-ft from springs. If one-fourth of the permitted water right were used, about 10,000 acre-ft annual recharge from irrigation could range from 0 acre-ft (sprinkler irrigation) to about 5,000 acre-ft (flood irrigation). Because most of the irrigation observed was being applied with sprinklers, recharge from this mechanism is thought to be at the lower end of this range.

Ground-Water Movement

Ground water in the aquifer system of the upper Ash Creek drainage basin generally moves from the surrounding mountains toward the valley floor and thence from the valley-floor margins toward Ash and Kanarra Creeks. Water-level measurements in the basin-fill aquifer indicate that ground-water movement within the basin generally is south from Kanarraville and east from New Harmony toward Ash Creek Reservoir (fig. 18a). Water levels measured in a few wells that tap the alluvial-fan aquifer near its margin indicate that ground water moves in a similar direction as in the basin-fill aquifer (fig. 18b). Water levels in wells that tap the Pine Valley monzonite aquifer south and southeast of New Harmony indicate a similar movement of ground water, from the Pine Valley Mountains toward the valley floor and thence toward Ash Creek Reservoir (fig. 18c).

Vertical movement between aquifers and within aquifers is indicated by observed differences in water levels in nearby wells that are finished at different depths. A downward gradient is indicated within the basin-fill aquifer near the Hurricane Fault and less than 1 mi east of New Harmony. The downward gradient near the fault supports the concept of recharge from ephemeral streams, but not from east of the fault. Upward gradients are evident within the alluvial-fan aquifer 3 mi east of New Harmony and within the Pine Valley monzonite aquifer along Ash Creek between New Harmony and Ash Creek reservoir.

Discharge

Principal sources of discharge from the upper Ash Creek drainage basin ground-water system are well withdrawal, evaporation, transpiration by riparian

vegetation, spring discharge, surface-water seepage gains in Ash Creek, and subsurface outflow via the fractured basalt in the vicinity of Ash Creek Reservoir (fig. 15).

Wells

Annual municipal well discharge for New Harmony and Kanarraville has been sporadically recorded since 1979, and the amount of irrigation, stock, and domestic well discharge in the basin can only be estimated. Kanarraville and New Harmony each have one municipal well. Recorded discharge from the Kanarraville municipal well has varied from 12 acre-ft in 1979 to 65 acre-ft in 1994, averaging about 30 acre-ft/yr. New Harmony municipal well discharge has varied from 24 acre-ft in 1980 to 47 acre-ft in 1986, averaging about 33 acre-ft/yr. Both municipalities supplement well discharge with water from springs.

Total irrigation, stock watering, and domestic well discharge has been estimated to range from 1,200 to 1,500 acre-ft/yr from about 120 wells in the upper Ash Creek drainage basin. Most of these wells list irrigation as the principal use, with stock watering and household as secondary uses. Irrigation well discharge has not changed substantially for the last 30 years. Cordova, Sandberg, and McConkie (1972) estimated irrigation well discharge to be about 1,000 acre-ft in 1968, 1,340 acre-ft in 1969, and 1,250 acre-ft in 1970. On the basis of the increase in population, irrigated acreage, and several discharge ratings done in 1995, total well discharge in 1995 was estimated to range from 1,200 to 1,500 acre-ft.

Evapotranspiration

Evapotranspiration in upper Ash Creek drainage basin likely occurs along perennial and ephemeral stream channels and in low areas adjacent to these channels. About 300 acres of cottonwood trees were mapped from areal photographs (fig. 19). The most dense growths exist along Ash Creek and Kanarra Creek, but there also are groves along Camp, Taylor, and Sawyer Creeks. There are about 4,300 acres of pasture grasses along the upper reaches of Kanarra Creek and around New Harmony. Although unknown, ground water was assumed to supply the entire demand for the growth of this vegetation.

There have been several different estimates of water use by vegetation. Using the Blaney-Criddle method (Criddle, Harris, and Willardson, 1962), Cordova, Sandberg, and McConkie (1972) estimated use

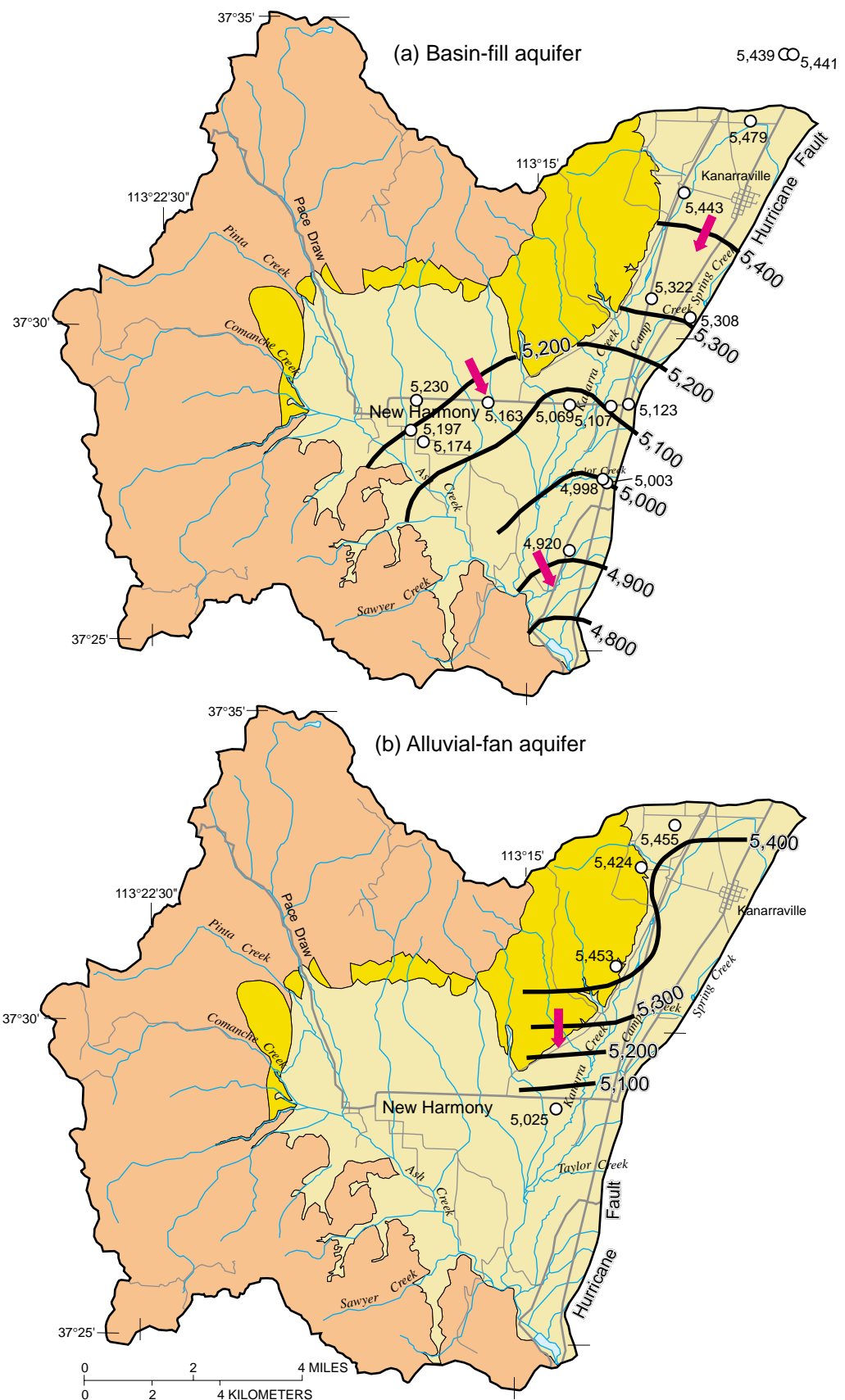


Figure 18. Approximate potentiometric contours in the three aquifers of the upper Ash Creek drainage basin, Utah

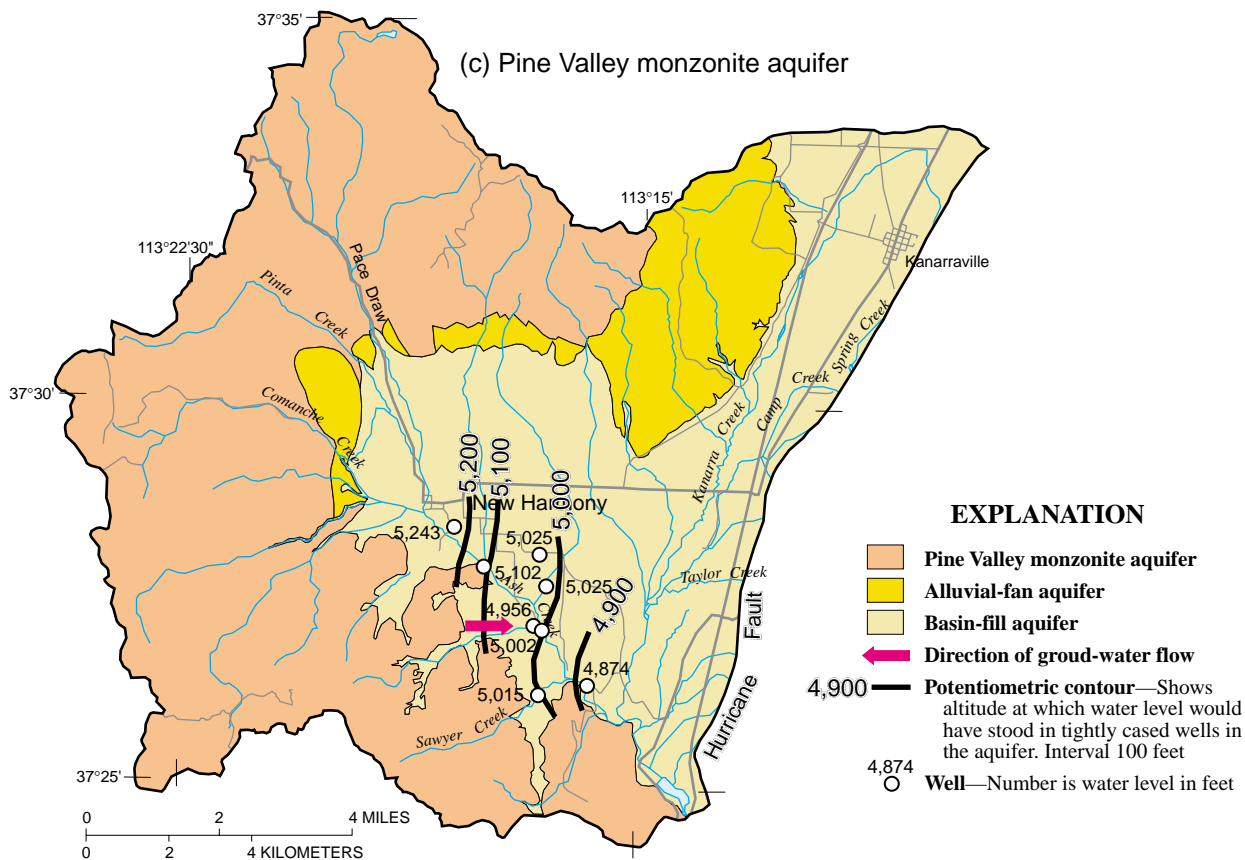


Figure 18. Approximate potentiometric contours in the three aquifers of the upper Ash Creek drainage basin, Utah—Continued

by cottonwood trees to be 3.6 ft/yr at 100 percent density, and by pasture grasses to be 2.9 ft/yr. Measurements of consumptive use by cottonwood trees in California (Muckel and Blaney, 1945) and in Arizona (Gatewood and others, 1950) indicate that annual use could be as much as 7 to 8 ft/yr. Because temperature varies, the amount of ground water consumed by riparian growth would vary seasonally; and because the depth to water varies, there could be areas where pasture grasses may not use any water from the saturated zone for transpiration. On the basis of this range of evapotranspiration rate and the extent and density of riparian growth, evapotranspiration loss in the upper Ash Creek drainage basin is estimated to range from 1,100 to 15,000 acre-ft/yr.

Springs

There are at least 25 springs in the upper Ash Creek drainage basin. Most are in the surrounding mountains and are near-surface, local-recharge-area systems that are not part of the basin-wide aquifer sys-

tem. All springs that discharge at the level of the valley floor and a few that discharge near the base of the surrounding mountains are likely part of the basin-wide aquifer system (fig. 20). A long-term record of the seasonal and year-to-year variability in discharge from these springs is not available. Users, have a water right of about 1,000 acre-ft/yr, thus, discharge was assumed to be 1,000 acre-ft/yr (excluding Sawyer Spring). Comanche and Lawson Springs are the largest of all the springs. Other smaller seeps and springs discharge from the basin fill where the water table intersects land surface. On the basis of water-right information, spring discharge was estimated to range from 200 to 1,000 acre-ft/yr. Sawyer Spring is discussed in the following section.

Ash, Sawyer, and Kanarra Creeks

Cordova, Sandberg, and McConkie (1972, p. 19) estimated that 2,200 acre-ft of ground water seeped to Ash Creek above Ash Creek Reservoir in 1970. The seepage study performed on Ash Creek in October

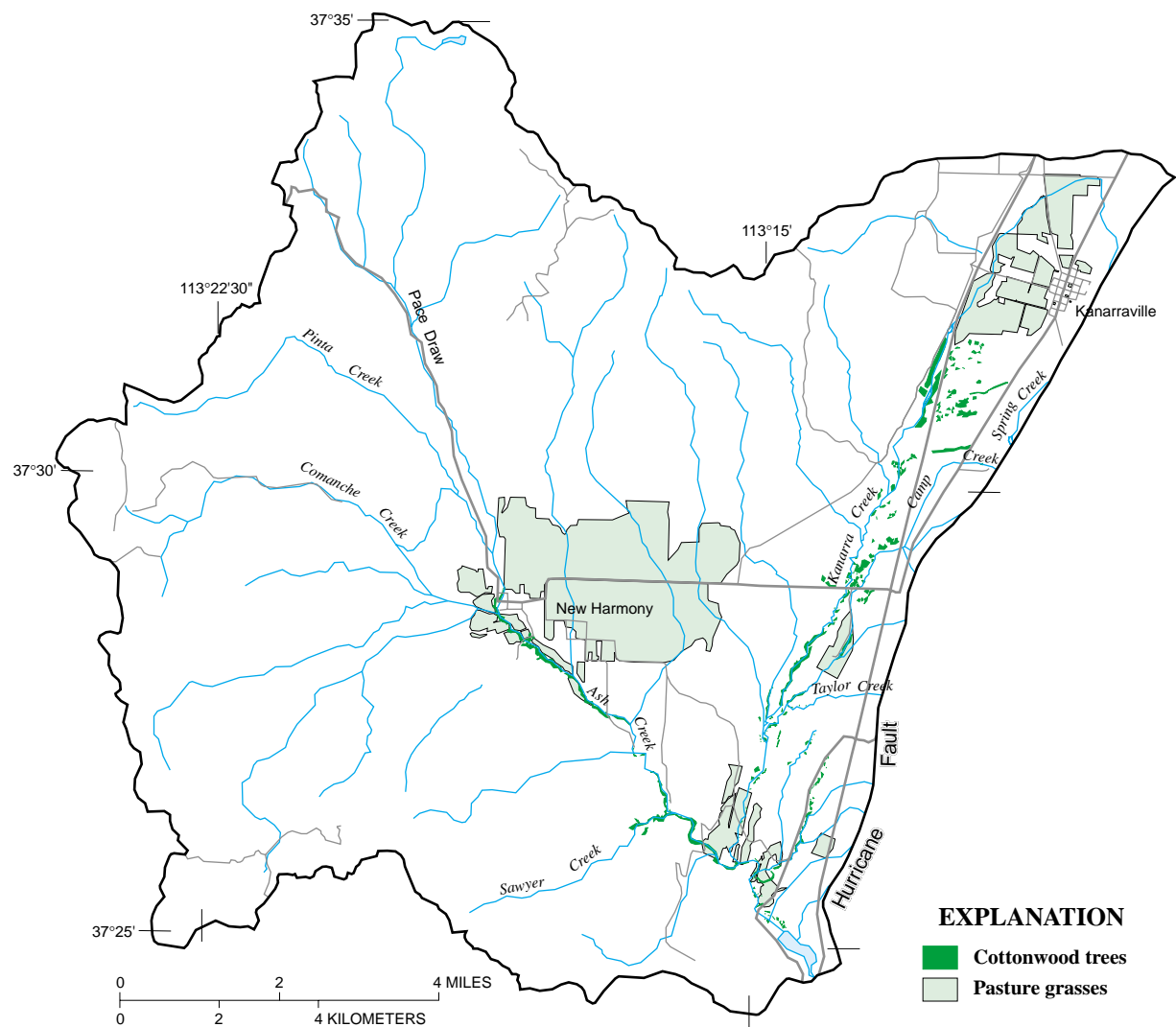


Figure 19. Areas of phreatophyte growth in the upper Ash Creek drainage basin, Utah.

1995, during a period of minimal evapotranspiration loss and inflow from runoff, showed that the stream gained about 1,400 acre-ft/yr, mostly in a 1.5- to 2-mi reach downstream from New Harmony (table 7, fig. 17). Sawyer Creek begins to flow at Sawyer Spring about 1/3 mi from its confluence with Ash Creek. This short reach, including Sawyer Spring, discharged about 1,100 acre-ft/yr from the Pine Valley monzonite aquifer in October 1995. Kanarra Creek begins to flow again about 1 mi upstream from its confluence with Ash Creek. In the first part of this perennial segment, the stream gained about 260 acre-ft/yr before losing flow in the last segment before the confluence. The seasonal and year-to-year variation in this discharge from the basin-wide aquifer system is unknown. The range of discharge by stream seepage is estimated to be 500 to 3,000 acre-ft/yr.

Subsurface Flow to Lower Ash Creek Drainage

The amount of ground water that potentially could discharge from the area as subsurface outflow through the deep alluvial deposits in the vicinity of Ash Creek Reservoir was estimated using Darcy's Law and approximations of aquifer geometry and water transmitting properties. Subsurface flow is calculated on the basis of the difference in water-level altitude in the aquifers at the reservoir and the aquifers to the south near Pintura, Utah. Well (C-39-13)25dcd-1, located about 3.5 mi south of Ash Creek Reservoir and finished in basalt, has a water level about 600 ft lower than the water level in the aquifer at the reservoir. This difference yields a head gradient of about 0.03 ft/ft. The aquifer through which ground water moves southward out of the upper Ash Creek drainage basin is of unknown thickness and width. However, on the basis of a descrip-

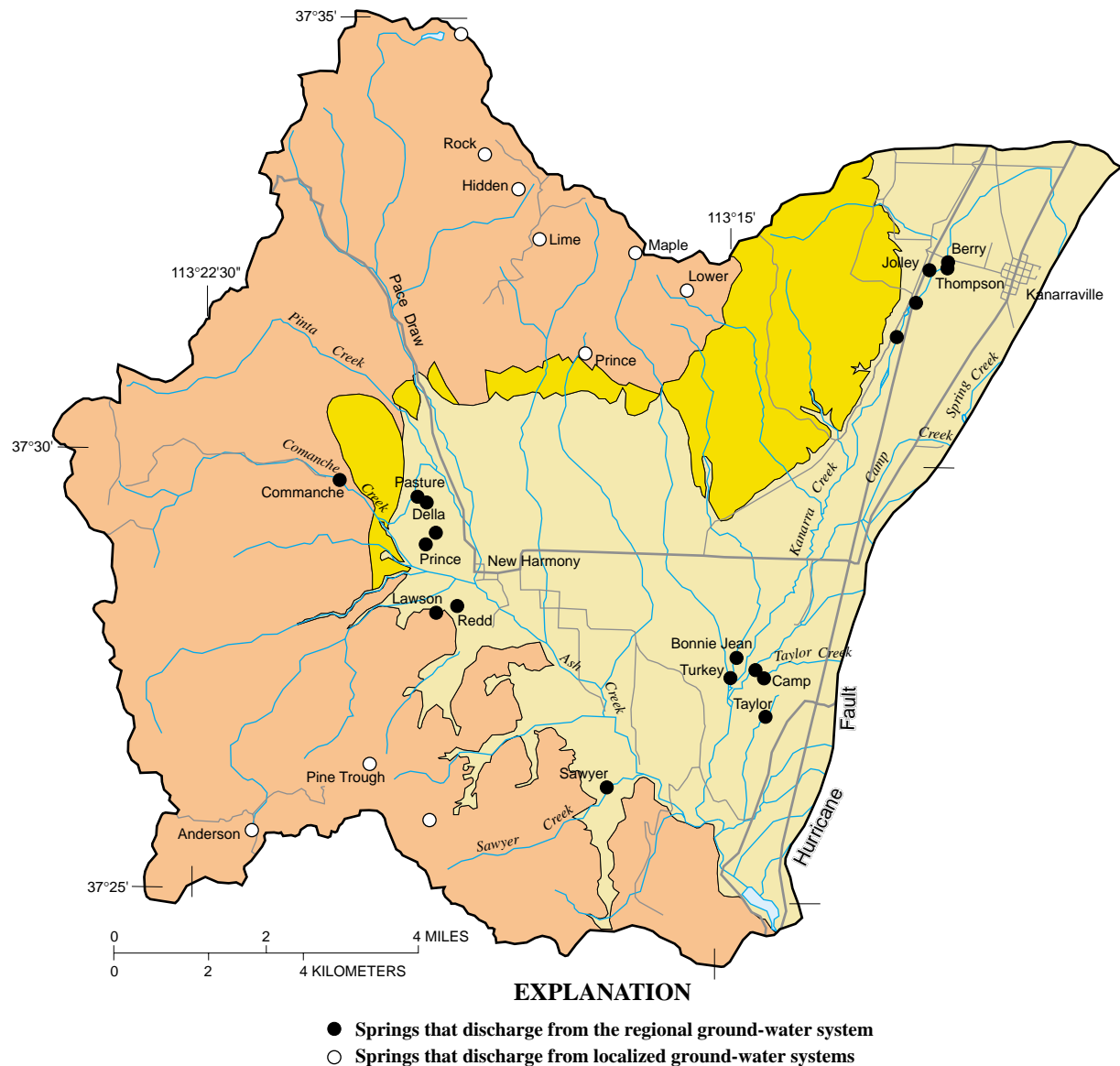


Figure 20. Location of local and regional springs in the upper Ash Creek drainage basin, Utah.

tion of the geologic framework by Hurlow (1998), thickness and width are estimated to be about 300 ft and 5,000 ft, respectively. Hydraulic conductivity of the interbedded alluvial deposits can be estimated to be similar to the lower values of the basin-fill aquifer because of compaction and cementation. A value of about 20 ft/d was estimated. Use of these numbers in Darcy's Law yields a maximum potential outflow of about 7,500 acre-ft/yr. Because of a general lack of information about geometry and hydraulics in this outflow area, this estimate is uncertain.

Ground-Water Budget

A compilation of potential inflow to and outflow from the upper Ash Creek drainage basin ground-water system is shown in table 9. Except for well discharge, all ground-water budget components have a large estimated range.

Navajo and Kayenta Aquifer System

The saturated parts of the Navajo Sandstone and Kayenta Formation, referred to in this section as the

Table 9. Estimated ground-water budget for the upper Ash Creek drainage basin, Utah

Flow component	Rate, in acre-feet per year	Rate, in cubic feet per second
Recharge		
Infiltration of precipitation	2,100 to 9,200	2.9 to 12.7
Seepage from ephemeral streams	¹ 3,500	4.8
Infiltration of unconsumed irrigation water	² 0 to 5,000	0 to 6.9
Seepage from perennial streams	500 to 1,100	0.7 to 1.5
Total	6,100 to 18,800	8.4 to 25.9
Discharge		
Well discharge	1,200 to 1,500	1.7 to 2.1
Evapotranspiration	1,100 to 15,000	1.5 to 20.7
Spring discharge (excludes Sawyer Spring)	200 to 1,000	0.3 to 1.4
Seepage to Ash, Sawyer, and Kanarra Creeks (includes Sawyer Spring)	500 to 3,000	0.7 to 4.2
Subsurface outflow to lower Ash Creek drainage	0 to 7,500	0 to 10.4
Total	3,000 to 28,000	4.2 to 38.8

¹This is likely a minimum value.

²Actual amount is thought to be nearer the lower end of this range.

Navajo and Kayenta aquifers, provide most of the potable water to the municipalities of Washington County, Utah. Because of large outcrop exposures, uniform grain size, and large stratigraphic thickness, these formations are able to receive and store large amounts of water. In addition, structural forces have created extensive fracture zones, enhancing ground-water recharge and movement within the aquifers. A generalized conceptualization of how water recharges to and discharges from the Navajo and Kayenta aquifers is shown in figure 21.

Aquifer System Geometry and Hydrologic Boundaries

The hydrologic boundaries of the Navajo and Kayenta aquifers are similar to the structural boundaries of the geologic formations. The aquifers are bounded to the east by the Hurricane Fault, which completely offsets these formations. Because the fine-grained fault-gouge material likely acts as a barrier to flow across the fault (discussed under “Hydrogeologic framework”), the Hurricane fault is assumed to be a lateral no-flow boundary. To conclusively determine if ground water crosses the fault into the Navajo Sandstone and Kayenta Formation to the west, it would be necessary to drill a pair of observation wells into the

Navajo Sandstone south of Hurricane, just west of fault, as well as into the formations just east of the fault.

Like the Hurricane Fault, the Gunlock Fault is assumed to be a lateral no-flow boundary that divides the Navajo and Kayenta aquifers within the study area into two parts: (1) the main part, located between the Hurricane and Gunlock Faults; and (2) the Gunlock part, located west of the Gunlock Fault. Hurlow (1998) states that little or no hydrologic connection likely exists across the Gunlock Fault. The Gunlock Fault completely offsets the Navajo Sandstone and Kayenta Formations (fig. 5) along the outcrop (Hintze and Hammond, 1994, pl. 1). The offset is unknown to the north where the Navajo Sandstone is buried by younger formations. Only a small amount of ground-water recharge to the Navajo aquifer is thought to occur where it is buried by poorly permeable overlying formations. Therefore, water within the buried parts of the Navajo aquifer is most likely stagnant, with little movement across the Gunlock Fault. Additional well drilling and aquifer testing would be needed to conclusively determine the exact hydrologic characteristics of the fault.

The southern boundaries of the Navajo Sandstone and Kayenta Formation are defined by their erosional extents (pl. 1). However, the formations are likely unsaturated along this southernmost edge, espe-

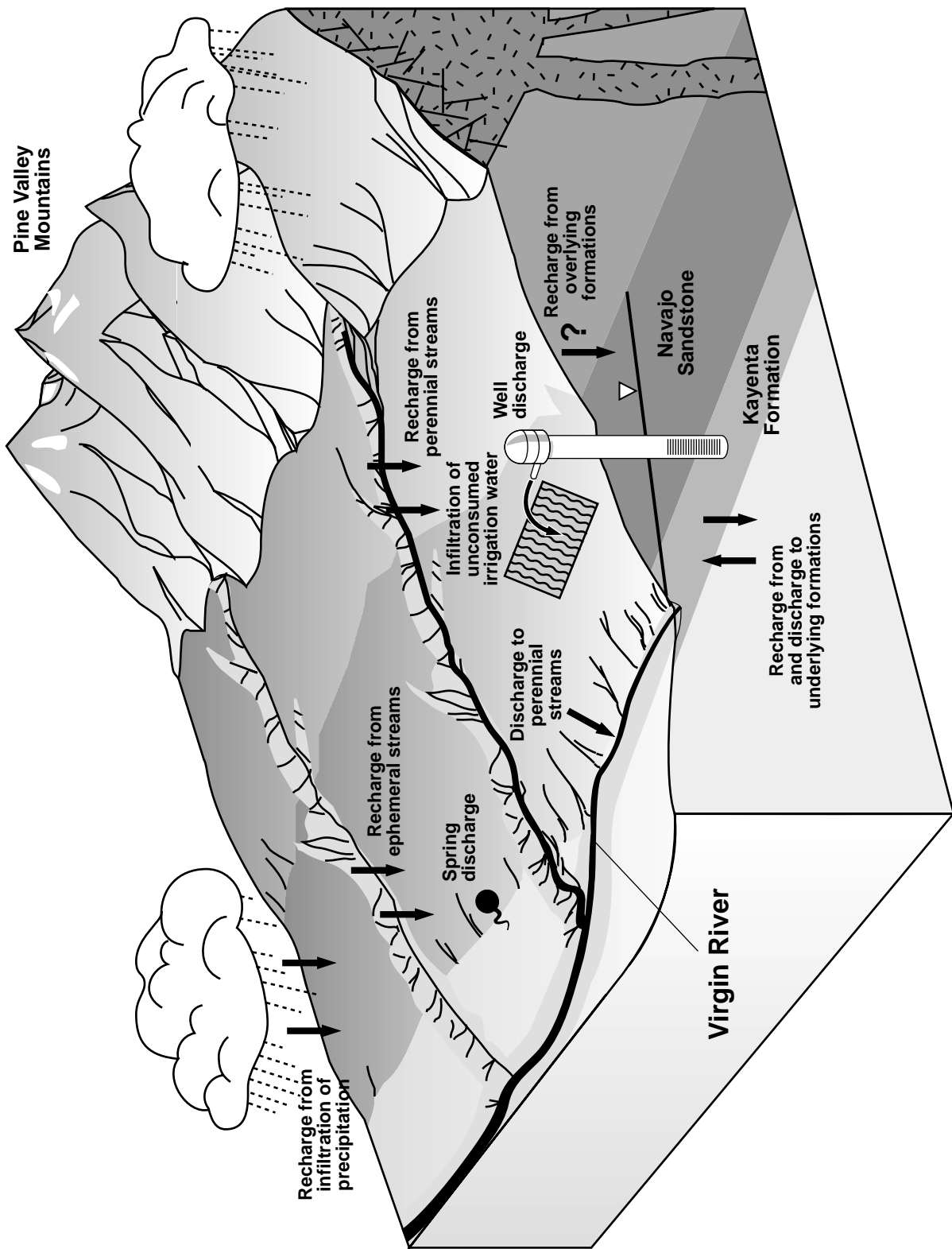


Figure 21. Generalized diagram showing sources of recharge to and discharge from the Navajo and Kayenta aquifers within the central Virgin River basin study area, Utah.

cially where they are locally uplifted, such as the southern part of the Red Mountains east of the Gunlock Fault. The Navajo Sandstone and Kayenta Formation become deeply buried toward the north. A structure contour map of the top of the Navajo Sandstone by Hurlow (1998, pl. 5B) indicates that the top of the Navajo Sandstone is about 8,000 ft below land surface (2,000 ft above sea level) in the Pine Valley Mountains. It is unknown how far to the north the Navajo Sandstone and Kayenta Formation extend under younger formations, but the ARCO Three Peaks #1 oil exploration drill hole 10 mi northwest of Cedar City (about 50 mi northeast of St. George) reached the top of the Navajo Sandstone at a depth of 6,286 ft beneath land surface (Van Kooten, 1988). Although the Navajo Sandstone and Kayenta Formation extend to the north beyond the study area, little recharge is thought to enter the aquifers where they are buried by younger formations. Therefore, it is assumed that little ground-water flow occurs in this region.

Because of the homogeneous nature of the Navajo Sandstone, the Navajo aquifer is assumed to be unconfined throughout the outcrop area. However, there may be local areas where the aquifer is confined as a result of variations in grain size, cementation, or bedding planes. One example of this is Winchester Hills well (C-41-16)24cba-1, where petrographic analysis of borehole cuttings indicated a 10-ft-thick layer of silt and clay at a depth of 850 ft. Another example is Washington County Water Conservancy District (WCWCD) Anderson Junction well (C-40-13)28dcc-1, where the driller noted that after water was reached at a depth of 190 ft, the water level rose in the borehole to a depth of 31 ft. However, such areas of confined conditions generally are not thought to be prevalent within the Navajo aquifer.

At some unknown distance north of the outcrop, the Navajo aquifer is assumed to become confined as it is buried by younger formations. A drillers' log from Dameron Valley Well (C-40-16)17dad-1 indicates that the Navajo Sandstone was reached at a depth of 440 ft with a reported water level of 1,280 ft beneath land surface (pl. 2), indicating unconfined conditions at this location about 1 mi north of the contact with younger formations. Assuming a flat potentiometric surface farther north (based on the assumption that little recharge reaches the aquifer where it is deeply buried) and a northeastward dip of the Navajo Sandstone of 3 to 10 degrees (Hurlow, 1998, pl. 5B), confined conditions may occur between 2 and 4 mi northeast of the outcrop in the Dameron Valley area. The location of the uncon-

fined/confined boundary of the Navajo aquifer north of the contact with younger formations would vary, depending on the local dip of the Navajo Sandstone and the altitude of the water table. The saturated thickness of the aquifer would be about 2,400 ft where confined and vary from 0 to 2,400 ft in the unconfined part.

The Navajo and Kayenta aquifers are assumed to be hydraulically connected. The potentiometric gradient between the two aquifers indicates that ground water moves from the Navajo aquifer to the Kayenta aquifer (Cordova, 1978). No observation wells have been finished exclusively in the Kayenta aquifer where it underlies the Navajo aquifer. However, if the potentiometric surface from wells along the Kayenta outcrop to areas where observation wells are finished in the Navajo aquifer is extended, the estimated vertical gradient between the Navajo and Kayenta aquifers is generally downward. Water-level differences are estimated to be less than 100 ft. Cordova (1978) suggested that ground-water movement from the Navajo aquifer to the Kayenta aquifer occurs along the entire part of the outcrop within the study area. This theory is based on (1) the general direction of ground-water movement, inferred from potentiometric maps, toward the escarpment that forms the erosional extent of the Navajo Sandstone outcrop; (2) the absence of natural discharge by springs, seeps, or phreatophytes along the escarpment above the base of the Navajo Sandstone; and (3) water levels at a few wells finished in both the Navajo Sandstone and the Kayenta Formation that indicate the saturated zone is in the Kayenta Formation. If a layer with low hydraulic-conductivity separates the two aquifers, this would be manifested by substantial discharge along the contact between the Navajo Sandstone and Kayenta Formation. Rather, most of the natural discharge from the aquifer system occurs within the Kayenta Formation, which indicates a less permeable boundary at or near the base of the Kayenta Formation.

The lowest part of the Kayenta Formation consists of siltstones and mudstones (Hurlow, 1998) that are relatively impervious and most likely act as a confining layer at the base of the Navajo and Kayenta aquifer system. Evidence for this hydrologic boundary includes (1) many springs that emanate from the lower part of the Kayenta Formation between Santa Clara and St. George; (2) seepage studies that show gain in the Santa Clara River as it crosses the lower Kayenta Formation; and (3) the Sullivan flowing well (C-41-13)16bcd-1, which is an artesian well drilled along the Kayenta Formation outcrop near Sandstone Mountain but is finished in the underlying Springdale Sandstone

member of the Moenave Formation (Wilkowske and others, 1998, table 1). There may be localized areas, however, where through-going fractures may act as conduits for vertical ground-water movement across this lower boundary, such as are hypothesized for (1) the higher dissolved-solids parts of the aquifer north of St. George and east of Hurricane (discussed under the “Sources of salinity to the Navajo and Kayenta aquifers” section); and (2) locations where seepage to the Santa Clara and Virgin Rivers occurs as they traverse older sedimentary layers underlying the Kayenta Formation.

Like the Navajo aquifer, the Kayenta aquifer is unconfined along its outcrop. Because of its hydraulic connection to the Navajo aquifer, the transition to confined conditions within the Kayenta aquifer likely is the same as in the Navajo aquifer—toward the north where both formations become deeply buried.

Aquifer Properties

Knowledge of aquifer properties is necessary to understand the occurrence of ground water. These properties include (1) effective porosity, (2) hydraulic conductivity or transmissivity, and (3) storage capacity. Aquifer properties are typically estimated from laboratory analyses and multiple-well aquifer testing.

Navajo Aquifer

The Navajo Sandstone is well sorted, as is shown by grain-size distribution curves (Cordova, 1978, fig. 2). Average total porosity, determined from resistivity and neutron logs of 13 boreholes in the Navajo Sandstone within the study area, is about 32 percent (Cordova, 1978, table 4). Effective porosity, determined from laboratory analysis of 12 rock samples from selected outcrops within the study area, is about 17 percent (Cordova, 1978, table 3).

Because of the uniformly well-sorted lithologic character of the Navajo Sandstone throughout the study area, variations in hydraulic conductivity are most likely caused by secondary fracturing, both vertical and along bedding planes. Laboratory analysis of rock samples from eight outcrop locations within the study area indicate that average saturated hydraulic conductivity of the Navajo aquifer is about 2.1 ft/day (Cordova, 1978). Because these outcrop samples were collected along the outcrop, the measured hydraulic-conductivity values are probably higher than the actual matrix hydraulic conductivity because of weathering. Dissolution of the cement surrounding the silica grains during

weathering would likely increase the effective permeability of the rock samples.

As part of the study, aquifer tests were done within the Navajo aquifer at Anderson Junction (WCWCD wells), Hurricane Bench (Winding Rivers wells), Grapevine Pass (Washington City well), and downstream from Gunlock Reservoir (St. George City wells) (table 10, appendix A). Transmissivity determined from these tests ranged from 100 to 19,000 ft²/d, corresponding to horizontal hydraulic-conductivity values of 0.2 to 32 ft/d. Higher hydraulic-conductivity values are assumed to be associated with highly fractured parts of the aquifer. Hydraulic conductivity was highest at the Anderson Junction site and ranged from 1.3 ft/d along the north-northeast direction to 32 ft/d along the east-southeast direction. Hurlow (1998, p. 27) stated that “the Navajo Sandstone in this area is densely fractured and is cut by numerous northeast-striking faults, implying relatively high permeability.” The lowest hydraulic-conductivity value of 0.2 ft/d was at Grapevine Pass. Although surface fractures are present nearby, little fracturing can be seen at the site itself (Hugh Hurlow, Utah Geological Survey, oral commun., 1997). In addition, petrographic analysis of borehole cuttings from the Grapevine Pass well showed much finer average grain size than samples from other Navajo Sandstone wells, possibly indicating a much thicker transition zone at the base of the Navajo Sandstone than at other locations (Janae Wallace, Utah Geological Survey, oral commun., 1997).

Results of the aquifer tests downstream from Gunlock Reservoir and at Anderson Junction indicate that fracture-related anisotropy can strongly influence directional permeability within the Navajo aquifer. The north-south directional anisotropy of hydraulic-conductivity values (1.0 ft/d north-south and 0.3 ft/d east-west) determined from the Gunlock Reservoir aquifer test (appendix A) is consistent with observations of large-scale fracturing aligned north-south parallel to the Santa Clara River, and with one of the three areal photograph rose diagrams from nearby outcrops. However, surface-fracture orientation data are not always consistent with the anisotropic hydraulic-conductivity values determined from aquifer tests. This is because the subsurface connectivity of fractures strongly influences anisotropy in hydraulic conductivity, which can only be predicted from rose diagrams in the simplest cases. At the Gunlock test site, the scan-line rose diagrams of the outcrop and two of the three rose diagrams based on areal photographs indicate that the predominant fracture orientation generally is in the east-west

Table 10. Aquifer-test results from the Navajo aquifer, central Virgin River basin study area, Utah
(See appendix A for additional information; \pm , plus or minus)

Location	Pumping well number	Number of observation wells	Pumping/recovery period (days)	Horizontal hydraulic conductivity (feet/day)	Saturated thickness (feet)	Transmissivity (feet squared per day)	Storage coefficient
Anderson Junction	(C-40-13)28dcb-2	2	4	1.3 to 32	600	¹ 800 \pm 19% to 19,000 \pm 21%	.0007 to .0025
Hurricane Bench	(C-42-14)12dbb-2	5	5	2.2	500	1,075	.002
Grapevine Pass	(C-41-15)28dcb-2 (single-well test)	0	1	.2	500	100	—
Downstream from Gunlock Reservoir	(C-41-17)8acc-1	6	6	.3 to 1.0	1,100	360 to 1,100	.001

¹See figure A-8.

direction (Hurlow, 1998, pl. 6) rather than north-south direction, as indicated by aquifer testing. At Anderson Junction, the direction of maximum transmissivity indicated by aquifer testing is in the east-southeast orientation, yet the rose diagram of scan-line outcrop data indicates that the predominant orientation of surface fracturing is north-northeast. Anisotropy could not be determined from the aquifer-test results at the Hurricane Bench and Grapevine Pass sites because of the lack of observation wells.

Although there may not be a direct correlation between the direction of maximum aquifer transmissivity and the predominant orientation of surface fracturing at nearby outcrops, a strong correlation was shown between hydraulic-conductivity estimates based on specific-capacity data and the product of fracture density and average aperture (Hurlow, 1998, fig. 14). Thus, although inferring the direction of aquifer anisotropy from surface-fracture orientation data remains uncertain, other outcrop fracture data such as fracture density and aperture (fracture width) can provide a good indication of the degree of permeability enhancement caused by fracturing. Such data would be valuable in locating potentially high-yielding production wells in the Navajo aquifer.

Cordova (1978) reported the results of multiple-well aquifer tests in the Navajo aquifer at three sites: below the Gunlock Reservoir, City Creek, and Hurricane Bench. However, all of the measurements at

observation wells during that study were problematic. Measurements during the Gunlock test did not include monitoring of Santa Clara River discharge. Because decreases in stream discharge were noted during this study's aquifer test in the Gunlock area, streamflow likely was induced into the aquifer. Assuming that this leakage was unaccounted for, transmissivity and storage values determined from observation-well measurements are not accurate. The aquifer test at City Creek was not a constant-drawdown test. Instead, a step-drawdown test was done, pumping first at 470 gal/min and then at 1,100 gal/min. However, an average pumping rate was used for the analysis that resulted in inaccurate determinations of transmissivity and storage. Finally, aquifer-test results at Hurricane Bench were considered inaccurate because water from the pumped well was not removed from the site and infiltrated the saturated zone, affecting observation-well drawdown measurements.

Two other aquifer tests done by Cordova (1978) at Mill Creek and City Creek did not produce drawdown at any observation wells, so the reported transmissivity values were based only on drawdown in the pumped wells. However, assuming that a constant pumping rate was maintained and the pumped water was removed sufficiently far from the site, the reported transmissivity and hydraulic-conductivity values of 2,400 ft²/d and 3.4 ft/d for the Mill Creek site and 5,000 ft²/d and 5.0 ft/d for the City Creek site may be reasonable.

No aquifer testing was done to determine vertical hydraulic conductivity of the Navajo aquifer within the study area. Horizontal and vertical hydraulic-conductivity values determined from laboratory analysis of Navajo Sandstone samples within the Upper Colorado River Basin were compiled by Weigel (1987, table 5). The average vertical and horizontal hydraulic conductivity of 24 samples was about 0.8 ft/d and 1.1 ft/d, respectively. The ratio of vertical to horizontal hydraulic-conductivity values for the 24 pairs of samples ranged from 0.13 to 2.7, averaging about 0.4. However, these discrete vertical samples may not be an accurate representation of the vertical hydraulic conductivity or vertical-to-horizontal anisotropy ratios for the Navajo aquifer within the study area. The lowest vertical hydraulic conductivity of a layered sedimentary formation controls the overall vertical hydraulic conductivity of that layer. Therefore, it is likely that in some regions of the Navajo aquifer, the vertical movement of ground water may be more restricted than is indicated by the average of the laboratory-determined values. Lower overall vertical hydraulic-conductivity values and vertical-to-horizontal hydraulic-conductivity ratios may result from thin, low-permeability horizontal layers that consist of fine-grained interdunal deposits or have greater-than-average cementation that may not be within the sampled zone for laboratory analyses. Conversely, vertical fracturing would greatly increase the vertical hydraulic conductivity and vertical-to-horizontal hydraulic-conductivity ratios for the aquifer above the laboratory ratios.

Storage values for the Navajo aquifer were determined from the three multiple-well aquifer tests done during this study and ranged from 0.0007 to 0.0025 (both from the Anderson Junction site). This narrow range indicates the general uniformity of storage values for the Navajo aquifer within the study area. Because storage values less than 0.001 generally indicate confined storage (Lohman, 1979), the aquifer-test results indicate that the Navajo aquifer acts as a partly confined system. However, the Navajo Sandstone, as indicated above, is generally homogeneous and well sorted. Drillers' logs and lithologic logs generally do not indicate finer grain-size layers, which normally are associated with confined conditions. One possible explanation is the existence of very thin fine-grained zones or increased cementation associated with bedding planes within the sandstone that are too small to be detected from borehole cuttings. Another explanation is that the small storage values may be a combination of short durations of aquifer testing and observation-well

perforated intervals far below the water table. Although the tests showed a short-term confined response at the observation wells, longer-term drawdown observations at these wells might yield higher storage values, approaching the 17-percent effective porosity determined by Cordova (1978).

Kayenta Aquifer

No aquifer testing was done to determine the horizontal or vertical hydraulic conductivity of the Kayenta aquifer as part of this study. However, an earlier multiple-well aquifer test by Cordova (1978) at the Goddard and Savage well (C-41-13)5bbc-1 near Leeds (Wilkowske and others, 1998, table 1) indicated a transmissivity of 3,500 ft²/d. The geology of this area is complicated by the Virgin River Anticline and associated faulting, which precludes an exact determination of the saturated thickness. However, assuming a saturated thickness of about 600 ft at the site, the estimated hydraulic conductivity is about 6 ft/d. This value is similar to the higher hydraulic-conductivity values for the Navajo aquifer and may indicate a highly fractured area within the Kayenta aquifer.

Additionally, Cordova (1972, table 11) reported a horizontal hydraulic-conductivity value of 1 ft/d on the basis of specific-capacity data from a well in St. George. The storage value estimated from this specific-capacity data is 0.006. Also, estimated horizontal hydraulic conductivity from slug tests in the Kayenta Formation near Sheep Springs, about 2 mi northwest of St. George, ranged from 0.1 to 0.6 ft/d (Jensen and others, 1997).

Horizontal and vertical hydraulic-conductivity values were determined from laboratory analysis of Kayenta Formation samples within the Upper Colorado River Basin, Utah and Colorado (Weigel, 1987, table 5). The average horizontal hydraulic-conductivity value of 12 core samples was about 0.5 ft/d and ranged from 8.2×10^{-4} to 1.4 ft/d. The vertical hydraulic-conductivity value of two samples ranged from 8.2×10^{-4} to 0.5 ft/d. The large range in values reflects the alternating siltstone, silty mudstone, and sandstone layers within the formation. The ratio of vertical-to-horizontal hydraulic conductivity for these two samples ranged from 0.36 and 1.0. As with laboratory analyses of core samples from the Navajo aquifer, these discrete vertical samples may not be an accurate representation of the hydraulic conductivity or vertical-to-horizontal anisotropy ratios for the Kayenta aquifer. Also, hydraulic properties of the Kayenta aquifer may vary regionally

between the Upper Colorado River Basin and the central Virgin River basin.

As in the Navajo aquifer, fracturing within the Kayenta Formation is thought to enhance the permeability of the aquifer. Sheep Springs, which emanate from a fracture zone in the Kayenta Formation, is evidence of this. In the vicinity of Sheep Springs, the predominant joints are orientated north-south and have a near-vertical dip (Jensen and others, 1997, fig. 21, 22). This is similar to the predominant north-south direction and vertical dip of the Navajo Sandstone fractures at nearby outcrops between City Creek and Snow Canyon (Hurlow, 1998, pl. 6). Therefore, it generally is assumed that directional anisotropy of hydraulic conductivity within the Kayenta aquifer is similar to that in the Navajo aquifer.

Recharge

The Navajo and Kayenta aquifers are recharged primarily by infiltration of precipitation on the Navajo Sandstone and Kayenta Formation outcrop and seepage from streams crossing the outcrop. Additional sources of recharge include seepage from overlying and underlying formations, infiltration of unconsumed irrigation water, and seepage from Gunlock Reservoir. The total amount of recharge for the main and Gunlock parts of the aquifer is estimated to range from 12 to 49 ft³/s (about 8,700 to 36,100 acre-ft/yr) and from 2 to 10 ft³/s (about 1,400 to 7,300 acre-ft/yr), respectively.

Precipitation

Infiltration of precipitation as either rain or snow on the Navajo Sandstone and Kayenta Formation outcrop is thought to be the largest source of recharge to the main aquifer but not the Gunlock part of the aquifer. The total average annual precipitation on the outcrop is estimated to be about 205 ft³/s (148,800 acre-ft/yr) and 18.5 ft³/s (13,400 acre-ft/yr), respectively, for the main and Gunlock parts of the aquifers. The percentage of precipitation that moves through the unsaturated zone to the water table is assumed to vary widely based on such factors as topographic slope, density of fractures extending to the surface, surficial material on the outcrop, season, vegetation, and storm intensity.

The topography of Navajo Sandstone and Kayenta Formation outcrops within the study area ranges from steep escarpments to nearly flat surfaces. Rapid runoff and potentially lower infiltration rates are characteristic of the steeper sloped areas, whereas slower runoff and potentially higher infiltration rates are char-

acteristic of the more flatter areas. The outcrop surface consists of areas of consolidated rock, unconsolidated sand, and fractured basalt. The exposed sandstone and siltstone along the outcrop varies from highly fractured to relatively unfractured. Fractures that are exposed along the outcrop can greatly enhance recharge by providing conduits for rapid transport of water to the saturated zone (Pruess, 1998). Also, infiltration rates likely are higher where thin surficial deposits of sand and basalt cover the outcrop. Sand deposits can trap and temporarily store precipitation that would otherwise run off of unfractured areas of the outcrop, allowing more time for infiltration into the consolidated rock outcrop (Dincer and others, 1974). Likewise, fractured basalt can rapidly transmit water beneath the evapotranspiration zone and result in more available recharge.

Once infiltration to the subsurface occurs, evaporation from the shallowest part of the unsaturated zone can occur and reduce recharge, especially during the warmer seasons. Similarly, in areas of thick vegetative cover, much of the potential recharge to the aquifer can be intercepted within the evapotranspiration (root) zone during the warmer seasons. The frequency and intensity of precipitation also are important factors that affect the amount of recharge. Recharge from short-lived storms with small amounts of precipitation is probably minimal, with most of the water intercepted in the shallow subsurface by evapotranspiration. However, long-lasting storms of high precipitation intensity, especially during the winter months when evaporation and evapotranspiration effects are minimal, likely account for a large part of recharge to the aquifer. The increased soil-moisture content during longer precipitation events greatly increases the effective permeability of the unsaturated sandstone and its ability to transmit water downward toward the saturated zone.

Recharge to the Navajo and Kayenta aquifers is estimated to be from 5 to 15 percent of precipitation on the outcrop, and ranges from about 10 to 30 ft³/s (7,200 to 21,700 acre-ft/yr) for the main part and from about 1 to 3 ft³/s (700 to 2,200 acre-ft/yr) for the Gunlock part. No measurements of the infiltration rates were taken during this study. The minimum estimated infiltration rate is based on a study site in New Mexico in fine-grained soils (Scanlon, 1992). The infiltration rate from tritium analysis of unsaturated-zone pore water was estimated to be about 4.8 percent of the 8-in. average annual precipitation. This infiltration rate is assumed to be at the low end of recharge to the outcrop in the study area because (1) average annual precipitation on the

outcrop ranges from 8 to 19 in. and the rate of infiltration is generally assumed to increase in areas of higher precipitation; (2) the study area has lower average annual temperatures and lower potential soil-water evaporation than the New Mexico site; and (3) the surficial material along the outcrop (sand dunes, fractured basalt, and fractured sandstone) may capture and transport water to the saturated zone more readily than the soils at the New Mexico study sites. The maximum 15-percent infiltration rate is based on estimated recharge along consolidated-rock outcrops in Tooele County, Utah, where average annual precipitation ranges from 16 to 20 in/yr (Hood and Waddell, 1968, table 5). Also, a study of recharge beneath the Dahna sand dunes in Saudi Arabia, where annual precipitation is much less, indicated infiltration rates of as much as 29 percent (Dincer and others, 1974). The measured infiltration rate in Saudi Arabia may be higher than along sand dunes overlying the Navajo aquifer because the Dahna sand is coarser grained.

Streams

Seepage from streams traversing the Navajo Sandstone and Kayenta Formation outcrop is another important source of ground-water recharge to the Navajo aquifer. Six of the seven perennial streams that traverse the outcrop in the study area had a net loss of water from the stream into the Navajo aquifer. Also, numerous ephemeral washes traverse the outcrop and most likely are an additional source of recharge to the Navajo aquifer.

Perennial Streams

All six perennial streams which originate in the Pine Valley Mountains and traverse the outcrop recharge the Navajo aquifer. These streams include South Ash Creek, Wet Sandy Creek, Leeds Creek, Quail Creek, Cottonwood Creek/Heath Wash, and the Santa Clara River (fig. 22). Total recharge to the Navajo aquifer from these perennial streams was estimated from seepage studies to range from 1.8 to 4.4 ft³/s (1,300 to 3,200 acre-ft/yr) and from 0.78 to 4.1 ft³/s (570 to 3,000 acre-ft/yr) for the main and Gunlock parts of the Navajo and Kayenta aquifers, respectively. The Virgin River, which traverses the outcrop near Sand Mountain, is the only perennial stream that did not show net seepage to the aquifer during seepage studies.

Reconnaissance-level seepage studies were done along all of the perennial creeks that originate in the Pine Valley Mountains and traverse the outcrop. These

studies were done from October through December 1995, during base-flow conditions when little or no evapotranspiration was occurring. Therefore, measured loss in streamflow was assumed to be recharge to the Navajo aquifer. Streamflow was measured in the Santa Clara River, Leeds Creek, and Quail Creek where the streams first cross the contact between the Navajo Sandstone and the overlying Carmel Formation, and again where the streams cross the contact between the Navajo Sandstone and the Kayenta Formation. The downstream measurement in South Ash Creek was at the contact with unconsolidated Quaternary sediments, about 0.7 mi upstream from the contact between the Navajo Sandstone and the Tertiary formations (pl. 1). The downstream measurement in Wet Sandy Creek was at the contact with unconsolidated Quaternary sediments about 2 mi upstream from where it was noted to be dry as the wash crosses underneath highway I-15. Streamflow was measured in Cottonwood Creek (and the Heath Wash tributary) at the Navajo Sandstone/Carmel Formation contact, and the stream was observed to be dry at the Navajo Sandstone/Kayenta Formation contact. Estimated recharge from perennial streams on the basis of the seepage studies is shown in table 11. The estimated recharge to the Navajo aquifer from perennial streams may be low because the seepage studies were done during base-flow conditions. Higher flow conditions would increase the stage and width of the stream and should increase recharge from the stream to the aquifer.

Decreases in streamflow were measured for all perennial streams that cross the outcrop (fig. 22). Upper Cottonwood, Quail, Wet Sandy, and South Ash Creeks had measured seepage losses of 0.47 ft³/s (360 acre-ft/yr), 0.19 ft³/s (140 acre-ft/yr), 0.37 ft³/s (270 acre-ft/yr), and 1.38 ft³/s (1,000 acre-ft/yr), respectively (table 11). Although seepage studies along Leeds Creek on 10/07/95 and 12/07/95 showed small net gains in streamflow as the creek crossed the outcrop, these gains were within the error limitations of the measurement equipment. Therefore, these two seepage studies were determined to be inconclusive. An earlier seepage study by Cordova (1978) indicated a seepage loss from Leeds Creek to the Navajo aquifer of 0.22 ft³/s (160 acre-ft/yr).

Downstream from the Navajo Sandstone outcrop, Wet Sandy and South Ash Creeks flow along Quaternary alluvial deposits that overlie the Navajo Sandstone (pl. 1). During the October 1995 seepage study, discharge in Wet Sandy Creek decreased along this reach of coarse alluvium from 0.63 ft³/s, eventually drying

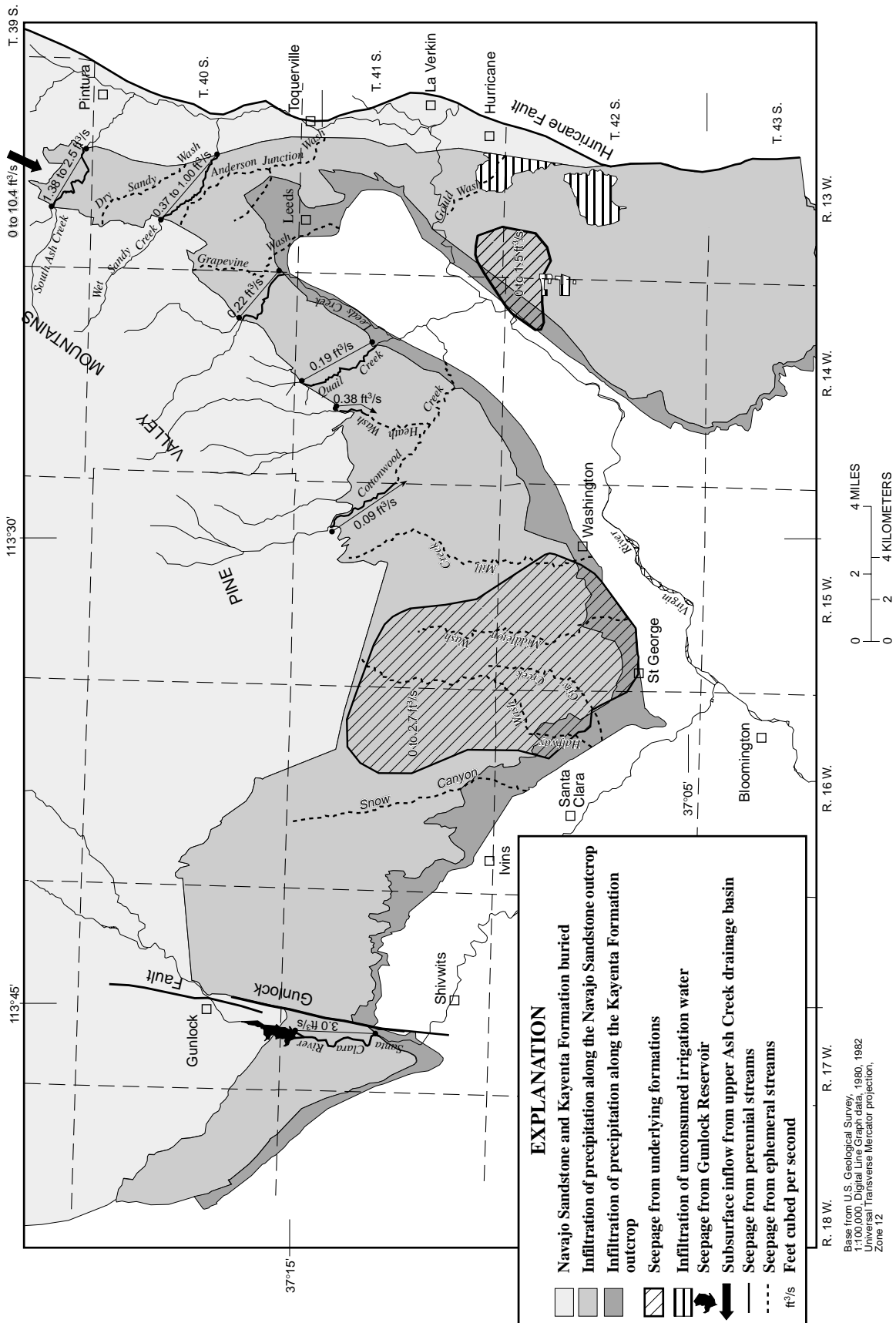


Figure 22. Potential sources of recharge to the Navajo and Kayenta aquifers in the central Virgin River basin study area, Utah.

Table 11. Seepage measurements and estimated recharge from perennial streams to the Navajo aquifer in the central Virgin River basin, Utah

[acre-ft/yr, acre-feet per year; ft³/s, cubic feet per second; NA, not available]

Stream	Average annual discharge from streamflow-gaging stations (acre-ft/yr)	Date	Upper discharge measurement, (ft ³ /s)	Lower discharge measurement, (ft ³ /s)	Measured seepage from stream, (ft ³ /s)	Estimated recharge to aquifer, in ft ³ /s (acre-ft/yr)
Main part of Navajo aquifer¹						
Cottonwood Creek (upper) ²	NA	10/08/95	.47	0	.47	.47 (360)
Quail Creek	NA	10/24/95	3.537	.345	.19	.19 (140)
Leeds Creek	45,610	12/07/95	4.99	5.27	5NA	0 to ⁶ .22 (160)
Wet Sandy	NA	10/06/95	1.00	.63	.37	.37 to ⁷ 1.00 (270 to 720)
South Ash Creek	85,000	10/09/95	3.58	2.20	1.38	6.48 to ⁹ 3.6 (350 to 2,600)
Total (rounded)						1.5 to 5.5 (1,300 to 4,000)
Gunlock part of Navajo aquifer						
Santa Clara River	¹⁰ 17,170	12/06/95 02/15/96	18.8 .78	14.7 0	4.1 .78	¹¹ .78 to 4.1 (570 to 3,000)

¹ Combination of discharge in Bitter Creek and Heath Wash.

² A seepage study was done for upper Cottonwood Creek, however, it is only a perennial stream along the upper part of Navajo Sandstone outcrop.

³ Combination of discharge in Quail Creek and Water Canyon.

⁴ Based on measurements from USGS streamflow-gaging station 0940800 for water years 1965-1996 (Herbert and others, 1997).

⁵ Because of possible measurement error (as much as 10 percent), the upper contact and lower contact discharge values are too close to quantify seepage.

⁶ Based on a USGS seepage study reported by Cordova (1978, p. 17).

⁷ Assumes all seepage to the subsurface through alluvial deposits recharges the Navajo aquifer.

⁸ Based on measurements from USGS streamflow-gaging station 09406700 for water years 1966-82 (ReMillard and others, 1982).

⁹ Assumes all seepage to the subsurface through alluvial deposits recharges the Navajo aquifer.

¹⁰ Based on USGS streamflow-gaging station 09410100 for water years 1973-96 (Herbert and others, 1997).

¹¹ Average annual recharge is estimated to be 3.0 cubic feet per year based on a seepage rate of 4.1 ft³/s for 8 months per year and 0.78 ft³/s for 4 months per year.

out before the reach crossed under Interstate I-15. Therefore, in addition to the measured 0.37 ft³/s seepage loss along Wet Sandy Creek as it traversed the outcrop, it is probable that there was 0.63 ft³/s of seepage to the Navajo aquifer through overlying alluvial deposits. Similarly, the flow in South Ash Creek decreased from 2.2 ft³/s along Quaternary alluvial deposits downstream of the outcrop, eventually drying out before the reach crossed under Interstate I-15. Therefore, in addition to the measured 1.38 ft³/s seepage loss along South Ash Creek as it traversed the outcrop, it is possible that there was up to 2.2 ft³/s of seepage to the Navajo aquifer through overlying alluvial deposits. Thus, total recharge to the Navajo aquifer during these base-flow conditions was up to 1.00 ft³/s (720 acre-ft/yr) along Wet Sandy Creek and 3.6 ft³/s (2,600 acre-ft/yr) along South Ash Creek.

Because the city of St. George diverts several large springs that previously flowed into Cottonwood Creek, this once perennial stream flows year round only in the upper section of its reach along the outcrop. On the basis of a 15-year record from the city of St. George, an average of 2,500 acre-ft/yr of water from springs is diverted from the upper Cottonwood Creek drainage. During the seepage study, the creek bed was dry along the lower two-thirds of its reach as it traverses the outcrop. Therefore, it is assumed that the base-flow component of the creek is removed by diverting the springs, effectively shortening its perennial reach. Observations by local residents indicate that after a precipitation event, Cottonwood Creek remains flowing longer than other nearby ephemeral drainages (Morgan Jenson, Washington County Water Conservancy District, oral commun., 1998). This is consistent with the assumption that Cottonwood Creek was perennial along the entire

reach that traverses the Navajo Sandstone prior to spring development by the city of St. George.

Discharge in the Santa Clara River traversing the Navajo Sandstone and Kayenta Formation outcrop is controlled by releases from Gunlock Reservoir. Discharge records from the Gunlock Reservoir outlet beginning in 1971 (Utah State Division of Water Rights, written commun., 1998) indicate that water is released from the reservoir for about 8 months per year. Discharge from the reservoir averages about $20 \text{ ft}^3/\text{s}$ during this period (Rodney & Helen Leavitt, written commun., 1998). When the reservoir release valve is closed (for about 4 months per year), about $0.8 \text{ ft}^3/\text{s}$ seeps from the base of the dam into the stream channel. Two seepage studies were done on the Santa Clara River during winter when little or no evapotranspiration is thought to occur. The first seepage study, during which $18.8 \text{ ft}^3/\text{s}$ was being released from the reservoir, indicated that $4.1 \text{ ft}^3/\text{s}$ of seepage loss occurred. The second seepage study, during which the release valve was shut and streamflow was $0.78 \text{ ft}^3/\text{s}$, indicated that $0.78 \text{ ft}^3/\text{s}$ of seepage loss occurred because the stream stopped flowing a few miles downstream from the dam. If the higher seepage rate of $4.1 \text{ ft}^3/\text{s}$ occurs on average 8 months per year and the lower seepage rate to occur on average 4 months per year, the average annual seepage rate from the Santa Clara River into the Navajo aquifer is estimated to be about $3.0 \text{ ft}^3/\text{s}$ (table 11). A seepage study done by the USGS in 1974 (Cordova, 1978) indicated a seepage gain into the river along the same reach of about $1.5 \text{ ft}^3/\text{s}$. This indicates that a reversal of head gradient between the aquifer and the river has occurred since 1974, most likely as a result of increased discharge at the St. George municipal well field.

Geochemical evidence also indicates that most of the water that recharges the St. George municipal well field in the Gunlock part of the Navajo aquifer (west of the Gunlock Fault) originates as seepage from the Santa Clara River. A trilinear plot of major-ion chemistry of water from both the Santa Clara River and the St. George municipal well field near Gunlock is shown in figure 23. With the exception of the water sample of St. George City Gunlock Well #2, the ground-water samples have a geochemical signature very similar to that of Santa Clara River water sampled near Gunlock and Windsor Dam. This indicates that most of the recharge to the municipal well field is from seepage from the Santa Clara River and Gunlock Reservoir where they cross the Navajo Sandstone and Kayenta Formation outcrop. Gunlock Well #2, located about 1,500 ft from

the Santa Clara River, contains water with higher dissolved-solids concentrations than the other wells, including higher concentrations of sulfate and chloride (fig. 15; Wilkowske and others, 1998, tables 1 and 4). This well, located farther from the Santa Clara River than the other St. George City municipal wells, was drilled closer to the base of the Navajo Sandstone and Kayenta Formation than the other wells. Thus, it may receive part of its recharge from infiltration of precipitation or upward movement of water from underlying formations.

CFC data also indicate that the Santa Clara River is a source of recharge to the Navajo aquifer. Seven wells in the Gunlock part of the Navajo aquifer and four surface-water sites along the Santa Clara River were sampled for CFCs (fig. 24). Average CFC-12 concentrations from Gunlock Wells #7 and #8, east of the Santa Clara River, were about 0 and 0.11 pmoles/kg , respectively, indicating apparent recharge ages from pre-1950 to 1958 (table 4; fig. 25). These values are much lower than for wells adjacent to the Santa Clara River on the west side. Gunlock Wells #3, #4, and #5, west of the Santa Clara River, had measured CFC-12 concentrations of about 0.35 , 0.42 , and 1.14 pmoles/kg , respectively, indicating apparent recharge ages from 1966 to 1977 (table 4; fig. 25). The average CFC-12 concentration at four sites along the Santa Clara River was about 1.5 pmoles/kg (table 4). The analysis of the CFC-12 data indicates that in the area of the St. George municipal well field, the Santa Clara River recharges the Navajo aquifer to the west. This is consistent with (1) general-chemistry data that show that the Santa Clara River is likely the principal source of recharge to this part of the Navajo aquifer, (2) seepage studies along the Santa Clara River that show it to be a losing reach in the area of the well field, and (3) contoured water-level data from the well field that show the direction of ground-water flow from northeast to southwest under the river (fig. 26).

Ephemeral Streams

Two methods for estimating recharge to the Navajo aquifer along ephemeral streams in Washington County, Utah, have been developed. In the first method, a theoretical average annual discharge in ephemeral streams is calculated and recharge to the aquifer is assumed to be a percentage of this amount. In the second method, an experimentally determined rate of infiltration per unit length of ephemeral stream is applied to calculate recharge. Both methods were applied to ephemeral streams with drainage-basin areas greater

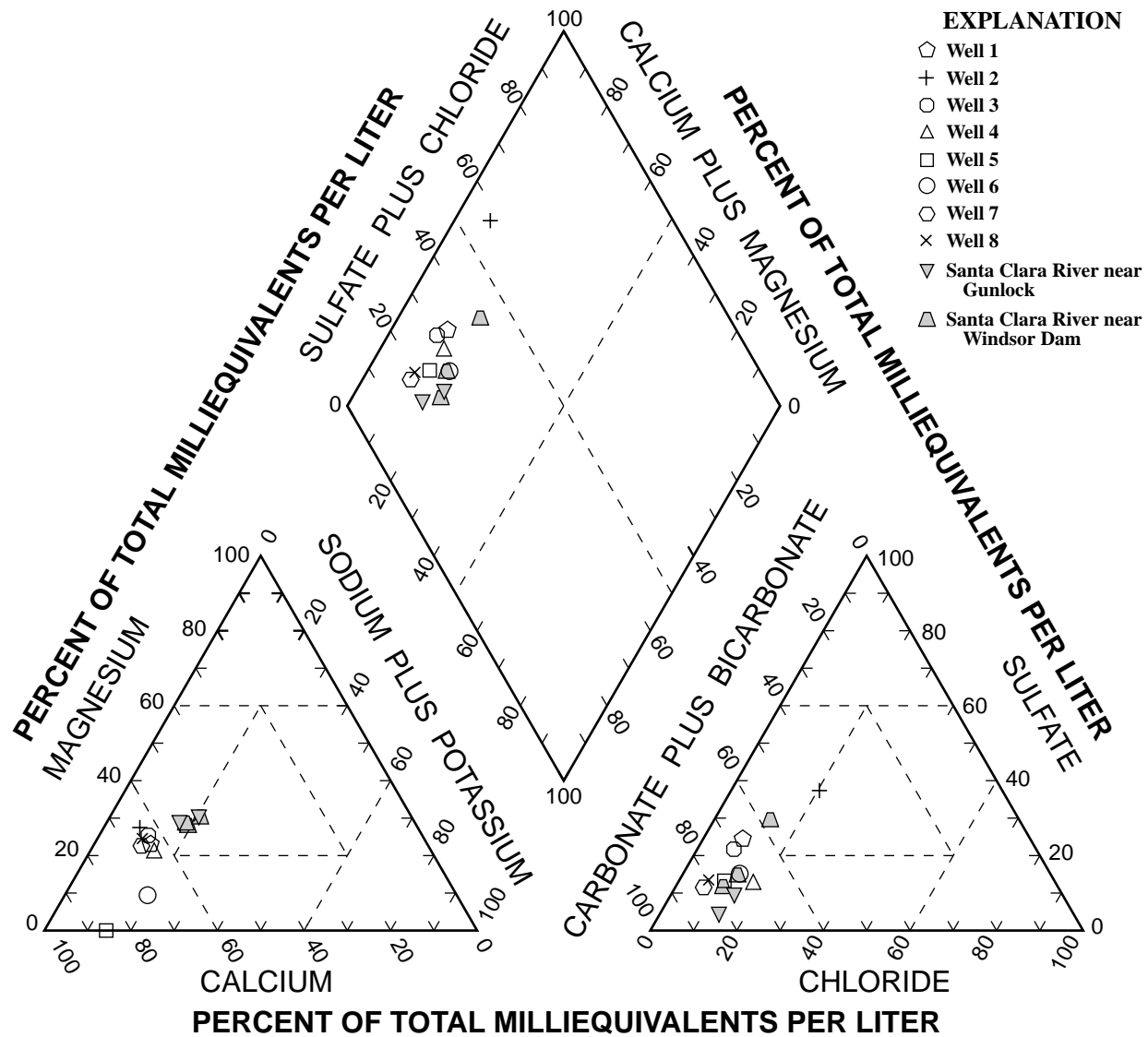


Figure 23. Chemical composition of water from the Santa Clara River and the St. George municipal well field in the Gunlock part of the Navajo aquifer within the central Virgin River basin study area, Utah.

than 5 mi² that cross the main part of the outcrop. No ephemeral streams with drainage basin areas greater than 5 mi² cross the Gunlock part of the outcrop. The drainage-basin area for the perennial and larger ephemeral streams that recharge the Navajo aquifer in the study area are shown in figure 27. Recharge to the main part of the Navajo aquifer from ephemeral streams is estimated to range from 0.28 to 6.3 ft³/s (200 to 3,000 acre-ft/yr).

Method 1

Average annual discharge for streams in southern Utah can be estimated by using two equations developed by Christensen and others (1985, tables 3 and 4):

$$\text{Southwestern plateaus region: } Q = 7.02 + .583 A \quad (2)$$

$$\text{Central plateaus region: } Q = 4.13 \times 10^{-4} A^{.709} P^{1.46} S^{.554} \quad (3)$$

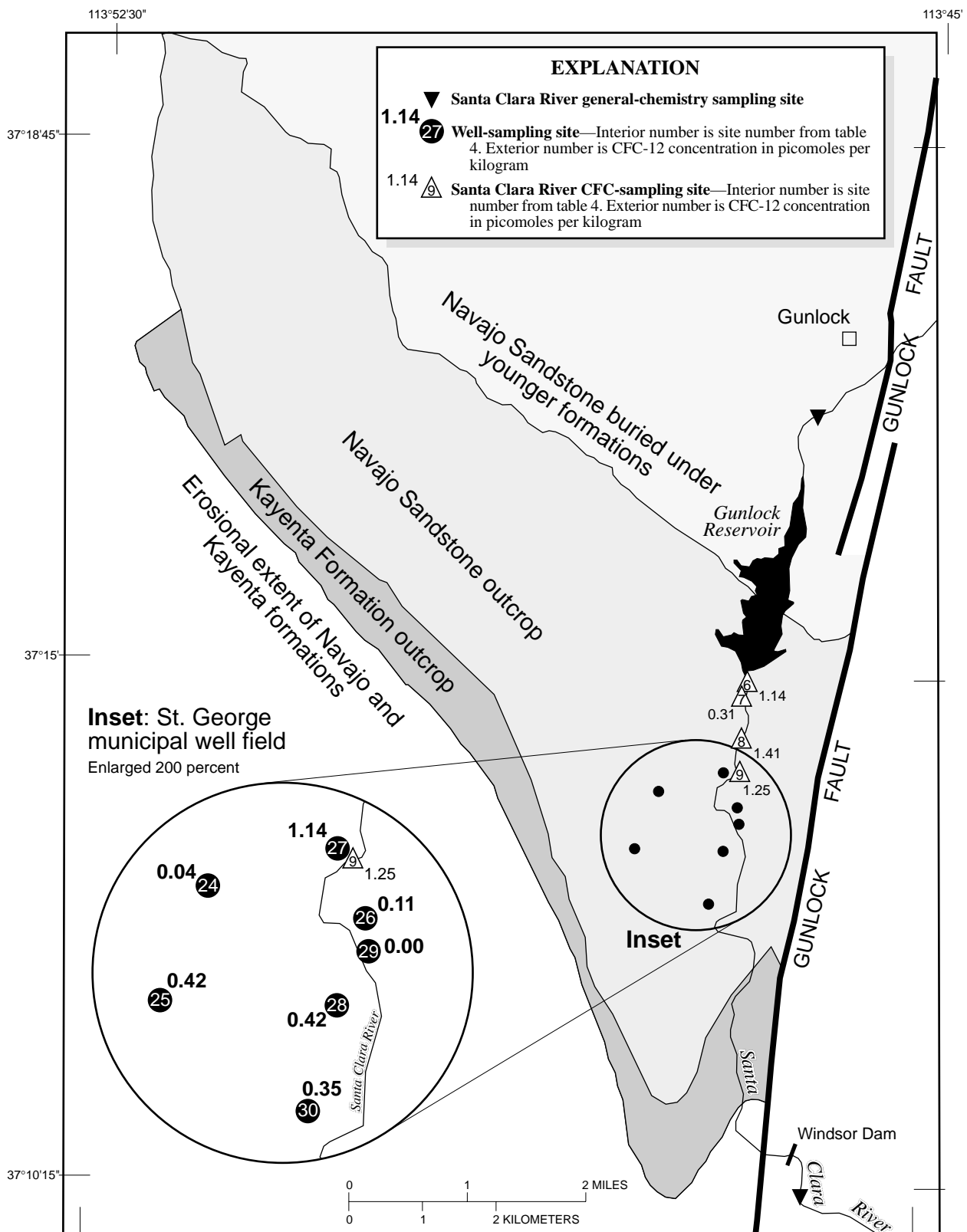
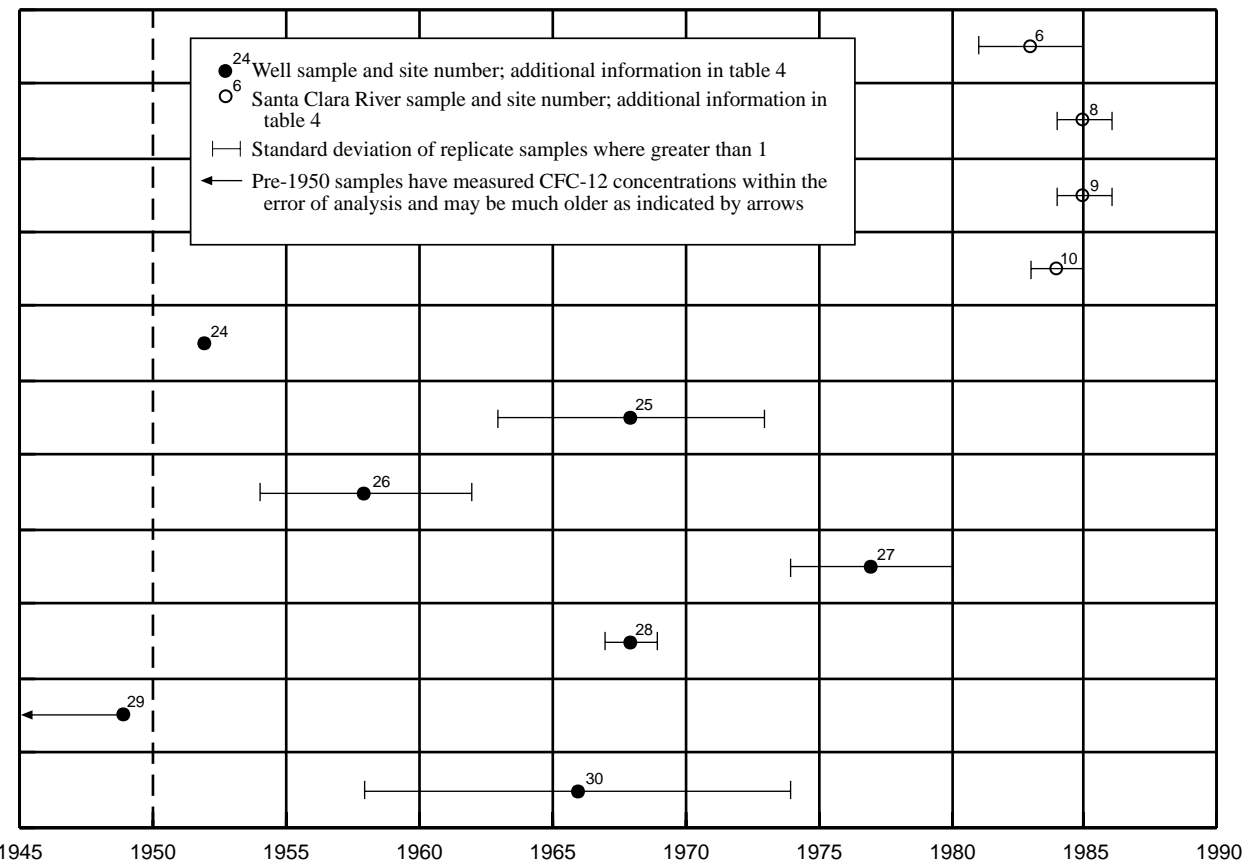


Figure 24. Location of general-chemistry sampling sites and CFC-12 sampling sites in the Gunlock part of the Navajo aquifer, central Virgin River basin study area, Utah.



APPARENT GROUND-WATER RECHARGE YEAR DETERMINED FROM CFC-12 CONCENTRATION

Figure 25. Apparent ground-water recharge year determined from CFC-12 concentration at Santa Clara River sites and in water from wells in the Gunlock part of the Navajo aquifer within the central Virgin River basin study area, Utah.

where

Q is discharge in acre-ft/d,

A is the area of the drainage basin in mi²,

P is average annual precipitation in., and

S is the main channel slope in ft/mi.

Equation 2 was developed for streams in the southwestern plateaus region of Utah and was calibrated with perennial streams including South Ash Creek and Leeds Creek. Equation 3 was developed for the central plateaus region of Utah. The ephemeral streams in the central part of the study area southwest of and including Cottonwood Creek and along Hurricane Bench have quite different characteristics from South Ash Creek and Leeds Creek. These streams receive little or no gain from snowmelt runoff; therefore, it is believed that the equation developed for the central plateaus region more accurately predicts discharge of these lower-altitude streams. The parameters for each of the drainage basins are reported in table 12.

Only the higher altitude ephemeral stream basins northeast of Cottonwood Creek are assumed to be affected by snowmelt runoff. These streams, labeled "E2" in table 12, are similar to Leeds and South Ash Creeks, upon which the southwestern plateaus region discharge equation, equation 3, was based (Christensen and others, 1985, tables 3 and 4). Ephemeral streams that drain the Pine Valley Mountains to the southwest of and including Cottonwood Creek are probably not affected by snowmelt runoff and are similar to streams in the central plateaus region. Discharge in these streams is calculated by using equation 3 and is labeled "E3" in table 12. The last column of the table shows the estimated average annual discharge for both the ephemeral and perennial creeks that cross the outcrop. Discharge for the perennial streams is calculated by using equation 2.

The estimated discharge in acre-ft/yr is shown in the first column of table 13. Average annual discharge, estimated by using equation 2 for Leeds Creek, is 5,770

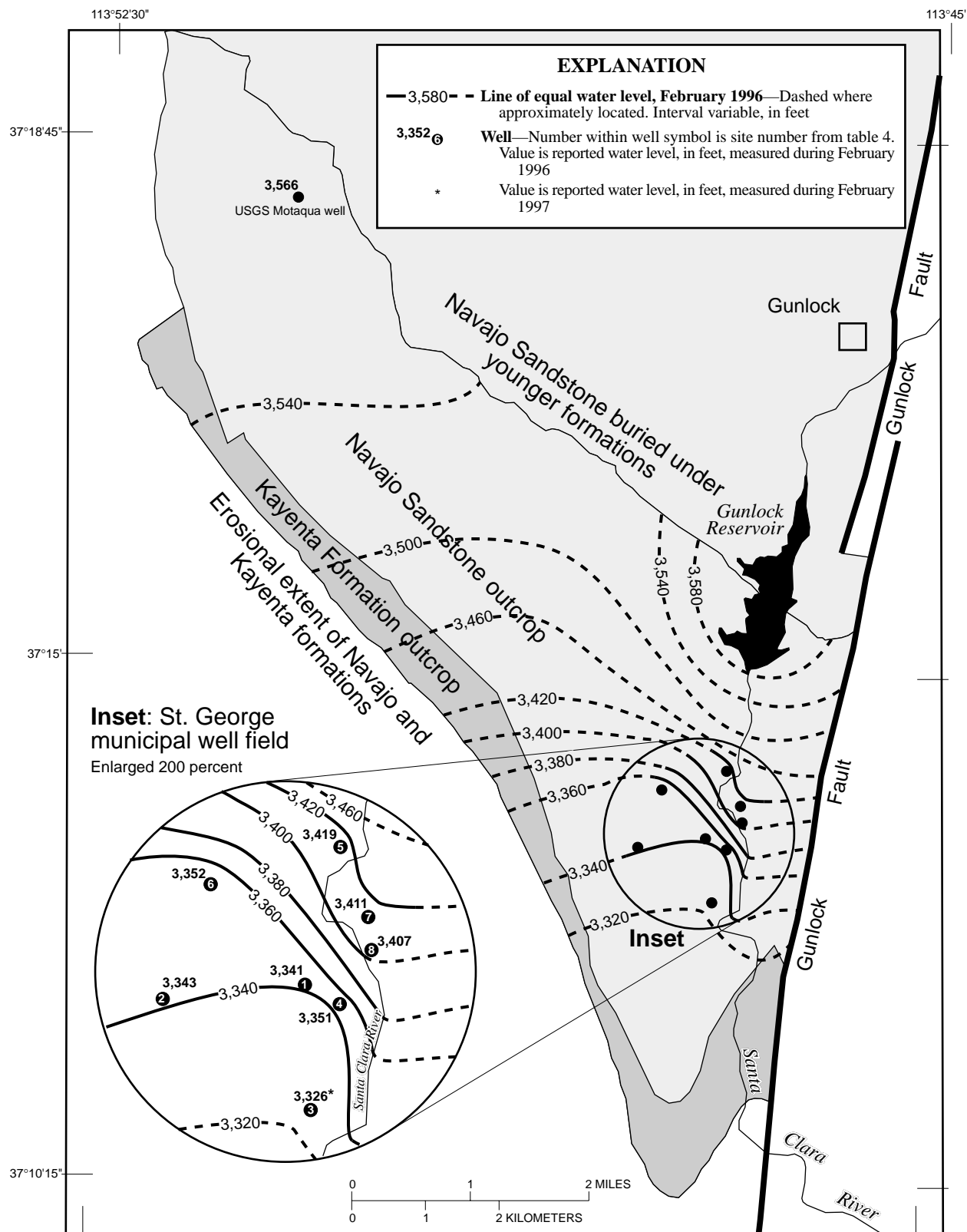


Figure 26. Approximate potentiometric surface in the Gunlock part of the Navajo aquifer within the central Virgin River basin study area, Utah, February 1996.

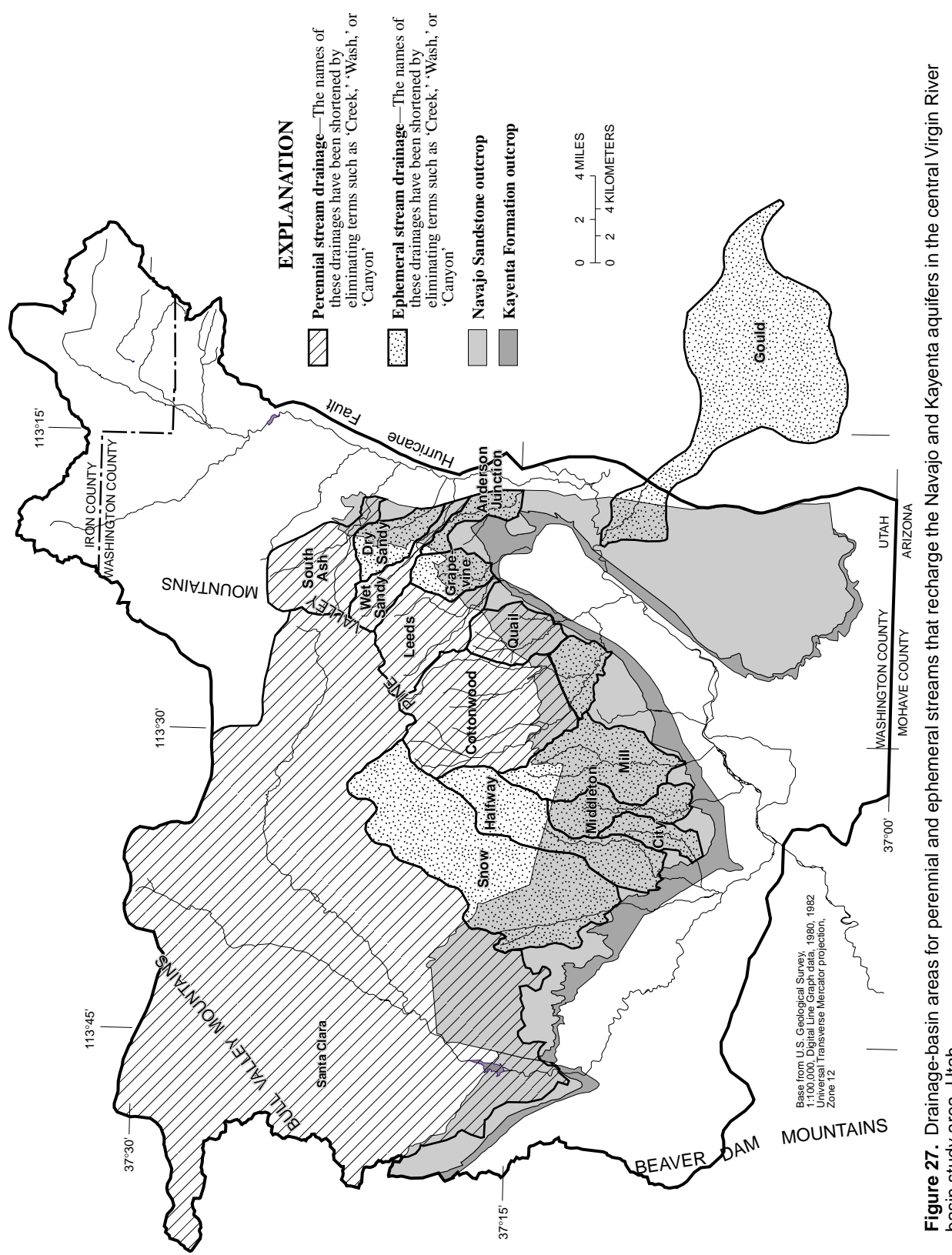


Figure 27. Drainage-basin areas for perennial and ephemeral streams that recharge the Navajo and Kayenta aquifers in the central Virgin River basin study area, Utah.

Table 12. Drainage-basin parameters for perennial and ephemeral streams that recharge the Navajo aquifer in the central Virgin River basin, Utah

Stream type: E2 indicates an ephemeral stream located northeast of Cottonwood Creek with discharge calculated using equation 2; E3 indicates an ephemeral stream located southwest of, and including, Cottonwood Creek and along Hurricane Bench, with discharge calculated using equation 3; P indicates a perennial stream with discharge calculated using equation 2.

Drainage basin	Stream type	Drainage area (square miles)	Average annual precipitation (inches)	Main channel slope (feet per mile)	Estimated average annual discharge (acre-feet per day)	Estimated average annual discharge (acre-feet per year)
Ephemeral streams:						
Snow Canyon	E3	49	14.7	180	5.9	2,140
Halfway Wash	E3	19	12.7	260	3.0	1,080
City Creek	E3	5	9.14	130	0.48	180
Middleton Wash	E3	9	10.5	150	.97	360
Mill Creek	E3	19	11.0	330	2.7	1,000
Gould Wash	E3	62	14.0	78	4.1	1,480
Cottonwood Creek	E3	40	16.1	250	7.0	2,540
Grapevine Wash	E2	6	13.0	210	10.5	3,830
Anderson Junction Wash	E2	5	12.2	220	9.9	3,610
Dry Sandy Wash	E2	7	16.6	610	11.1	4,050
Perennial streams:						
Quail Creek	P	9	12.9	340	12.3	4,490
Leeds Creek	P	15	19.0	410	15.8	5,770
Wet Sandy	P	7	19.8	570	11.1	4,050
South Ash Creek	P	16	23.4	290	16.4	5,990

acre-ft/yr, similar to the 5,610 acre-ft/yr average based on 32 years of measurements at USGS streamflow-gaging station 0940800 (table 11). Average annual discharge, estimated by using equation 2, for South Ash Creek is 5,990 acre-ft/yr. However, when using the smaller drainage basin area (11.0 mi^2) upstream of USGS streamflow-gaging station 09406700, the average annual discharge is 4,900 acre-ft/yr, similar to the 5,000 acre-ft/yr average based on 16 years of streamflow-gaging station measurements (table 11).

The estimated annual recharge from ephemeral streams also is shown in table 13. It is assumed that between 5 and 15 percent of the estimated average annual discharge, or 1,000 to 3,000 acre-ft/yr, is estimated to recharge the Navajo aquifer from ephemeral streams that cross the outcrop. To evaluate the accuracy of this method, the estimated average annual discharge was calculated for the perennial streams by using equation 2. The same percentage of discharge (5 to 15 percent) was compared to values measured during the seepage investigations of perennial streams (not including the Santa Clara River, whose discharge is regulated by dam releases and irrigation diversions). By using method 1, the total estimated recharge from perennial streams would be 1,000 to 3,000 acre-ft/yr, similar to

the 900 to 2,800 acre-ft/yr of measured seepage from perennial streams. When compared to another ephemeral stream seepage study, the estimated 5- to 15-percent infiltration of stream discharge for this study brackets the 9 percent of total streamflow estimated to recharge the alluvial aquifer system beneath the ephemeral Rillito Creek in southern Arizona based on microgravity surveying (Parker and others, 1998). The two primary limitations of this method are: (1) no long-term recharge from ephemeral streams in the study area has been measured; and (2) there are no perennial streams southwest of Cottonwood Creek to compare with discharge estimates obtained by using equation 3.

Method 2

This alternative method of estimating ephemeral stream recharge is based on an infiltration experiment done during February and March 1997 along City Creek where it traverses the Navajo Sandstone outcrop (pl. 1, fig. 22). The St. George City Creek Well #2 (Wilkowske and others, 1998, table 1) was pumped at 540 gal/min and discharged into the dry stream channel. Flow measured 4 mi downstream at Dixie-Red Hills Golf Course was 250 gal/min. The test, done in

Table 13. Estimated annual recharge from ephemeral streams to the Navajo aquifer based on estimated annual stream discharge, central Virgin River basin, Utah

Drainage basin	Estimated average annual discharge (acre-feet per year)	Estimated recharge assuming:			Measured seepage, in acre-feet per year (see table 11)
		15 percent infiltration of discharge (acre-feet per year)	10 percent infiltration of discharge (acre-feet per year)	5 percent infiltration of discharge (acre-feet per year)	
Ephemeral streams					
Snow Canyon	2,140	320	210	110	
Halfway Wash	1,080	160	110	50	
City Creek	180	30	20	10	
Middleton Wash	360	50	40	20	
Mill Creek	1,000	150	100	50	
Gould Wash	1,480	220	150	70	
Cottonwood Creek (lower)	2,450	380	250	130	
Grapevine Wash	3,830	570	380	190	
Anderson Junction Wash	3,610	540	360	180	
Dry Sandy Wash	4,050	610	400	200	
Total (rounded)	20,200	3,000	2,000	1,000	
Perennial streams¹					
Quail Creek	4,490	670	450	220	140
Leeds Creek	5,770	870	580	290	² 160
Wet Sandy	4,050	610	400	200	270-720
South Ash Creek	5,990	900	600	300	² 350-1,800
Total (rounded)	20,300	3,000	2,000	1,000	900-2,800

¹ Excludes the perennial reach of Cottonwood Creek because stream discharge is affected by spring diversions.

² Based on seepage studies from Cordova (1978, p.17).

early spring when evapotranspiration effects are considered negligible, showed a net seepage loss of 290 gal/min, or 53 percent of the total flow. The loss per mile during this experiment was about 70 gal/min or about 0.31 (acre-ft/d)/mi. When making the simplifying assumption that this infiltration rate is constant for all ephemeral streams crossing the Navajo Sandstone in the study area, the following method was used to calculate total ephemeral stream recharge: (1) this rate was multiplied by the length of each ephemeral stream reach along the outcrop; and (2) this product was then multiplied by the estimated number of days of flow in each ephemeral drainage.

The duration of the flow and length of stream reach along the outcrop in the larger ephemeral stream drainages are shown in table 14. These estimates are based on observations from local residents (Morgan

Jensen, oral commun., 1998), as well as on the hydrograph of discharge along Leeds Creek for the past 19 years (fig. 28). Base flow on Leeds Creek, determined from annual discharge hydrographs, is about 2.8 ft³/s, and is represented by a horizontal dashed line on figure 28. Two distinct types of higher flows can be seen on the hydrograph: (1) narrow spikes representing rainstorms and (2) wider peaks of longer duration representing periods of snowmelt runoff. Factors assumed to affect the duration of flow in ephemeral stream drainages are the estimated number of larger rainstorms, the frequency and length of snowmelt-runoff events, and the presence of springs. On the basis of anecdotal information from local residents, large rainstorms are estimated to occur on average five times per year, causing ephemeral streamflow lasting about 1 day in the larger drainages. Periods of snowmelt are identified on the

Table 14. Estimated recharge from ephemeral streams to the Navajo aquifer based on the City Creek infiltration experiment, February to March 1997, central Virgin River basin, Utah

Factors affecting streamflow: R, rainfall events; SP, spring flow; SN, snowmelt-runoff events.

Drainage basin	Stream reach on outcrop ¹ (miles)	Infiltration rate (acre-feet per day per mile)	Factors affecting streamflow	Flow duration (days per year)	Estimated recharge (acre-feet per year)	Measured seepage (acre-feet per year)
Ephemeral Streams						
Snow Canyon	7.7	0.31	R	5	12	
Halfway Wash	9	.31	R	5	14	
City Creek	5.2	.31	R	5	8	
Middleton Wash	7.7	.31	R	5	12	
Mill Creek	8.9	.31	R	5	14	
Gould Wash	2.8	.31	R+SP	15	13	
Cottonwood Creek (lower)	7.3 ²	.31	R+SN+SP	25	57	
Grapevine Wash	4.2	.31	R+SN+SP	25	33	
Anderson Junction Wash	5.6	.31	R	5	9	
Dry Sandy Wash	3.7	.31	R+SN	15	17	
Total (rounded)					200	
Perennial streams³						
Quail Creek	4.1	.31		365	470	140
Leeds Creek	2.8	.31		365	310	⁴ 160
Wet Sandy	2.8	.31		365	310	270 -720
South Ash Creek	3.1	.31		365	360	⁴ 350-1,800
Total (rounded)					1,500	900-2,800

¹ Length of stream reach along either the Navajo Sandstone or Navajo Sandstone and Kayenta Formation outcrop.

² Lower Cottonwood Creek (ephemeral part) is about 2/3 of the 11.0-mi stream reach along the Navajo Sandstone and Kayenta Formation.

³ Excludes the perennial reach of Cottonwood Creek because stream discharge is affected by spring flow diversions.

⁴ Based on seepage studies from Cordova (1978, p. 17).

Leeds Creek hydrograph as those multiple-month flows during late winter through early summer with a discharge greater than 10 ft³/s. On the basis of the Leeds Creek hydrograph, longer periods of snowmelt runoff are estimated to occur on average once every third year. Local residents have observed that these snowmelt-runoff flows last about 30 days (or 10 days per year) for higher altitude ephemeral streams, such as Cottonwood Creek, Grapevine Wash, and Dry Sandy Wash. The presence of springs in an ephemeral wash is assumed to increase the duration of flow by enhancing the discharge. It is estimated that the presence of springs would lengthen rain and snowmelt-runoff flows each by 10 days. Cottonwood Creek, Grapevine Wash, and

Gold Wash have springs that discharge into the stream channel (table 14).

The estimated recharge from ephemeral streams to the Navajo aquifer calculated using method 2 is shown in table 14. The total estimated recharge from ephemeral streams is about 200 acre-ft/yr. To verify the accuracy of this method, the same infiltration rates per river mile were applied to the perennial streams and compared to values measured during the seepage investigations (not including the Santa Clara River and Cottonwood Creek, whose discharge is regulated by dam releases, irrigation diversions, and/or spring-flow diversions). With this method, the total estimated recharge from perennial streams would be about 1,500 acre-ft/yr.

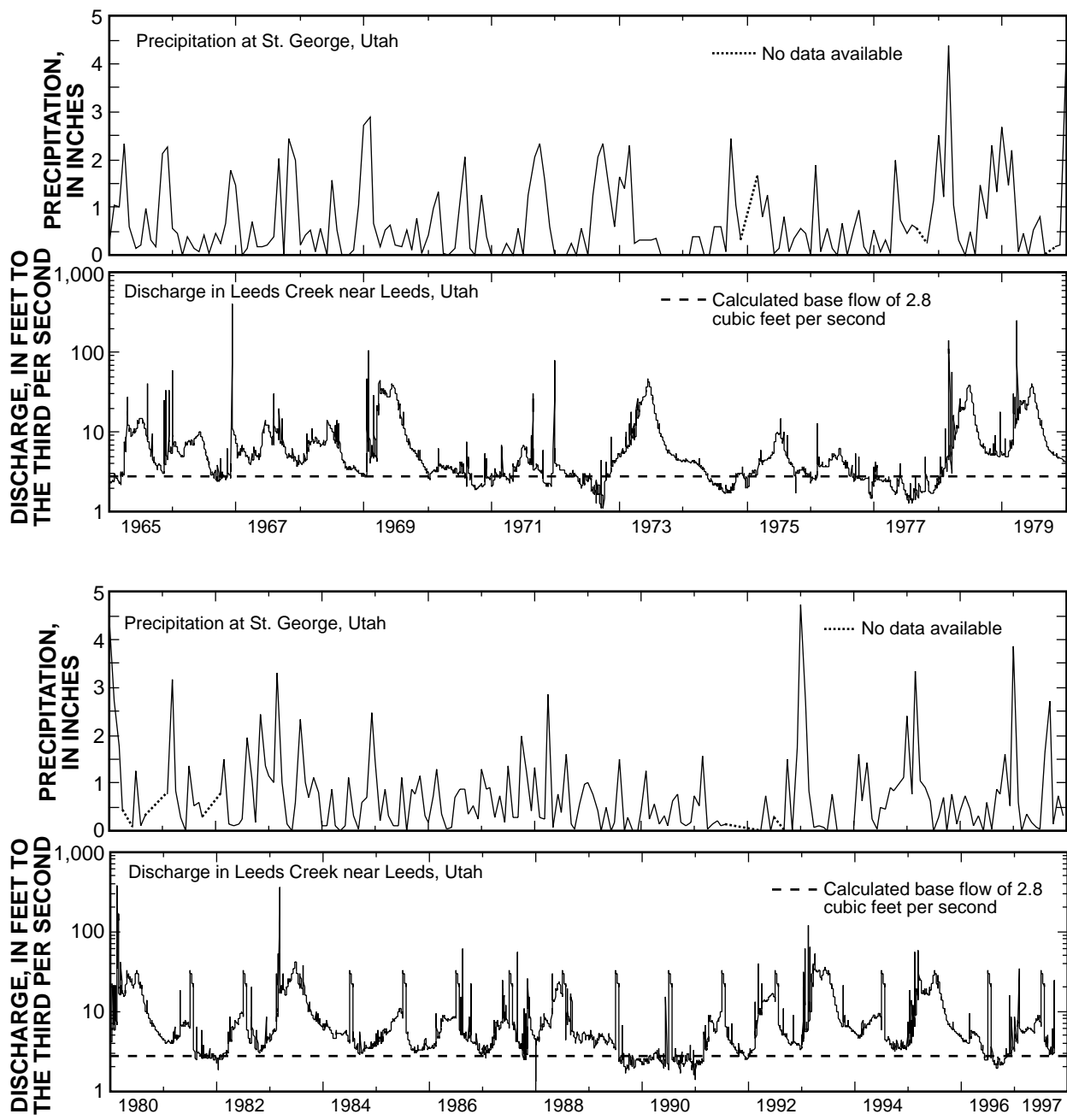


Figure 28. Discharge of Leeds Creek and precipitation at St. George, Utah, from 1965 through 1997.

This value is within the range of 900 to 2,800 acre-ft/yr estimated from base-flow seepage measurements for the same perennial streams. The limitation of this method is the assumption that infiltration occurs at a constant rate, independent of factors such as streambed geometry, total discharge, or evapotranspiration losses during warmer months. It is unlikely that the 0.3 acre-ft/d/mi infiltration rate measured at City Creek would apply for different channel conditions (slope, width, thickness of unconsolidated stream deposits) and dif-

ferent times of year. Also, the City Creek experiment simulated base-flow conditions by adding a constant but small flow to the channel. During an actual flash flood or snowmelt-runoff event, the discharge and corresponding rate of infiltration would be larger. The amount of infiltration from ephemeral streams estimated using method 2 may represent the lower values in the range of possible recharge from ephemeral streams. However, because infiltration values estimated for perennial streams with the experimental infiltration

rate are within the measured range of seepage, they may provide a reasonable estimate for recharge from ephemeral streams.

In summary, both methods for estimating recharge from ephemeral streams closely approximate or bracket the measured base-flow seepage to the Navajo aquifer from perennial streams. The amount of ephemeral stream recharge based on the method 1 ranges from 1,000 to 3,000 acre-ft/yr. The amount of ephemeral stream recharge based on method 2 is 200 acre-ft/yr. Therefore, the overall estimated range of ephemeral stream recharge is from 200 to 3,000 acre-ft/yr.

Overlying and Underlying Formations

The Carmel Formation overlies the Navajo Sandstone and consists of limestone, sandstone, shale, and gypsum deposits. Little vertical ground-water movement is likely through these low-permeability sedimentary rocks. However, because of higher precipitation toward the Pine Valley Mountains where the Navajo and Kayenta aquifers are covered by the Carmel Formation, the possible infiltration of small amounts of water downward into the Navajo aquifer cannot be entirely ruled out. Hurlow (1998) suggested that the large thickness and low permeability of overlying formations likely minimizes recharge to the Navajo aquifer. In a study by Cordy, Seiler, and Stolp (1993) of springs in Zion National Park, higher dissolved-solids concentrations were measured in water samples from the Navajo aquifer near where it is covered by the gypsum beds of the Carmel Formation. Lower dissolved-solids concentrations were associated with areas where the Navajo Sandstone outcrop is exposed at land surface. Also, surface water sampled from Bitter Creek (Wilkowske and others, 1998, tables 4, 6) contained high dissolved-solids concentrations in the reach that crosses the Carmel Formation. If large amounts of recharge from the overlying Carmel Formation were moving into the Navajo aquifer, this likely would cause an increase in dissolved-solids concentration in the parts of the aquifer near this contact, compared with parts of the aquifer, such as south of Hurricane, where there is no overlying Carmel Formation. However, the areas of higher dissolved-solids concentration within the study area do not correlate with parts of the Navajo aquifer near the Carmel Formation contact. Therefore, it is assumed that downward infiltration of water through the Carmel Formation is not a substantial source of recharge to the Navajo aquifer.

The Kayenta Formation is underlain by progressively older sedimentary formations including the Moenave Formation, the Chinle Formation, and the Moenkopi Formation (table 2; fig. 5). Although these finer grained formations generally are considered less permeable than the Navajo Sandstone and Kayenta Formation, ground water may migrate upward along fractures into the Navajo and Kayenta aquifers. Two flowing wells in the study area, well (C-41-17)29aba-1 drilled into the Shinarump Conglomerate of the Chinle Formation, and well (C-41-13)16bcd-1 drilled into the Springdale Sandstone of the Moenave Formation (Wilkowske and others, 1998, table 1), each have water levels similar to those of nearby wells in the Navajo aquifer, which indicates that an upward gradient towards the Navajo and Kayenta aquifers may exist at some locations.

Solute mass balances were developed to quantify recharge to the Navajo and Kayenta aquifers in the areas north of St. George and west of Hurricane (fig. 9). The mass balances were developed on the basis of 4 assumptions: (1) That the principal source of dissolved solids in the aquifer originate from underlying formations, (2) that other sources of dissolved solids were not considered, (3) that there is no change in storage in the aquifer, and (4) that the dissolved-solids concentration does not change with time. The water- and solute-mass balance equations used are:

$$Q_1 + Q_2 = Q_3 \quad (4)$$

and

$$Q_1 C_1 + Q_2 C_2 = Q_3 C_3 \quad (5)$$

where

Q_1 is recharge (ft^3/s) from surface infiltration;

Q_2 is recharge (ft^3/s) from underlying formations;

Q_3 is discharge (ft^3/s) from the high dissolved-solids concentration parts of the Navajo and Kayenta aquifers;

C_1 is average dissolved-solids concentration (mg/L) of ground-water samples from the low dissolved-solids concentration parts of the Navajo and Kayenta aquifers, which represents water recharged predominantly from surface infiltration that interacts with the aquifer solids;

C_2 is average dissolved-solids concentration (mg/L) of ground-water samples from the underlying Triassic and Permian Formations; and

C_3 is average dissolved-solids concentration (mg/L) of water that discharges from the high dissolved-solids concentration parts of the Navajo and Kayenta aquifers.

Equation 4 is the water-budget mass balance. Equation 5 is a solute mass balance that describes the mixing of two water sources with different dissolved-solids concentrations while retaining conservation of mass. The amount of discharge, Q_3 , from the aquifer in the area north of St. George is estimated to be about 8.2 ft³/s, equal to the average annual well pumpage and spring discharge for that area. The amount of discharge, Q_3 , west of Hurricane is estimated to be about 4.5 ft³/s, equal to the average annual well pumpage and seepage to the Virgin River. Assuming steady-state conditions, equation 4 indicates that these amounts of discharge are equal to the two sources of recharge, Q_1 (infiltration of surface water) and Q_2 (recharge from underlying formations). Equation 5 indicates that the amount of each source of recharge, multiplied by the average dissolved-solids concentration of that recharge, will equal the amount of discharge, multiplied by the average dissolved-solids concentration of the discharge. The two unknown parameters, Q_1 and Q_2 , can be determined by simultaneous solution of equations 4 and 5. C_1 , C_2 , and C_3 are estimated to be about 300 mg/L, 2,500 mg/L, and 1,020 mg/L, respectively for both areas of dissolved-solids concentration.

The results indicate that in the area of high dissolved-solids concentration north of St. George, as much as 2.7 ft³/s enters the Navajo aquifer from underlying formations and 5.5 ft³/s or more enters the aquifer from infiltration of surface water. West of Hurricane, as much as 1.5 ft³/s enters the aquifer from underlying formations and 3.0 ft³/s or more enters the aquifer from infiltration of surface water. These estimated amounts of recharge from underlying formations should be considered a maximum because it is assumed that the only source of water with a dissolved-solids concentration greater than 300 mg/L is the underlying formations. It is possible that another source is seepage from streams traversing the Navajo Sandstone outcrop after dissolution of higher-solubility minerals as the streams cross overlying layers such as the Carmel Formation.

On the basis of these calculations, the estimated recharge to the Navajo and Kayenta aquifers from underlying formations in the higher dissolved-solids concentration parts of the aquifer north of St. George and west of Hurricane, is as much as 4.2 ft³/s.

Irrigation

Irrigation of alfalfa occurs along a small part of the Navajo Sandstone outcrop west and southwest of Hurricane, Utah. Most of the alfalfa (2,100 acres) is flood irrigated in townships/ranges C-41-13 and C-42-13 (fig. 22). These alfalfa fields are located along thick alluvial deposits associated with Gould Wash and Frog Hollow Wash (pl. 1). A drillers' log for well (C-42-13)15bad-1 at the mouth of Frog Hollow Wash shows alternating layers of clay, sand, and gravel to a depth of 400 ft. A much smaller area of about 200 acres directly on the Navajo Sandstone outcrop in section 12 of Township 42 S., Range 14 W. (fig. 22) is sprinkler irrigated. A study of recharge beneath sprinkler- and flood-irrigated fields near Milford, Utah, indicated that there was no recharge beneath the sprinkler-irrigated field, whereas about 30 in. of recharge occurred beneath the flood-irrigated field (Susong, 1995). On the basis of this study, no recharge is assumed to occur beneath the sprinkler-irrigated fields on the Navajo Sandstone outcrop within the study area. The amount of recharge from unconsumed irrigation water on the flood-irrigated fields cannot be accurately measured because no information is available regarding the amount of water applied annually to the fields. The consumptive use of water by alfalfa at Milford (altitude 5,000 ft) is about 34 in/yr, whereas the consumptive use near Hurricane (altitude 2,900 ft) is about 43 in/yr, because of higher mean annual temperatures and lower relative humidity (Hill, 1994). Therefore, it is assumed that the amount of recharge from unconsumed irrigation water near Hurricane is less than the infiltration measured at Milford. Assuming an infiltration rate of 0 to 20 in/yr beneath the flood-irrigated fields near Hurricane, estimated recharge is from 0 to 5 ft³/s (4,400 acre-ft/yr). But without information concerning the amount of water applied yearly to the flood-irrigated fields, this estimated range is poorly constrained.

Gunlock Reservoir

Recharge to the Navajo aquifer most likely is occurring beneath the southern half of the Gunlock Reservoir, which overlies about 125 acres (5,450,000 ft²) of the Navajo Sandstone outcrop (fig. 24). It is assumed that about 20 ft of silt has been deposited at the base of the reservoir since it was constructed. The water level in the reservoir generally is about 3,580 ft. It is assumed that a mound has developed beneath the reservoir so that the water in the reservoir is in hydraulic connection with the water table of the Navajo aquifer.

Assuming that the water table in the Navajo aquifer at the base of the reservoir is at about 3,470 ft and the vertical conductivity is about 0.01 ft/d for silts (Freeze and Cherry, 1979), Darcy's law calculations indicate that up to 3 ft³/s (2,200 acre-ft/yr) may seep into the Navajo aquifer. However, this estimate is based on many unknown parameters such as the actual thickness and hydraulic conductivity of the silt layer at the base of the reservoir.

Ground-Water Movement

Ground water moves from areas of high hydraulic head to areas of low hydraulic head. In an unconfined aquifer, this is generally from higher elevation areas to lower elevation areas. Based on water levels measured in wells during February and March of 1996 and 1997 (Wilkowske and others, 1998) ground water in the Navajo and Kayenta aquifers generally moves from the base of Pine Valley Mountains southward towards the Santa Clara and Virgin Rivers (pl. 2, fig. 26). The exception to this is the part of the aquifers southwest of Hurricane, where ground water moves northwestward toward the Virgin River. The potentiometric surface within the Navajo Sandstone and Kayenta Formation outcrop (unconfined) part of the aquifers is similar to the topography; ground water moves perpendicular to the potentiometric contours, generally from higher-altitude areas of the outcrop toward lower-altitude areas. There are three areas of the outcrop with very sparse water-level data: the eastern part of the outcrop west of Hurricane Fault, the area between Leeds Creek and Grapevine Pass Wash, and the area northwest of the St. George municipal well field in the Gunlock part of the Navajo aquifer (pl. 1). In these areas, the direction of ground-water movement can only be inferred from distant water-level measurement sites. Also, many of the water levels on plate 1 and in figure 26 are from production wells, many of which are pumped for most of the year. Although water levels were measured near the end of the winter when pumping is minimal, water levels may still be recovering from earlier pumping and may not be representative of the regional potentiometric surface.

Vertical movement of ground water between the Navajo and Kayenta aquifers likely occurs, as indicated by small vertical gradients inferred from nearby pairs of wells finished in the two formations. Small downward vertical gradients likely exist near the Navajo Sandstone/Kayenta Formation contact southwest of Hurricane, northwest of Toquerville, and north of

Washington. The vertical gradients estimated in these areas generally are less than 0.10 and were determined by dividing the difference in water-level altitude (generally less than 50 ft) by the vertical distance between the perforated intervals of the well pairs (generally about 500 ft). There are no nested pairs of wells finished in the Navajo and Kayenta aquifers for direct measurement of vertical gradient. Smaller vertical gradients are consistent with the assumption that water moves easily between the two aquifers.

In the high dissolved-solids concentration parts of the aquifers, upward vertical gradients likely exist between the Kayenta Formation and underlying formations as a result of hydrothermal circulation. The evidence of this, as discussed above, includes a strong correlation between elevated dissolved-solids concentration and elevated ground-water temperature. Also, flowing well (C-41-17)29aba-1 in the Shinarump Member of the Chinle Formation had a reported water level similar to that in the nearby Navajo aquifer, indicating the possible upward vertical gradient.

Discharge

The principal sources of discharge from the Navajo and Kayenta aquifers are well discharge, spring discharge, and seepage to streams. Additional possibilities for discharge include seepage to underlying formations and evapotranspiration. Measured and estimated sources of discharge from the Navajo and Kayenta aquifers are shown in figure 29. The total amount of discharge is estimated to range from 23 to 39 ft³/s (17,000 to 28,000 acre-ft/yr) and from 5 to 8 ft³/s (3,800 to 5,900 acre-ft/yr), respectively, for the main and Gunlock parts of the Navajo aquifer. These ranges of discharge values are much narrower than the range of recharge reported above. This is because the larger discharge components, including well discharge, spring discharge, and stream seepage, can be more accurately measured than many of the recharge components, especially infiltration of precipitation.

Wells

Well pumpage is the largest source of discharge from both the main and Gunlock parts of the Navajo and Kayenta aquifers. Except for an irrigation-well area southwest of Hurricane, most well discharge is for potable use. Historical well-pumpage records are incomplete for some municipalities and for many private potable and irrigation wells. The best source of data is St. George, where accurate discharge measure-

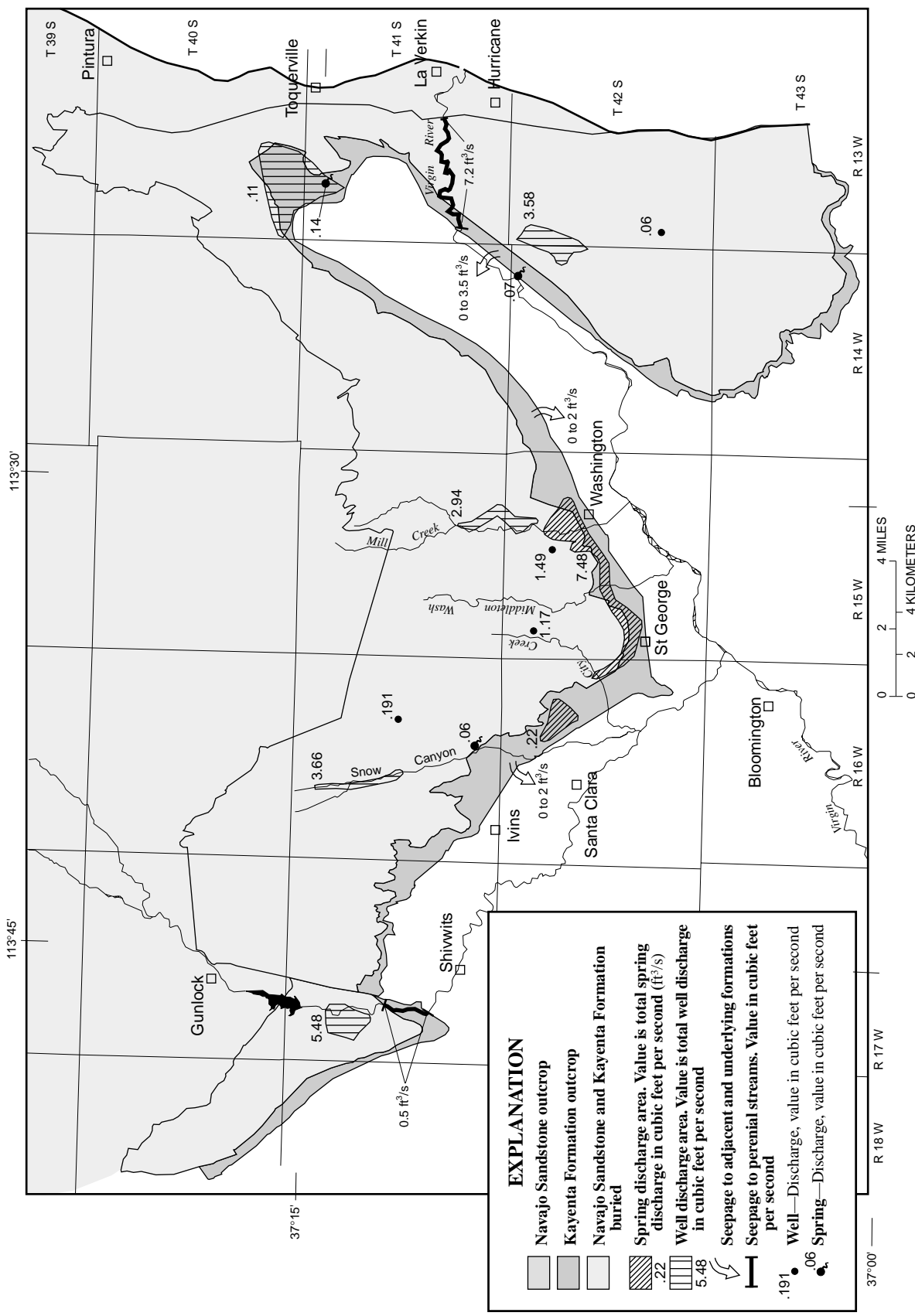


Figure 29. Measured and estimated sources of discharge from the Navajo and Kayenta aquifers in the central Virgin River basin study area, Utah.

ments have been kept since the late 1980s (Phillip Solomon, City of St. George, oral commun., 1995). Well discharge from St. George municipal wells in the main and Gunlock parts of the Navajo and Kayenta aquifers from 1987 through 1996 is shown in figure 30. Average well discharge from 1987 through 1996 for the Gunlock part of the aquifers was $5.5 \text{ ft}^3/\text{s}$ (4,200 acre-ft/yr), and varied from 4.7 to $7.6 \text{ ft}^3/\text{s}$ (3,400 and 5,500 acre-ft/yr). Average St. George well discharge in the main part of the aquifers for this period was $4.4 \text{ ft}^3/\text{s}$ (3,200 acre-ft/yr), and varied from 3.6 to $5.4 \text{ ft}^3/\text{s}$ (2,600 to 3,900 acre-ft/yr) (Jerry Olds, Utah Division of Water Rights, written commun., 1998). Except for 1995 data, total pumpage for the main part is not known because irrigation-well discharge and some potable-well discharge from subdivisions and municipalities is not regularly reported to the Utah Division of Water Rights.

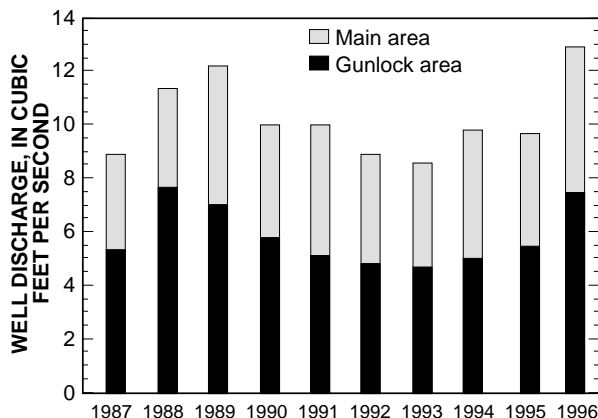


Figure 30. Well discharge from St. George municipal wells in the main and Gunlock parts of the Navajo and Kayenta aquifers from 1987 through 1996.

The total 1995 well discharge for the main part of the Navajo and Kayenta aquifers is estimated to be $12.7 \text{ ft}^3/\text{s}$ (9,200 acre-ft/yr) based predominantly on St. George City Water and Power Department (Phillip Solomon, written commun., 1996) and Utah Division of Water Rights (Jerry Olds, written commun., 1996) reported usage. About 70 percent, or $9.1 \text{ ft}^3/\text{s}$ (6,600 acre-ft/yr), of well discharge is for potable use by municipalities and subdivisions. The 1995 well pumpage also includes about $3.6 \text{ ft}^3/\text{s}$ (2,600 acre-ft/yr) from private potable and irrigation wells southwest of Hurricane. This amount was determined with discharge measurements from each well taken with either a sonic velocity device or bucket and stopwatch. The discharge measurements are then combined with power-meter

readings to determine average annual pumpage for each well (calculated by multiplying the ratio of discharge rate to power consumption by the total power consumption for the year).

Because 1995 discharge from the St. George wells is similar to the 1987-96 average St. George pumpage, it is assumed that the 1995 total discharge of $12.7 \text{ ft}^3/\text{s}$ (9,200 acre-ft/yr) from the main part of the Navajo and Kayenta aquifers is close to the 10-year average. Assuming that the 20 percent variation in St. George well discharge between 1987 and 1996 is similar to variations in well discharge for the entire main part of the aquifers, well discharge is estimated to range from about 10 to $15 \text{ ft}^3/\text{s}$ (7,200 to 10,900 acre-ft/yr).

The trend in St. George well discharge from 1987 through 1996 (fig. 30) is generally related to the amount of precipitation, which determines the availability of surface water. However, to keep up with population growth there have been numerous wells drilled since 1995, including the St. George municipal wells downstream from Gunlock Reservoir and in Mill Creek, a Washington City well in Grapevine Pass, and a WCWCD well at Anderson Junction. In addition, there have been recent acquisitions of private wells and water rights south and west of Hurricane by the cities of Hurricane and St. George, and the WCWCD. As these new and redeveloped wells become fully operational and if the population of the region continues to grow, it is likely that a general trend of increased well discharge will occur and be magnified during periods of less-than-normal precipitation.

In the main part of the Navajo and Kayenta aquifers, about 80 percent of the well discharge is estimated to be from the Navajo aquifer and 20 percent from the Kayenta aquifer. Most of the Navajo aquifer discharge occurs along Snow Canyon, City Creek, in the Mill Creek area, and southwest of Hurricane (fig. 29). Most of the Kayenta aquifer discharge occurs from wells along Snow Canyon, Mill Creek, and near Leeds that are drilled into the Navajo Sandstone but also perforated in the upper part of the Kayenta Formation. In the Gunlock part, all of the well discharge is from the Navajo aquifer.

Because drawdown associated with pumping rapidly decreases with distance away from production wells in an unconfined to partly confined aquifer there likely is not much drawdown in areas at large distances (generally more than a mile) from a production well in the Navajo and Kayenta aquifers. However, in areas such as Millcreek, Snow Canyon, and downstream from Gunlock Reservoir, where many large production

wells are located in close proximity, the drawdown effects are additive and farther reaching. Although only a few feet of drawdown likely occurs regionally along the perimeter of these wells fields, such change could be large enough to (1) reverse the direction of flow between ground water and surface water, as seen by the change in the Santa Clara River near the St. George municipal well field from gaining reach to losing reach during the past few decades; or (2) capture naturally occurring discharge that, prior to ground-water development, emanated at springs and gaining stream reaches. It is possible that additional ground-water development in areas upgradient of naturally occurring discharge (springs or gaining streams) may eventually capture some of this water. Anderson Junction is one such location where additional pumping may divert some of the ground water from seeping into the Virgin River.

Springs

Springs are the second-largest source of discharge from the main part of the Navajo and Kayenta aquifers. There is no known spring discharge from the Gunlock part of the aquifers. Total spring discharge for the main part is estimated to be about $7.7 \text{ ft}^3/\text{s}$ plus or minus 10 percent, or 6.9 to $8.5 \text{ ft}^3/\text{s}$ ($5,200$ to $6,200$ acre-ft/yr) (fig. 29), based on two spring inventories done in December 1995 and April 1996 (Wilkowske and others, 1998, table 3). All of the larger springs discharge from the lower Navajo Sandstone and upper Kayenta Formation between Snow Canyon and Mill Creek (fig. 29). It is estimated that there is little seasonal variation in spring discharge from the Navajo and Kayenta aquifers. Six springs measured during both the 1995 and 1996 surveys had less than 10-percent variation in discharge, within the error of the measurement methods. Similarly, a total spring discharge of $2,655$ gal/min was measured at seven springs (Snow, Mill Creek, Warm, Huntington, Cox, East City, and West City Springs) during November 1974 (Cordova, 1978, table 2). Total discharge from the same springs measured during 1995 and 1996 was $2,635$ gal/min, a variation of less than 1 percent from the earlier study. Finally, discharge at Sheep Springs showed little variation (1.9 to 2.1 gal/min) during 12 monthly measurements from November 1990 through October 1991 (Jensen and others, 1997, table 14).

The location of springs within the Navajo and Kayenta aquifers may be related to permeable fractures. Jensen and others (1997) noted that Beecham,

Gray, and Sheep Springs are located along a fracture identifiable on areal photographs. These springs trend on a line that extends northwestward along the axis of the inferred Snow Canyon Fault. Similarly, Warm Spring, north of Washington, may be associated with hydrothermal circulation along the nearby Washington Fault (Budding and Sommer, 1986).

Streams

A seepage study done during November 1994 along the Virgin River documented about $7.2 \text{ ft}^3/\text{s}$ ($5,200$ acre-ft/yr) streamflow gain across the Navajo Sandstone outcrop west of La Verkin (Herbert, 1995). Assuming a temporal variation in discharge of 10 percent, the estimated discharge from the Navajo is 6.5 to $7.9 \text{ ft}^3/\text{s}$ ($4,700$ to $5,700$ acre-ft/yr). The Virgin River cuts deeply into the Navajo Sandstone, and it is assumed that the source of this gain in streamflow is discharge from the Navajo aquifer (fig. 29). Because the study was done in late fall, it is assumed that evapotranspiration losses were minimal.

A larger gain of $13.8 \text{ ft}^3/\text{s}$ ($10,000$ acre-ft/yr) in the Virgin River was determined during a seepage study done in 1974 by Cordova (1978). The decrease in aquifer discharge since the 1970s may be caused by increased well discharge from the Navajo aquifer in the residential area northeast of Leeds and in the agricultural area southwest of Hurricane.

As part of this study, two seepage studies were done along the Santa Clara River (Wilkowske and others, 1998, table 6). On the basis of these discharge measurements, an estimated average streamflow gain of about $0.5 \text{ ft}^3/\text{s}$ (400 acre-ft/yr) was calculated in the Santa Clara River as it crossed the Kayenta Formation outcrop.

Adjacent and Underlying Formations

The November 1994 seepage study along the Virgin River showed additional streamflow gains of about $3.5 \text{ ft}^3/\text{s}$ along the Kayenta Formation outcrop and downstream Quaternary sediments (Qs) in contact with underlying formations (fig. 29, pl. 1) (Herbert, 1995). The part of this discharge coming from the Kayenta Formation could not be determined because no measurement was taken at the contact between the Kayenta Formation and the Quaternary sediments. However, it is assumed that most of this water originates in the Navajo Sandstone and Kayenta Formation, is discharged into the Quaternary and Tertiary basalt (Qtb), infiltrates into the Quaternary sediments, and finally seeps into the

Virgin River. On the basis of discharge measurements along the Santa Clara River (Herbert and others, 1997) and observations by local residents (R. Levitt, oral commun., 1998), an estimated streamflow gain of from 0 to 2 ft³/s (1,400 acre-ft/yr) between Ivins and St. George originates from the Navajo and Kayenta aquifers (fig. 29). This water may seep into the Santa Clara River from Quaternary sediments and basalt in contact with the Navajo Sandstone and Kayenta Formation near Snow Canyon, or through fractures in the underlying Moenave and Chinle Formations (pl. 1). Likewise, there are numerous seeps and small springs along the Moenave and Chinle Formation outcrop between St. George and Leeds (pl. 1). From 0 to 2 ft³/s (1,400 acre-ft/yr) of discharge is estimated to migrate from the Navajo Sandstone and Kayenta Formation through fractures into these underlying formations before seeping to the surface (fig. 29). A total estimated discharge of from 0 to 7.5 ft³/s (0 to 5,400 acre-ft/yr) moves from the main part of the Navajo and Kayenta aquifers into adjacent unconsolidated or consolidated formations, eventually discharging as seepage to springs or streams.

Evapotranspiration

Transpiration occurs from phreatophytes growing along perennial stream reaches that cross the Navajo Sandstone and Kayenta Formation outcrops. Except for the Virgin River, phreatophyte growth along the perennial reaches is generally sparse because of the steep canyon topography along the streams. Except for the Virgin River, all the perennial streams lose water to the aquifer. Thus, only the net amount of water recharging the aquifer (after removal by transpiration) is estimated and was based on seepage studies conducted during the autumn when transpiration is minimal. While transpiration losses are larger during the spring and summer, flow is also generally higher. Therefore, it is likely that the increased transpiration losses during the warmer months is offset by higher stream flow.

For the Virgin River, seepage studies were also conducted in the late autumn (Herbert, 1995) when transpiration losses were minimal and total discharge from the aquifer to the river could be accurately estimated. Therefore, transpiration did not need to be considered for the ground-water budget.

Ground-water budget

The estimated ground-water budgets for the main and Gunlock parts of the Navajo and Kayenta aquifers are shown in tables 15 and 16.

NUMERICAL SIMULATION OF GROUND-WATER FLOW

Computer models were developed to simulate various concepts of how ground water moves through the upper Ash Creek aquifer system and the Navajo and Kayenta aquifers. Computer models are able to test the viability of conceptual models and to determine the sensitivity of simulation results to uncertainty in data and interpretations based on those data. A model should reasonably represent most aspects of ground-water recharge, movement, and discharge, and results of simulations should reasonably match measured ground-water budget components and measured water levels in wells. The differences between simulation results and the measured aquifer flows and water levels should be "acceptable" for the intended use of the model.

Another equally important purpose for developing a ground-water flow model is to guide the collection of additional data. Data-collection priority can be set for parameters that are not well known by determining the sensitivity of simulation results to different types of data. Data to which the simulation results are sensitive should be given a high priority in future data-collection efforts. Only then can a model be successfully improved and updated in the future.

The purpose for developing the three models described in this report was to (1) evaluate the practicality of the conceptual models described, (2) evaluate alternative conceptual models, and (3) determine the sensitivity of simulation results to uncertainty in properties and flows to help prioritize future data collection.

The ground-water flow models were constructed with the latest version of the MODFLOW finite-difference simulation code (McDonald and Harbaugh, 1988). The updated version (Harbaugh and McDonald, 1996), known as MODFLOW-96, adds double precision to budget calculations and new input and output capability but retains the same programming structure for solving the ground-water flow equation.

The mathematical boundaries used to represent hydrologic boundaries of the aquifers include no-flow boundaries, specified-flux boundaries, and head-dependent flux boundaries. A no-flow boundary does not allow water to move through it. A specified-flux bound-

Table 15. Estimated ground-water budget for the main part of the Navajo and Kayenta aquifers, central Virgin River basin, Utah

Flow component	Volume, in cubic feet per second	Volume, in acre-feet per year
Recharge		
Infiltration of precipitation	10 to 30	7,200 to 21,700
Seepage from perennial streams	1.8 to 5.5	1,300 to 4,000
Seepage from ephemeral streams	.28 to 4.2	200 to 3,000
Seepage from underlying formations	0 to 4.2	0 to 3,000
Infiltration of unconsumed irrigation water	0 to 5	0 to 4,400
Total (rounded)	12 to 49	8,700 to 36,100
Discharge		
Well discharge	10 to 15	7,200 to 10,900
Spring discharge	6.9 to 8.5	5,000 to 6,200
Seepage to the Virgin River	6.5 to 7.9	4,700 to 5,700
Seepage to underlying formations	0 to 7.5	0 to 5,400
Total (rounded)	23 to 39	17,000 to 28,000

Table 16. Estimated ground-water budget for the Gunlock part of the Navajo and Kayenta aquifers, central Virgin River basin, Utah

Flow component	Volume, in cubic feet per second	Volume, in acre-feet per year
Recharge		
Infiltration of precipitation	1 to 3	700 to 2,200
Seepage from the Santa Clara River (rounded)	1 to 4	700 to 2,900
Seepage from the Gunlock Reservoir	0 to 3	0 to 2,200
Total (rounded)	2 to 10	1,400 to 7,300
Discharge		
Well discharge	4.7 to 7.6	3,400 to 5,500
Seepage to the Santa Clara River	.5	400
Total (rounded)	5 to 8	3,800 to 5,900

ary allows water to move across it at a fixed rate. A head-dependent flux-boundary allows the amount of water moving across it to vary when the head in the aquifer varies (see Franke, Reilly, and Bennett, 1987). No-flow boundaries representing the erosional and fault-controlled extend or ground-water divides in the aquifers are fairly well defined. Other boundaries, such as those representing flow to and from underlying, adjacent, and overlying formations, are not well understood. In general, the contact between the aquifers and underlying or overlying formations are represented by no-flow boundaries except where hydrologic or geochemical evidence indicates that ground water may be crossing these boundaries. Where the aquifers are unconfined, the boundary is a free surface. A specified-

flux is applied across the free-surface boundary to represent infiltration from precipitation, streams, and unconsumed irrigation water. There also are areas on the free surface boundary where head dependent fluxes are applied to simulate discharge from the system, such as spring discharge and seepage to streams.

Upper Ash Creek Drainage Basin Ground-Water System

Ground-water development in the upper Ash Creek drainage basin was negligible prior to 1995. Water-level variation in a well that has been measured since 1934 indicates no long-term effect from pumping, but seasonal and longer-term water-level changes indi-

cate that recharge to the system is probably affected by climatic variability (fig. 31). Because there have been no long-term changes in water levels, changes in ground-water storage are negligible and the system is considered to be in steady-state. Thus, a steady-state computer model was developed to examine how the hydrologic system functions and to test and evaluate the conceptual model and test the estimated water budget. The baseline period was 1995.

A baseline simulation was developed to represent how the system is conceptualized to function. Alternative simulations, which represent variations to the conceptual model, were tested to determine which were reasonable and which were not. Because of uncertainties about the flows and properties of the hydrologic system, sensitivity analyses were done on the baseline simulation to test how variations in these parameters within reasonable limits affected simulation results.

Model Characteristics and Discretization

The model is discretized into a grid of rectangular blocks or cells, each assumed to have homogeneous properties. The ground-water flow system for the upper Ash Creek drainage basin is divided into 67 rows, 49 columns, and 3 layers with a total of 9,849 cells (fig. 32). The model grid is designed to emphasize flow in the basin-fill aquifer, for which the most information is available. All but a few cells that represent the basin-fill aquifer are 1,000 ft by 1,000 ft (about 23 acres). The southernmost cells are as much as 34 acres. Cells that represent the alluvial-fan aquifer range from 1,000 ft by 1,000 ft to 1,000 by 1,500 ft (about 34 acres). Cells that represent areas in the Pine Valley Mountains and the Pine Valley monzonite aquifer are as large as 3,000 ft by 3,000 ft (about 207 acres). The three aquifers are each represented by a model layer and the areal extent of each layer becomes larger with depth. Layer 1 represents the basin-fill aquifer and includes about 28 mi² and 875 active cells. Layer 2 represents the alluvial-fan aquifer and includes about 50 mi² and 1,251 active cells. Layer 3 represents the Pine Valley monzonite aquifer and includes about 99 mi² and 1,865 active cells. The Pine Valley monzonite aquifer is assumed to underlie the entire modeled area, but this is not based on fact, merely supposition. The orientation of the grid is rotated clockwise about 35 degrees from true north to better align with physical boundaries of the system and the dominant fracture orientation in the Pine Valley monzonite aquifer.

The model layers correspond to geologic units and vary in thickness. Layer 1 represents the Quaternary basin fill and ranges from less than 100 to as much as 1,500 ft thick. Layer 2 represents semiconsolidated Tertiary alluvial-fan deposits and ranges from less than 100 to as much as 1,500 ft thick. Layer 3 represents the Pine Valley monzonite aquifer and is assigned a thickness of no more than 3,000 ft. The thickness of the Pine Valley monzonite aquifer is not known, but 3,000 ft was arbitrarily chosen as a depth below which ground-water movement is negligible. Figure 32 shows the model layering used for the flow simulation.

Boundary Conditions

No-flow, specified flux, and specified-head boundaries were used to represent the hydrologic boundaries in the Ash Creek basin model (fig. 33).

Recharge Boundaries

The top of the uppermost layer throughout the modeled area represents a specified-flux recharge boundary, where simulated recharge includes infiltration of precipitation, seepage from ephemeral and perennial streamflow, and infiltration of unconsumed irrigation water. No recharge from subsurface flow was conceptualized or simulated.

Precipitation

Infiltration of precipitation is simulated with the recharge package (Harbaugh and McDonald, 1966, p. 28). The distribution of annual precipitation for the modeled area was obtained from the Utah Climate Center (1996). Initially recharge from infiltration was applied as 8.5 percent of total precipitation, but as the steady-state model was refined, the percentage was increased as total precipitation increased with altitude. The areal distribution of recharge from infiltration of precipitation is shown in figure 34.

Ephemeral Streams

Recharge from streams flowing onto the valley floor from the surrounding mountains and plateaus also is simulated as part of the recharge package but is not represented in figure 34. In the areas where Kanarra, Spring, Camp, and Taylor Creeks flow onto the valley floor the recharge package was used to apply about half the total estimated flow in these streams as infiltration into layer 1. The recharge package also was used to apply additional infiltration to cells that represent areas

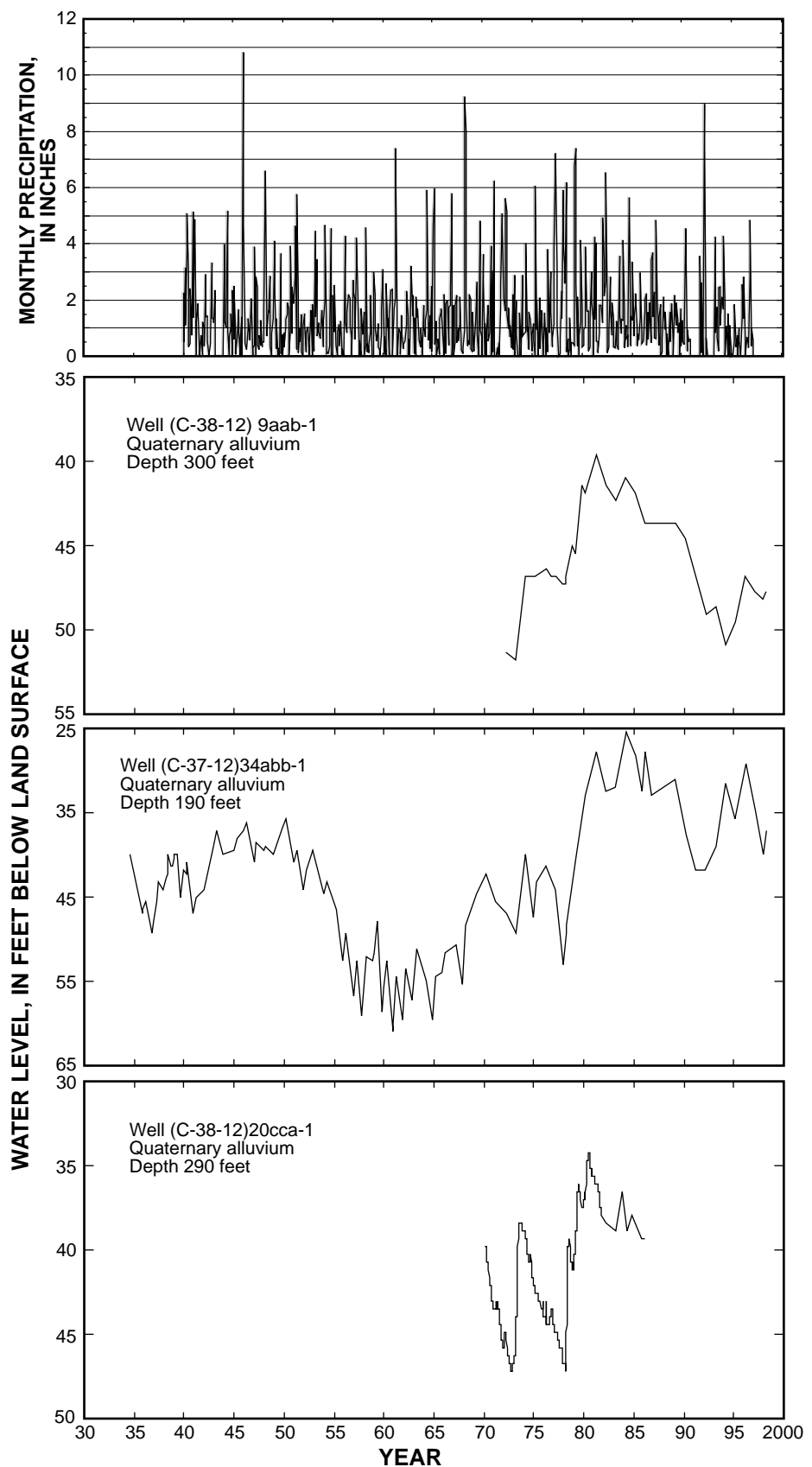


Figure 31. Water levels in three wells in the upper Ash Creek drainage basin, Utah, 1934-95.

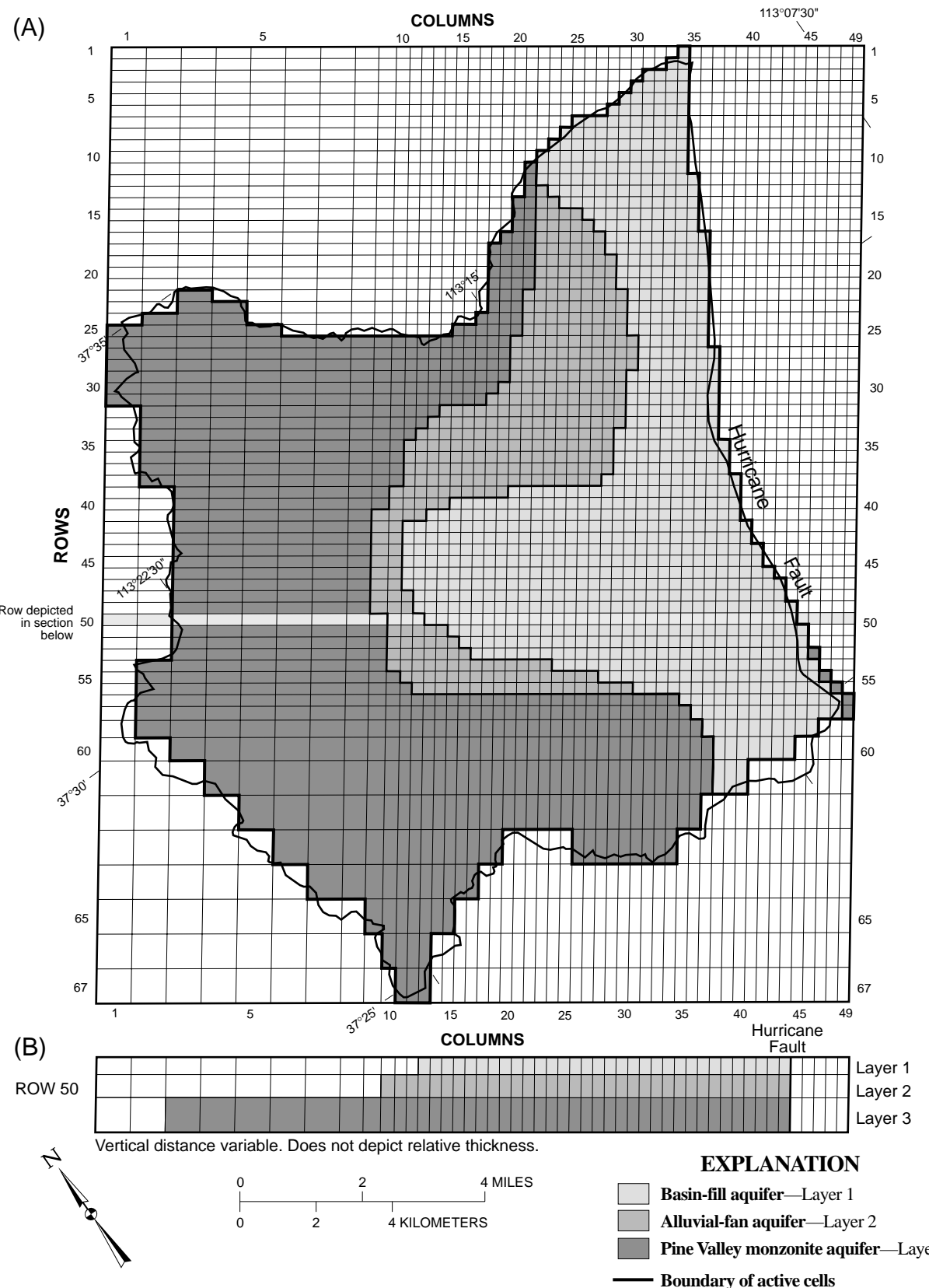


Figure 32. Map and section showing (a) finite-difference model grid and (b) layering scheme for the ground-water flow model of the upper Ash Creek drainage basin, Utah.

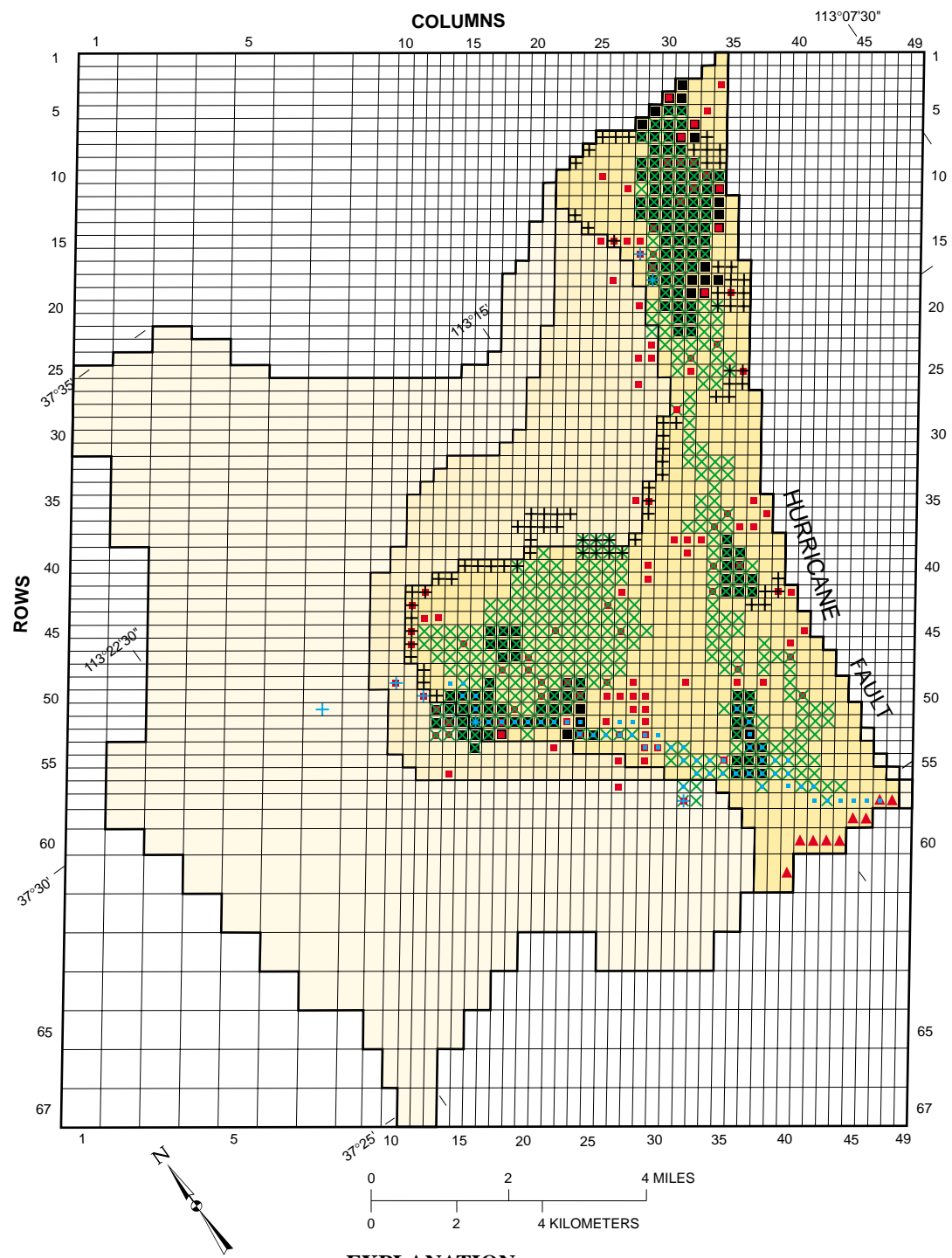


Figure 33. Boundary conditions and cell assignments for the ground-water flow model of the upper Ash Creek drainage basin, Utah.

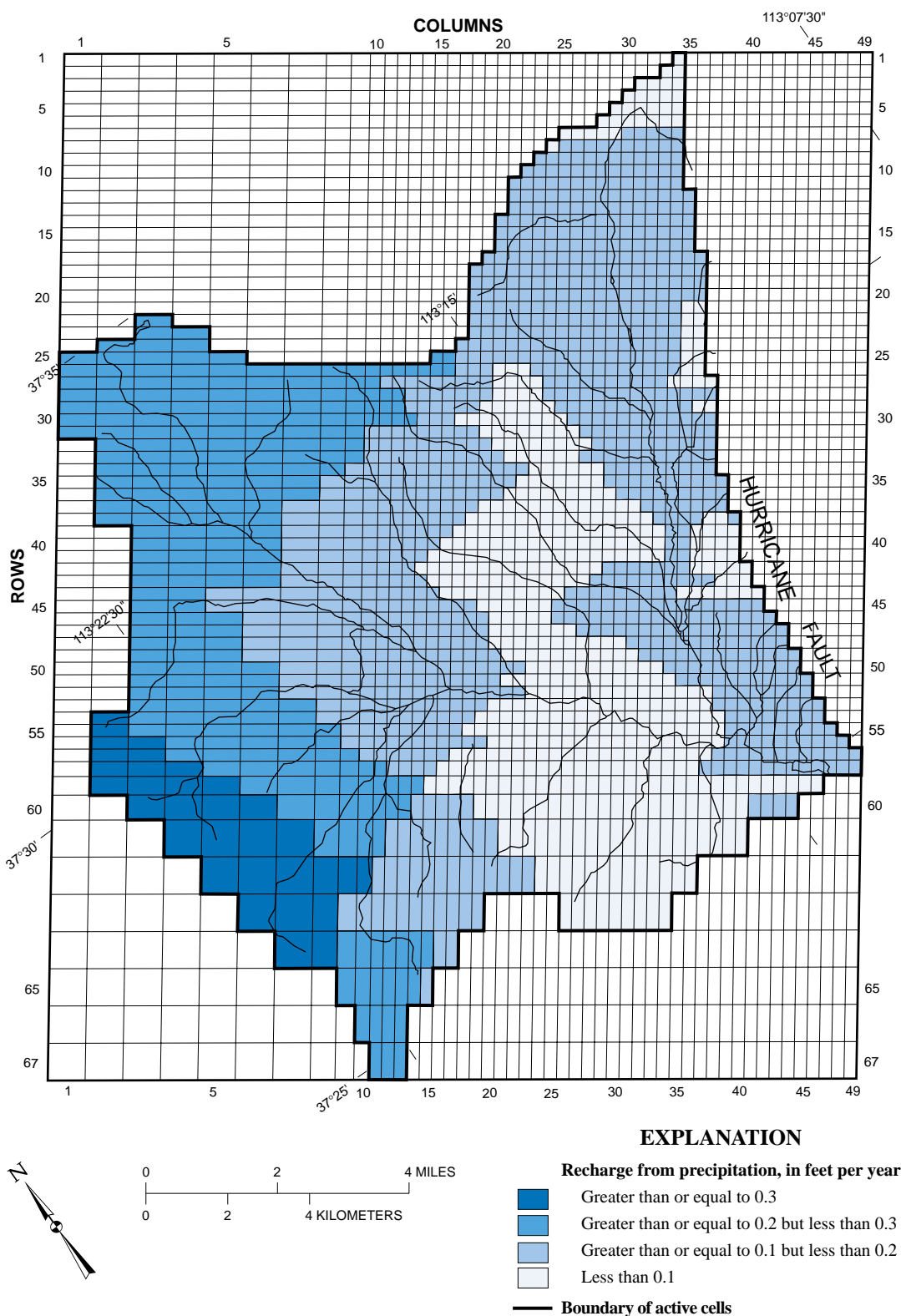


Figure 34. Areal distribution of recharge from infiltration of precipitation in the ground-water flow model of the upper Ash Creek drainage basin, Utah.

where ephemeral streams flow from the Harmony and Pine Valley Mountains onto the valley floor. The amount was arbitrary because there is no record of streamflow for these washes. The amount was adjusted during steady-state model refinement to closely approximate steady-state water levels but not beyond the estimated runoff for the drainage area represented by the wash.

Ash Creek

The river package (Harbaugh and McDonald, 1996, p. 26) simulates stream seepage from Ash Creek to the basin-fill aquifer (recharge). The river package represents a head-dependent flux boundary and one reach per cell is simulated (fig. 35). Stream leakage occurs whenever the water level in the aquifer is below the stage in the stream. When the stream is not in hydraulic connection with the aquifer (when there is an unsaturated zone beneath the streambed), the flux is controlled by the difference between the altitude of the stream stage and the bottom of the streambed material (RBOT) and the hydraulic conductance of the streambed. In cases where the stream is in hydraulic connection with the aquifer, the rate of leakage is controlled by (1) the difference between the altitude of the stream stage and the calculated head at the node of the cell underlying the stream reach; and (2) the conductance of the streambed (the product of vertical hydraulic conductivity and cross sectional area divided by streambed thickness). The cross sectional area is the area of streambed within each cell. Values for conductance of a small stream traversing basin fill are probably quite variable, but most were assigned a value equal to one-tenth of the horizontal hydraulic-conductivity value of the basin-fill aquifer times the length of the stream across the cell divided by a 1-ft thick streambed. The cells that represent Ash Creek Reservoir were assigned a value equal to one-hundredth of the horizontal hydraulic-conductivity value of the basin-fill aquifer times the reservoir area in the cell divided by a 1-ft thick lake bed because the reservoir bottom likely consists of much finer grained sediments than the streambed. The average altitude of the stream/lake bed was obtained from topographic maps with a contour interval of 20 ft. The stream/reservoir altitude was assigned a value 10 ft higher than the bottom altitude, thereby allowing stream or lake leakage to be driven by a hydraulic head of 10 ft. The actual driving head is probably more than 10 ft in the reservoir and less than 10 ft in the stream. A model that is intended for use as a predictive tool should be constructed so that this interac-

tion between stream and aquifer and between reservoir and aquifer is more realistically depicted using vertical hydraulic conductivity values and varying stream/reservoir stage.

Irrigation

Irrigation areas were delineated from land-use maps developed by the Utah Division of Water Resources. Recharge of 880 acre-ft/yr was simulated with the recharge package to account for unconsumed irrigation that infiltrates to the water table (fig. 33). During steady-state model refinement, recharge rates for selected cells were adjusted within reason to obtain a better simulated match with measured water levels. The total recharge simulated for irrigation is consistent with the application method being used.

Discharge boundaries

Several types of head-dependent flux and specified-flux discharge boundaries are used in the baseline simulation (fig. 35). Evapotranspiration is simulated with the evapotranspiration package, well discharge is simulated with the well package, and discharge from springs is simulated with the drain package. Seepage to Ash, Sawyer, and the lower reach of Kanarra Creek was simulated with the river package. Subsurface flow to the south into the lower reaches of the Ash Creek drainage is simulated with the general-head package.

Evapotranspiration

Simulated evapotranspiration from the saturated zone in areas where cottonwood trees and pasture grasses grow is dependent on the depth of the water table, the average rate of consumption by each type of vegetation present, and the depth below land surface at which transpiration ceases for each type of vegetation. The evapotranspiration package simulates the effects of direct evaporation and plant transpiration by using a linear variation in the evapotranspiration rate. The maximum rate occurs when the water table is at or near land surface. The rate drops to zero when the water table is deeper than a specified extinction depth for each type of vegetation. The two dominant types of phreatophytes, cottonwood trees and pasture grasses, have different rates of water consumption and different maximum depths from which they can use ground water. The baseline numerical simulation described in this report uses extinction depths of 25 ft (Robinson, 1958, p. 62) for cottonwoods and 5 ft for pasture grass. Because of lower temperatures and density of the

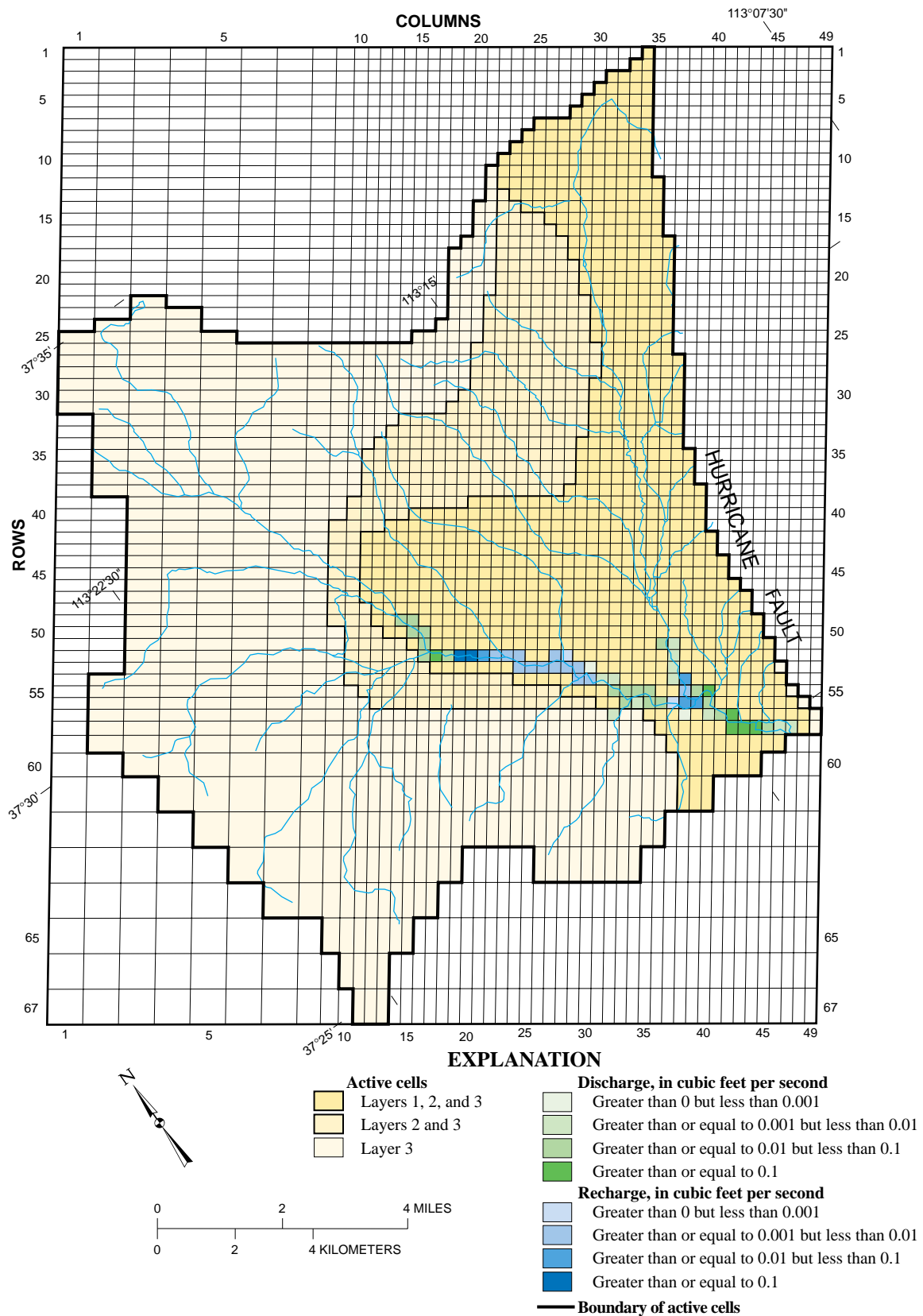


Figure 35. Simulated recharge to and discharge from the aquifers by stream seepage in the ground-water flow model of the upper Ash Creek drainage basin, Utah.

growth in the upper Ash Creek drainage, consumptive use rates were set at 3.5 ft/yr for cottonwood trees and 1.75 ft/yr for pasture grass, somewhat less than the rates from other studies. Evapotranspiration represents a head-dependent discharge boundary at the top of the saturated zone that functions only when the water-table altitude is above the extinction depth or above land surface.

Wells

Well discharge is simulated as a specified-flux discharge with the well package. Because water use for the upper Ash Creek drainage basin is not well documented, the amount of discharge simulated for each cell was estimated on the basis of type of water use, well diameter, and length of open interval. Relative to the water right, household wells were assigned a fixed discharge of 0.67 acre-ft/yr, wells used for stock were assigned a fixed discharge of 0.23 acre-ft/yr, and wells used for domestic, stock, and irrigation were assigned a fixed discharge of 3.3 acre-ft/yr. These rates combined with the rate for irrigation wells yielded a total discharge of 1,440 ft/yr. Discharge from irrigation wells was estimated based on average discharge from four irrigation wells measured with a sonic velocity device. The average discharge per square foot of screen for the four measured wells was 0.85 (gal/min)/ft². This factor was multiplied by the screen area of all other irrigation wells, and assuming 3 months of pumping per year, was used to obtain the estimated discharge in the baseline simulation. The distribution and magnitude for simulated well discharge is shown in figure 36.

Springs

Spring discharge is simulated with the drain package. The drain package represents a head-dependent discharge boundary for each cell to which it is assigned. The amount of discharge simulated depends on the assigned conductance value and the difference between the assigned drain altitude and the simulated water level in that cell. Drain altitudes were taken from topographic maps and were adjusted during model refinement within the accuracy of the map contour intervals. The drain simulates no discharge when the computed head is lower than the specified drain altitude. The conductance values were adjusted during the model refinement procedure to approximate the measured discharge at selected springs.

Ash and Kanarra Creeks

Discharge from the aquifer into the perennial reaches of Ash and Kanarra Creeks is simulated with the river package (fig. 33). The river package represents a head-dependent boundary at the contact between perennial streams and the uppermost saturated zone. Discharge from the ground-water system to the streams is controlled by (1) the difference between the simulated head in a river cell and the altitude of the stream or lake bottom, (2) the streambed area in each cell, and (3) the assigned conductance value for the streambed. The streambed area in each cell and the assigned conductance values are explained above in the "Ash Creek" section.

Subsurface Flow to Lower Ash Creek Drainage

Subsurface flow from the upper Ash Creek drainage basin ground-water system to the south into the lower Ash Creek drainage (fig. 33) is simulated with the general-head package. This package represents a head-dependent boundary between the assigned cells and a fixed-head boundary outside of the modeled area. When the fixed head is lower in altitude than the simulated water-level altitude in the general-head cells, discharge from those cells is simulated. The amount of discharge simulated depends on the simulated head difference and the assigned conductance value. The conductance value is approximated by dividing the product of the horizontal hydraulic conductivity of the material and the cross-sectional area by the distance traveled through that material. This value is somewhat speculative for the area south of Ash Creek Reservoir because the hydraulic properties of the material through which ground water moves are uncertain. Values of conductance assigned for the baseline simulation were 20 ft²/d for the basin-fill and Pine Valley monzonite aquifers and 15 ft²/d for the alluvial-fan aquifer. A fixed head of 3,850 ft was assigned to represent a well 3.5 mi to the south.

No-Flow Boundaries

It is conceptualized that no ground water enters or exits the upper Ash Creek drainage basin at the drainage-basin boundaries or at the Hurricane Fault. The model was developed so that the appropriate layer boundaries terminate at the drainage-basin boundaries and the fault. No flow was simulated for all lateral boundaries except at the general head cells south of Ash Creek Reservoir. Also, no flow was simulated for the base of the Pine Valley monzonite aquifer (layer 3).

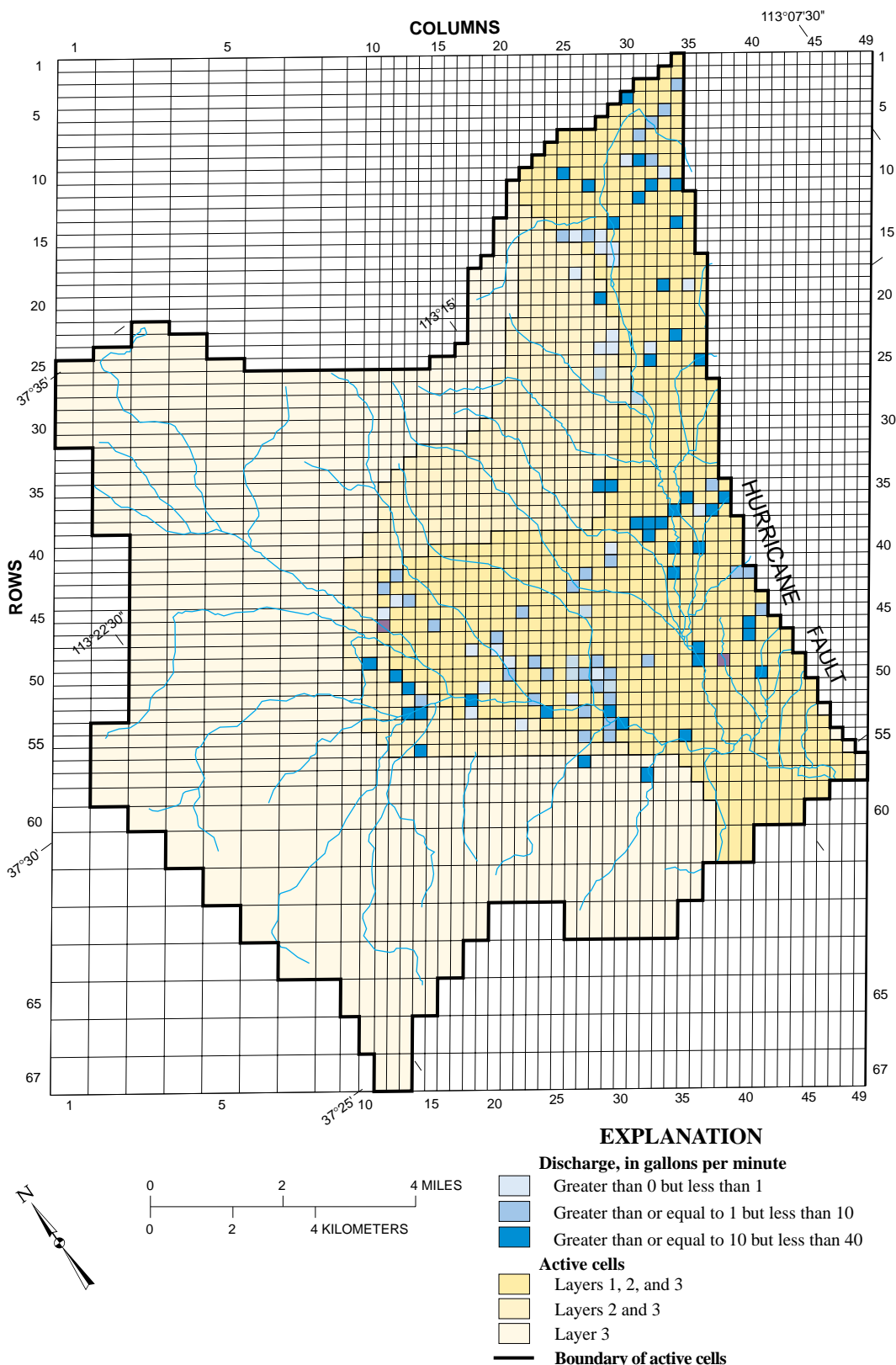


Figure 36. Location and magnitude of simulated well discharge in the ground-water flow model of the upper Ash Creek drainage basin, Utah.

Ground-Water Divide

The ground-water divide between the upper Ash Creek drainage basin and Cedar Valley ground-water systems represents a no-flow boundary whose position varies with time. Withdrawals from the Cedar Valley ground-water system to the north apparently have moved this boundary 2 mi farther south since the mid-1940s. These withdrawals were not simulated in the upper Ash Creek drainage basin.

Faults

A no-flow boundary is simulated for the Hurricane Fault. Cross sections from geologic mapping indicate that the offset of the fault is many thousands of feet. Water levels and streamflow measurements indicate that there is little or no ground water moving through the fault system into the basin-fill aquifer.

Underlying Formations

The nature of the material that underlies the Pine Valley monzonite aquifer is not known. As stated previously, this aquifer is thought to be more than 2,000 ft thick. The bottom of the aquifer was chosen to be at 3,000 ft below land surface. This allows the simulated transmissivity to be calculated from the product of hydraulic conductivity and saturated thickness. Compaction and cementation associated with deeper burial are presumed to have resulted in low hydraulic conductivity, so that no ground water is moving from depth up into the aquifer; thus, it is simulated as a no-flow boundary.

Divides

The surface drainage divide for the Ash Creek drainage basin was assumed to be a ground-water divide and thus is simulated as a no-flow boundary.

Distribution of Aquifer Characteristics

Each model layer represents a different aquifer and is assigned hydrologic properties on the basis of aquifer-test results reported in the literature, specific-capacity tests, and lithologic descriptions from drillers' logs. Available data with which to estimate aquifer properties are scant. The initial distribution of transmissivity for layer 1, the basin-fill aquifer, was developed by comparing the values reported from a few aquifer tests with values from specific-capacity tests done by drillers. A rough map of the most likely values and their areal distribution was created and appropriate values

for aquifer top, bottom, and hydraulic conductivity were assigned to the cells that represent that aquifer. Transmissivity in the model is calculated from the product of the hydraulic conductivity and the saturated thickness. The distribution for layers 2 and 3 was determined in the same way but is based on fewer data.

While trying to match measured and model-computed water levels and estimated and model-computed flows, initial distributions were altered within reasonable limits to obtain the best match between measured and computed values. Final distributions of transmissivity are shown in figure 37. The distribution values for layer 2 are 10 times smaller than values in the other layers. This is speculative and was based on the relative differences in a few specific-capacity values. The distribution for layer 3 is largely uncertain for all areas except south of New Harmony, where several irrigation wells have been drilled. Layer 3 for the Harmony and Pine Valley Mountains and where the monzonite aquifer is at depth under basin fill, was assigned a small transmissivity value. A line of cells across the Harmony structural basin also were assigned a small value to simulate the potential impedance of west-to-east ground-water movement across the fault zone mapped by Hurlow (1998). Slightly higher values were assigned to a zone of cells that represent a more structurally disturbed transition from Pine Valley monzonite to the Quachapa Group and Claron Formation, roughly along the stream course of Comanche Creek.

Vertical-Head Gradients

No wells with multiple completions are finished in any of the three aquifers; however, anomalous water levels in some closely spaced wells indicate possible vertical-head gradients within and between aquifers (discussed in "Ground-water movement" section). To simulate vertical-head differences, the values for vertical conductance between layers must be small enough to create an impedance to vertical ground-water movement. Laterally uniform values are used for the baseline simulation and were chosen during model development to approximate measured water levels. Final vertical-conductance values were 1×10^{-4} (ft/d)/ft between layers 1 and 2 and 1 (ft/d)/ft between layers 2 and 3. This simulates little or no vertical impedance to flow between layers 2 and 3 and substantial impedance between layers 1 and 2. Because of the uncertainty in the values for aquifer properties and geometry, vertical-conductance values were assigned during model refinement, not on the basis of calculations of vertical hydraulic conduc-

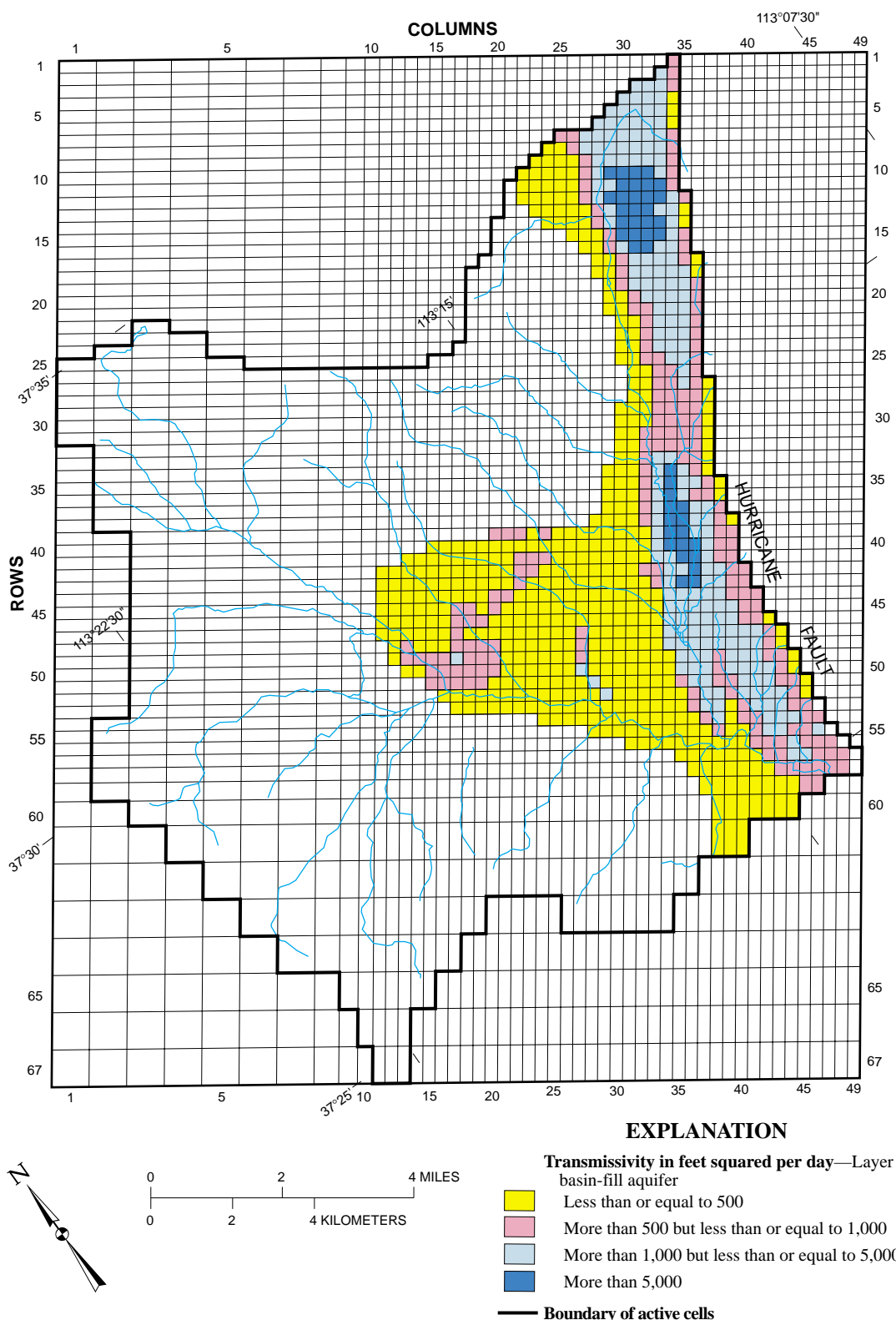


Figure 37. Final distribution of transmissivity simulated in the ground-water flow model of the upper Ash Creek drainage basin, Utah.

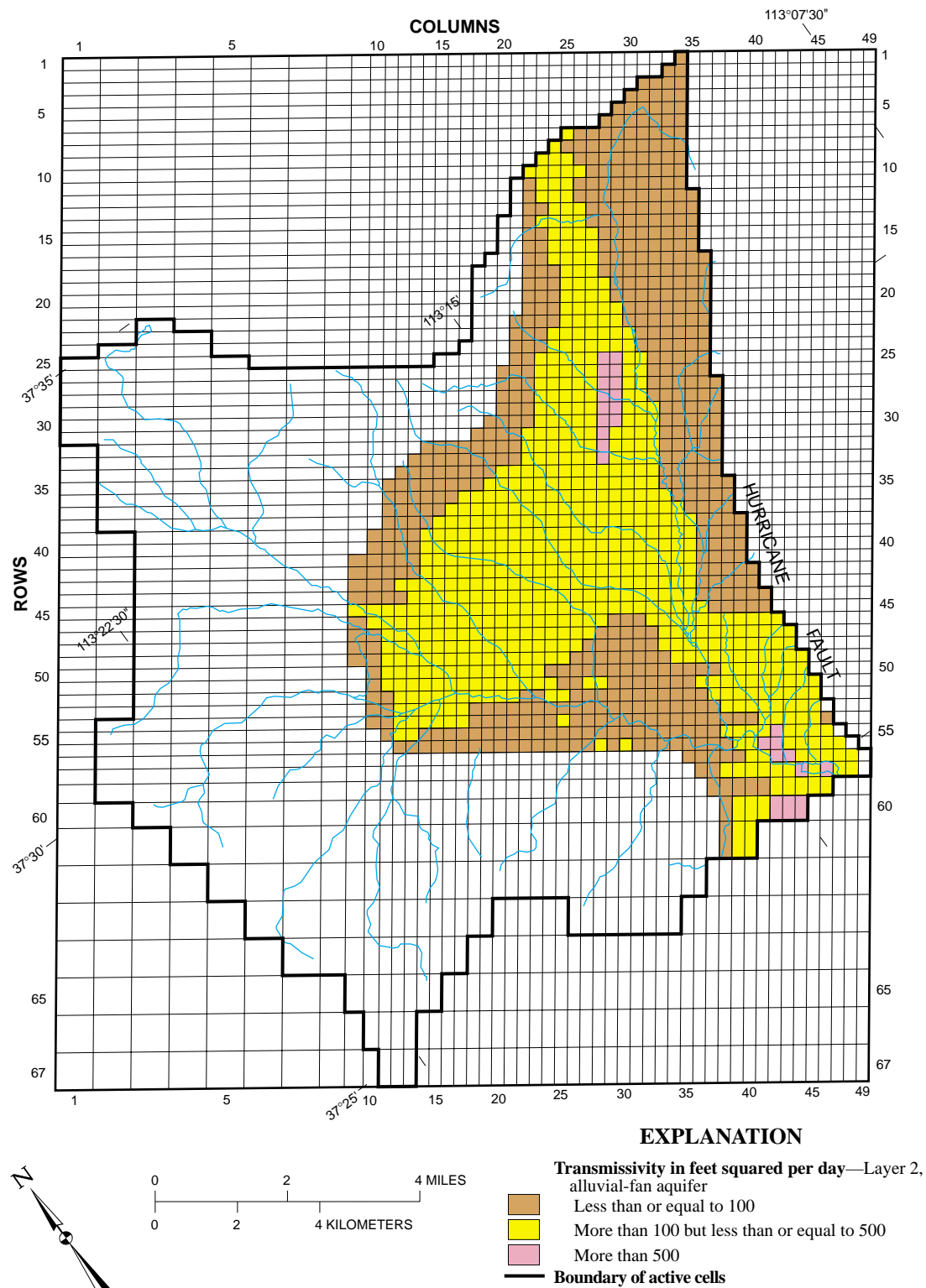
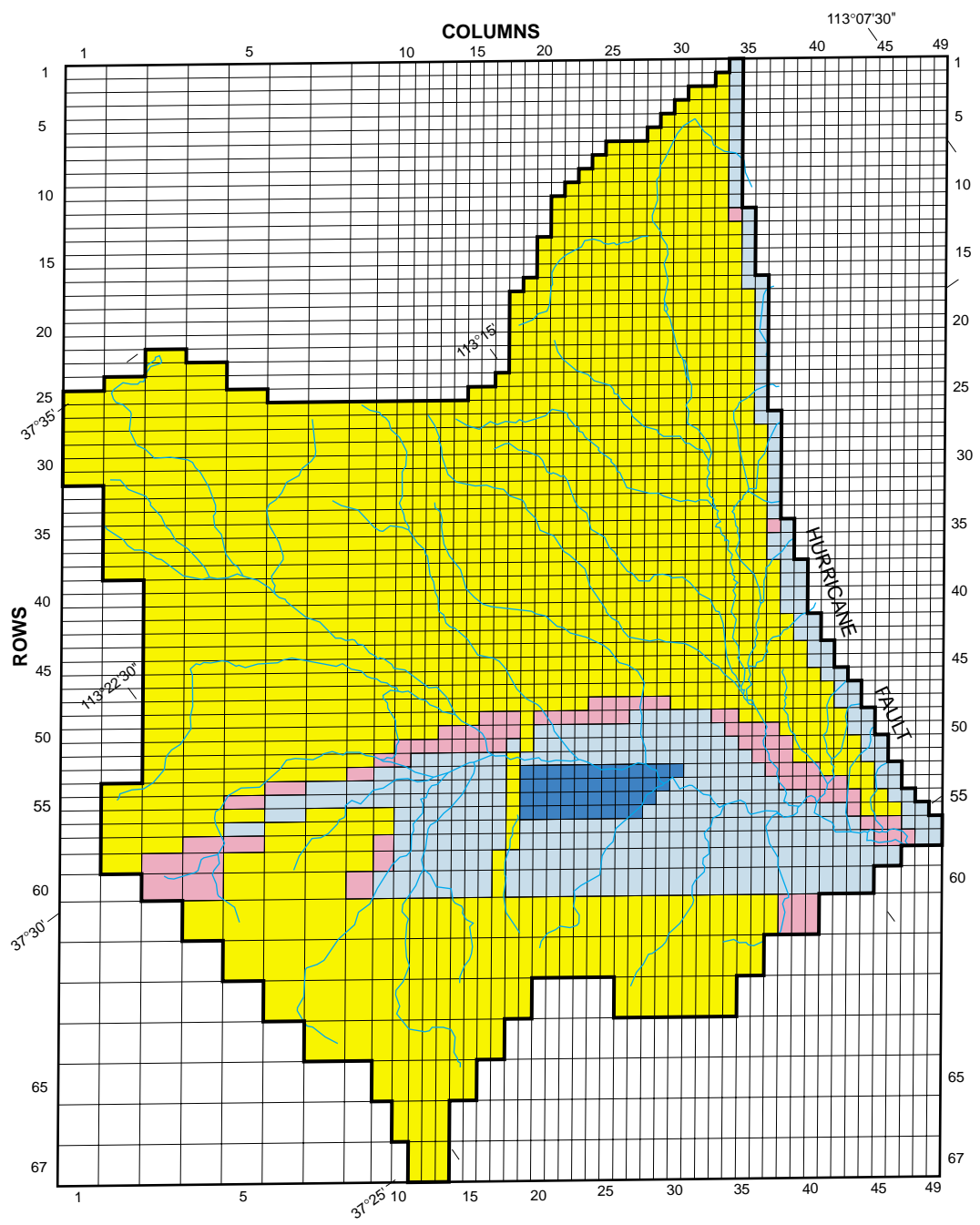


Figure 37. Final distribution of transmissivity simulated in the ground-water flow model of the upper Ash Creek drainage basin, Utah—Continued.



EXPLANATION

Transmissivity in feet squared per day—Layer 3,
Pine Valley monzonite aquifer

Less than or equal to 500

More than 500 but less than

More than 1,000 but less than or equal to 5,000

More than 5,000

Boundary of active

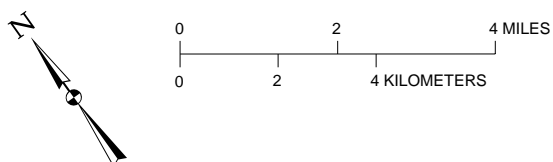


Figure 37. Final distribution of transmissivity simulated in the ground-water flow model of the upper Ash Creek drainage basin, Utah—Continued.

tivity multiplied by cross sectional area divided by distance between the center of layers.

Conceptual Model and Numerical Simulations

Two factors are typically used to determine how closely a numerical simulation compares to a conceptual ground-water flow model: (1) comparison of computed and measured water levels in wells, and (2) comparison of the model's volumetric-balance calculation and the estimated ground-water budget. Although there are similarities between the budgets, computed water levels in layer 3 of the upper Ash Creek drainage basin model are substantially higher than measured water levels, and there is considerable variation among

the four computed and measured water levels for layer 2 (table 17). These comparisons indicate that although the conceptual model could be correct, there are many details about aquifer-property distribution and system heterogeneity that are not accurately represented by this baseline simulation. The direction of ground-water movement depicted by the baseline simulation (fig. 38a, b, and c) is similar to that depicted in figure 18, indicating flow from recharge areas in the surrounding mountains to discharge points at springs and streams.

Model Applicability

The model was developed to help understand the ground-water flow system in the upper Ash Creek

Table 17. (a) Conceptual and simulated ground-water budgets and (b) simulated versus measured water-level differences for the upper Ash Creek drainage basin ground-water system, Utah

(a) Ground-water budget		
Flow component	Conceptual	Baseline simulation ¹ (rounded)
Recharge, in acre-feet per year		
Infiltration of precipitation	2,100 to 9,200	10,410
Seepage from ephemeral streams	1,000 to 6,000	2,650
Infiltration of unconsumed irrigation water	0 to 5,000	880
Seepage from perennial streams	500 to 1,100	380
Total	3,600 to 21,300	14,320
Discharge, in acre-feet per year		
Well discharge	1,200 to 1,500	1,440
Evapotranspiration	1,100 to 15,000	8,410
Spring discharge	200 to 1,000	340
Seepage to Ash, Sawyer, and Kanarra Creeks	500 to 3,000	1,630
Subsurface outflow to lower Ash Creek drainage	0 to 7,500	2,500
Total	3,000 to 28,000	14,320

¹Budget amounts in italics are specified and not computed by the model.

(b) Difference between simulated and measured water levels, in feet			
Water-level comparison	Layer 1 basin fill	Layer 2 alluvial fan	Layer 3 Pine Valley monzonite
Number of water levels compared	18	4	8
Maximum computed above measured, in feet	54	51	97
Maximum computed below measured, in feet	-36	-110	-35
Mean of differences, in feet	.8	-4.4	34.0
Root mean square error, in feet	24	63	57

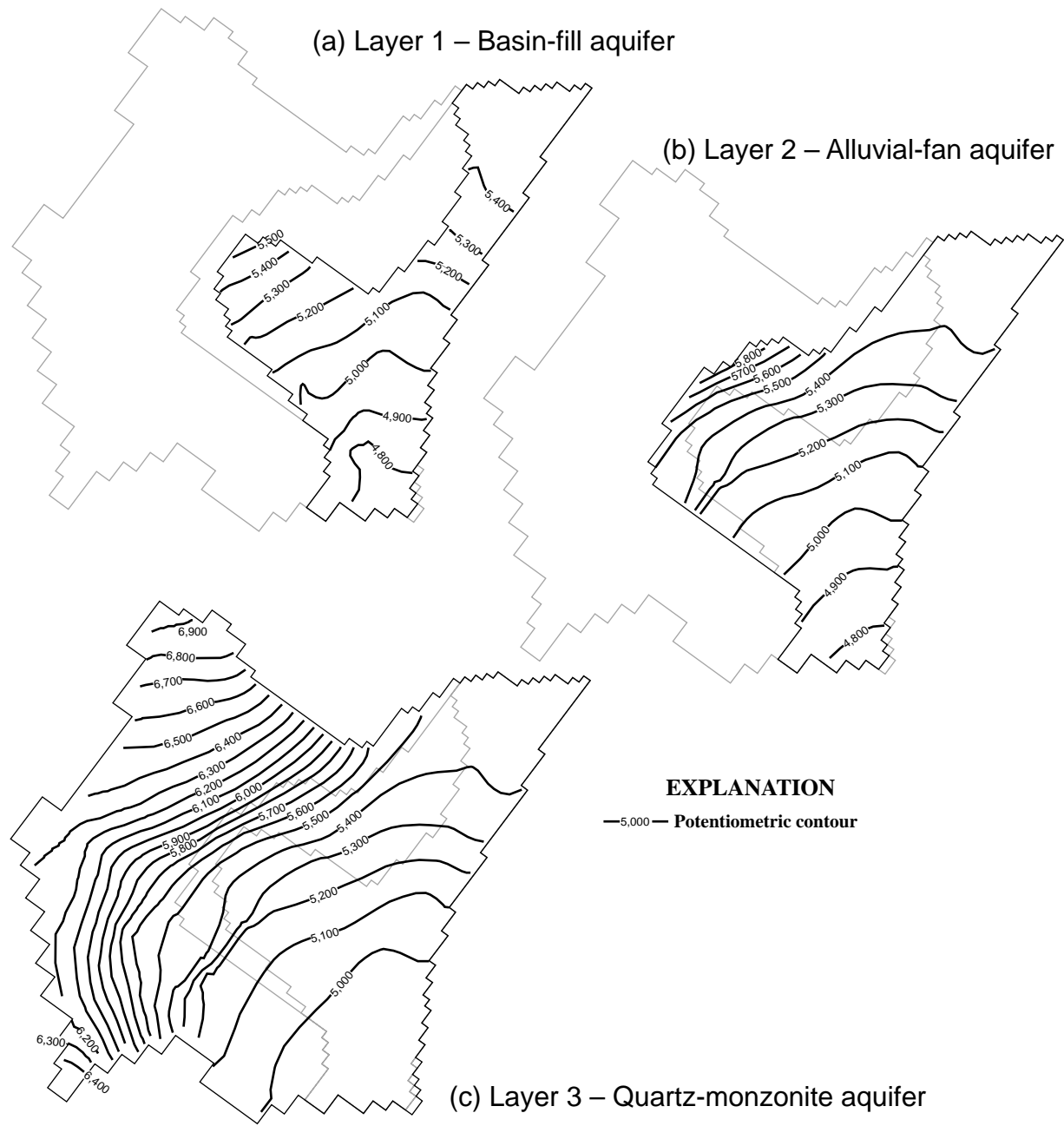


Figure 38. Simulated potentiometric contours in (a) layer 1, (b) layer 2, and (c) layer 3 from the baseline simulation of the upper Ash Creek drainage basin, Utah. [New figure]

drainage basin. It is the first computer simulation of the upper Ash Creek drainage basin. Because of the many uncertainties regarding boundaries, geometry, and aquifer properties, it is not considered a “calibrated” steady-state model. It should be thought of as a tool to use to explore the viability of alternative conceptualizations about the flow system.

Alternative Conceptualizations

Numerous alternative conceptual models might match the measured ground-water budget components and water levels. Much more hydrologic data are needed before a calibrated model can be developed. This model is the mathematical representation of one of those conceptual models. This numerical model was used to explore the validity of other conceptualizations about the upper Ash Creek drainage basin ground-water system. Four different conceptualizations were simulated.

Alternative 1—Flow Across the Hurricane Fault

On the basis of the relation between recharge and average annual precipitation in excess of 8 in. defined for the basin-fill aquifers of Nevada and Utah (Harrill and Prudic, 1998), about 1,000 acre-ft/yr of “mountain-front” recharge could be generated by precipitation on the Markagunt Plateau east of the Hurricane Fault. If this amount of recharge were added as inflow to the basin-fill aquifer at the eastern boundary of the upper Ash Creek drainage basin, water levels in all three layers would rise along the boundary by 5 to 15 ft. Water levels in the area around Ash Creek Reservoir and New Harmony would increase by less than 2 ft. Most of the increase in recharge would be counterbalanced by an increase in evapotranspiration, which would be well within conceptual estimates. Seepage to Ash Creek, discharge at springs, and underflow to the lower Ash Creek drainage area would also increase slightly. Seepage from Ash Creek would decrease by less than 1 acre-ft/yr.

In summary, the alternative 1 simulation did not improve the water-level match for layers 1 and 2 and slightly improved the match for layer 3 (table 18). Recharge along the east boundary across the Hurricane Fault is plausible, but not an improvement over the baseline simulation. Simulated ground-water movement through the system did not change substantially in this alternative (fig. 39a, b, and c).

Alternative 2—No Subsurface Outflow to Lower Ash Creek Drainage

Because no physical evidence of ground-water seepage to lower Ash Creek drainage has been observed, an alternative simulation without this seepage was tested. Simulating no subsurface outflow to the lower Ash Creek drainage was done by changing the conductance values for these general-head boundary cells to zero in the baseline model. The budget components in Alternative 2 were within reasonable ranges; seepage into Ash Creek and spring discharge were increased to values that were closer to those initially conceptualized. The match between measured and simulated water levels were about the same for layer 1 and layer 2. The layer 3 water-level match was slightly worse than in the baseline simulation. Simulated water levels rose as much as 98 ft, but no measured water levels are available for the area where these increases occurred (table 19). The configuration of the potentiometric surfaces was not substantially different than that of the baseline simulation (fig. 40).

Alternative 3—Increased Transmissivity of the Pine Valley Monzonite Aquifer

The hydrologic character of the Pine Valley monzonite aquifer is largely unknown, especially in the mountains and beneath the main part of the alluvial basin between Kanarraville and Ash Creek Reservoir. The aquifer is assumed to have low transmissivity everywhere except south of New Harmony where irrigation wells have high yields. Transmissivity values for these unknown areas were increased to about 10 times the values used in the baseline simulation. Higher transmissivity values for layer 3 could not be numerically simulated. The model would not converge to the prescribed closure criteria and water-level declines caused numerous cells in layer 2 to be eliminated from the simulation because water levels fell below the defined bottom of the aquifer. This was likely caused by the conductive vertical connection simulated between layers 2 and 3. Increasing the transmissivity of layer 3 likely is not a viable conceptualization.

Alternative 4—Variation in anisotropy of the Pine Valley Monzonite Aquifer

The Pine Valley monzonite contains numerous fractures in outcrops (Hurlow, 1998, p. 29) and the primary orientation of these fractures has been observed to be generally north-south. An anisotropy ratio for hydraulic conductivity of 1.5-to-1 along the column direction (south-southwest to north-northeast) was used

Table 18. (a) Conceptual and simulated ground-water budgets and (b) simulated versus measured water-level differences for the baseline simulation and the simulation testing flow across the Hurricane Fault in the upper Ash Creek drainage basin ground-water system, Utah

(a) Ground-water budget			
Flow component	Conceptual	Baseline simulation (rounded)	Hurricane Fault simulation (rounded)
Recharge, in acre-feet per year			
Infiltration of precipitation	2,100 to 9,200	10,410	10,410
Seepage from ephemeral streams	1,000 to 6,000	2,650	2,650
Infiltration of unconsumed irrigation water	0 to 5,000	880	880
Seepage from perennial streams	500 to 1,100	380	370
Underflow across Hurricane Fault	—	—	950
Total	3,600 to 21,300	14,320	15,260
Discharge, in acre-feet per year			
Well discharge	1,200 to 1,500	1,440	1,440
Evapotranspiration	1,100 to 15,000	8,410	9,320
Spring discharge	200 to 1,000	340	350
Seepage to Ash, Sawyer, and Kanarra Creeks	500 to 3,000	1,630	1,650
Subsurface outflow to lower Ash Creek drainage	0 to 7,500	2,500	2,500
Total	3,000 to 28,000	14,320	15,260

(b) Difference between simulated and measured water levels, in feet						
Water level	Layer 1 basin fill		Layer 2 alluvial fan		Layer 3 Pine Valley monzonite	
	Baseline simulation	Hurricane Fault simulation	Baseline simulation	Hurricane Fault simulation	Baseline simulation	Hurricane Fault simulation
Number of water levels compared	18		4		8	
Maximum computed above measured, in feet	54	64	51	54	97	92
Maximum computed below measured, in feet	-36	-34	-110	-108	-35	-37
Mean of differences, in feet	-0.8	3.9	-4.4	-.3	34.0	29.3
Root mean square error, in feet	24	26	63	63	57	54

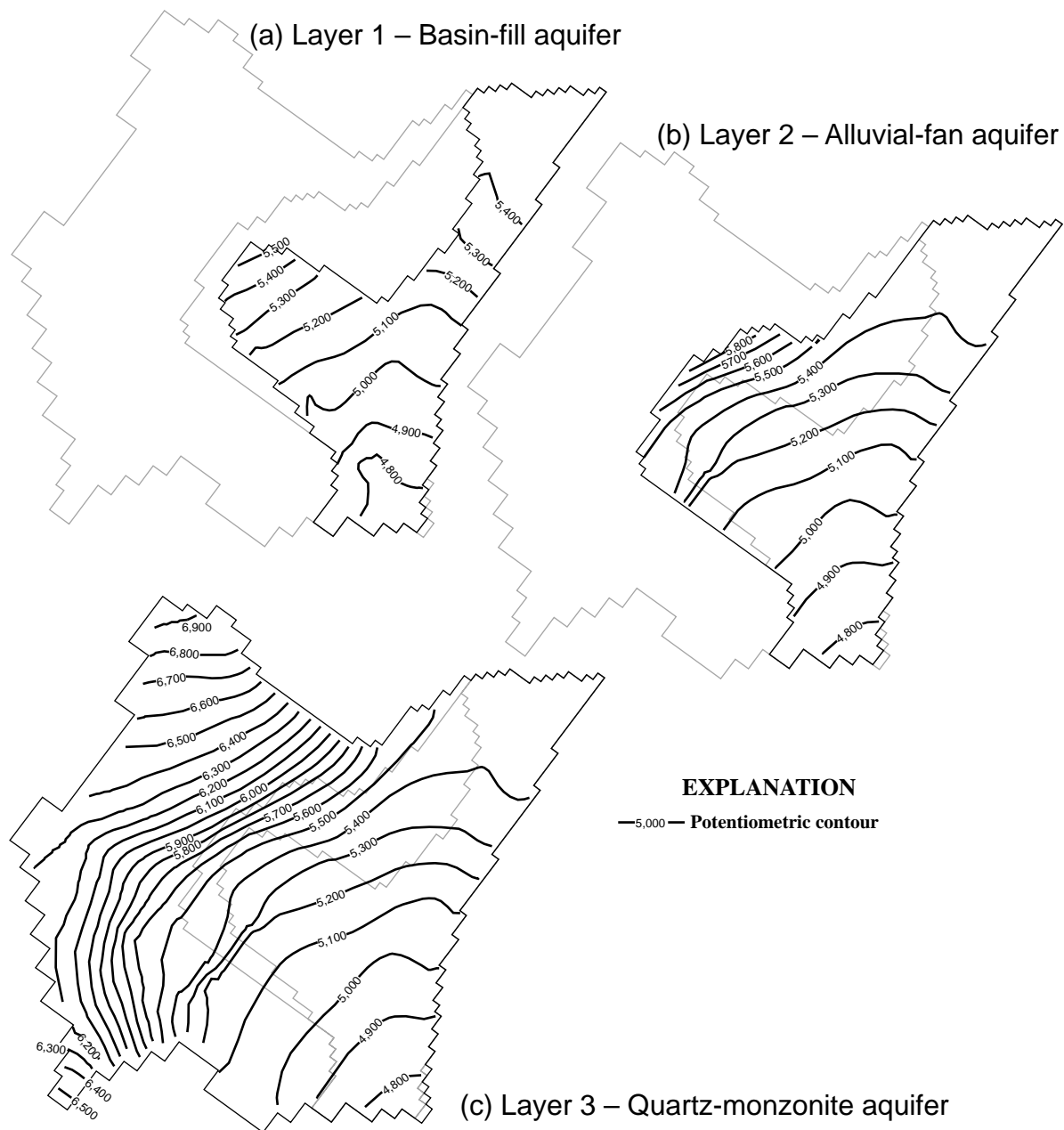


Figure 39. Simulated potentiometric contours in (a) layer 1, (b) layer 2, and (c) layer 3 from alternative simulation depicting flow across the Hurricane Fault, the upper Ash Creek drainage basin, Utah.

Table 19. (a) Conceptual and simulated ground-water budgets and (b) simulated versus measured water-level differences for the baseline simulation and the simulation of no subsurface outflow to the lower Ash Creek drainage basin, Utah

(a) Ground-water budget			
Flow component	Conceptual	Baseline simulation	No subsurface outflow simulation
Recharge, in acre-feet per year			
Infiltration of precipitation	2,100 to 9,200	10,410	10,410
Seepage from ephemeral streams	1,000 to 6,000	2,650	2,650
Infiltration of unconsumed irrigation water	0 to 5,000	880	880
Seepage from perennial streams	500 to 1,100	380	350
Total	3,600 to 21,300	14,320	14,290
Discharge, in acre-feet per year			
Well discharge	1,200 to 1,500	1,440	1,440
Evapotranspiration	1,100 to 15,000	8,410	10,290
Spring discharge	200 to 1,000	340	390
Seepage to Ash, Sawyer, and Kanarra Creeks	500 to 3,000	1,630	2,170
Subsurface outflow to lower Ash Creek drainage	0 to 7,500	2,500	0
Total	3,000 to 28,000	14,320	14,290

(b) Difference between simulated and measured water levels						
Water level	Layer 1 basin fill		Layer 2 alluvial fan		Layer 3 Pine Valley monzonite	
	Baseline simulation	No under- flow simulation	Baseline simulation	No under- flow simulation	Baseline simulation	No underflow simulation
Number of water levels compared	18		4		8	
Maximum computed above measured, feet	54	54	51	51	97	98
Maximum computed below measured, in feet	-36	-36	-110	-110	-35	-35
Mean of differences, in feet	-0.8	-0.4	-4.4	-4.4	34.0	35.3
Root mean square error, in feet	24	24	63	63	57	58

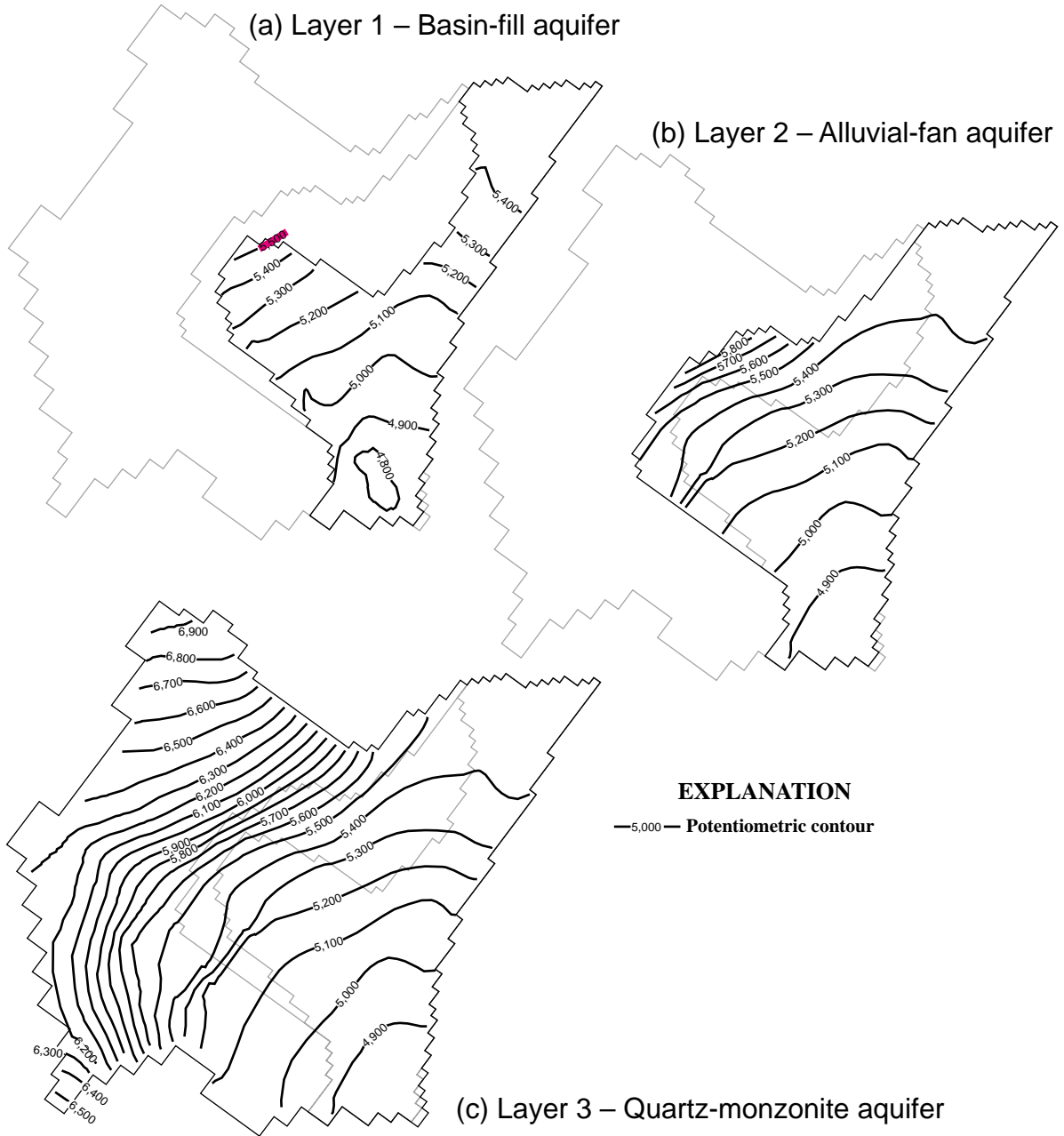


Figure 40. Simulated potentiometric contours in (a) layer 1, (b) layer 2, and (c) layer 3 from alternative simulation depicting no outflow from the basin near Ash Creek reservoir, upper Ash Creek drainage basin, Utah.

in the baseline simulation; however, this ratio is speculative. Because of uncertainty about the relative magnitude of hydraulic conductivity in the direction of primary fracture orientation, the anisotropy ratio conceptually could be lower or higher than the value used in the baseline model. To test this alternative, the anisotropy ratio was increased from 1.5-to-1 to 3-to-1, and then decreased to 1-to-1.

The simulations (table 20) indicate that an anisotropy of 3-to-1 in layer 3 is a plausible hydrologic conceptualization. This ratio, however, did not provide as close a match to measured water levels in layers 1 and 2 as an anisotropy ratio of 1.5-to-1. An anisotropy ratio of 1-to-1 in layer 3 also is a plausible hydrologic conceptualization. Water-budget discharge to springs and streams was within the desired range, and simulated water levels were closer to measured values for layers 2 and 3. The configuration of the potentiometric surfaces was not substantially different than that of the baseline simulation.

Model Sensitivity

Sensitivity analyses are an important part of developing ground-water flow models. They help to understand which properties and budget components are most important to simulation results, and thus, which should be given the highest priority when considering additional analysis or data collection. The upper Ash Creek drainage basin ground-water flow model described in this report is considered the most plausible and probable representation of the ground-water flow system for 1995 conditions. It is not considered to be "calibrated." There are numerous uncertainties about the hydrologic boundaries, the amount of water moving across these boundaries, and about the geometry and properties of the aquifers. Relative sensitivity of the baseline model to variations in different parameters is shown in figure 41. The height of each bar is subjective and is based on an overall evaluation of how variations in the parameters affected computed water levels and head-dependent flux. More detailed analyses and results of all sensitivity runs are in appendix B.

The baseline model was acutely sensitive to variations in the water transmitting properties of the layers that represent the basin-fill and the Pine Valley monzonite aquifers and of the vertical conductance in the basin fill. The model appears to be insensitive to vertical conductance between the alluvial-fan and Pine Valley monzonite aquifers, but this was a result of setting

the baseline value for conductance high. If conductance values were decreased to those for the basin-fill aquifer, the model would indicate a comparable sensitivity to this value. The amount of water simulated as recharge from unconsumed irrigation and as direct infiltration from precipitation also affected baseline model results. Other parameters such as transmissiveness of the alluvial-fan aquifer, streambed conductance, and recharge attributed to ephemeral stream flow affected results moderately to slightly.

Need for Additional Study

On the basis of model sensitivity to selected parameters, collection of specific types of data would help refine the present hydrologic conceptualization. Data needed to update this preliminary model might include the amount of (1) water applied for irrigation, (2) water used by different crops, (3) applied water that evaporates, and (4) applied water that runs off into drainage channels. Recharge from precipitation and how it is distributed laterally throughout the upper Ash Creek drainage basin also warrants additional attention.

Appropriately designed multiple-observation-well aquifer testing is needed for the basin-fill and Pine Valley aquifers. The variability in transmissivity of the basin-fill aquifer, created by variations in thickness and lithologic character, needs to be well delineated to decrease the uncertainties in this important parameter. Additional data on the variability of transmissivity in the monzonite aquifer are equally needed. Water from snowmelt and precipitation infiltrating into the surrounding mountains eventually moves from this fractured crystalline aquifer into shallow alluvial deposits where it is discharged by evapotranspiration, springs, wells, and seepage to streams. Better understanding of the flow paths through the fractured monzonite aquifer and how water moves from fractured crystalline rock to unconsolidated sediments are critical to developing accurate numerical simulations of this flow system.

Water-Resource Management

Probably the most important aspects of effectively managing the surface- and ground-water resources of the upper Ash Creek drainage basin are the amount of water that moves through the system from year to year and where, why, and how that water is being used within the system. Much of that information has been documented by observations, measurements, and development of a preliminary simulation. The simulations described herein should not be used to manage

Table 20. (a) Conceptual and simulated ground-water budgets and (b) simulated versus measured water-level differences for the baseline simulation and the simulation testing anisotropy in the Pine Valley monzonite aquifer in the upper Ash Creek drainage basin ground-water system, Utah

(a) Ground-water budget					
Flow component	Conceptual model		Baseline simulation (anisotropy 1.5:1)	Higher-anisotropy simulation (3:1)	No-anisotropy simulation (1:1)
Recharge, in acre-feet per year					
Infiltration of precipitation	2,100 to 9,200		10,410	10,410	10,410
Seepage from ephemeral streams	1,000 to 6,000		2,650	2,650	2,650
Infiltration of unconsumed irrigation water	0 to 5,000		880	880	880
Seepage from perennial streams	500 to 1,100		380	360	370
Total	3,600 to 21,300		14,320	14,300	14,310
Discharge, in acre-feet per year					
Well discharge	1,200 to 1,500		1,440	1,440	1,440
Evapotranspiration	1,100 to 15,000		8,410	8,150	8,550
Spring discharge	200 to 1,000		340	450	260
Seepage to Ash, Sawyer, and Kanarra Creeks	500 to 3,000		1,630	1,730	1,570
Subsurface outflow to lower Ash Creek drainage	0 to 7,500		2,500	2,530	2,490
Total	3,000 to 28,000		14,320	14,300	14,310

(b) Difference between simulated and measured water levels, in feet									
Water level	Layer 1 basin fill			Layer 2 alluvial fan			Layer 3 Pine Valley monzonite		
	Baseline simula- tion	Higher anisotropy simulation (3:1)	No anisotropy simulation (1:1)	Baseline simula- tion	Higher anisotropy simulation (3:1)	No anisotropy simulation (1:1)	Baseline simula- tion	Higher anisotropy simulation (3:1)	No anisotropy simulation (1:1)
Number of water levels compared		18			4			8	
Maximum computed above measured, in feet	54	47	57	51	48	52	97	96	90
Maximum computed below measured, in feet	-36	-38	-36	-110	-120	-104	-35	-41	-36
Mean of differences, in feet	-0.8	-5.9	0.5	-4.4	-13.6	-0.8	34.0	32.2	27.4
Root mean square error, in feet	24	24	25	63	65	61	57	56	53

K1 Basin-fill horizontal hydraulic conductivity
 K2 Alluvial-fan horizontal hydraulic conductivity
 K3 Pine Valley monzonite horizontal hydraulic conductivity
 VC1 Basin-fill vertical leakance
 VC2 Alluvial-fan vertical leakance
 RIV Streambed conductance

ETD Evapotranspiration extinction depth
 ETR Maximum evapotranspiration rate
 IRR Recharge rate from irrigation
 ESTR Recharge rate from ephemeral streams
 PPT Recharge rate from precipitation

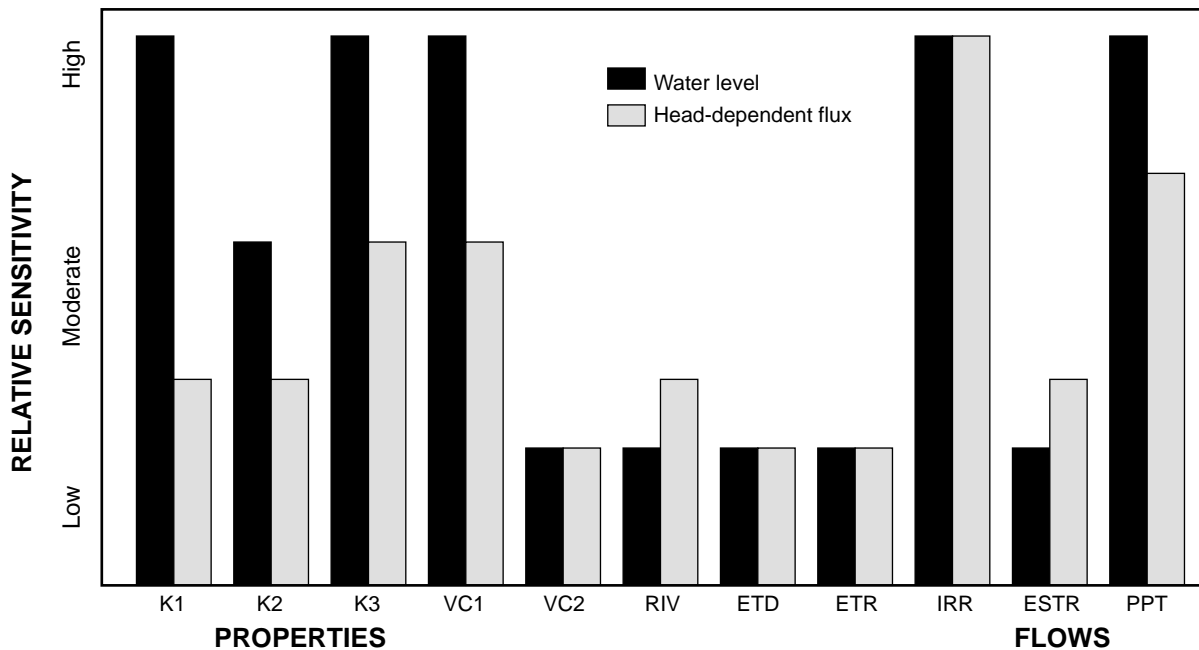


Figure 41. Relative sensitivity of the baseline model representing the upper Ash Creek drainage ground-water flow system to uncertainty in selected properties and flows.

the basin's ground water, but only to visualize the interdependencies of hydrologic processes and the possible effects of climate change or human-caused change.

Model Limitations

The limitations of the model have been implied in previous sections. The baseline simulation is considered to be the most reasonable representation for the upper Ash Creek ground-water system, but because the model has no storage component, it can only simulate the ultimate result of changes in stress on aquifer properties. Other representations may also be realistic, and thus the baseline simulation may need to be revised after additional hydrologic or geologic data about the system become available.

Alternate steady-state simulations could be devised to show the potential effect of (1) decrease in areal recharge because of drought, (2) removal of riparian vegetation, or (3) increased or decreased pumpage, but simulations such as these should not be used to

manage the water resources but rather to better understand interaction of hydrologic processes.

Navajo and Kayenta Aquifer System

Because the Gunlock Fault completely offsets the Navajo Sandstone and Kayenta Formation outcrops (pl. 1), two separate ground-water flow models were developed for the main and Gunlock parts of the Navajo and Kayenta aquifers. The two computer models share similar aquifer properties and boundary conditions; for example, a shared no-flow boundary represents the Gunlock Fault. They were developed independently on the basis of the conceptual model ground-water budgets presented earlier (tables 15 and 16). Recharge to and discharge from the aquifers varies both seasonally and yearly as a result of both climatic changes and water use; however, there has generally been little overall water-level change at wells measured both in 1974 and as part of this study (fig. 42). Although at least 30 ft of water-level decline was measured at three of the Gunlock wells, those measurement were at productions

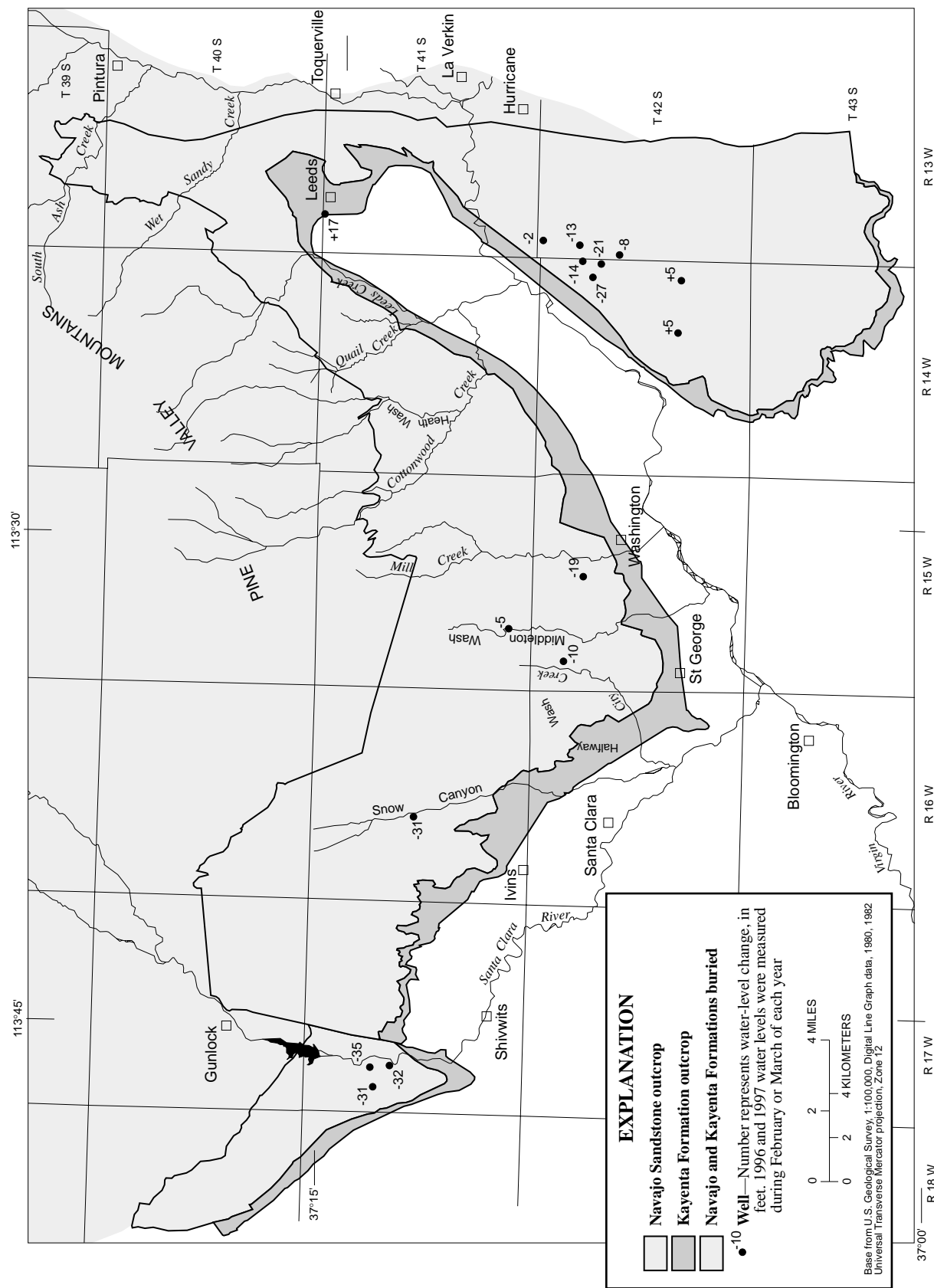


Figure 42. Water-level changes in the Navajo and Kayenta aquifers from 1974 to February/March 1996, 1997 in the central Virgin River basin study area, Utah.

wells and may reflect localized drawdown cones rather than regional declines. Also, these declines are small relative to the overall saturated thickness of the aquifer. Unfortunately, there are no long-term water-level data from the Navajo or Kayenta aquifer observation wells to show historical trends. Therefore, only steady-state models were developed for the main and Gunlock parts of the Navajo and Kayenta aquifers. The most recent year for which complete well discharge information was available was 1995. Water levels in wells were measured in 1996 and additional measurements were acquired in 1997 to fill in gaps. To evaluate the use of 1995 pumpage and 1996 to 1997 water levels for the steady-state model, February and March 1996 water levels were compared to measurements at 9 wells measured in February and March 1995 and 38 wells measured during June and July 1995. The average difference for the nine wells measured in February and March 1995 was a 1.6-ft decline in water levels, ranging from a rise of 2.5 ft to a decline of 12.8 ft. The average difference for the 38 wells measured in June and July 1996 was a 2.9-ft rise in water levels, ranging from a rise of 44.5 ft to a decline of 10.0 ft (Wilkowske and others, 1998, table 2). However, as stated earlier, most of the measured wells were production wells, so the larger changes (plus or minus more than 5 ft) were likely due to effects of seasonal pumping. Thus, while not ideal, the baseline simulation for the main Navajo-Kayenta model represents average conditions for the period 1995 to 1997. Although pumping did increase in 1996 and 1997, the 1995 withdrawals were an acceptable long-term average to try and represent in a steady-state simulation.

Main Part of the Navajo and Kayenta Aquifers

The ground-water flow model developed for the main part of the Navajo and Kayenta aquifers includes the area west of the Hurricane Fault and east of the Gunlock Fault where the Navajo Sandstone and Kayenta Formation are exposed, as well as an area extending up to 4 mi north of the Navajo Sandstone/Carmel Formation contact, where the formations are buried. The model was developed as a simplified representation of a complicated and extensive aquifer system. The approach was to create a baseline model with which to test various alternative conceptualizations of aquifer properties.

Model Characteristics and Discretization

The model is divided into 58 rows, 65 columns, and 2 layers with a total of 7,540 model cells (fig. 43). The model grid was designed to emphasize more detailed simulation of ground-water flow along the exposed outcrop part of the aquifers between the Hurricane Fault and Snow Canyon, where most hydrologic information is available. Therefore, the size of model cells ranges from about 2,000 ft by 2,000 ft along the center of the outcrop to about 2,000 ft by 5,000 ft along the northeast and the western parts of the simulation area. Layer 1 represents the Navajo aquifer and includes about 2,020 active cells simulating an area of about 330 mi². Layer 2 represents the Kayenta aquifer and includes about 2,340 active cells simulating an area of about 390 mi². The orientation of the grid was rotated clockwise about 10 degrees from true north so that the columns are parallel to the general orientation of predominant faulting and jointing.

The altitude of the base of layer 2 that represents the Kayenta aquifer is shown in figure 44. Generally this corresponds to altitudes 850 ft below the base of the Navajo Sandstone (Hurlow, 1998, pl. 5a), except where the base of the Kayenta aquifer is inferred to be lower than 1,850 ft below sea level in the northeast corner of the model. The saturated thickness of layer 1 ranges from 2,400 ft where the Navajo aquifer is confined by overlying formations towards the north, to less than 200 ft near its erosional extent. The saturated thickness of layer 2 ranges from 850 ft where the Kayenta aquifer is confined by overlying formations toward the north, to less than 200 ft near its erosional extent. A cross section of the model grid along column 20 shows the layer geometry used in the ground-water flow model (fig. 45).

Boundary Conditions

The hydrologic boundaries that represent the main part of the Navajo and Kayenta aquifers include no-flow boundaries, specified-flux boundaries, and head-dependent (general-head) boundaries. No-flow boundaries representing the erosional and fault-controlled extent of the aquifers are fairly well defined. However, other boundaries, such as those representing flow to and from underlying, adjacent, and overlying formations, are not well understood. In general, these underlying and overlying formations are represented by no-flow boundaries except where hydrologic or geochemical evidence indicates that ground water may be crossing these boundaries. Where the aquifers are

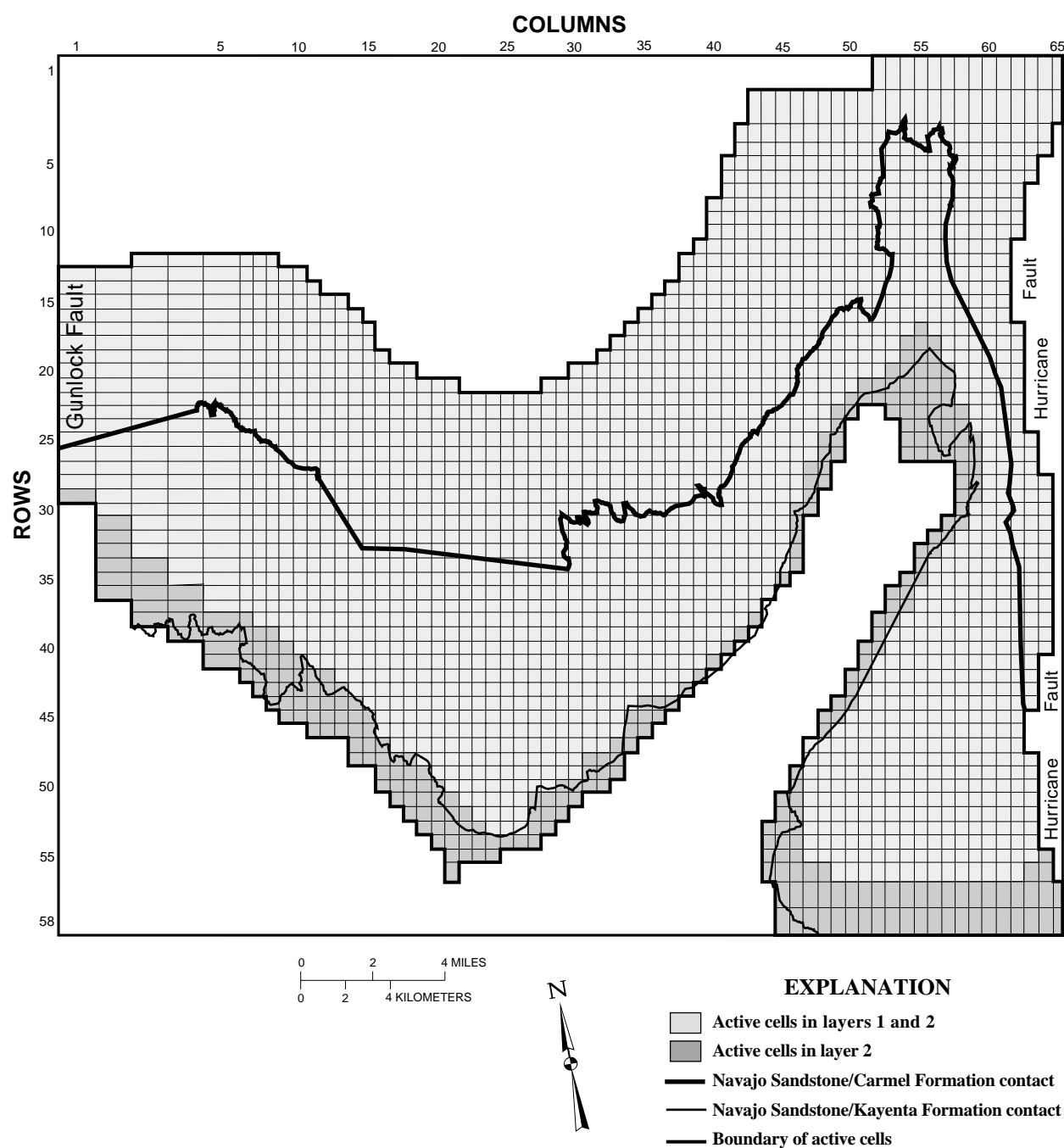


Figure 43. Model grid of the ground-water flow model of the main part of the Navajo and Kayenta aquifers within the central Virgin River basin study area, Utah.

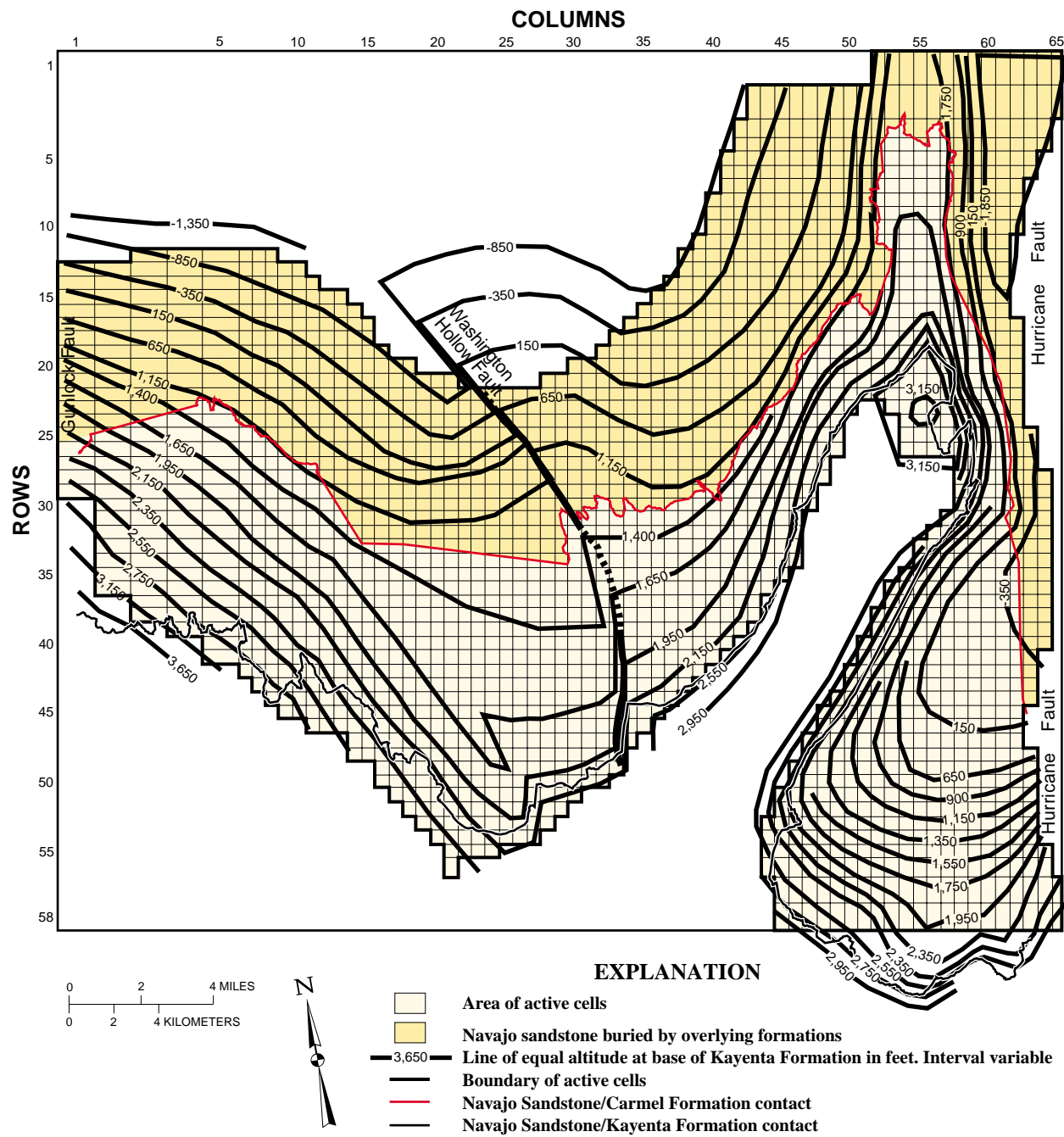


Figure 44. Altitude of the base level of layer 2, representing the base of the Kayenta Formation, in the ground-water flow model of the main part of the Navajo and Kayenta aquifers within the central Virgin River basin study area, Utah (Hurlow, 1998, pl. 5a).

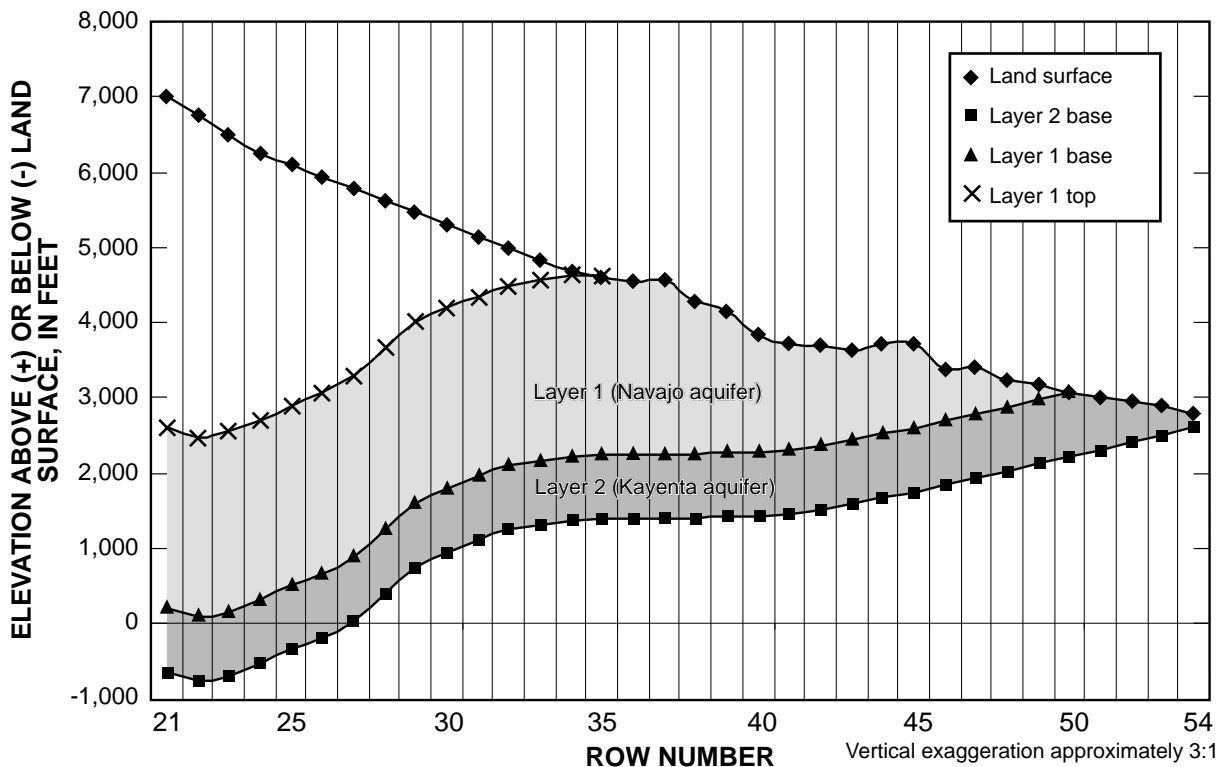


Figure 45. Generalized cross section along column 20 of the ground-water flow model of the main part of the Navajo and Kayenta aquifers within the central Virgin River basin study area, Utah.

unconfined along the Navajo Sandstone and Kayenta Formation outcrops, the water table generally is simulated as a recharge boundary to represent infiltration from precipitation, streams, and unconsumed irrigation water, but there are areas where the water table is simulated as a discharge boundary to represent spring discharge and seepage to the Virgin River.

Recharge Boundaries

The water table is simulated as a recharge boundary where the Navajo Sandstone and Kayenta Formation becomes fully saturated. The depth of this boundary could range from land surface to as much as 800 ft below land surface. Simulated sources of recharge along this boundary include infiltration from precipitation, perennial and ephemeral streams, and unconsumed flood-irrigation water. Recharge from underlying formations was simulated along parts of the base of layer 2 where higher dissolved-solids concentrations are contained within the Navajo and Kayenta aquifers.

Precipitation

Infiltration of precipitation was simulated with the recharge package at model cells that represent the outcrop of the Navajo Sandstone and the Kayenta Formation. The distribution of precipitation (fig. 3) was based on the average annual precipitation map (Utah Climate Center, 1996). Recharge from infiltration was initially specified as 10 percent of total annual precipitation. But as model refinement for the steady-state solution progressed, the percentage was increased along the part of the outcrop north of Anderson Junction where average annual precipitation exceeds 14 in/yr. A higher recharge rate was applied to this area because the Navajo Sandstone outcrop is more highly fractured and partially covered by more permeable alluvial material than elsewhere in the study area (Hurlow, 1998). The distribution of recharge from infiltration of precipitation simulated in the ground-water flow model is shown in figure 46.

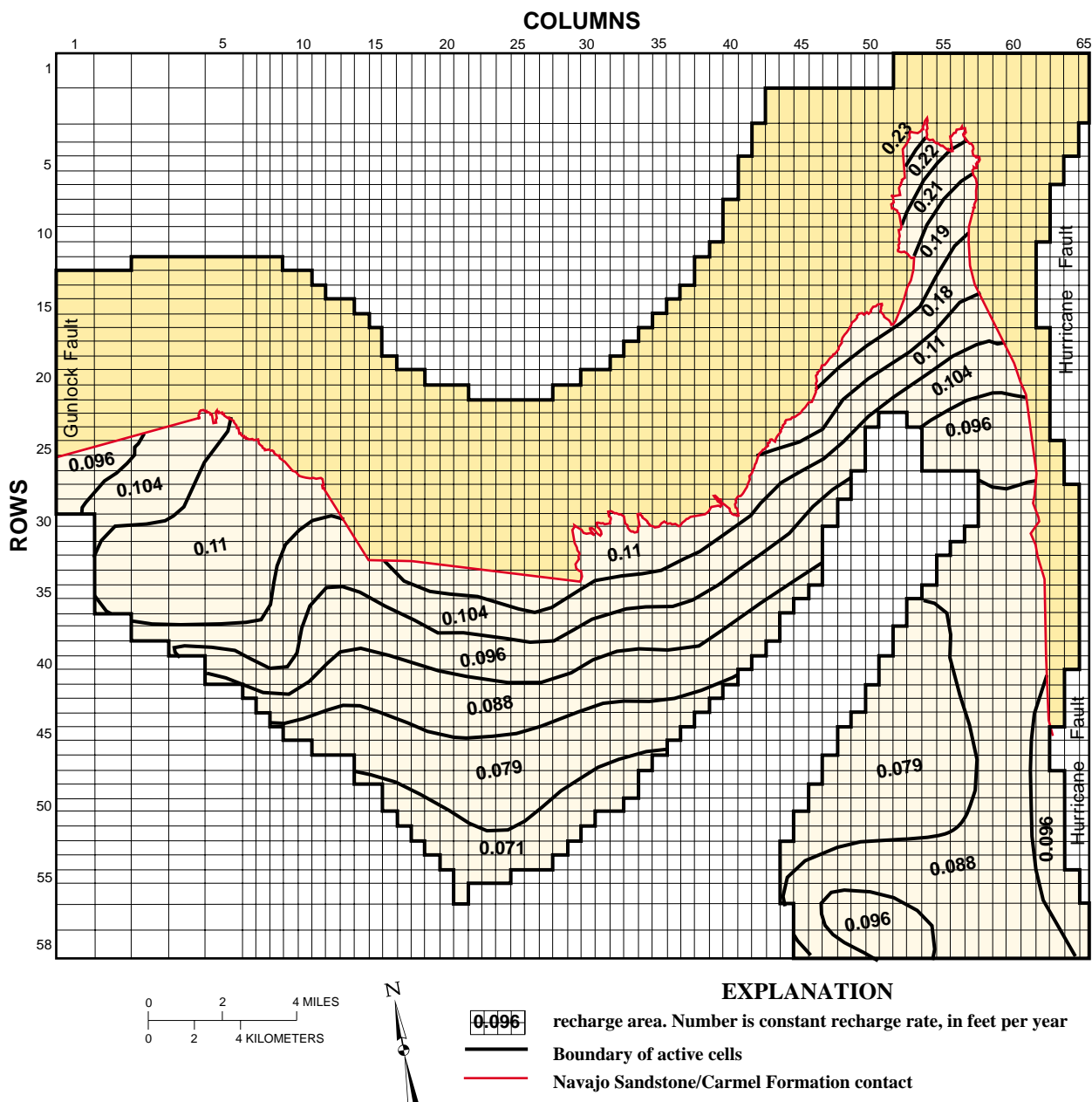


Figure 46. Distribution of recharge from infiltration of precipitation simulated in the ground-water flow model of the main part of the Navajo and Kayenta aquifers within the central Virgin River basin study area, Utah.

Streams

Recharge from perennial and ephemeral streams flowing along the Navajo Sandstone outcrop was simulated with the river package (fig. 47). When the water level in the aquifer is below the bottom of the stream, a constant amount of water is simulated to recharge the aquifer and is determined by the difference between the stream stage and the altitude of stream bottom multiplied by the vertical hydraulic conductivity of the stre-

ambed deposits. When the water level in the aquifer is between the stream-bottom altitude and the stream stage, simulated recharge to the aquifer is variable and depends on this head difference. When the water level in the aquifer is above the stream stage, the aquifer discharges water to the stream, depending on the difference between the stream stage and the aquifer water level. Therefore, the river package can either simulate recharge to or discharge from the aquifer.

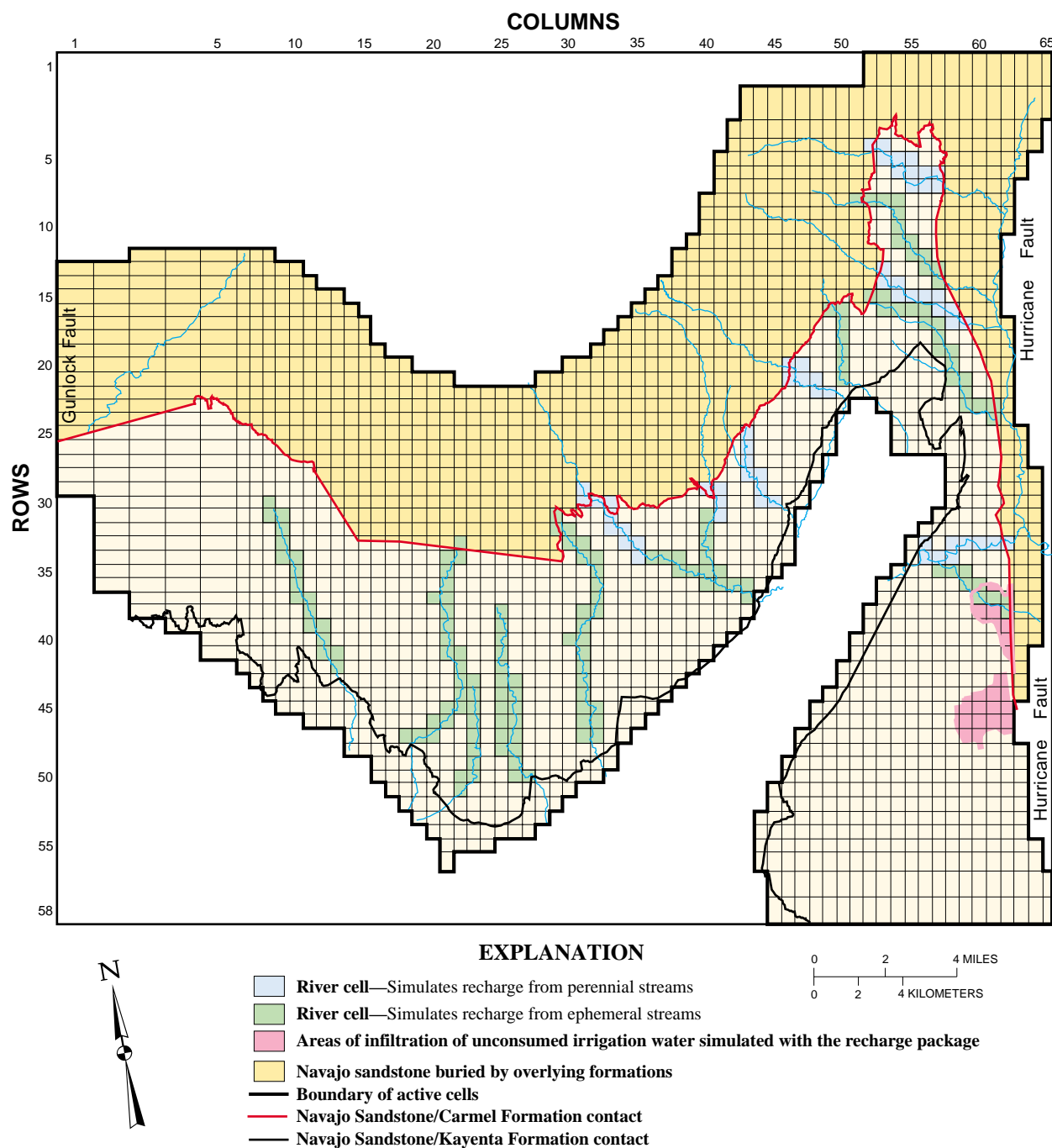


Figure 47. Distribution of recharge from streams and infiltration of unconsumed irrigation water simulated for layer 1 of the ground-water flow model of the main part of the Navajo and Kayenta aquifers within the central Virgin River basin study area, Utah.

The perennial streams that cross the Navajo Sandstone and Kayenta Formation outcrops within the study area are assumed to be in hydraulic connection with the water table. A test of the model's accuracy in representing the Navajo and Kayenta aquifers is its ability to simulate this surface-water/ground-water interaction. Therefore, it was important to evaluate whether stream reaches that are known to recharge water to the aquifer also simulate recharge in the model; conversely, streams reaches that are known to gain water from aquifer discharge are expected to simulate this flow. The model does simulate recharge along the same five stream reaches where seepage studies indicate recharge (South Ash Creek, Wet Sandy Creek, Leeds Creek, Quail Creek, and Cottonwood Creek) (table 11). Conversely, simulated discharge to the Virgin River is consistent with the seepage study done in November 1994 that indicated discharge from the Navajo and Kayenta aquifers (Herbert, 1995).

The simulated amount of recharge or discharge depends on the streambed conductance, the elevation of the streambed, the stream stage, and the head at the node in the cell underlying the stream. Streambed conductance is the product of the vertical hydraulic conductivity and the cross sectional area of the streambed divided by the thickness of the streambed. Field data on actual streambed conductance were not available. Therefore, for the five perennial creeks draining southeastward from the Pine Valley Mountains, an initial stream-bed conductance value of about $0.01 \text{ ft}^2/\text{d}$ was assumed. This value represents a vertical hydraulic conductivity that is 1 to 2 orders of magnitude less than the estimated 2 ft/d horizontal hydraulic conductivity of the Navajo aquifer. The altitude of the stream assigned for each river cell was estimated from topographic maps with 40-ft contour intervals. On the basis of measurements made during seepage studies, the width of all five streams is estimated to be about 10 ft. The stream stage was originally estimated to be 2 ft above the bottom altitude of each stream reach. However, with these conductance values, simulated recharge was much less than measured recharge for all five streams. To more closely approximate measured recharge, stage was uniformly increased to 20 ft above the streambed elevation for all five streams. This was a simplistic way of increasing stream seepage to the aquifer and might not be appropriate for any other conditions or stresses on this system. A model intended for use as a predictive tool should be structured to more realistically depict this interaction between stream and aquifer. After these

changes, simulated recharge rates along Leeds, Quail, and Cottonwood Creeks more closely approximated measured values. To closely approximate measured recharge along Wet Sandy and South Ash Creeks, the streambed conductance was increased five-fold and ten-fold, respectively, to 0.05 and 0.1 ft/d . This is consistent with surficial geologic studies, which indicate that the unconsolidated deposits along the streambeds north of Anderson Junction are coarser and more permeable (Hurlow, 1998).

Ephemeral streams that cross the Navajo Sandstone and Kayenta Formation outcrops within the study area are not assumed to be in hydraulic connection with the water table because of their sporadic nature. However, to allow prospective users of the model to keep line recharge mechanisms separate from aerial recharge mechanisms such as precipitation, the river package was chosen to simulate recharge from ephemeral streams. In this initial simulation, a constant flow was assumed for each ephemeral stream reach. To do this, the stream bottom and stage were assigned a higher altitude than the potentiometric surface of the aquifer and the stream stage was assigned a value 1 ft higher than the stream bottom. This allowed a constant flow to be specified on the basis of the streambed conductance and length of the reach. The total specified amount of ephemeral stream recharge for layer 1 was initially $4.1 \text{ ft}^3/\text{s}$ ($3,000 \text{ acre-ft/yr}$). This corresponds to the median values (assuming 10 percent infiltration) determined above from estimated annual stream discharge (method 1, table 13). However, to be consistent with the increased infiltration rates for precipitation north of Anderson Junction, the infiltration rate for Dry Sandy (the only ephemeral stream north of Anderson Junction) was increased to 15 percent, so that the total simulated recharge from ephemeral streams in layer 1 is $4.4 \text{ ft}^3/\text{s}$ ($3,200 \text{ acre-ft/yr}$).

Some recharge is assumed along the ephemeral streams north of where Leeds Creek crosses the Kayenta Formation outcrop. Assuming the same infiltration rates specified for the reaches that cross the Navajo Sandstone outcrop, an estimated $0.6 \text{ ft}^3/\text{s}$ recharges the Kayenta aquifer along Anderson Junction and Grapevine Wash (fig. 48). Because the Kayenta aquifer to the south between Snow Canyon and Mill Creek is a major area of discharge, it is assumed that ephemeral streams along the Kayenta Formation outcrop in this southern area do not recharge the aquifer.

Underlying Formations

Recharge as seepage from underlying formations was simulated with the general-head package. This represents inflow of water with a higher dissolved-solids concentration assumed to come from the area north of St. George and southwest of Hurricane (fig. 22). The cells in layer 2 that simulate this recharge are shown in figure 48. The amount of simulated recharge is a function of (1) the head difference between the cell and a fixed head that represents the water level in the underlying formation and (2) the conductance of the material between the cell and the fixed-head location. Both of these parameters are very speculative for the two areas of higher dissolved-solids concentration because the potentiometric surface and the vertical hydraulic conductivity of the underlying formations in these areas are unknown. A conductance value of 2.5×10^{-5} (ft/d)/ft was assigned to both general-head boundary areas. This value was determined during model refinement and assumes that the hydraulic conductivity of the material between the Kayenta aquifer and the underlying formations was 2.5×10^{-3} ft/d, or about three orders of magnitude less than the estimated vertical hydraulic conductivity of layer 2. For both areas the fixed general head was assumed to be about 200 ft higher than the average head in the aquifer, which is about 3,250 ft for the area north of St. George and 3,130 ft for the area southwest of Hurricane. A vertical distance of 1,000 ft between layer 2 and the location of the fixed general head was assumed for both areas.

Irrigation

Recharge from unconsumed irrigation water beneath the flood-irrigated fields southwest of Hurricane is simulated as a specified flux with the recharge package (fig. 47). A recharge rate of about 0.5 ft/yr over the flood-irrigated area of 2,100 acres (1,050 acre-ft/yr) was applied at this location. This amount is within the estimated range of 0 to 5 ft³/s (3,600 acre-ft/yr) of recharge.

Discharge Boundaries

Discharge is simulated as both constant-flow and head-dependent boundaries in the ground-water flow model. Sources of discharge include well discharge, spring discharge, seepage to the Virgin River, and seepage to adjacent and underlying formations.

Wells

Simulated pumpage was based on well discharge records from various city, county, and state water agencies. A total of about 14 ft³/s (10,100 acre-ft/yr) of well discharge is simulated with the well package. About 80 percent, or 11 ft³/s (8,000 acre-ft/yr) of the well discharge is simulated from layer 1 (fig. 49), whereas about 20 percent, or 3 ft³/s (2,200 acre-ft/yr) is simulated from layer 2 (fig. 50). Originally, an estimated discharge of 12.7 ft³/s (9,200 acre-ft/yr) was specified for 1995. However, simulated water levels were much higher than measured water levels in the Mill Creek area. Although 1991 and 1993 well discharge at Washington City's Mill Creek wells was not reported to the Utah Division of Water Rights, 1992 and 1994 well discharge in the Mill Creek area was about 40 percent higher than reported 1995 pumpage. Because the Navajo and Kayenta aquifers may buffer short-term variations in pumping, measured water levels do not likely reflect the anomalously small amount of 1995 Mill Creek well discharge. Therefore, specified well discharge was increased by 40 percent, or about 1.3 ft³/s (900 acre-ft/yr), at the Mill Creek area to reflect longer-term average pumping rates.

Springs

Spring discharge was simulated with the drain package. Because of coarse vertical discretization, spring discharge from the Navajo aquifer could not be accurately simulated in layer 1 because numerical oscillation would cause drying of these cells. Therefore, all of the spring discharge was simulated in layer 2. This is a reasonable approximation because most of the spring discharge from the Navajo aquifer occurs just above the contact with the Kayenta Formation. The location of drain cells that represent spring discharge is shown in figure 50. The discharge from drain cells is head-dependent and is determined by the difference in head (the simulated water level at the cell compared with the specified altitude of the spring) multiplied by the spring conductance. Altitude of each spring was determined from 1:24,000 USGS topographic maps. Because of the 40-ft contour interval on these maps, specified spring altitudes may have as much as plus or minus 20 ft in error. As with the river package, the conductance represents the permeability of material at the spring location. Because of the strong influence of fracturing, this conductance is highly variable and could not be measured. Therefore, conductance values were adjusted during model refinement to approximate the

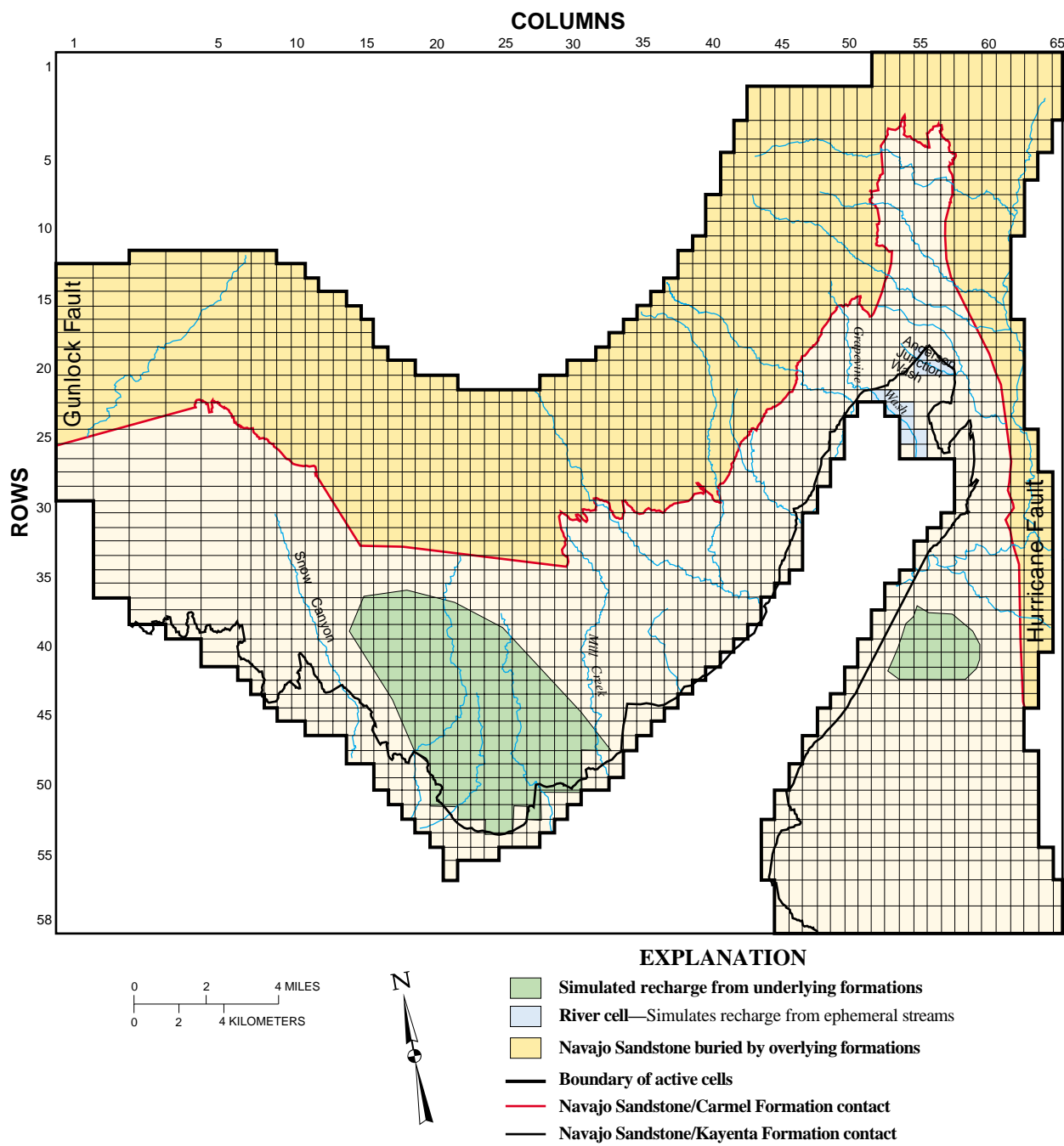


Figure 48. Location of recharge from ephemeral streams and inflow from underlying formations simulated for layer 2 of the ground-water flow model of the main part of the Navajo and Kayenta aquifers within the central Virgin River basin study area, Utah.

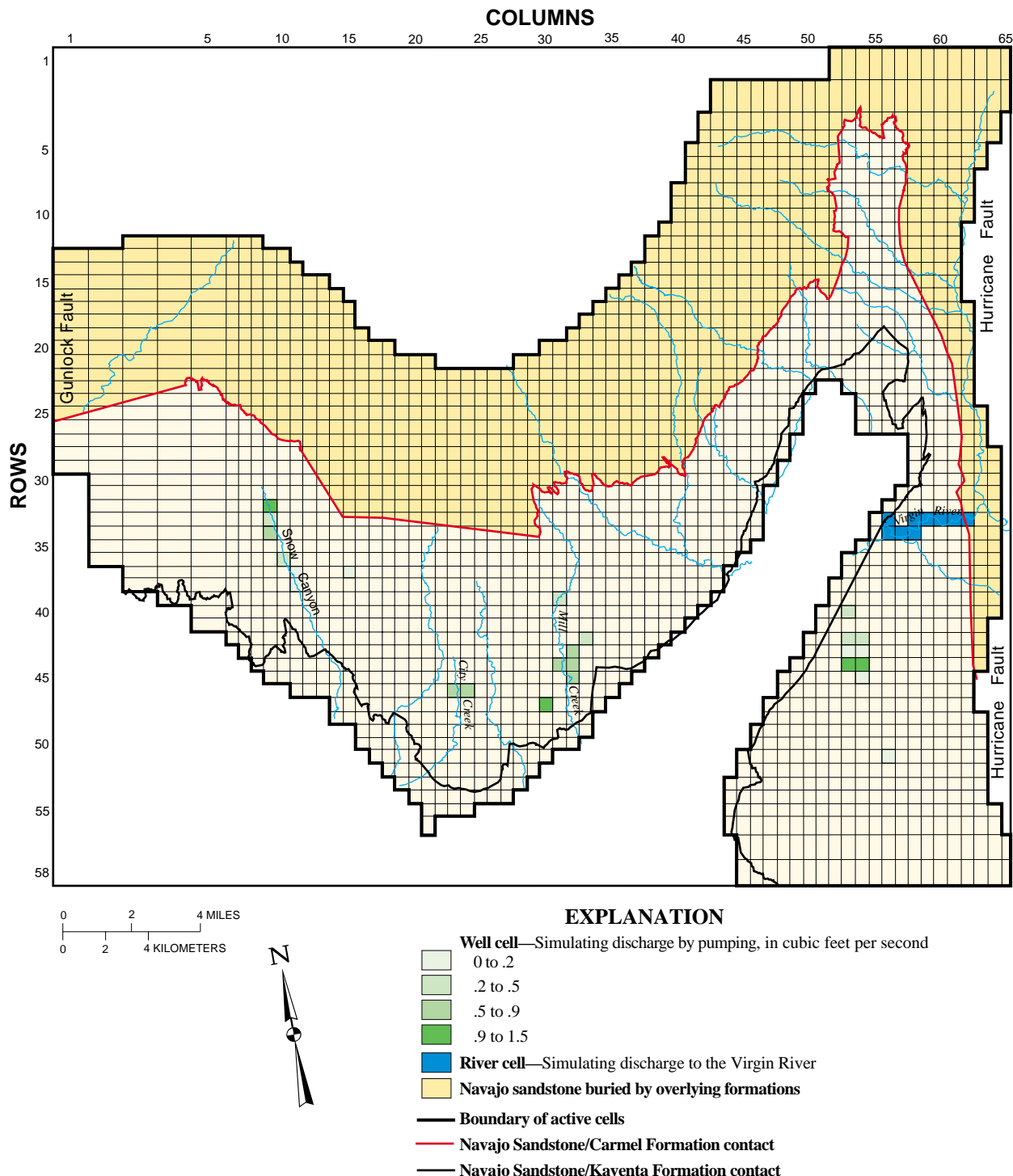


Figure 49. Discharge to wells and to the Virgin River from layer 1 of the ground-water flow model of the main part of the Navajo and Kayenta aquifers within the central Virgin River basin study area, Utah.

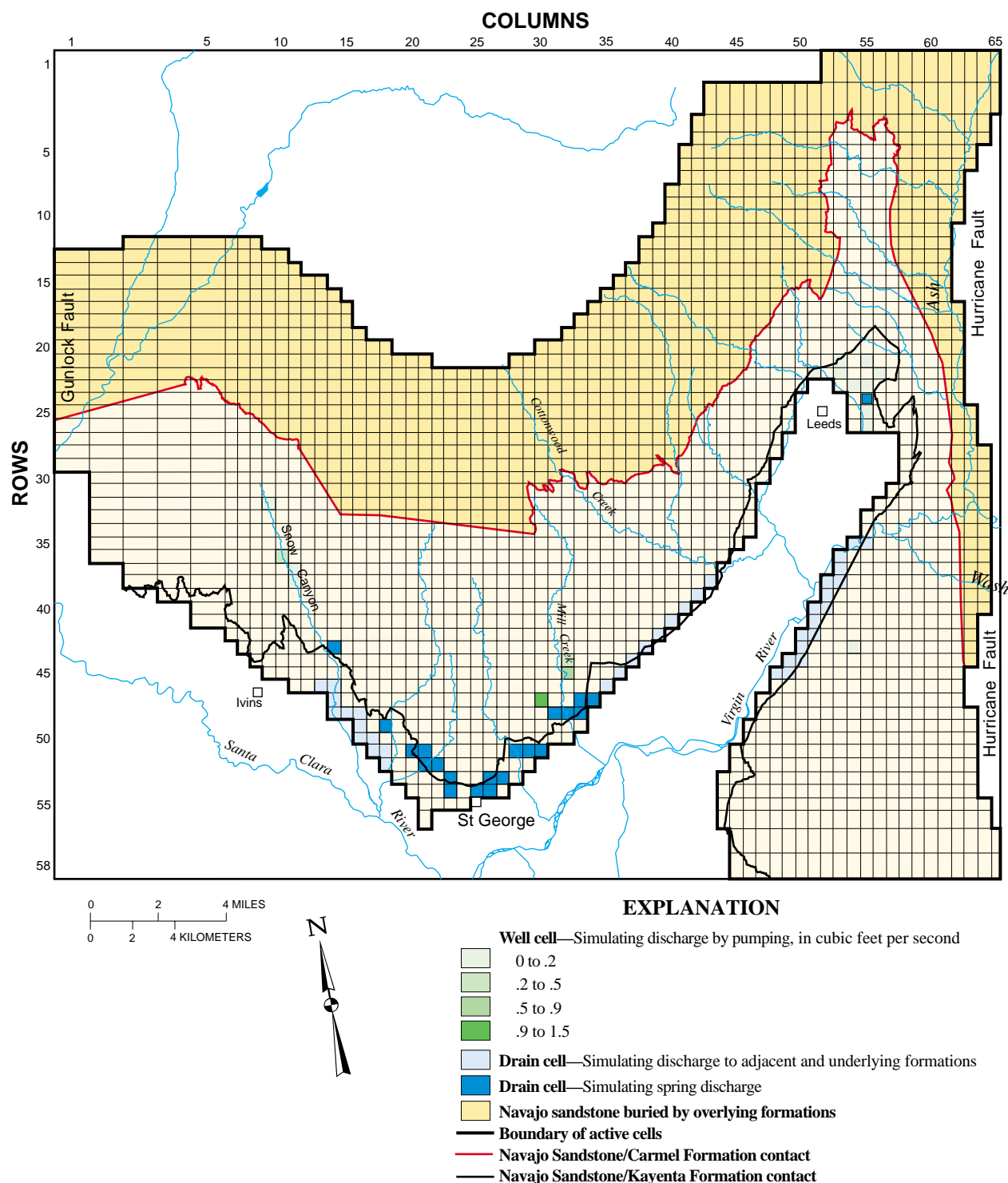


Figure 50. Discharge to wells, springs, and subsurface outflow to adjacent and underlying formations from layer 2 of the ground-water flow model of the main part of the Navajo and Kayenta aquifers in the central Virgin River basin study area, Utah.

discharge measured at each spring area. The final specified conductance ranges from about 0.02 to 0.8 ft²/s (1,700 to 70,000 ft²/d).

Virgin River

The river package is used to simulate seepage to the Virgin River from layer 1 (fig. 49). Riverbed conductance was estimated at about 0.1 ft²/d. The vertical hydraulic conductivity used in this conductance term is more than one order of magnitude less than the estimated 2 ft²/d horizontal hydraulic conductivity of the Navajo aquifer. On the basis of measurements made during seepage studies, the width of the river is estimated to be about 100 ft and the stage altitude is estimated to be about 3 ft above the bottom altitude of each stream reach. The altitude assigned for each river cell was based on 1:24,000 USGS topographic maps with 40-ft contour intervals.

Adjacent and Underlying Formations

Seepage to adjacent and underlying formations is simulated as a head-dependent flux boundary with the drain package. The drain cells simulating discharge to adjacent and underlying formations shown in figure 50 represent (1) discharge to the Virgin River downstream of the Navajo Sandstone outcrop, (2) discharge to the Santa Clara River on the reach between Ivins and St. George, and (3) discharge to numerous seeps and springs along the Moenave and Chinle Formation outcrop between St. George and Leeds. The altitude assigned for each drain cell was based on topographic maps with 40-ft contour intervals. For simplicity, a uniform conductance of about 0.1 ft²/d was assigned for all three areas.

No-Flow Boundaries

In general, no ground-water movement is simulated to enter or exit the Navajo and Kayenta aquifers at the erosional extents of the formations toward the south, where the aquifers are deeply buried toward the north, across the Hurricane and Gunlock Faults, or at the base of the Kayenta aquifer (layer 2). However, exceptions to this include two areas of general-head boundary cells at the base of layer 2 that simulate inflow of water with higher dissolved-solid concentrations from underlying formations and drains along part of the erosional extent of the Kayenta aquifer that represent subsurface outflow to adjacent or underlying formations.

Because little recharge is thought to enter the Navajo and Kayenta aquifers where they are deeply buried by younger formations to the north, little ground-water flow is assumed in this region. Therefore, an arbitrary no-flow boundary was assigned at the northern edge of the ground-water flow model about 4 mi north of the contact with the Carmel Formation (fig. 43). This was considered sufficiently far from any potential ground-water development so that additional well discharge would not cause drawdown effects along these boundaries.

Distribution of Aquifer Characteristics

Although horizontal hydraulic-conductivity values for the Navajo aquifer, determined from aquifer tests, varied by more than two orders of magnitude because of fracturing and other heterogeneities, not enough information was available to accurately simulate this variation throughout the model area. Therefore, uniform hydraulic-conductivity values were simulated for each layer of the baseline model. The simulated hydrologic properties were within the range of measured values for the Navajo and Kayenta aquifers (see sections on Navajo and Kayenta aquifer properties). While keeping within this range, horizontal hydraulic-conductivity values for layers 1 and 2 were varied more than one order of magnitude to yield the best matches to measured or estimated water levels and fluxes. The final specified horizontal hydraulic-conductivity values are 2 ft/d for layer 1 (the Navajo aquifer) and 0.5 ft/d for layer 2 (the Kayenta aquifer) (table 21).

There are no nearby pairs of wells perforated in the Navajo and Kayenta aquifers. Therefore, vertical gradients between the two aquifers can only be inferred. If potentiometric gradients are extended from Kayenta aquifer wells to the closest Navajo aquifer wells, water-level differences are estimated to be generally less than 100 ft and indicate a slight downward vertical gradient. This is consistent with the conceptualization that most recharge to the Kayenta aquifer is from downward vertical migration of water from the Navajo aquifer. At certain locations, such as the two areas of higher dissolved-solids concentration, there may be an upward vertical gradient between the Kayenta and Navajo aquifers. The vertical hydraulic-conductivity value for each layer was varied by up to one order of magnitude to determine the best match to water levels and ground-water budget components. The final specified values for vertical hydraulic conductivity are 1.5

Table 21. Measured, estimated, and simulated hydraulic-conductivity values for the main part of the Navajo and Kayenta aquifers, central Virgin River basin, Utah

	Measured or estimated, in feet per day	Baseline simulation, in feet per day
Layer 1 (Navajo aquifer) horizontal hydraulic conductivity	¹ 0.2 to 32	2
Layer 1 (Navajo aquifer) vertical hydraulic conductivity	² 0.08 to 22	1.5
Layer 2 (Kayenta aquifer) horizontal hydraulic conductivity	³ 8.2 × 10 ⁻⁴ to 6	.5
Layer 2 (Kayenta aquifer) vertical hydraulic conductivity	³ 8.2 × 10 ⁻⁴ to 0.5	.25

¹ From table 10.

² Determined by assuming a vertical-to-horizontal hydraulic conductivity ratio of 0.4 to 0.7.

³ Discussed earlier in the “Aquifer properties—Kayenta aquifer” section.

ft/d for layer 1 (the Navajo aquifer) and 0.25 ft/d for layer 2 (the Kayenta aquifer) (table 21).

Conceptual Model and Numerical Simulation

Comparison between the conceptual and numerical ground-water budgets shows that simulated flows are within the estimated ranges (table 22a). The two head-dependent recharge flows, seepage from perennial streams and seepage from underlying formations, are near or at the maximum of the estimated ranges. Of the three head-dependent discharge flows, spring discharge and seepage to underlying formations are at or near the maximum of the estimated ranges. Simulated discharge to the Virgin River is the same as measured during the seepage investigation.

Water-level comparisons, however, are not as close (table 22b). In general, simulated water levels are higher in the central area and lower in the Anderson Junction area than measured water levels at selected observation wells (fig. 51). The simulated water levels in the Hurricane Bench area are similar to measured values. It was not considered important to match measured water levels exactly because of several factors: (1) most measured water levels were from production wells and may have been influenced by residual drawdown cones (depending on the time interval since pumping ceased); (2) simulated water levels are the calculated average water levels for each cell, which may not be the same as the water level at a point within the area (at least 2,000 ft by 2,000 ft) of each model cell, especially at pumping wells. However, the relatively large water-level differences in the central and Anderson Junction areas indicate that the baseline simulation only offers a general approximation to the actual hydrologic system. Various factors, such as heterogeneity of

aquifer properties and inaccurate estimates for some of the ground-water budget components may be the reason for these differences.

The potentiometric surface for the baseline simulation shows a pattern of ground-water movement (fig. 52) similar to that conceptualized from sparse water-level measurements (pl. 2).

Model Applicability

The baseline simulation was developed to better understand ground-water flow in the main part of the Navajo and Kayenta aquifers. It is the first computer model developed to represent these aquifers and represents a very simplified conceptualization of a complicated ground-water flow system. Certain boundaries and boundary conditions are well understood, but others have not been well defined. Therefore, rather than being considered a “calibrated” model, it should be considered as a tool for testing alternative conceptualizations of the flow system. Although the baseline simulation is a viable representation of the ground-water system, there likely are other combinations of aquifer properties that may yield a similar or improved representation of measured or estimated hydrologic properties.

Alternative Conceptualizations

The baseline numerical simulation concentrated on testing the effects of simulating various combinations of fluxes and uniform hydraulic properties; however, heterogeneous aquifer properties were not tested. Because of sparse spatial information about aquifer properties and the large model area, localized heterogeneity in aquifer properties was not simulated. However, generalized, non-uniform alterations of hydraulic con-

Table 22. (a) Conceptual and simulated ground-water budgets and (b) simulated versus measured water-level differences for the main part of the Navajo and Kayenta aquifers, central Virgin River basin, Utah

(a) Ground-water budget		
Flow component	Conceptual model	Baseline numerical simulation ¹ (rounded)
Recharge, in acre-feet per year		
Infiltration of precipitation	7,200 to 21,700	14,500
Seepage from perennial streams	1,300 to 4,000	4,000
Seepage from ephemeral streams	200 to 4,500	3,600
Seepage from underlying formations	0 to 3,000	2,400
Infiltration of unconsumed irrigation water	0 to 4,400	1,100
Total	8,700 to 37,600	² 25,600
Discharge, in acre-feet per year		
Well discharge	7,200 to 10,900	10,200
Spring discharge	5,000 to 6,200	5,900
Seepage to the Virgin River	4,700 to 5,700	5,200
Seepage to underlying formations	0 to 5,400	4,500
Total	16,900 to 28,200	² 25,800

¹Budget amounts listed in italics were specified fluxes. All others are head -dependent fluxes determined by the model.

²Numbers do not match due to slight rounding error.

(b) Difference between simulated and measured water levels			
Water level	Central area	Anderson Junction area	Hurricane Bench area
Number of water levels compared	18	7	17
Maximum computed above measured, in feet	160	61	197
Maximum computed below measured, in feet	-158	-305	-58
Mean of differences, in feet	62	-158	12
Root mean square, in feet	91	196	58

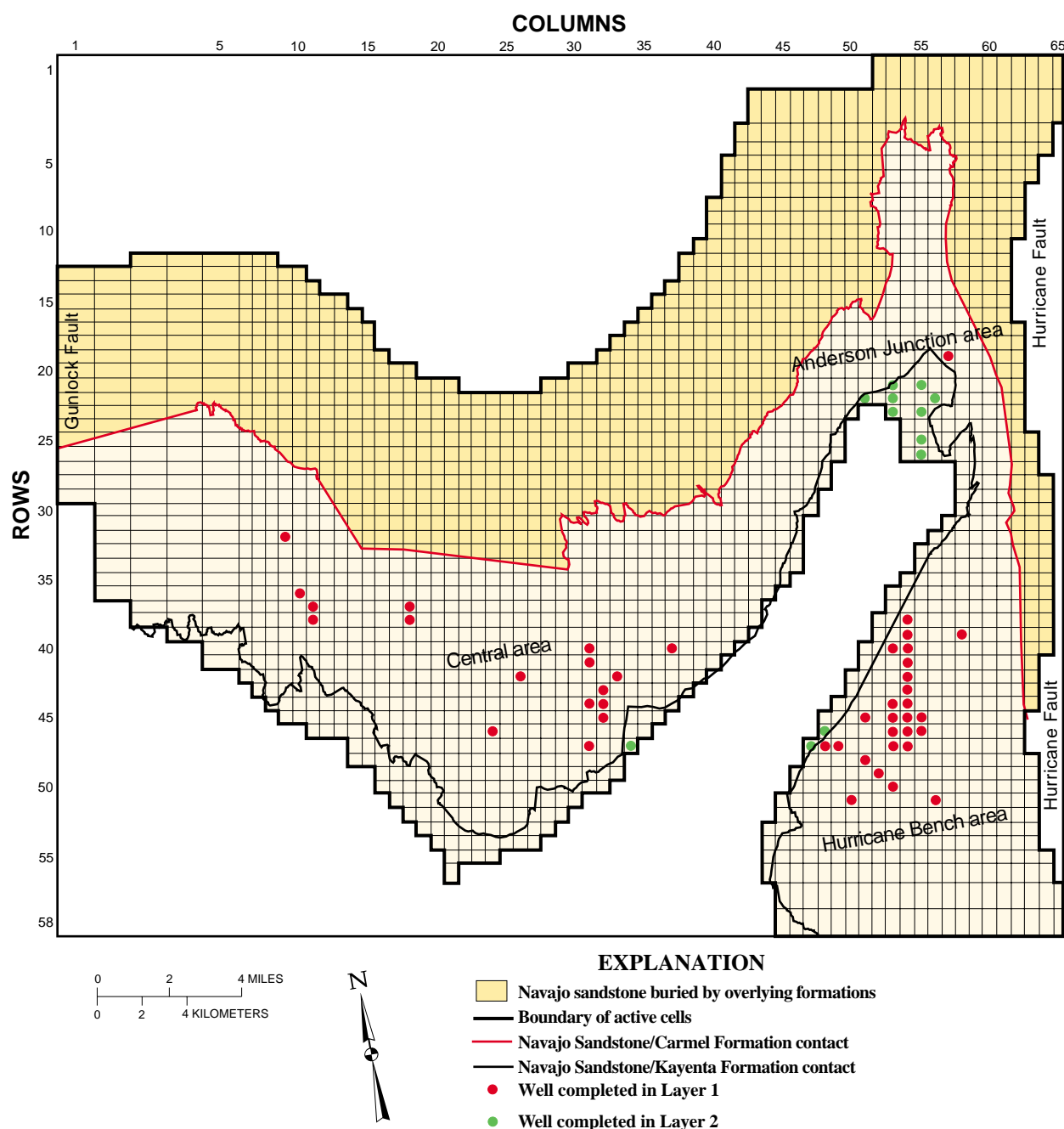


Figure 51. Location of observation wells used for comparison of computed and measured water levels for the ground-water flow model of the main part of the Navajo and Kayenta aquifers within the central Virgin River basin study area, Utah.

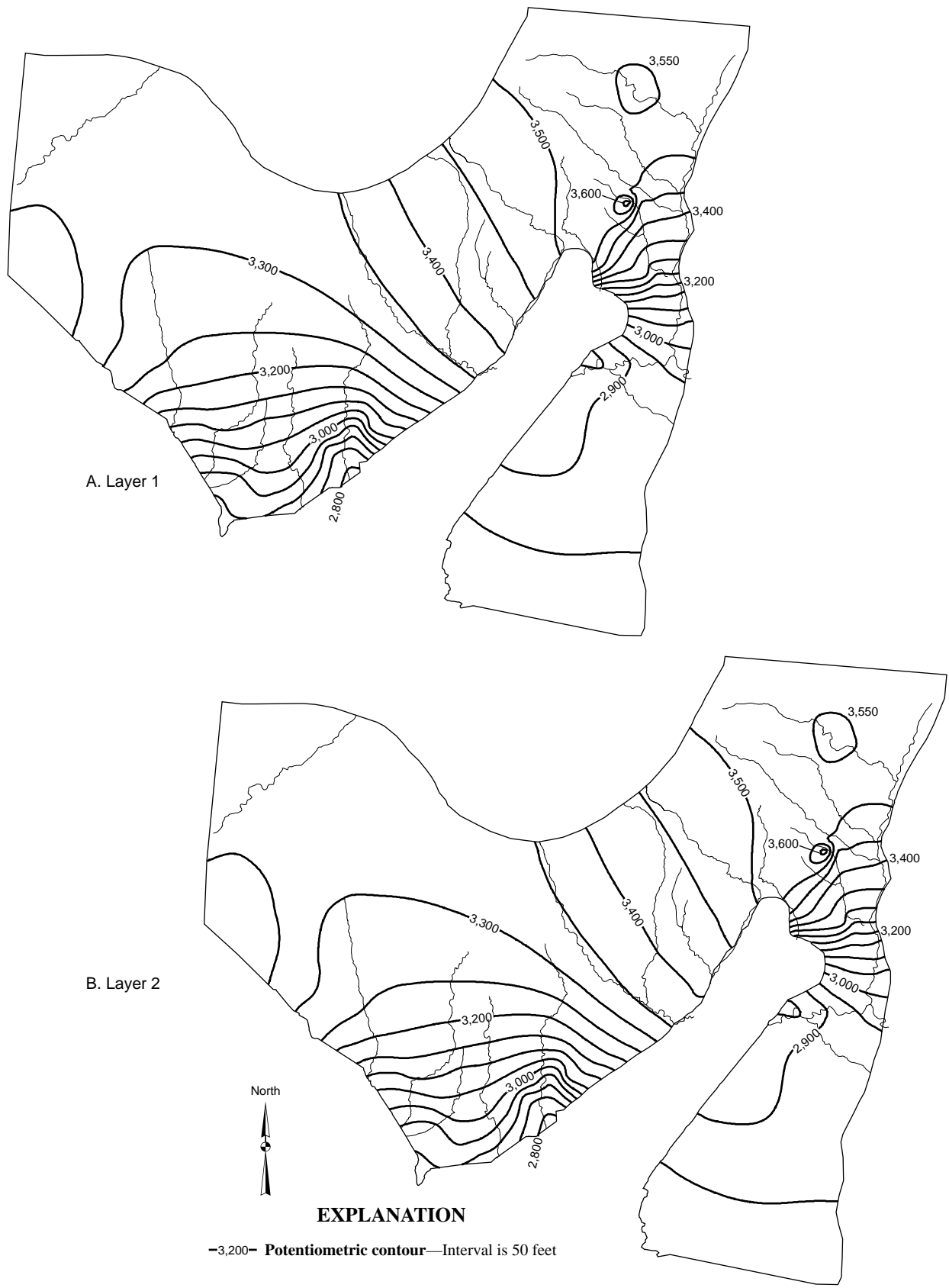


Figure 52. Simulated potentiometric contours for (a) layer 1 and (b) layer 2 of the baseline main Navajo aquifer ground-water flow model.

ductivity, related to fracturing, were examined. Two types of alternative simulations were tested that explored the effects of decreased ground-water flow perpendicular to large faults and increased ground-water flow parallel to predominant fracture orientations.

Alternative 1—Effects of Faulting

Several faults have been mapped in the Navajo Sandstone and the Kayenta Formation between the Gunlock Fault and the Hurricane Fault. Actual offset along most of these faults is difficult to determine and may be minor; however, the Washington Hollow Fault and an unnamed fault near Anderson Junction are assumed to have substantial offset (Hurlow, 1998). Ground-water flow is assumed to be impeded across formations substantially offset by faults as a result of shearing within the fault zone, which likely creates fine-grained fault gouge and increased remineralization. To explore the possibility of decreased flow across these faults, the horizontal hydraulic-conductivity value of both model layers was reduced by one order of magnitude for a line of cells along the two fault traces (fig. 53). Horizontal hydraulic conductivity was decreased from 2.0 ft/d to 0.2 ft/d for these “fault” cells in layer 1 (the Navajo aquifer). Likewise, horizontal hydraulic conductivity was decreased from 0.5 ft/d to 0.05 ft/d for “fault” cells in layer 2 (Kayenta aquifer).

The most important effect of this simulation is a rise in water levels in the Anderson Junction area between the two faults (fig. 54). The mean of the difference between simulated and measured water levels in this area was reduced from -158 ft in the baseline simulation to -2 ft in alternative simulation 1 (table 23). Simulated water levels in alternative 1 were somewhat higher in the Snow Canyon part of the central area and somewhat lower in the Mill Creek and City Creek parts. Simulated water levels in the Hurricane Bench area were essentially unchanged. The primary ground-water budget effects were decreased spring discharge in the central area and decreased seepage to the Virgin River, offset by increased seepage to underlying formations (table 23). These simulated ground-water budget components were generally within the ranges estimated in the conceptual model. Because of the improved match between simulated and measured water levels in the Anderson Junction area, the simulation of decreased horizontal hydraulic conductivity along the two faults is an improvement over the baseline simulation.

Alternative 2—Combined Effects of Faulting and Anisotropy

Extensive fracturing within the Navajo and Kayenta aquifers likely causes anisotropic conditions with increased ground-water flow along predominant fracture orientations. Outcrop-scale scan-line surveys and areal-photograph analyses (Hurlow, 1998, pl. 6) indicate that the predominant fracture orientation changes across the study area. On the basis of surface fracturing and multiple-well aquifer testing (appendix 1), the general fracture orientation is interpreted to be in a north-south direction in the central area and in an east-west direction in the Anderson Junction area. Although a multiple-well aquifer test at the Winding Rivers property did not indicate anisotropic conditions within the Navajo aquifer at that site, surface-fracture data indicate a predominant northeast-southwest fracture orientation for the Hurricane Bench area.

To investigate the possibility of anisotropic conditions, two simulations testing anisotropy ratios of 1.5 to 1 along the column direction (roughly north-south; alternative 2a) and 1.5 to 1 along the row direction (roughly east-west; alternative 2b) for both layers were tested, while maintaining the decreased flow across major faults simulated with alternative 1. Because of limitations with the finite-difference numerical method, anisotropy could not be evaluated at oblique angles to the model-grid orientation. For the north-south anisotropy simulation, horizontal hydraulic-conductivity values were increased in the north-south direction from 2 ft/d to 3 ft/d in layer 1 and from 0.5 ft/d to 0.75 ft/d in layer 2. For the east-west anisotropy simulation, horizontal hydraulic-conductivity values were increased in the east-west direction by the same amount.

Results from these simulations (table 23) indicate that increased horizontal hydraulic conductivity in the north-south direction (alternative 2a) substantially improves the match of simulated to measured water levels in the central area (generally higher water levels (fig. 55) and generally stays within the ground-water budget constraints estimated in the conceptual model. However, simulated water levels in the Anderson Junction area, although closer to measured values than the baseline simulation, showed a poorer match than in the homogeneous alternative with faulting only (alternative 1). The water-level match in the Hurricane Bench area was better than in both the baseline and alternative 1 simulations.

The anisotropic simulation with increased hydraulic conductivity in the east-west direction (alternative 2b) did not produce close matches to measured

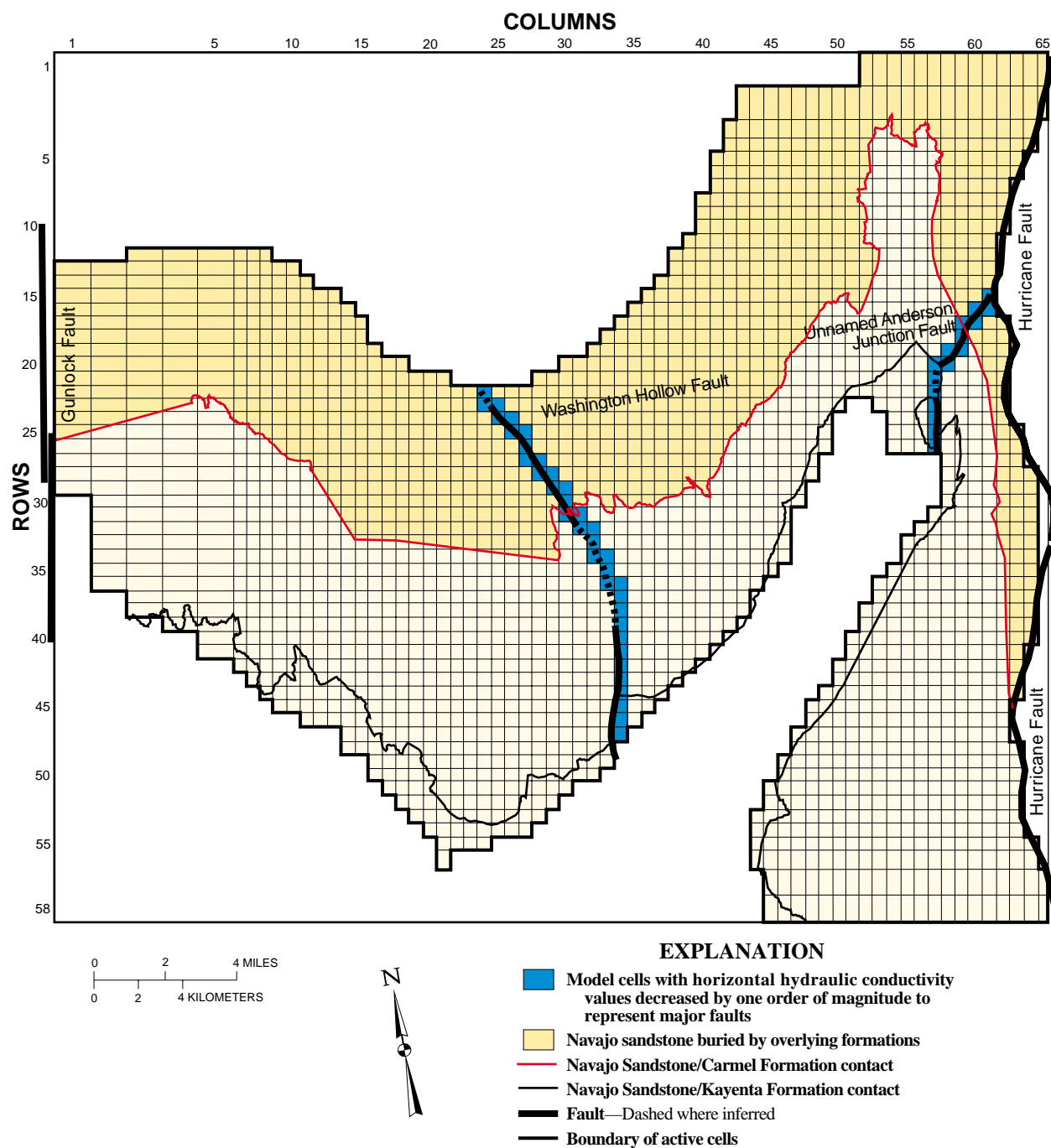


Figure 53. Location of model cells that simulate effects of faulting in the ground-water flow model of the main part of the Navajo and Kayenta aquifers within the central Virgin River basin study area, Utah.

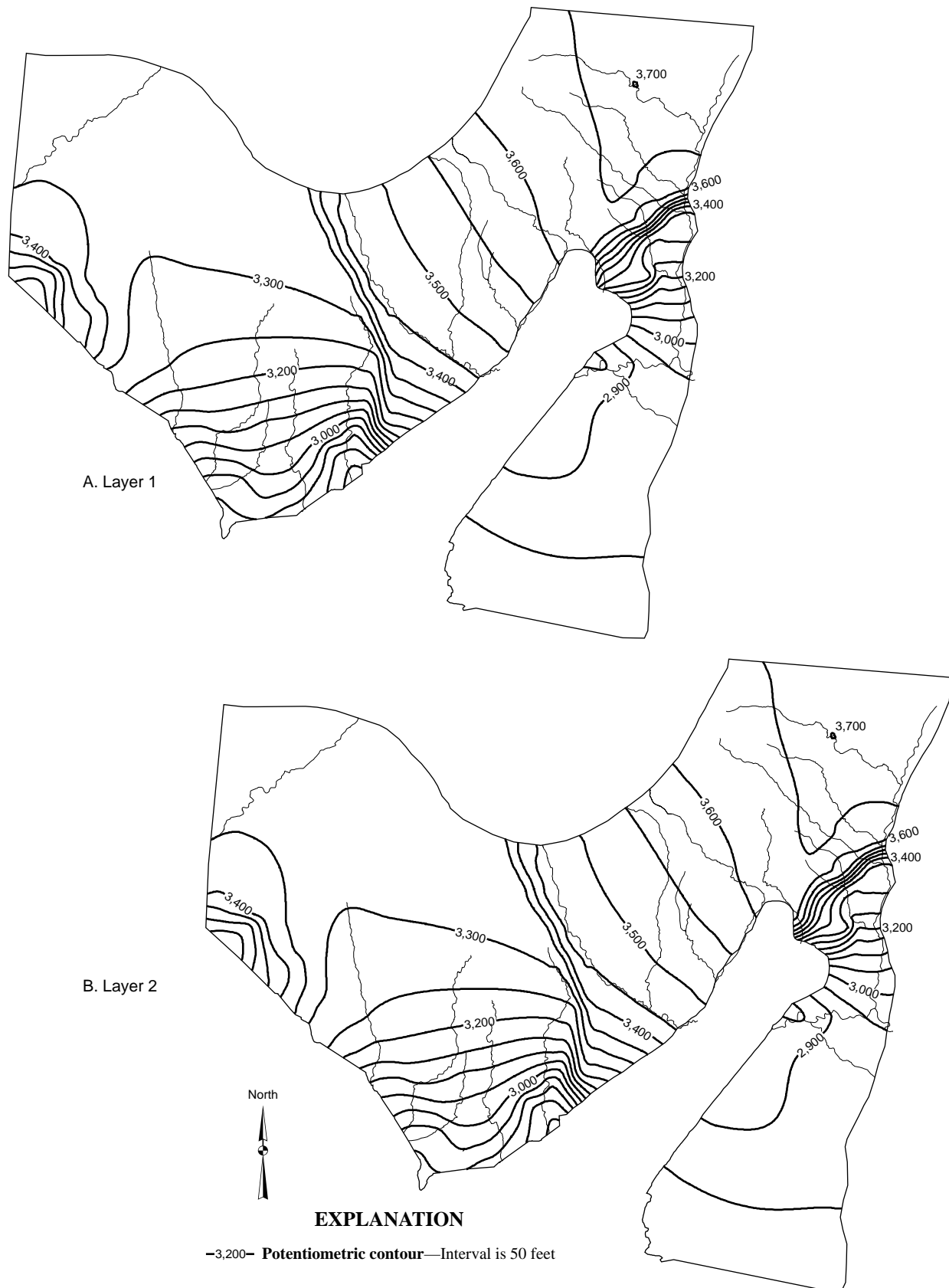


Figure 54. Simulated potentiometric contours for (a) layer 1, and (b) layer 2 of the alternative depicting effects of faulting, main Navajo aquifer ground-water flow model.

Table 23. (a) Conceptual and simulated ground-water budgets and (b) simulated versus measured water-level differences for the baseline simulation and simulations testing faulting and anisotropy in the main part of the Navajo and Kayenta aquifers, central Virgin River basin, Utah

(a) Ground-water budget					
Flow component	Conceptual	Baseline simulation	Alternative 1: decreased fault-flow simulation	Alternative 2a: increased north-south anisotropy simulation (1.5:1)	Alternative 2b: increased east-west anisotropy simulation (1.5:1)
Recharge, in acre-feet per year					
Infiltration of precipitation	7,200 to 21,700	14,500	14,500	14,500	14,500
Seepage from perennial streams	1,300 to 4,000	4,000	4,000	4,000	4,000
Seepage from ephemeral streams	200 to 4,500	3,600	3,600	3,600	3,600
Seepage from underlying formations	0 to 3,000	2,400	2,300	2,800	2,400
Infiltration of unconsumed irrigation water	0 to 4,400	1,100	1,100	1,100	1,100
Total (rounded)	8,700 to 37,600	² 25,600	² 25,500	² 26,000	² 25,600
Discharge, in acre-feet per year					
Well discharge	7,200 to 10,900	10,200	10,200	10,200	10,200
Spring discharge	5,000 - 6,200	5,900	5,600	6,200	5,900
Seepage to the Virgin River	4,700 to 5,700	5,200	4,600	4,800	4,200
Seepage to underlying formations	0 to 5,400	4,500	5,300	5,200	5,500
Total (rounded)	17,000 to 28,000	² 25,800	² 25,700	² 26,400	² 25,800

¹Budget amounts listed in italics are specified fluxes. All others are head-dependent fluxes determined by the model.

²Numbers do not match due to slight rounding error.

(b) Difference between simulated and measured water levels												
Water-level comparison	Central area				Anderson Junction area				Hurricane Bench area			
	Baseline simulation	Decreased fault-flow simulation	Decreased fault flow and increased north-south anisotropy simulation (1.5:1)	Decreased fault flow and increased east-west anisotropy simulation (1.5:1)	Baseline simulation	Decreased fault-flow simulation	Decreased fault flow and increased north-south anisotropy simulation (1.5:1)	Decreased fault flow and increased east-west anisotropy simulation (1.5:1)	Baseline simulation	Decreased fault-flow simulation	Decreased fault flow and increased north-south anisotropy simulation (1.5:1)	Decreased fault flow and increased east-west anisotropy simulation (1.5:1)
Number of water levels compared	18				7				17			
Maximum computed above measured, feet	160	183	132	187	61	253	164	234	197	196	182	194
Maximum computed below measured, feet	-158	-160	-160	-161	-305	-197	-295	-210	-58	-60	-64	-63
Mean of differences, feet	62	67	16	73	-158	-2	-101	-22	12	11	2	13
Root mean square, feet	91	97	69	104	196	137	174	138	58	58	57	58

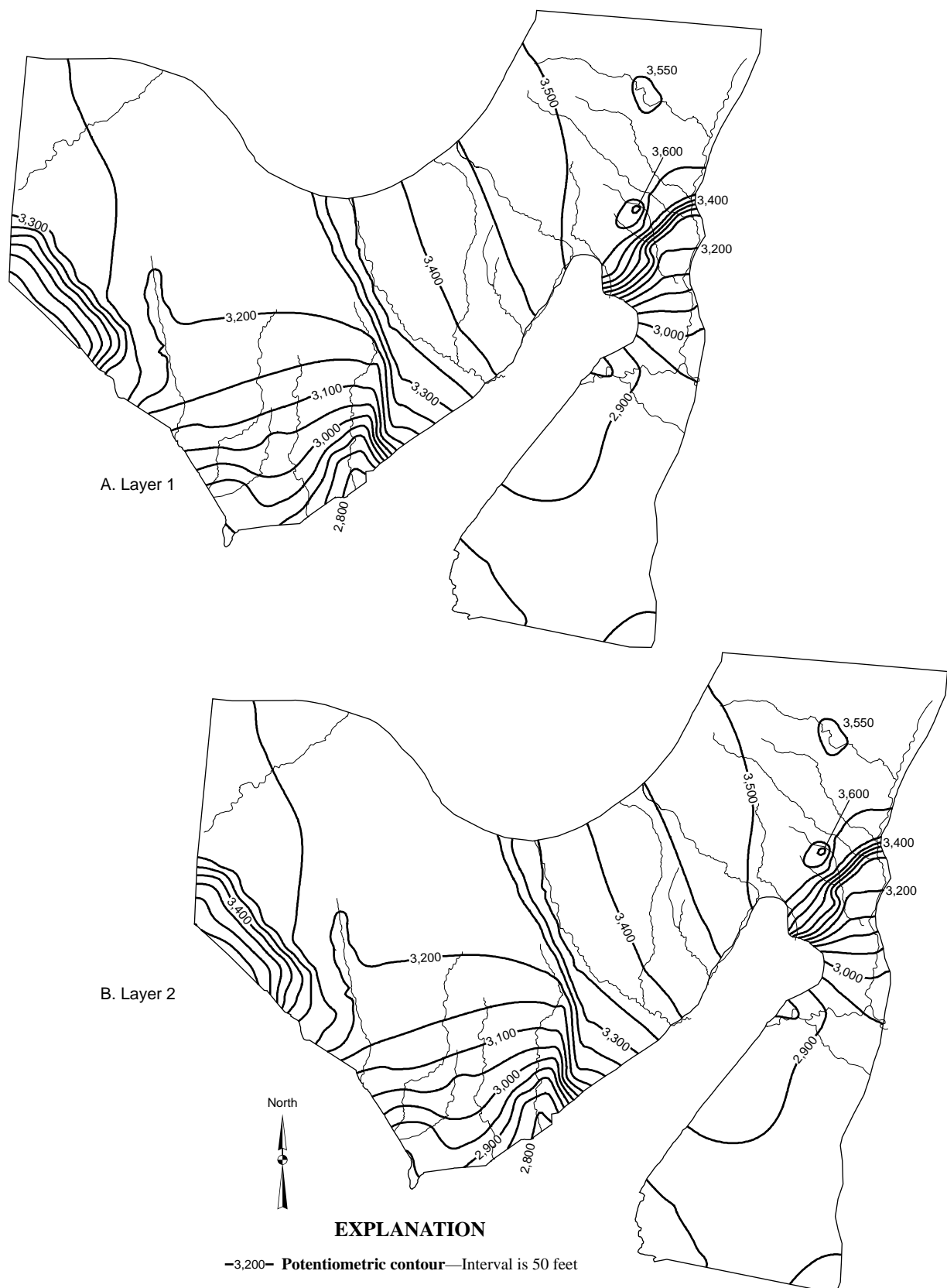


Figure 55. Simulated potentiometric contours for (a) layer 1, and (b) layer 2 of the alternative depicting effects of faulting and north-south anisotropy of the main Navajo aquifer ground-water flow model.

water levels, except for the Anderson Junction area where water levels are higher than in the baseline model (figs. 52, 56). The improvement at Anderson Junction is consistent with the directional anisotropy determined from the aquifer test. Also, the seepage to the Virgin River with this simulation was about 20 percent less than measured. Therefore, the east-west anisotropy simulation is not viewed as an improvement to the overall model. However, if future versions of the MODFLOW software package permit directional changes in anisotropy at different parts of the model, both the east-west anisotropy at Anderson Junction and the north-south anisotropy elsewhere could be accommodated.

In summary, the alternative 1 simulation (decreased flow across faults) substantially improved water-level matches in the Anderson Junction area. Adding north-south anisotropy (alternative 2a) substantially improved water-level matches in the central and Hurricane bench areas. Unfortunately, the MODFLOW software program does not allow for variable anisotropy. However, if this capability were added to the program, a closer match to measured water levels likely could be achieved by using the alternative 1 simulation, along with increased north-south hydraulic conductivity in the central and Hurricane Bench areas, and increased east-west hydraulic conductivity in the Anderson Junction area.

Model Sensitivity

The baseline model for the main part of the Navajo and Kayenta aquifers is considered to be a reasonable, albeit simplified, representation of the ground-water flow system. It is not considered to be "calibrated." There are numerous uncertainties about the hydrologic boundaries, the amount of water moving across these boundaries, and the geometry and properties of the aquifers. Relative sensitivity of computed water level and independent flux to variations in different parameters is shown in figure 57. It is presented to show the relative importance of the different parameters in the computer model. More detailed analyses and results of all sensitivity runs are described in Appendix B2.

Simulated water levels in the baseline model are very sensitive to variations in the horizontal hydraulic conductivity of layer 1 (Navajo aquifer), streambed conductance, and areal recharge. Simulated water levels are only slightly to moderately affected by variations in the horizontal hydraulic conductivity of layer 2 (Kayenta aquifer), vertical leakance between the

Navajo and Kayenta aquifers, as well as the conductance of general-head boundary cells and drain cells.

Simulated ground-water budget components are very sensitive to streambed conductance of river cells, the conductance of general-head boundary cells, and areal recharge. Simulated ground-water budget components are only slightly to moderately sensitive to variations in horizontal hydraulic-conductivity values for layers 1 and 2, vertical leakance between the Navajo and Kayenta aquifers, and the conductance of drain cells.

Need for Additional Study

The above analysis indicates that the baseline model of the main part of the Navajo and Kayenta aquifers is very sensitive to some of the simulated parameters. A better understanding of these parameters would help to improve and refine this initial modeling effort. Suggestions for additional data collection are (1) quantify diffuse infiltration of precipitation and how it varies across the Navajo outcrop within the study area; (2) carry out additional multiple-well aquifer testing to better characterize the variation in horizontal and vertical hydraulic conductivity of the Navajo aquifer; (3) do seepage studies along the Santa Clara and Virgin Rivers upstream of their confluence to better estimate seepage to underlying and adjacent formations; (4) take additional spring measurements to better determine variation in spring discharge under different hydrologic conditions; (5) quantify recharge along the larger ephemeral stream drainages; and (6) undertake a more in-depth age-dating study, including the installation of nested piezometers for investigating vertical stratification of ground water and particle-tracking computer analysis, to better-define aquifer residence times.

In addition, periodic measurements of water levels in observation wells located away from pumping wells would provide information for the development of a transient ground-water flow model to examine shorter-term effects of drought cycles and increased well discharge. There are presently no long-term water-level data available for any Navajo or Kayenta aquifer wells.

Water-Resource Management

This preliminary simulation of ground-water flow in the main part of the Navajo and Kayenta aquifers provides a useful tool for evaluating the validity of the conceptual model and the relative importance of different hydrologic processes and hydraulic proper-

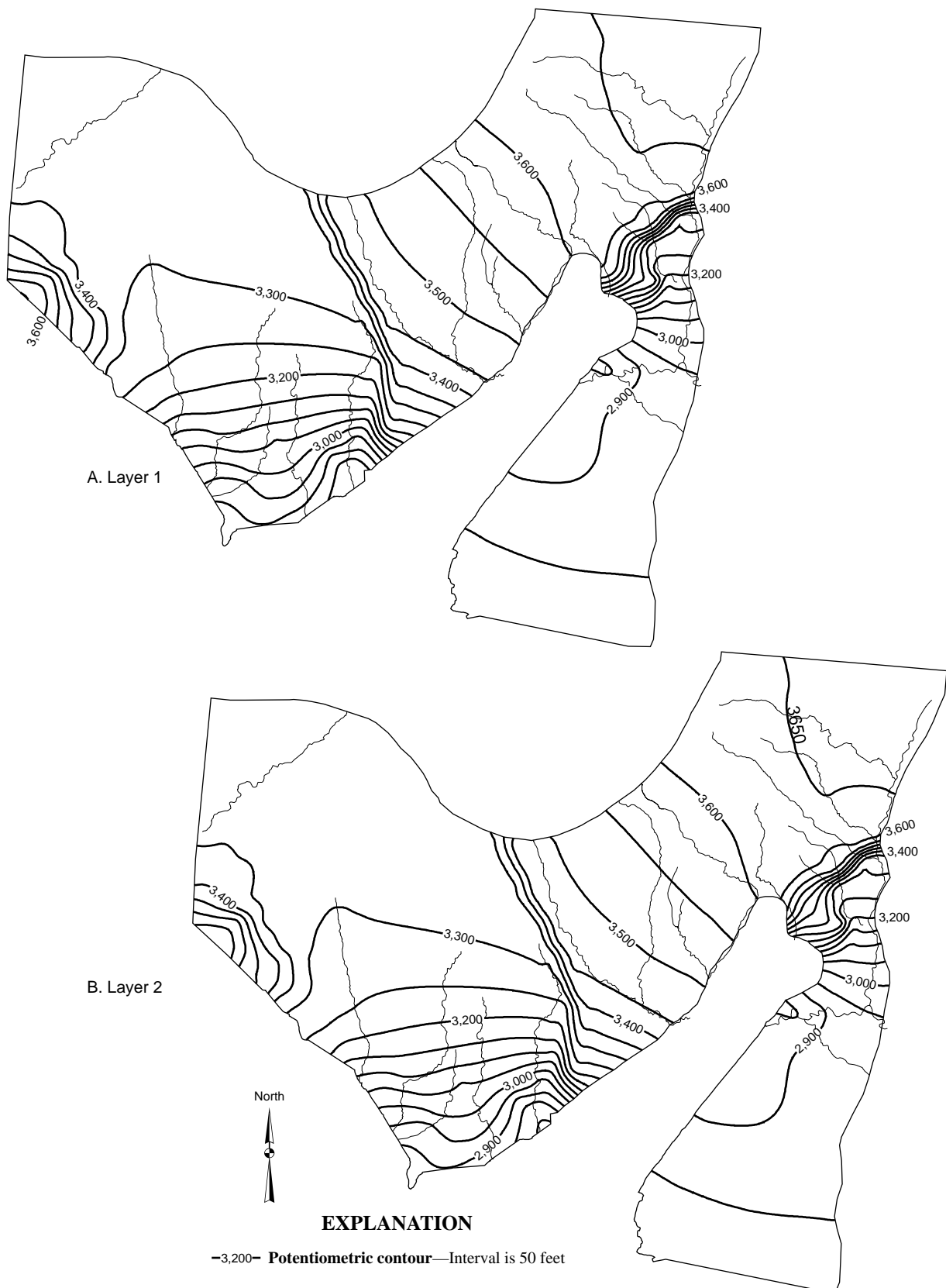


Figure 56. Simulated potentiometric contours for (a) layer 1, and (b) layer 2 of the alternative depicting effects of faulting and east-west anisotropy of the main Navajo aquifer ground-water flow model.

K1	Horizontal hydraulic conductivity of Navajo aquifer
K2	Horizontal hydraulic conductivity of Kayenta aquifer
VCNT	Vertical leakance between Navajo and Kayenta aquifers
RIV	Streambed conductance
GHB	Conductance of general-head boundaries representing subsurface inflow
DRN	Conductance of drain cells representing springs and simulating leakage to underlying formations
RCH	Recharge rate from precipitation and unconsumed irrigation

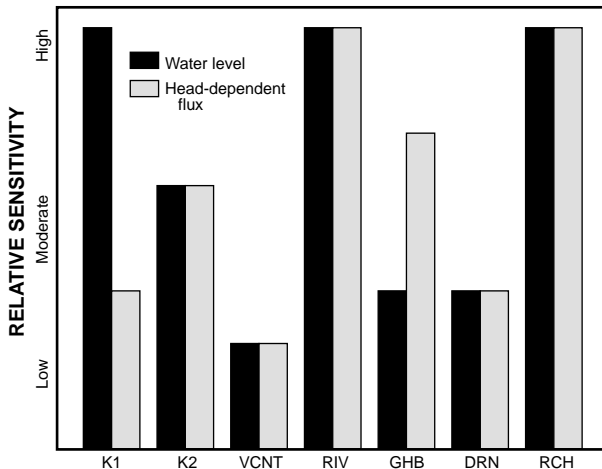


Figure 57. Relative sensitivity of the baseline model representing the main part of the Navajo and Kayenta aquifers to uncertainty in selected properties and flows.

ties. Although the model was constructed with all available hydrologic information, many unknown or poorly-defined hydrologic parameters need to be further investigated. In its present state, the model should not be used as a ground-water management tool, but rather to illustrate the interdependence of hydrologic processes and potential effects of climate change or water use.

Model Limitations

As previously stated, the alternative 1 simulation is considered to be a reasonable approximation to the aquifer system of the main part of the Navajo and Kayenta aquifers. However, it is evident from both aquifer testing and computer modeling of anisotropic conditions that aquifer properties vary throughout the study area. Because of sparse hydraulic-property data and limitations of the modeling software, such variability was not simulated. Likewise, important ground-water fluxes, such as recharge from precipitation and ephemeral streams, were only estimated; the spatial location and rates of recharge may vary substantially from the simulated fluxes. Therefore, the model is a reasonable representation of the aquifer system on a regional scale but may not accurately represent hydrologic conditions at particular locations. Thus, the model should be used

as a tool for testing general cause-and-effect scenarios rather than evaluating site-specific processes.

In addition, the model simulates steady-state conditions based on the underlying assumption that hydrologic data collected during 1995 and 1996 are representative of average conditions. If either natural or man-induced stresses to the hydrologic system substantially change different ground-water budget components, these components would need to be revised in the computer model. Subsequently, the revised model's ability to accurately represent the hydrologic system would need to be reevaluated. Finally, because the model is a steady-state simulation, it can only indicate the ultimate effects of imposed changes rather than the changing effects over time. For example, if the effect of a new well field were to be evaluated, the model would only show the potential ultimate decrease in ground-water levels, rather than year-to-year declines.

Gunlock Part of the Navajo Aquifer

The Gunlock part of the Navajo and Kayenta aquifers is defined by the Gunlock Fault on the east and the erosional extent of the Kayenta Formation on the south and west. These aquifers are in hydrologic contact with the Santa Clara River and stores a major portion of the potable water supply of St. George. To examine the hydrologic characteristics of the Gunlock aquifers, a steady-state baseline ground-water flow model was developed. The flow model was used to study pumping at the St. George municipal well field, flow in the Santa Clara River, and alternative hydrologic boundaries. The steady-state simulation incorporates an average recharge and discharge for the system. Simulated well discharge is the 1987-96 average; simulated precipitation recharge represents the 1961-90 average.

Model Characteristics and Discretization

The ground-water flow model presented here is an initial effort at simulating hydrologic conditions in the Gunlock part of the Navajo and Kayenta aquifers. Most model parameters were not adjusted from initial estimates and the model is not considered to be "calibrated." Limited data are available to describe conditions in the Gunlock part and a determination of whether adjusted model parameters result in a more acceptable or "better" simulation of the system than initial values is difficult to make.

The 59-mi² area that represents the Gunlock part of the Navajo and Kayenta aquifers is divided into 132

rows, 67 columns, and 2 layers with a total of 17,688 model cells (fig. 58). The modeled area is defined by the Gunlock Fault on the east, the saturated extent of the Navajo Sandstone and Kayenta Formation on the south and west, and extends up to 4 miles north of the Carmel Formation and Navajo Sandstone contact. Model cells are 530 ft by 530 ft (0.01 mi^2); cell size was determined so that each well in the St. George municipal well field would be represented by an unique cell. Layer 1 represents the Navajo aquifer and includes 5,058 active cells simulating an area of about 52 mi^2 . Layer 2 represents the Kayenta aquifer and includes 5,585 active cells that simulate an area of about 59 mi^2 . The model grid is orientated 10 degrees east of true north so that columns run parallel to the general orientation of the Gunlock Fault. The vertical dip of both layers is about 20 degrees to the northeast, consistent with the structural geology of the area.

Vertical model discretization is referenced from the top and bottom of the Navajo Sandstone (fig. 59). The base of model layer 2 was set at 850 ft below the base of the Navajo Sandstone (table 2); where the Kayenta Formation is overlain by the Navajo Sandstone, model layer 2 is 850 ft thick. Where the Kayenta Formation is exposed, the simulated thickness of model layer 2 corresponds to model-computed water levels in the layer (200 ft to 850 ft thick). The base of model layer 1 (equivalent to the top of model layer 2) was determined from the structure contour map of the base of the Navajo Sandstone (Hurlow, 1998, pl. 5a). Where the Navajo Sandstone is exposed, the thickness of model layer 1 depends on computed water levels for the layer (200 ft to 2,400 ft). Where the Navajo Sandstone is overlain by Carmel Formation, the top of model layer 1 is based on the contour map of the top of the Navajo Sandstone (Hurlow, 1998, pl. 5b). The average thickness of the Navajo aquifer where it is overlain by the Carmel Formation is about 2,400 ft.

Boundary Conditions

Hydrologic boundaries used in the baseline model of the Gunlock part of the Navajo and Kayenta aquifers include no-flow, specified-flux, and head-dependent (general-head) boundaries. Similar to the main part, no-flow boundaries represent the erosional extent of the aquifers and are fairly well defined. Other boundaries, such as those that represent flow to and from underlying and overlying formations, and across the Gunlock Fault, are not well defined and therefore are represented by no-flow boundaries. Where the aquif-

fers are unconfined along the Navajo and Kayenta Formation outcrops, the water table is treated as a free surface with a specified flux recharge boundary to simulate infiltration of precipitation and seepage from Gunlock Reservoir. Model cells corresponding to the Santa Clara River include a head-dependent boundary that allows for interaction between the free surface and the river.

Recharge Boundaries

Precipitation

Recharge from precipitation is simulated with the recharge package at model cells that represent the surface exposure of Navajo Sandstone and Kayenta Formation. Where average annual precipitation is estimated to be 14 in. or less, recharge is specified as 10 percent of total precipitation. For areas where precipitation exceeds 14 in., recharge is specified as 15 percent of total precipitation. These estimated rates are based on water-budget calculations. The distribution of precipitation was derived from the 30-year average annual precipitation contours (1961-90) compiled by the Utah Climate Center (fig. 2). The distribution and amount of precipitation that becomes recharge used in the baseline model is shown in figure 60.

Santa Clara River

Recharge as seepage from the Santa Clara River is simulated as head-dependent flux with the streamflow package (Prudic, 1989). Properties that control the rate of simulated recharge are (1) the difference between the computed water level for the appropriate model cell and the altitude of the water surface in the Santa Clara River (stream stage), (2) the width and thickness of the alluvial streambed material that separates the Santa Clara River from the underlying Navajo Sandstone, and (3) the hydraulic conductivity of the streambed material. Altitude of the top of the streambed was determined from the appropriate USGS 1:24,000-scale topographic map, which has a contour interval of 40 ft, and surveyed altitudes at four selected sites. Width of the alluvial material is specified as 100 ft and thickness is specified at 20 ft. These dimensions are rough estimates made on the basis of field observations and correspond to values used in the analysis of the Gunlock well-field aquifer test. Hydraulic-conductivity values specified for the streambed range from 1.4 to 290 ft/day. The distribution of hydraulic conductivity is shown on figure 61, and was also made on the basis of

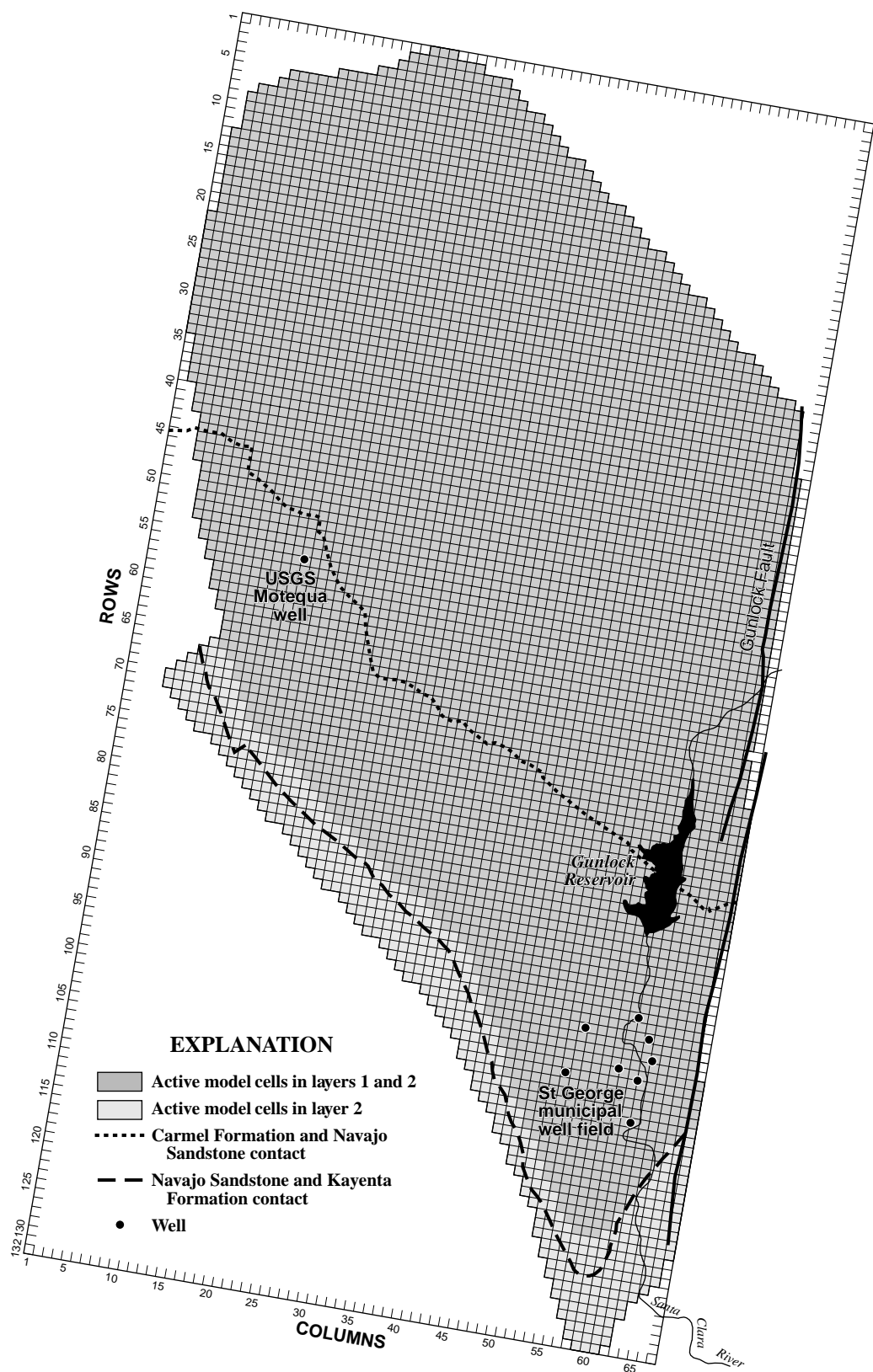


Figure 58. Model grid of the Gunlock part of the Navajo and Kayenta aquifers within the central Virgin River basin study area, Utah.

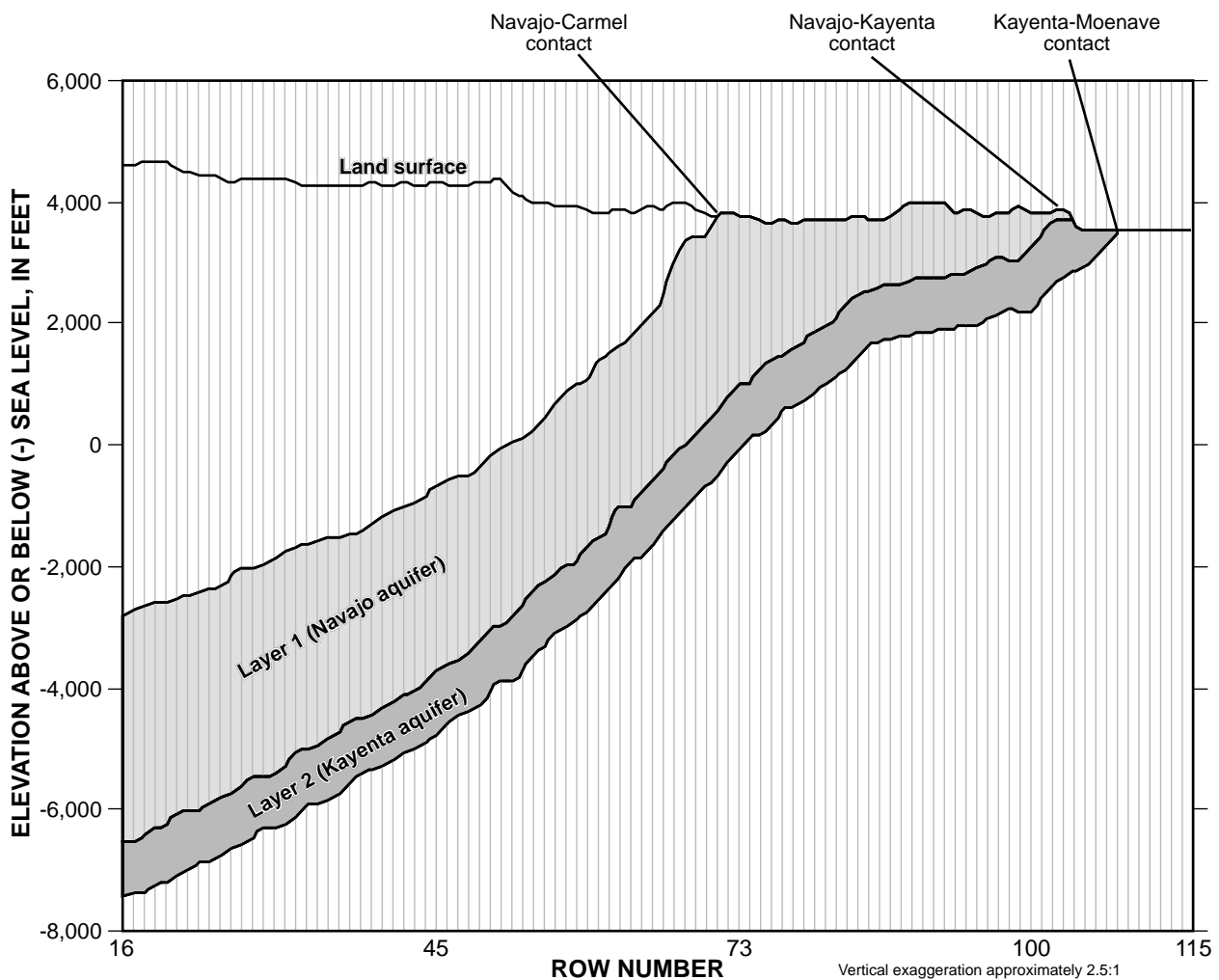


Figure 59. Generalized cross section along column 45 of the ground-water flow model of the Gunlock part of the Navajo and Kayenta aquifers within the central Virgin River basin study area, Utah.

the Gunlock well-field aquifer test. The degree of variability in hydraulic conductivity is large and reflects (1) averaging and uncertainty associated with the width and thickness of the streambed alluvium, and (2) heterogeneity of the underlying Navajo Sandstone that is caused by joints and fractures. The Santa Clara River alternates from running along and perpendicular to facutes that exist in the Navajo Sandstone.

As mentioned, the distribution of hydraulic conductivity of the streambed alluvium was determined from results of the Gunlock well field aquifer test. However, conductivity values used in this simulation are one order of magnitude less than those from the aquifer test. This discrepancy is likely caused by the fact that simulated stream seepage in the aquifer test model is considered a combined effect from the river and release of water from storage in the alluvial stre-

ambed material (appendix A, fig. A-10). Streambed conductivities in this simulation were reduced in an attempt to replicate measured stream channel losses from the Santa Clara River.

In addition to simulating interaction with the Gunlock aquifer, the streamflow package also accounts for surface flow in the Santa Clara River; surface flow changes in accordance with seepage losses from the river. Streamflow in the Santa Clara River, at the point where water is released from Gunlock Reservoir, is specified at $6.0 \text{ ft}^3/\text{s}$ (4,300 acre-ft/yr). Surface flow in successive stream reaches is determined by the computer model. Stream stage for the Santa Clara River is specified at 1 ft above the top of the streambed, on the basis of field observations made at several locations along the stream. The location and course of the Santa Clara River also was determined from the 1:24,000-

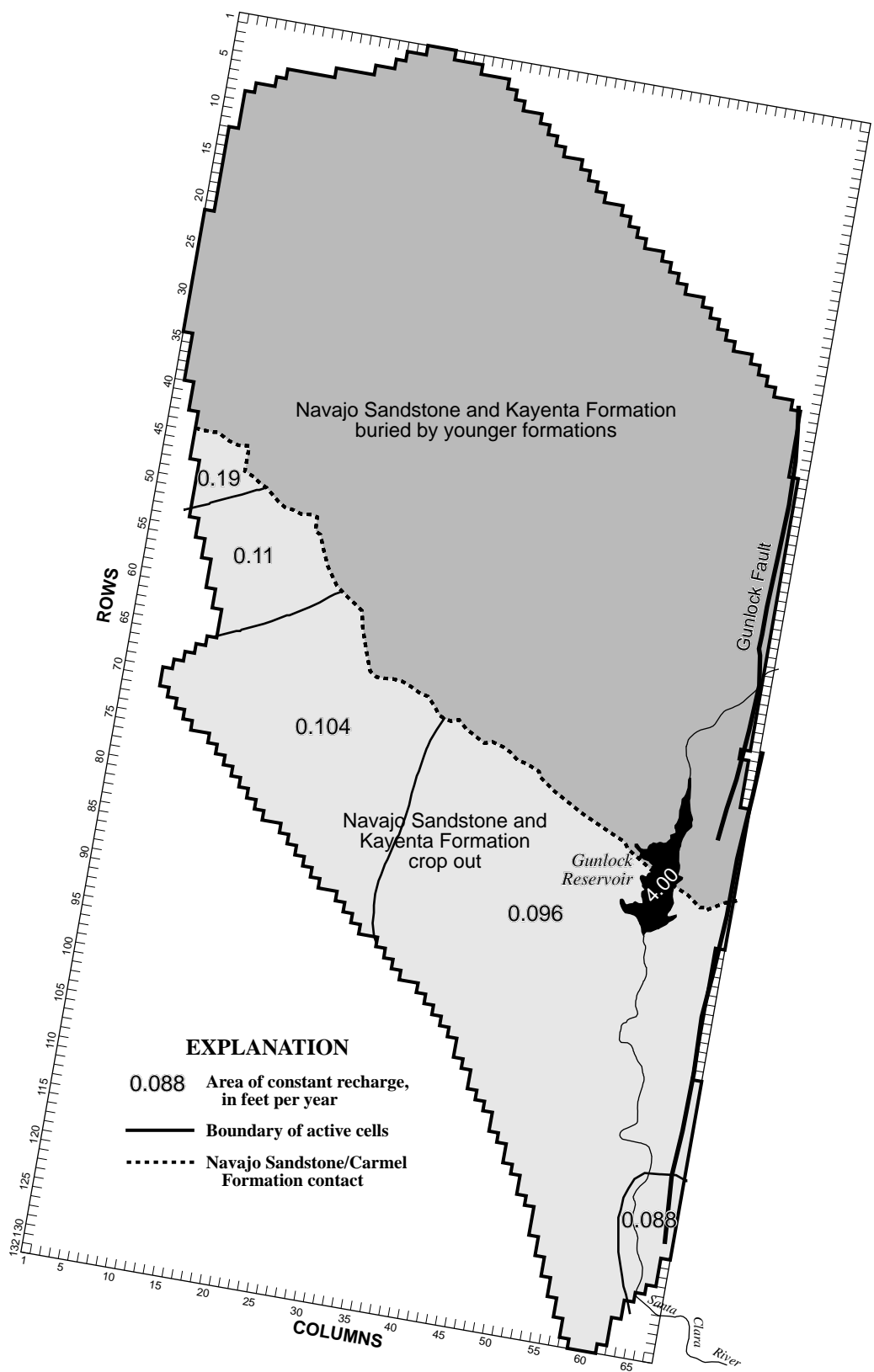


Figure 60. Distribution of recharge from infiltration of precipitation and reservoir leakage simulated in the ground-water flow model of the Gunlock part of the Navajo and Kayenta aquifers within the central Virgin River basin study area, Utah.

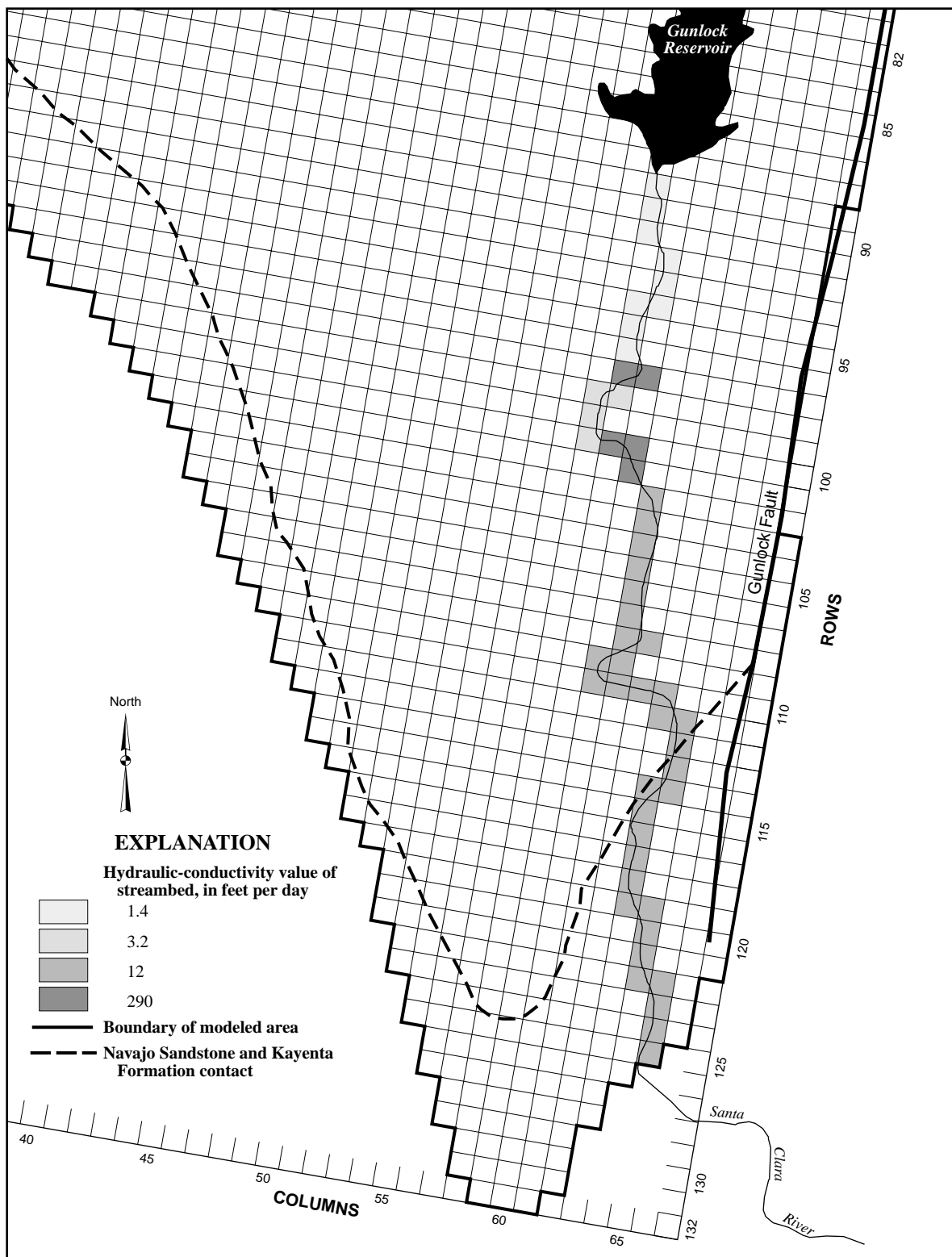


Figure 61. Distribution of streambed hydraulic conductivity that simulates seepage from the Santa Clara River in the ground-water flow model of the Gunlock part of the Navajo and Kayenta aquifers within the central Virgin River basin study area, Utah.

scale topographic map. Seventy-six model cells are used to simulate the river.

Gunlock Reservoir

Recharge as seepage from Gunlock Reservoir is specified with the recharge package at cells where the reservoir overlies the Navajo Sandstone (fig. 53). Total simulated recharge beneath the reservoir is $1.4 \text{ ft}^3/\text{s}$ ($1,000 \text{ acre-ft/yr}$), as determined from Darcy's law and seepage estimates discussed in the conceptual description of the Gunlock area. Because seepage from the reservoir is treated as a specified flux, recharge is independent of water levels in the Navajo aquifer and the pool altitude in the reservoir.

Discharge Boundaries

Wells

Discharge from eight wells in the St. George municipal well field is simulated with the well package. These wells are located in a cluster about 1 to 2 miles south of Gunlock Reservoir. The discharge rate used in the baseline simulation, $5.8 \text{ ft}^3/\text{s}$, is based on water-use information compiled by the city of St. George and represents the 1987-96 average. During that time, total discharge rates from the eight wells ranged from 4.1 to $7.1 \text{ ft}^3/\text{s}$. The location of the wells is shown in figure 51. All well discharge is simulated from the Navajo aquifer (model layer 1).

Santa Clara River

Discharge as seepage to the Santa Clara River is simulated as head-dependent flux with the streamflow package. Discharge is simulated when the model-computed water level for the aquifer is higher than the stream stage of the river. On the basis of field observations, seepage to the Santa Clara River occurs where the river flows across the southern extent of the Navajo Sandstone and across the Kayenta Formation. Model parameters required for the streamflow boundary and the methods used to estimate them are explained in the section titled "Recharge boundaries." Hydraulic conductivity of the streambed material where it is underlain by the Kayenta Formation was estimated at 12 ft/d (fig. 61). This value was not determined directly but was extrapolated from the hydraulic conductivity assigned to the southern most streambed material included in the Gunlock well-field aquifer test.

No-Flow Boundaries

No-flow boundaries are used to represent (1) the base of the Kayenta Formation, (2) the lateral extent of the Navajo and Kayenta aquifers to the south, west, east, and north, and (3) the top of the Navajo Sandstone where it is overlain by Carmel Formation. This boundary condition is based on the conceptual assumptions that (1) there is no hydraulic connection between the Kayenta aquifer and underlying formations, (2) there is no hydraulic connection across the Gunlock Fault with the main part of the Navajo and Kayenta aquifers, and (3) there is no ground-water recharge from the overlying Carmel Formation to the Navajo aquifer.

Distribution of Aquifer Characteristics

The Navajo and Kayenta aquifers are simulated as individual layers in the baseline model. Each layer is assigned a set of aquifer characteristics on the basis of aquifer tests and simulation results for the main part of the Navajo and Kayenta aquifers. Data describing the spatial distribution of aquifer properties are not available; therefore, both layers are considered homogeneous. Aquifer properties include horizontal hydraulic conductivity, vertical hydraulic conductivity, and anisotropy. These properties are assigned to all active cells in the modeled area. In conjunction with boundary conditions, aquifer properties determine the amount and pattern of simulated ground-water flow. Values assigned to each layer are listed in table 24.

The horizontal hydraulic conductivity of layer 1 (the Navajo aquifer) is specified as 0.33 ft/d and the east-west to north-south horizontal anisotropy ratio is specified as 3.0. This results in a simulated hydraulic conductivity of 0.33 ft/d in a generally east-to-west direction (along rows) and 1.0 ft/d in a generally north-to-south direction (along columns). Anisotropy and horizontal hydraulic conductivity of the Navajo aquifer are based on values determined from the Gunlock well-field aquifer test. A vertical hydraulic-conductivity value of 0.25 ft/d is specified for layer 1 and was calculated by multiplying the east-west horizontal-conductivity value by 0.75. This multiplier is the same as that used in the baseline simulation of the main part of the Navajo and Kayenta aquifers and is in agreement with laboratory hydraulic testing of Navajo Sandstone.

The horizontal hydraulic-conductivity value of layer 2 (the Kayenta aquifer) is specified as 0.25 ft/d . Initially, the conductivity value assigned to layer 2 was 0.085, which resulted in the same ratio of layer 1:layer 2 horizontal conductivity specified in the baseline sim-

Table 24. Hydraulic-conductivity values used in the baseline simulation of the Gunlock part of the Navajo and Kayenta aquifers, central Virgin River basin, Utah

	Navajo aquifer (layer 1), in feet per day	Kayenta aquifer (layer 2), in feet per day
East-west to north-south anisotropy	13.0	¹ 3.0
East-west horizontal hydraulic conductivity	.33	.25
North-south horizontal hydraulic conductivity	1.00	.75
Vertical hydraulic conductivity	.25	.125

¹Anisotropy is unitless.

ulation of the main part of the Navajo and Kayenta aquifers. The final value of 0.25 ft/d results in a better match to measured and estimated water levels and fluxes. The vertical hydraulic conductivity of layer 2 is specified as 50 percent of the horizontal value, maintaining the horizontal-to-vertical conductivity ratio specified in the baseline simulation of the main part. The Kayenta Formation contains zones of silts and clays, most likely causing overall conductivity values to be less than those estimated for the Navajo Sandstone. Assuming that fracture density and orientation within the Kayenta aquifer are similar to the Navajo aquifer, the anisotropy for layer 2 was specified at 3.0, the same value as in layer 1.

Conceptual Model and Numerical Simulation

Two factors were used to determine how closely the baseline numerical simulation matched the conceptual model: (1) a comparison of conceptual and model-computed ground-water budgets, and (2) a comparison of computed and measured water levels in wells (table 25). The computed ground-water budget indicates that simulated seepage from the Santa Clara River to the aquifers are at the upper limit of the range estimated in the conceptual model. Simulated seepage to the Santa Clara River from the aquifers is several times the estimated amount, although the excess represents less than 15 percent of the total ground-water budget. Other components of the simulated budget are specified and not computed by the model. The direction of ground-water movement depicted by the baseline simulating (fig. 62) is similar to that depicted in figure 26, indicating flow from recharge areas toward the Santa Clara River.

Water levels indicate considerable variation between simulated and measured values (table 25).

Although differences in excess of 25 ft occur only at wells 3 and 4, the root mean square error (a measure of overall error) indicates that the numerical simulation does not accurately simulate the detailed shape of the water table in the area of the municipal well field. Several factors may explain this, including the use of pumping wells as observation wells, and steep ground-water gradients (drawdown cones) near pumping wells. The overall hydraulic gradient from northwest to southeast in the Navajo aquifer, as measured by the difference in water levels at the USGS Motoqua well and well 3 (figs. 26 and 58) is reasonably represented. The measured difference is 240 ft; the simulated difference is 263 ft.

Model Applicability

The baseline model represents the conceptual understanding and available data for the Gunlock part of the Navajo and Kayenta aquifers. However, as is the case for the upper Ash Creek drainage basin ground-water system and the main part of the Navajo and Kayenta aquifers, other possible numerical simulations might match the recharge fluxes, discharge fluxes, and water-level distribution observed and estimated for the Gunlock aquifers. Because available data are limited and certain hydrologic boundaries of the Gunlock aquifers are not well defined, the baseline model should not be considered a “calibrated” model. Although other combinations of aquifer properties and fluxes may yield a similar or improved match to measured and estimated hydrologic properties, the baseline model is a viable representation that can be used as a tool for testing alternative combinations of aquifer properties and fluxes.

Table 25. (a) Conceptual and simulated ground-water budgets and (b) simulated versus measured water-level differences in the Gunlock part of the Navajo and Kayenta aquifers, central Virgin River basin, Utah

(a) Ground-water budget ¹		
Flow component	Conceptual	Baseline simulation ¹ (rounded)
Recharge, in acre-feet per year		
Infiltration of precipitation	700 to 2,200	1,400
Seepage from Gunlock Reservoir	0 to 2,200	1,000
Seepage from the Santa Clara River	700 to 2,900	2,900
Total	1,400 to 7,300	5,300
Discharge, in acre-feet per year		
Well discharge	3,400 to 5,500	4,200
Seepage to the Santa Clara River	400	1,100
Total	3,800 to 5,900	5,300

¹ Budget amounts listed in italics were specified fluxes. All others are head-dependent fluxes determined by the model.

(b) Measured and simulated water levels, in feet above sea level			
Well identifier	Measured water level	Simulated water level	Difference ³
Well #1 ¹	3,341	3,348	7
Well #2 ¹	3,343	3,356	13
Well #3 ²	3,326	3,290	-36
Well #4 ¹	3,351	3,318	-33
Well #5 ¹	3,419	3,418	-1
Well #6 ¹	3,352	3,376	24
Well #7 ¹	3,411	3,410	-1
Well #8 ¹	3,407	3,400	-7
Motoqua Well ¹	3,566	3,549	-17
Root mean square error, in feet			20

¹ Water level measured in February 1996, when pump in well was not operating. Motoqua well contains no pump.

² Water level measured in February 1997, when pump in well was not operating.

³ (-) indicates simulated water level is lower than measured water level.

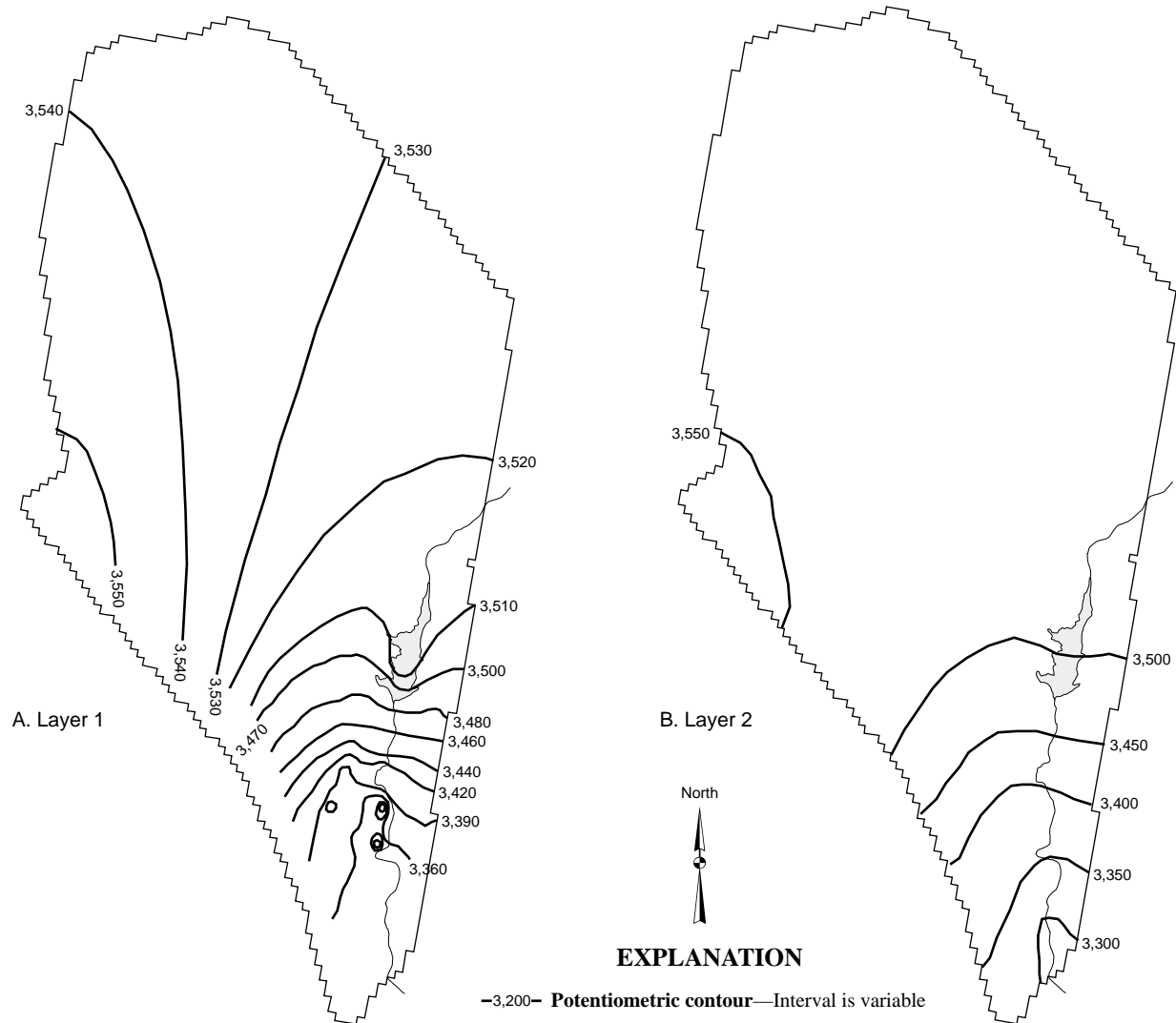


Figure 62. Simulated potentiometric contours for (a) layer 1 and (b) layer 2 of the baseline simulation of the Gunlock ground-water flow model.

Alternative Simulations

Conceptually, the Gunlock part of the Navajo and Kayenta aquifers is not considered to be hydraulically connected to underlying formations, nor to the main Navajo and Kayenta aquifers east of the Gunlock Fault. Reflecting that, the baseline model simulates the bottom of the Kayenta aquifer and the Gunlock Fault as no-flow boundaries. Only seepage to and from the Santa Clara River was simulated as being dependent on hydrologic conditions within the aquifers. To examine the effects of other hydraulically connected boundaries, two alternative simulations were tested.

Alternative 1—Seepage Across the Gunlock Fault.

In the baseline model, the Gunlock Fault is represented as a no-flow boundary. Because the fault has created a vertical offset between the main part of the Navajo and Kayenta aquifers and the aquifers of the Gunlock part. However, no direct evidence or field observations substantiate this concept. To explore the possible effects of ground-water flow across the fault, the no-flow baseline boundary was replaced with a head-dependent flow boundary with the general-head boundary package.

Required input parameters for the general-head boundary include hydraulic conductivity of the bound-

ary and water-level altitude outside of the modeled area. Computed flow across the boundary is directly proportional to the difference between computed water levels inside the model area and the water levels assigned outside the model area. The general-head boundary was placed in model layer 1 at cells that correspond to the segment of the Gunlock Fault with the vertical offset between the main and Gunlock aquifers.

To simulate seepage across the fault, the following assumptions were made: (1) the vertical face of the boundary is set to the 2,400-ft measured thickness of the Navajo Sandstone west of the Gunlock Fault; (2) the water level on the east side of the fault (3,345 ft) is the average water level simulated for the main part of the Navajo Sandstone at the fault; (3) the fault zone is 300 ft wide; and (4) the hydraulic conductivity of the fault zone is the average horizontal hydraulic-conductivity value of the Navajo Sandstone (1.2 ft/d) used in the main and Gunlock parts. Data are not available to describe the hydrology of the fault zone, and these assumptions are hypothetical.

Given the conditions listed above, the computer model simulated ground-water flow out of the Gunlock aquifers across the Gunlock Fault (fig. 63, table 26). This outflow has a moderate effect on the simulated interaction between the Navajo aquifer and the Santa Clara River. Seepage from the river increased from 2,900 to 3,400 acre-ft/yr. Seepage to the river decreased, from 1,100 to 900 acre-ft/yr, and is a closer match to measured seepage. Overall, simulated water levels at the St. George municipal well field decreased. This simulation indicates that some flow across the fault toward the main aquifer is plausible. However, only one of many possible representations of the fault is explored.

Alternative 2—Inflow from Underlying Formations

The formations underlying the Kayenta aquifer contain fine-grained material and are generally considered to have poor water-bearing characteristics. Because of this, the base of the Kayenta aquifer is treated as a no-flow boundary in the baseline model. However, as is the case with the Gunlock Fault, no direct hydrologic evidence substantiates the no-flow concept. Depending on the vertical extent of fractures, some ground-water flow across the base of the Kayenta aquifer is possible. Such flow could be induced or enhanced if water levels in the Navajo and Kayenta aquifers declined. Higher dissolved-solids concentrations at St. George Gunlock Well 2, (C-41-17)7ddb-1

(Wilkowske and others, 1998, table 4) indicate that there may be some upward movement of ground water from underlying formations at the municipal well field. To explore this possibility, the no-flow boundary at the base of the Kayenta Formation was replaced with a head-dependent flow boundary, with the general-head boundary package.

The general-head boundary was arbitrarily assigned to cells defining a 1-mi² area at the base of the Kayenta aquifer and centered at St. George Gunlock Well 2. The following assumptions were made for this alternative: (1) the water-level altitude in the underlying formation near St. George Gunlock Well 2 is about 100 ft higher than the average water level of 3,340 ft estimated for the area (fig. 26); (2) the point at which this water level exists in the underlying formation is 300 vertical feet below the base of the Kayenta aquifer; and (3) the vertical hydraulic conductivity of the underlying formations is about three orders of magnitude less than the estimated vertical hydraulic conductivity of the Kayenta aquifer. These values are consistent with the values specified to simulate flow from underlying formations in the main part of the Navajo and Kayenta aquifers. No data are available to determine the characteristics of this boundary with certainty.

Using the conditions stated above, the alternative model simulated about 300 acre-ft/yr of ground-water inflow from underlying formations (table 27). This inflow has a small effect on the simulated interaction between the Navajo aquifer and the Santa Clara River. Seepage from the river decreased slightly, from about 2,900 to 2,700 acre-ft/yr. Seepage to the river increased by about the same amount, from about 1,100 to 1,200 acre-ft/yr. Simulated water levels at the St. George municipal well field generally rose, increasing at seven wells and remaining the same at one well (table 27). The simulated water level at the Motoqua well increased by 6 ft. The direction of ground-water movement depicted by this alternative simulation (fig. 64a and b) is similar to the baseline simulation, but water levels are slightly higher in the northern part of the simulated area. Given the above conditions, the alternative of allowing a small amount of inflow to the area from underlying formations is plausible.

Model sensitivity

Although the baseline model is not “calibrated,” it is a viable tool for analysis of general concepts of ground-water flow for the Gunlock part of the Navajo and Kayenta aquifers. To get a feel for the relative importance of the aquifer properties and fluxes that

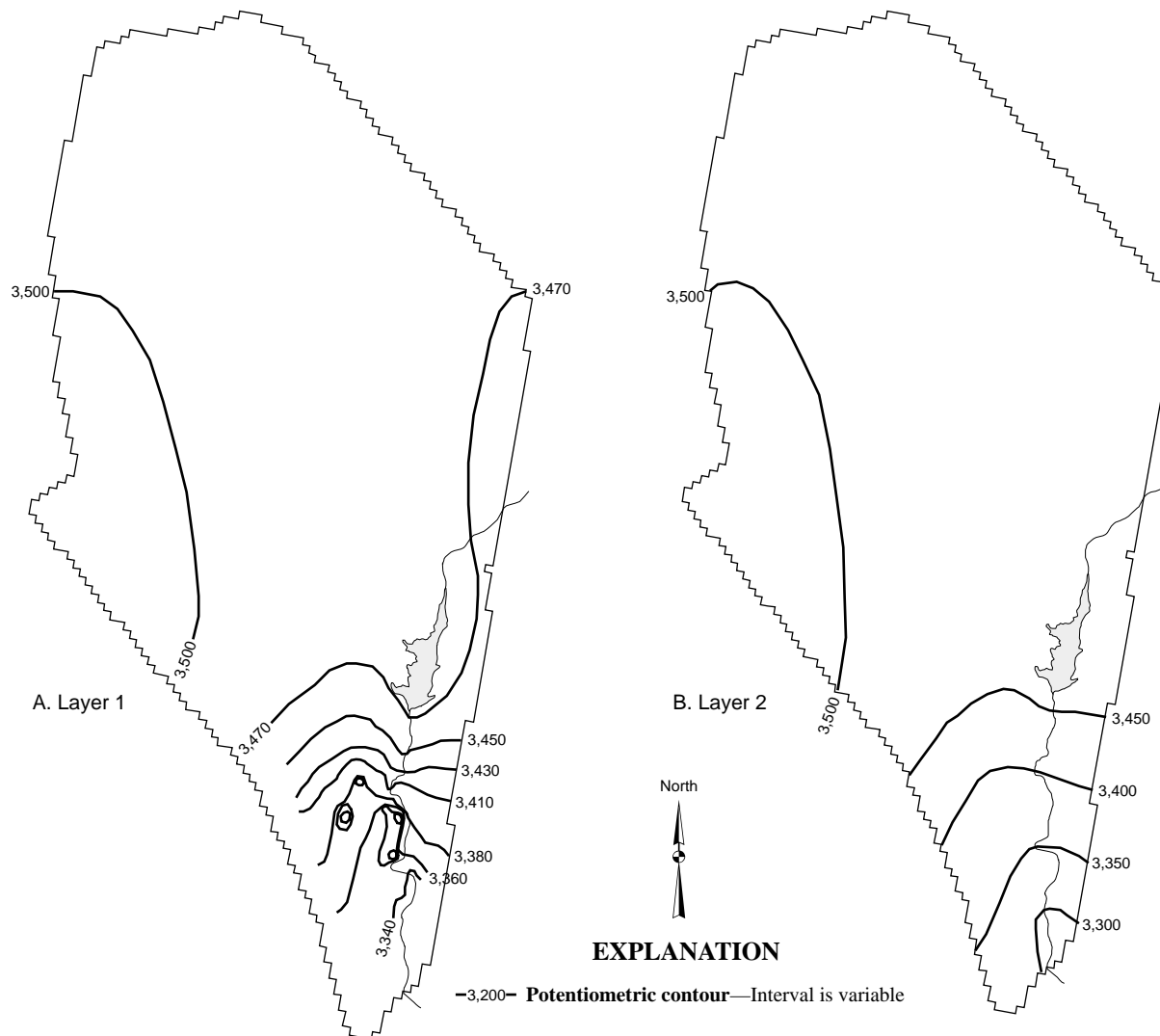


Figure 63. Simulated potentiometric contours for (a) layer 1, and (b) layer 2 of the alternative simulation depicting flow across the Gunlock Fault, Gunlock ground-water flow model.

make up the Gunlock aquifers, a sensitivity analysis of the baseline simulation was performed. A sensitivity analysis identifies which model parameters have the greatest influence on model simulations. Although there is no direct correlation between model sensitivity and the natural system, model sensitivity is useful when considering additional analysis or data collection.

The sensitivity of the baseline model to different parameters is shown in figure 65. The height of each bar is subjective and based on an evaluation of how variations in the parameter affected computed water-levels and fluxes. A more detailed analysis and the quantitative results of all sensitivity runs are described in appendix B.

Computed water levels in the baseline model are highly sensitive to both increases and decreases in horizontal anisotropy (the ratio between east-west and north-south horizontal hydraulic conductivity) and the distribution of infiltration of precipitation. Decreased horizontal hydraulic conductivity in the north-south orientation caused computed water levels in all parts of the modeled area to decrease dramatically. Increased anisotropy caused increased head-dependent flux into and out of the Santa Clara River. Changes in the distribution of infiltration of precipitation had the greatest affect on water levels in areas away from the Santa Clara River. Both seepage to and from the Santa Clara River are moderately sensitive to changes in streambed properties. Computed water levels were moderately

Table 26. (a) Conceptual and simulated ground-water budgets and (b) simulated versus measured water-level differences for the baseline simulation and the simulation testing flow across the Gunlock Fault in the Gunlock part of the Navajo and Kayenta aquifers, central Virgin River basin, Utah

(a) Ground-water budget ¹			
Flow component	Conceptual	Baseline simulation	Gunlock Fault flow simulation
Recharge, in acre-feet per year			
Infiltration of precipitation	700 to 2,200	1,400	1,400
Seepage from Gunlock Reservoir	0 to 2,200	1,000	1,000
Seepage from Santa Clara River	700 to 2,900	2,900	3,400
Total	1,400 to 7,300	5,300	5,800
Discharge, in acre-feet per year			
Well discharge	3,400 to 5,500	4,200	4,200
Seepage to Santa Clara River	400	1,100	900
Flow across Gunlock Fault	0	0	600
Total	3,800 to 5,900	5,300	5,700

¹ Budget amounts listed in italics were specified fluxes. All others are head-dependent fluxes determined by the model.

(b) Difference between simulated and measured water levels, in feet		
Well identifier	Baseline simulation	Gunlock Fault flow simulation
Well #1	7	2
Well #2	13	-2
Well #3	¹ -36	¹ -38
Well #4	-33	-35
Well #5	-1	-2
Well #6	24	8
Well #7	-1	-3
Well #8	-7	-9
Motoqua well	-17	-62
Root mean square error	20	27

¹ Difference determined from water level measured in February 1997; all other water levels measured in February 1996.

Table 27. (a) Conceptual and simulated ground-water budgets and (b) simulated versus measured water-level differences for the baseline simulation and the simulation testing inflow from underlying formations in the Gunlock part of the Navajo and Kayenta aquifers, central Virgin River basin, Utah

(a) Ground-water budgets ¹			
Flow component	Conceptual	Baseline simulation	Underlying-formation inflow simulation
Recharge, in acre-feet per year			
Infiltration of precipitation	700 to 2,200	1,400	1,400
Seepage from Gunlock Reservoir	0 to 2,200	1,000	1,000
Seepage from Santa Clara River	700 to 2,900	2,900	2,700
Flow from the Moenave	0	0	300
Total	1,400 to 7,300	5,300	5,400
Discharge, in acre-feet per year			
Well discharge	3,400 to 5,500	4,200	4,200
Seepage to Santa Clara River	400	1,100	1,200
Total	3,800 to 5,900	5,300	5,400

¹ Budget amounts listed in italics were specified fluxes. All others are head-dependent fluxes determined by the model.¹

(b) Differences between simulated and measured water levels, in feet		
Well identifier	Baseline simulation	Underlying-formation inflow simulation
Well #1	7	11
Well #2	13	27
Well #3	1-36	1-34
Well #4	-33	-32
Well #5	-1	-1
Well #6	24	33
Well #7	-1	0
Well #8	-7	-6
Motoqua	-17	-11
Root mean squared error	20	22

¹ Difference determined from water level measured in February 1997; all other water levels measured in February 1996.

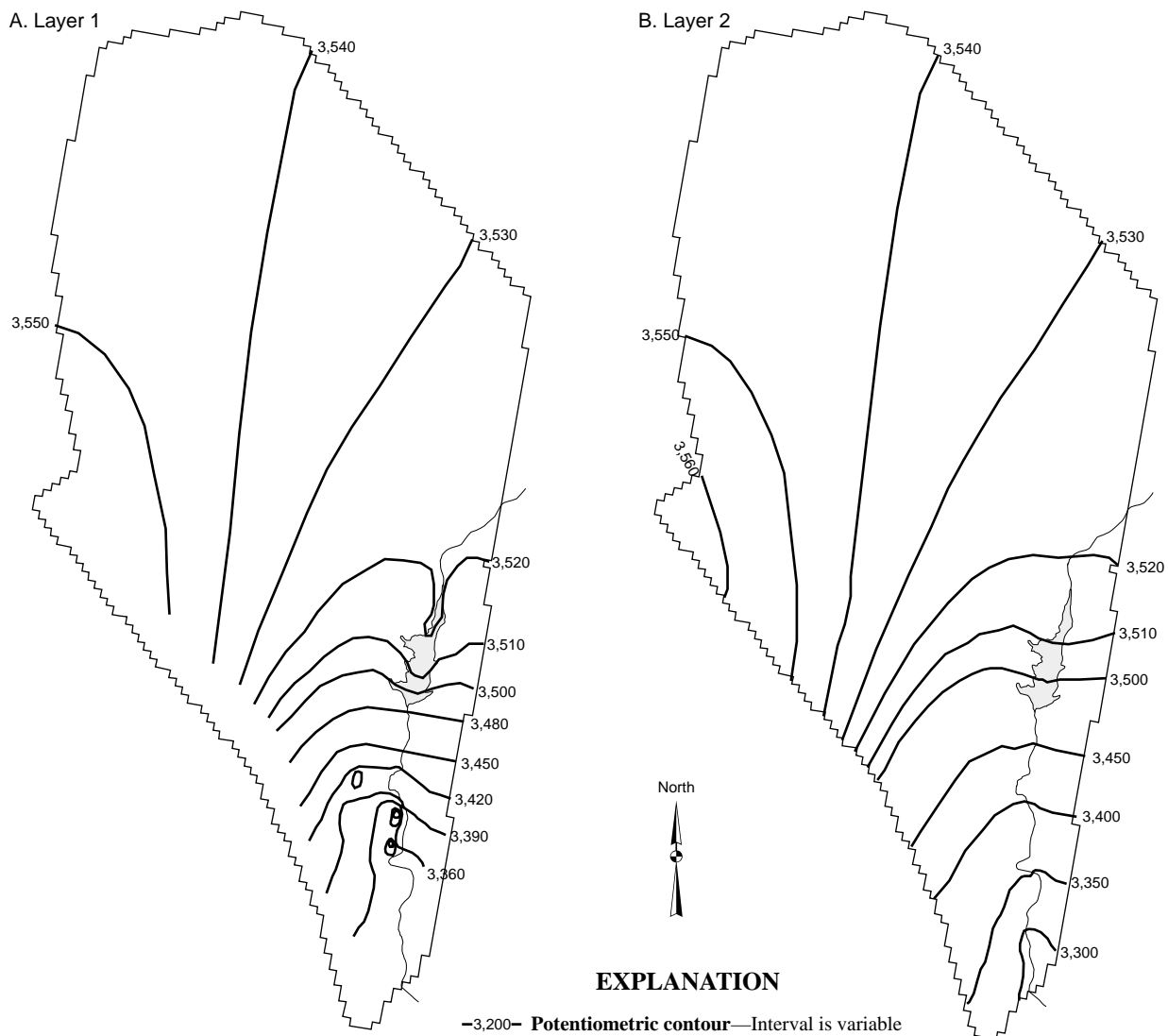


Figure 64. Simulated potentiometric contours for (a) layer 1, and (b) layer 2 of the alternative simulation depicting inflow from underlying formations, Gunlock ground-water flow model.

sensitive to changing aquifer properties of layer 1 near the Gunlock Fault. The baseline simulation is not very sensitive to changes in hydraulic properties of the Kayenta aquifer.

Need for additional study

On the basis of the alternative simulations and sensitivity analysis of the baseline model of the Gunlock part of the Navajo and Kayenta aquifers, the need for additional data became apparent. Better quantification of the hydrologic properties associated with the Gunlock Fault is needed to determine whether ground-water flow occurs across the fault, and the direction and amount of that flow. Design of an aquifer test with

observation wells located on both sides of the fault would answer some of those questions. Additional information regarding the interaction between the Santa Clara River and adjacent Navajo aquifer also would improve the conceptual model. Specifically, identifying aquifer properties associated with the streambed material would be helpful and could be determined with an appropriately designed multi-well aquifer test.

To better define the general shape and hydraulic gradient of the water table, water-level observation wells need to be constructed in areas away from the St. George municipal well field. Annual, seasonal, or monthly monitoring of water levels at observation wells

- A1 Anisotropy
 K1 Horizontal hydraulic conductivity of the Kayenta aquifer
 V1 Vertical hydraulic conductivity of the Kayenta aquifer
 S1 Streambed hydraulic conductivity
 K2 Hydraulic conductivity near the Gunlock Fault
 R1 Recharge from Gunlock Reservoir
 I1 Infiltration of precipitation

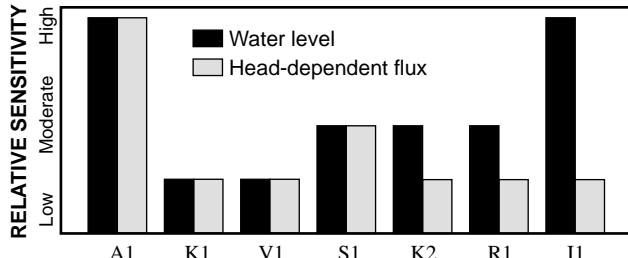


Figure 65. Relative sensitivity of the baseline model of the Gunlock part of the Navajo and Kayenta aquifers to uncertainty in selected properties and flows.

would help identify temporal variations in the potentiometric surface of the aquifers. Long-term water-level trends would help determine whether natural recharge to the aquifers is in balance with well discharge and seepage to the Santa Clara River.

Water-resource management

For the Gunlock part of the Navajo and Kayenta aquifers, the most important hydrologic parameter is the ground-water/surface-water interaction between the Santa Clara River and Navajo aquifer. Interaction is a function of aquifer boundaries and the hydraulic properties of the Navajo aquifer and streambed materials. Effective water-resource management must consider the effects of pumping at the St. George municipal well field on ground-water/surface-water interaction. The baseline model is a tool that can be used to better illustrate the role of pumping on streamflows.

Model Limitations

The ground-water flow model of the Gunlock part of the Navajo and Kayenta aquifers required simplification and, thus, could not accurately represent the actual heterogeneity of the system. Rarely are model simulations in perfect agreement with observations and field measurements. These factors are even more relevant for the baseline model, which, because of limited data, is not calibrated to reproduce a specific set of hydrologic conditions. Also, the model simulates steady-state conditions and does not account for the effects associated with any changes in the amount of

water stored in the aquifers. Although this model simulates the Gunlock aquifers reasonably well, the solution is not unique. Other numerical simulations could yield similar results. Model results should only be used for verifying concepts and indicating generalized effects associated with the hydrologic stresses that are simulated. Results should not be used to evaluate absolute water levels and flows at specific locations. The ability of this model to represent actual ground-water conditions could be better evaluated when additional data are collected and the system is observed under other stress conditions.

A specific limitation of the baseline model concerns flow at specified-flux boundaries. Because the model contains only one head-dependent flux boundary (the Santa Clara River), any change in specified flux will be exactly compensated for at the head-dependent flux boundary. For example, an increase in simulated pumping rates will be compensated for by a net increase in seepage from the Santa Clara River. Pumping cannot be increased beyond the point where seepage from the stream exceeds total streamflow, which is specified at 6.0 ft³/s. Therefore, any increase in pumping rates beyond that will result in the complete dewatering of the model area. Although this is consistent with the conceptual model, it represents a simplification that may not accurately reflect the natural system.

SUMMARY

This study focused on the two main ground-water reservoirs within the central Virgin River basin: the upper Ash Creek basin ground-water system and the Navajo and Kayenta aquifer system. On the basis of measurements, estimates, and numerical simulations of reasonable values for all inflow and outflow components, total water moving through the upper Ash Creek drainage basin ground-water system is estimated to be about 14,000 acre-ft/yr. Recharge to the upper Ash Creek drainage basin ground-water system primarily enters the system as infiltration of precipitation and seepage from ephemeral and perennial streams. The main source of discharge is assumed to be evapotranspiration; however, subsurface discharge near Ash Creek Reservoir also maybe important. The character of two of the hydrologic boundaries of the upper Ash Creek drainage basin ground-water system is speculative. The eastern boundary represented by the Hurricane Fault is assumed to be a no-flow boundary. Likewise, it is assumed that the principal drain for the system is subsurface outflow beneath Ash Creek Reservoir along the

southern boundary. However, these conceptualizations could be incorrect because alternative numerical simulations using different boundary conditions proved to be feasible. Major ion chemistry data from ground- and surface-water along the Ash Creek drainage were analyzed to determine possible sources for Toquerville and Ash Creek Springs. Although additional data are needed, the preliminary analysis indicates that the sources may be Ash Creek Reservoir surface water seeping in and mixing with ground water from the Pine Valley monzonite aquifer, the Navajo aquifer, or upper Ash Creek drainage.

Because of large outcrop exposures, uniform grain size, and large stratigraphic thickness, the Navajo Sandstone and Kayenta Formation receive and store large amounts of water and provide most of the potable water to the municipalities of Washington County. Aquifer tests of the Navajo aquifer indicate that horizontal hydraulic-conductivity values range from 0.2 to 32 ft/d at different locations and may be primarily dependent on the extent of fracturing. The Navajo and Kayenta aquifers are bounded to the south and west by the erosional extent of the formations and to the east by the Hurricane Fault, which completely offsets these formations and is assumed to be a lateral no-flow boundary. Like the Hurricane Fault, the Gunlock Fault is assumed to be a lateral no-flow boundary, dividing the Navajo and Kayenta aquifers within the study area into two parts: the main part, located between the Hurricane and Gunlock Faults; and the Gunlock part, located west of the Gunlock Fault.

Generally, water quality within the Navajo and Kayenta aquifers is very good with respect to dissolved-solids concentration. However, two distinct areas contain water with a dissolved-solids concentration greater than 500 mg/L and water temperatures greater than 20°C: a larger area north of St. George and a smaller area a few miles west of Hurricane. Mass-balance calculations indicate that in the higher dissolved-solids and higher water-temperature area north of St. George, as much as 2.7 ft³/s of hydrothermal water may be entering the aquifer from underlying formations. For the area west of Hurricane, as much as 1.5 ft³/s of hydrothermal water may be entering the aquifer from underlying formations. A relation between higher dissolved-solids concentrations and lighter stable isotopic ratios in these two areas indicates that mixing may be occurring between the upward seepage of hydrothermal water and recharge along the outcrop carrying isotopically light precipitation from the higher-elevation Pine Valley Mountains.

A preliminary investigation of aquifer residence times, based on CFC and radio-isotope techniques, indicates that the time it takes for water to move through the main part of the Navajo and Kayenta aquifers from points of recharge to points of discharge varies from less than 20 years to more than 50 years. However, additional sampling sites, age-dating techniques, and computer particle-tracking analysis are needed to more thoroughly define regional aquifer residence times. Also, CFC data, in combination with major-ion geochemical data, show that the Santa Clara River is likely the main source of recharge to the Gunlock part of the Navajo aquifer in the vicinity of the St. George municipal well field.

On the basis of measurements, estimates, and numerical simulations, total water moving through the Navajo and Kayenta aquifers is estimated to be about 25,000 acre-ft/yr for the main part and 5,000 acre-ft/yr for the Gunlock part. The primary source of recharge is assumed to be infiltration of precipitation in the main part and seepage from the Santa Clara River in the Gunlock part. The primary source of discharge is assumed to be well discharge for both the main and Gunlock parts of the aquifers. Numerical simulations indicate that faults with major offset may impede horizontal ground-water flow. Also, increased horizontal hydraulic conductivity along the orientation of predominant surface fracturing appears to be an important factor in regional ground-water flow. Computer simulations with increased north-south hydraulic conductivity substantially improved the match to measured water levels in the central area of the model between Snow Canyon and Mill Creek.

Numerical simulation of the Gunlock part of the Navajo and Kayenta aquifers, using aquifer properties determined for the St. George municipal well field, resulted in a reasonable representation of regional water levels and estimated seepage to and from the Santa Clara River. Analysis of hydrologic properties and flows indicates that horizontal hydrologic conductivity along the direction of regional fracturing and streambed aquifer properties are important to ground-water flow. Additional data needed to improve the conceptual model of ground-water flow within the Gunlock aquifers include better understanding of flow properties of the Gunlock Fault and better water-level information for areas away from the St. George municipal well field.

REFERENCES

- Anderson, T.W., 1995, Summary of the southwest alluvial basins, Regional Aquifer-System Analysis, south-central Arizona and parts of adjacent states: U.S. Geological Survey Professional Paper 1406-A, 33 p.
- Averitt, P., 1967, Geologic map of the Kanarraville Quadrangle, Iron County, Utah: U.S. Geological Survey Map GQ-694.
- Bjorklund, L.J., Sumsion, C.T., and Sandberg, G.W., 1978, Ground-water resources of the Parowan-Cedar City drainage basin, Iron County, Utah: State of Utah Department of Natural Resources Technical Publication No. 60, 93 p.
- Budding, K.E., and Sommer, S.N., 1986, Low-temperature geothermal assessment of the Santa Clara and Virgin River valleys, Washington County, Utah: Utah Geological and Mineral Survey Special Studies No. 67, 34 p.
- Busenberg, E., and Plummer, L.N., 1992, Use of chlorofluorocarbons (CCl_3F and CCl_2F) as hydrologic tracers and age-dating tools: The alluvium and terrace system of central Oklahoma: Water Resources Research, 28, p. 2257-2883.
- Christensen, R.E., Johnson, E.B., and Plantz, G.G., 1985, Manual for estimating streamflow characteristics of natural-flow streams in the Colorado River Basin in Utah: U.S. Geological Survey Water Resources Investigations Report 85-4297, 39 p.
- Clyde, C.G., 1987, Groundwater Resources of the Virgin River Basin in Utah: State of Utah Department of Natural Resources, Water Resources Draft Report, 97 p.
- Cook, E.F., 1957, Geology of the Pine Valley Mountains, Utah: Utah Geological and Mineralogical Survey Bulletin 58, 111 p.
- Cook, E.F., 1960, Geologic atlas of Utah, Washington County: Utah Geological and Mineralogical Survey Bulletin 70, 124 p.
- Cook, P.G. and Solomon, D.K., 1995, The transport of atmospheric trace gases to the water table: Implications for ground water dating with chlorofluorocarbons and krypton-85: Water Resources Research, 31, p. 263-270.
- Cordova, R.M., Sandberg, G.W., and McConkie, W., 1972, Ground-water conditions in the central Virgin River basin, Utah: State of Utah Department of Natural Resources Technical Publication No. 40, 64 p.
- Cordova, R.M., 1978, Ground-water conditions in the Navajo Sandstone in the central Virgin River basin, Utah: State of Utah Department of Natural Resources Technical Publication No. 61, 66 p.
- Cordy, G.E., Seiler, R.L., and Stolp, B.J., 1993, Hydrology of the L.C. Holding coal-lease tract and adjacent areas, southwestern Utah, and potential effects of coal mining: U.S. Geological Survey Water-Resources Investigations Report 91-4111, 84 p.
- Craig, H., 1961, Isotopic variations on meteoric waters: Science, v. 133, p. 1702-1703.
- Criddle, W.D., Harris, Karl, and Willardson, L.S., 1962, Consumptive use of water requirements for Utah: Utah State Engineer Technical Publication 8 (revised).
- Dettinger, M.D., 1989, Reconnaissance estimates of natural recharge to basins in Nevada, U.S.A., by using chloride-balance calculations: Journal of Hydrology, v. 106, p. 55-78.
- Dincer, T., A. Al-Mugrin, V. Zimmermann, 1974, Study of infiltration and recharge through sand dunes in arid zones with special reference to stable isotopes and thermonuclear tritium: Journal of Hydrology, v. 23, p. 79-109.
- Elkins, J.W., Thompson, T.M., Swanson, T.H., Butler, J.H., Hall, B.D., Cummings, S.O., Fisher, D.A., and Raffo, A.G., 1993, Decrease in growth rates of atmospheric chlorofluorocarbons 11 and 12: Nature, 364, p. 780-783.
- Fenneman, N.M., 1931, Physiography of the Western United States: New York, McGraw-Hill, 534 p.
- Franke, O.L., Reilly, T.E., and Bennett, G.D., 1987, Definition of boundary and initial conditions in the analysis of saturated ground-water flow systems—An introduction: Techniques of Water-Resources Investigations of the U.S. Geological Survey, TWRI Book 3, Chapter B5, 15 p.
- Freeze, R.A., and Cherry, J.A., 1979, Groundwater: New Jersey, Prentice-Hall, Inc., 604 p.
- Gatewood, J.S., Robinson, T.W., Colby, B.R., Hem, J.D., and Halpenny, L.C., 1950, Use of water by bottom-land vegetation in lower Safford Valley, Arizona: U.S. Geological Survey Water-Supply Paper 1103, 210 p.
- Harbaugh, A.W., and McDonald, M.G., 1996, User's documentation for MODFLOW-96, an update to the U.S. Geological Survey modular finite-difference ground-water flow model: U.S. Geological Survey Open-File Report 96-485, 56 p.

- Harrill, J.R., and Prudic, D.E., 1998, Aquifer systems of the Great Basin region of Nevada, Utah, and adjacent states—Summary Report: U.S. Geological Survey Professional Paper 1409-A, 66 p.
- Herbert, L.R., 1995, Seepage study of the Virgin River from Ash Creek to Harrisburg Dome, Washington County, Utah: State of Utah Department of Natural Resources Technical Publication No. 106, 8 p.
- Herbert, L.R., Tibbetts, J.R., Wilberg, D.E., Allen, D.V., and Canny, D.D., 1997, Water Resources Data, Utah, Water Year 1996: U.S. Geological Survey Water-Data Report UT-96-1, 299 p.
- Hershey, Ron, 1989, Hydrogeology and hydrogeochemistry of the Spring Mountains, Clark County, Nevada, Master's thesis, University of Nevada, Las Vegas, Department of Geosciences, 198 p.
- Hill, R.W., 1994, Consumptive use of irrigated crops in Utah: Utah State University/ Utah Agricultural Experiment Station Research Report 145, 361 p.
- Hintze, L.F., and Hammond, B.J., 1994, Geologic map of the Shivwits Quadrangle, Washington County, Utah: Utah Geological Survey Map 153.
- Hood, J.W., and Waddell, K.M., 1968, Hydrologic reconnaissance of Skull Valley, Tooele County, Utah: State of Utah Department of Natural Resources Technical Publication No. 18, 54 p.
- Hurlow, H.A., 1998, The geology of the central Virgin River Basin, southwestern Utah, and its relation to ground-water conditions, Utah Geological Survey Water-Resources Bulletin 26, 53 p.
- Jensen, M.E., Lowe, M. and Wireman, M., 1997, Investigation of hydrogeologic mapping to delineate protection zones around springs: Report of two case studies: U.S. Environmental Protection Agency Report 600/R-97/023, 60 p.
- Lehmann, B.E., Davis, S.N., and Fabryka-Martin, J.T., 1993, Atmospheric and subsurface sources of stable and radioactive nuclides used for groundwater dating, Water Resources Research 29, p. 2027-2040.
- Lohman, S.W., 1979, Ground-water hydraulics: U.S. Geological Survey Professional Paper 708, 70 p.
- Lovelock, J.E., 1971, Atmospheric fluorine compounds as indicators of air movements, Nature, 230, p. 379.
- Maxey, G.B., and Eakin, T.E., 1949, Ground water in White River Valley, White Pine, Nye, and Lincoln Counties, Utah: Nevada State Engineer Water Resources Bulletin 8, 59 p.
- Mazor, 1991
- McDonald, M.G., and Harbaugh, A.W., 1988, A modular three-dimensional finite-difference ground-water flow model: Techniques of Water-Resources Investigations of the U.S. Geological Survey, Chapter A-1, Book 6, Modeling Techniques.
- Mower, R.W., and Sandberg, G.W., 1982, Hydrology of the Beryl-Enterprise area, Escalante Desert, Utah, with emphasis on ground water: State of Utah Department of Natural Resources Technical Publication No. 73, 66 p.
- Muckel, D.C., and Blaney, H.F., 1945, Utilization of the waters of the lower San Luis Rey Valley, San Diego County, California: U.S. Department of Agriculture, Soil Conservation Service.
- Parker, J.T. and Pool, D.R., 1998, Use of microgravity to assess the affects of El Nino on ground-water storage in southern Arizona, U.S. Geological Survey Fact Sheet 060-98.
- Plummer, L.N., Michel, R.L., Thurman, E.M., and Glynn, P.D., 1993, Environmental tracers for age-dating young groundwater, *in* regional groundwater quality, Van Nostrand Reinhold, New York, N.Y., p. 255-294.
- Prudic, D.E., 1989, Documentation of a computer program to simulate stream-aquifer relations using a modular, finite-difference, ground-water flow model: U.S. Geological Survey Open-File Report 88-729, 113 p.
- Pruess, 1998, On water seepage and fast preferential flow in heterogeneous, unsaturated rock fractures: Journal of Contaminant Hydrology, v. 30, p. 333-362.
- ReMillard, M.D., Anderson, G.C., Hookano, E., and Sandberg, G.W., 1982, Water resources data, Utah, Water Year 1982, U.S. Geological Survey Water-Data Report UT-82-1, 497 p.
- Robinson, T.W., 1958, Phreatophytes: U.S. Geological Survey Water-Supply Paper 1423, 84 p.
- Rowland, F. S. and Molina, M.J., 1975, Chlorofluoromethanes in the environment, *in* Review of Geophysics and Space Physics, 13, p. 1-35.
- Russell, A.D., and Thompson, G.M., 1983, Mechanisms leading to enrichment of the atmospheric fluorocarbons CCL_3F and CCl_2F_2 in groundwater, Water Resources Research, 19, p. 57-60.
- Scanlon, B.R., 1992, Evaluation of liquid and vapor water flow in desert soils based on chlorine 36 and tritium tracers and nonisothermal flow simulations: Water Resources Research, v. 28, no. 1, p. 285-297.

- Spangler, L.E., Naftz, D.L., and Peterman Z.E., 1996, Hydrology, chemical quality, and characterization of salinity in the Navajo aquifer in and near the greater Aneth oil field, San Juan County, Utah, U.S. Geological Survey Water-Resources Investigations Report 96-4155, 90 p.
- Susong, D.D., 1995, Water budget and simulation of one-dimensional unsaturated flow for a flood- and a sprinkler-irrigated field near Milford, Utah: U.S. Geological Survey Water-Resources Investigations Report 95-4072, 32 p.
- Thiros, S.A., and Brothers, W.C., 1993, Ground-water hydrology of the upper Sevier River basin, south-central Utah, and simulation of ground-water flow in the valley fill aquifer in Panguitch Valley: State of Utah Department of Natural Resources Technical Publication No. 102, 121 p.
- Thomas, H.E., and Taylor, G.H., 1946, Geology and ground-water resources of Cedar City and Parowan Valleys, Iron County, Utah: U.S. Geological Survey Water-Supply Paper 993, 210 p.
- Utah Climate Center, 1996, 1961-90 normal precipitation contours: Utah State University, Logan, Utah.
- Van Kooten, G.K., 1988, Structure and hydrocarbon potential beneath the Iron Springs laccolith, southwestern Utah: Geological Society of America Bulletin, v. 100, p. 1533-1540.
- Weigel, J.F., 1987, Selected hydrologic and physical properties of Mesozoic formations in the Upper Colorado River Basin in Arizona, Colorado, Utah, and Wyoming--excluding the San Juan Basin: U.S. Geological Survey Water-Resources Investigations Report 86-4170, 68 p.
- Welch, A.H., and Preissler, A.M., 1986, Aqueous geochemistry of the Bradys Hot Springs geothermal area, Churchill County, Nevada, in Selected Papers in the Hydrologic Sciences: U.S. Geological Survey Water-Supply Paper 2290, p. 17-36.
- Wilkowske, C.D., Heilweil, V.M., and Wilberg, D.E., 1998, Selected hydrologic data for the central Virgin River basin area, Washington and Iron Counties, Utah, 1915-97, U.S. Geological Survey Open-File Report 98-389, 53 p.

APPENDICES

Appendix A

Results of aquifer testing within the study area

AQUIFER TEST ANALYSES

As part of this study, aquifer tests were done to evaluate the hydraulic properties of the Navajo Sandstone aquifer and the Pine Valley monzonite aquifer. Four aquifer tests were done in the Navajo Sandstone and one aquifer test was done in the Pine Valley monzonite. The locations of these five tests are shown in figure A-1.

Hurricane Bench Aquifer Test

The purpose of the Hurricane Bench aquifer test was to determine the transmissivity and storage properties of the Navajo aquifer about 5 mi southwest of Hurricane, Washington County, Utah (fig. A-2). The aquifer test was conducted in January and February 1996 by the USGS in coordination with the Winding Rivers Corpo-

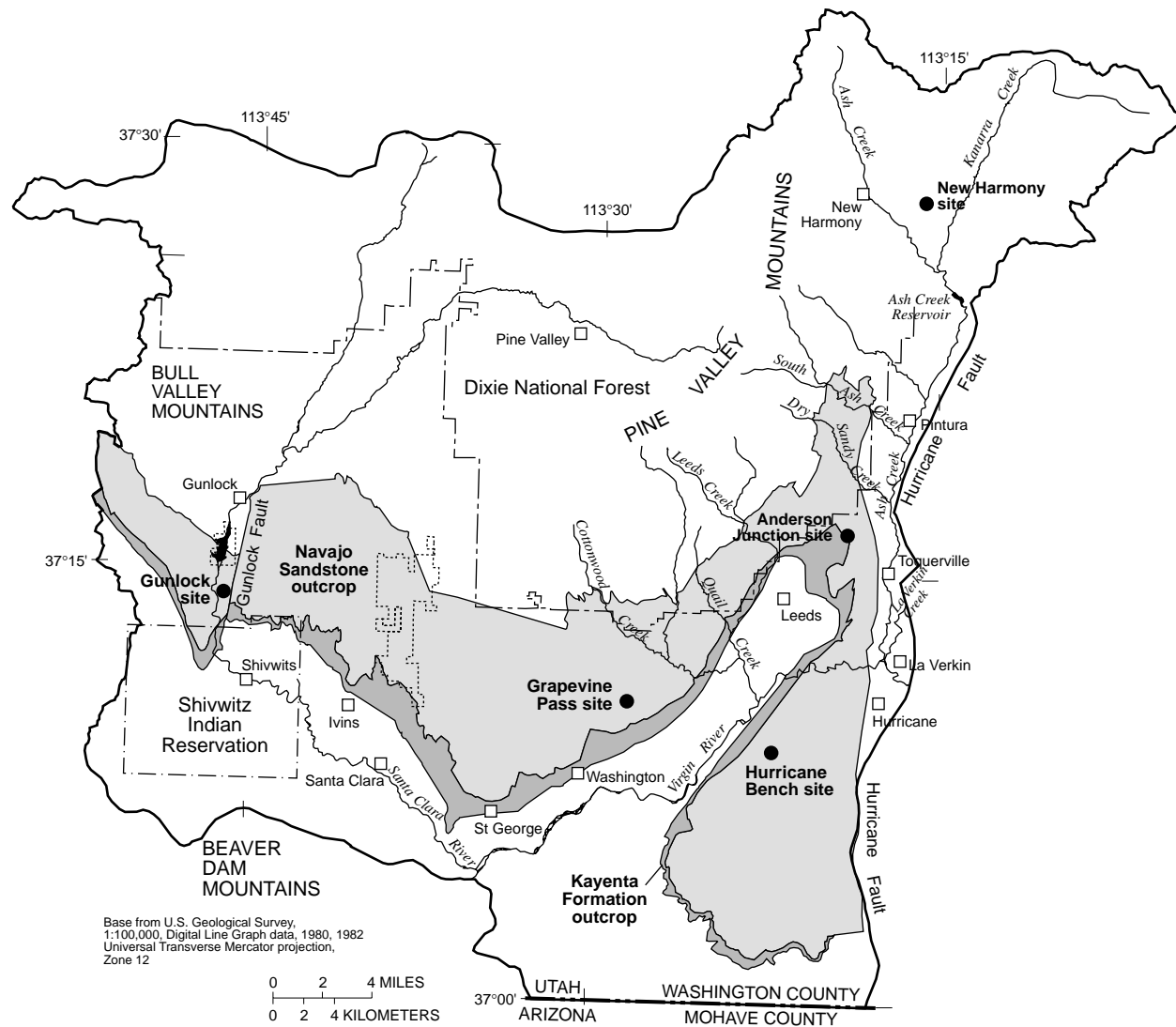


Figure A-1. Location of aquifer-test sites within the central Virgin River basin study area, Washington County, Utah, 1996.

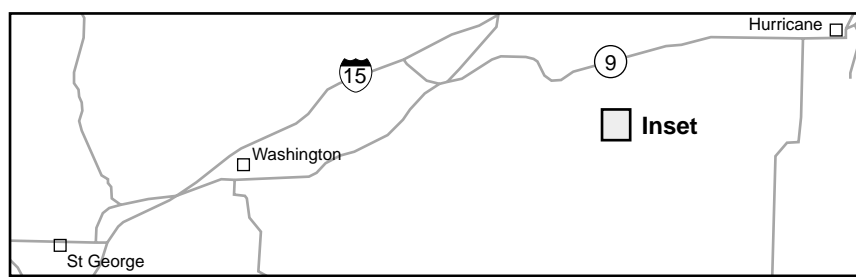
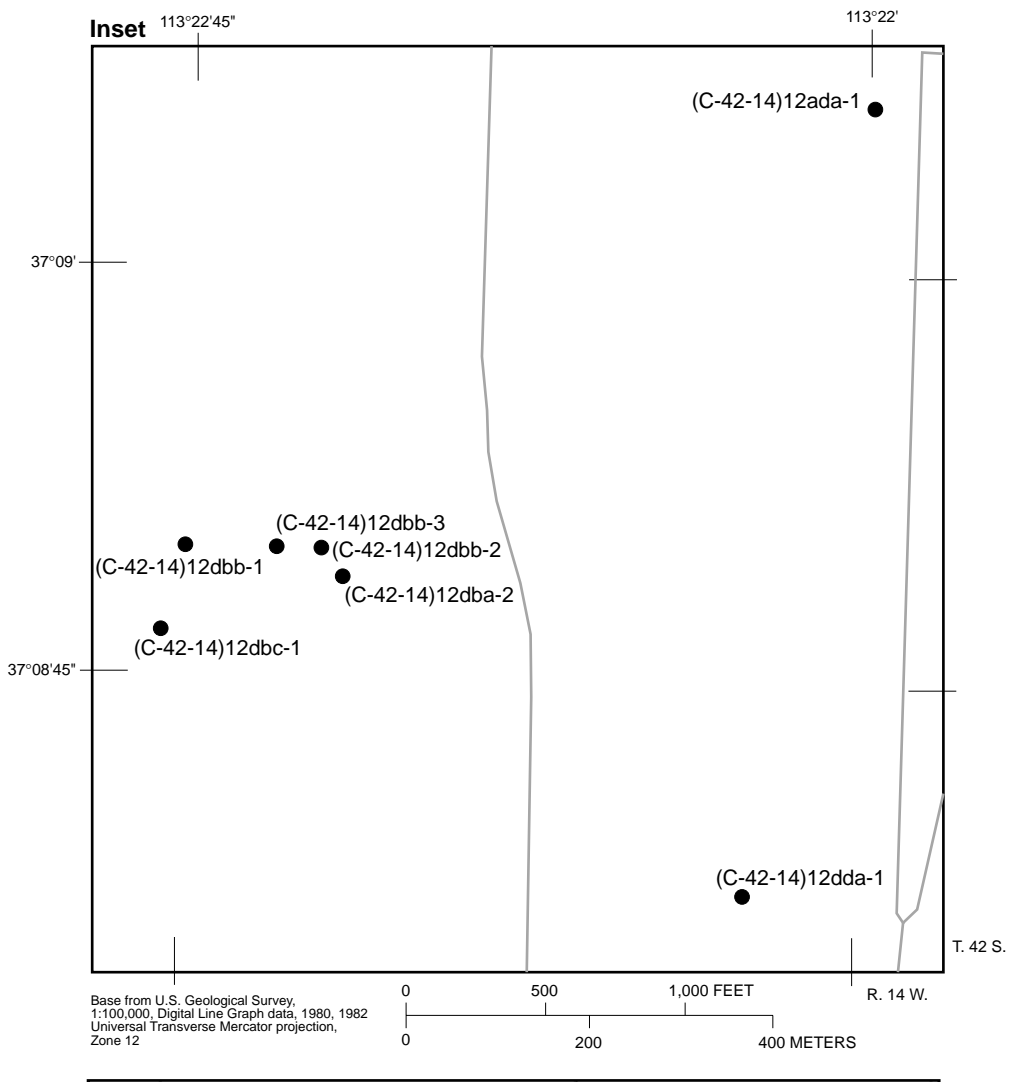


Figure A-2. Location of wells in the Hurricane Bench aquifer test, Washington County, Utah, January and February 1996.

ration. The multiple-well aquifer test involved pumping well (C-42-14)12dbb-2 at a rate of about 330 gal/min for almost 5 days. The discharge from the pumped well was diverted into an irrigation pipe, which transported the water more than 1 mi away from the well, where it was applied as irrigation water via sprinklers. Discharge was measured with a Clampatron flow meter, which was field checked by capturing discharge from one of the irrigation sprinkler nozzles and multiplying this by the total number of active nozzles. Because of problems with the circuit breaker controlling the submersible pump, some pumping occurred during the 2 days prior to the aquifer test. Therefore, only data from the recovery part of this aquifer test were analyzed.

Analysis of geologic maps and drillers' logs indicates that the Navajo Sandstone aquifer is areally extensive at the aquifer-test site and is underlain by the less permeable Kayenta Formation. Information from the drillers' log of well (C-42-13)7bcc-3 (0.45 mi from the pumping well) indicates that sandstone was found from 12 to 1,450 ft below land surface; and alternating siltstone and sandstone layers characteristic of the Kayenta Formation were found from 1,450 ft to 1,860 ft. Because of the shallow dip of the Navajo Sandstone to the northeast and the average prepumping depth to water of about 60 ft, the average saturated thickness of the Navajo aquifer at the aquifer-test site was assumed to be about 1,350 ft. According to a recent Utah Geological Survey fracture study of a nearby Navajo outcrop on Sand Mountain (about 3 1/2 mi to the south), the predominant fracture direction is northeast-southwest and the secondary direction is east-west.

Water levels were measured in six observation wells and the pumped well for 6 days preceding the test,

during the 7 days of pumping, and for 6 days after the pump was shut off. Data for the pumped well and observation wells are recorded in table A-1. Drawdown and recovery of sufficient magnitude to analyze were observed in five of the six observation wells. There was no noticeable drawdown or recovery at the observation well farthest from the pumped well, (C-42-14)12ada-1. All of the observation wells are finished in the Navajo Sandstone aquifer. The two observation wells nearest the pumped well have similar perforation intervals to the pumped well. The four observation wells farther away generally are open to the aquifer at shallower depths than the pumped well.

The measured water levels at five observation wells were corrected for barometric changes assuming 100 percent barometric efficiency. This barometric efficiency was chosen on the basis of observations of prepumping water-level changes at observation well (C-42-14)12dba-2 as a result of changes in barometric pressure. The 100-percent correction was verified by a comparison of the effects on water levels of barometric efficiencies ranging from 50 to 100 percent. Barometric data from a mercury barometer located at the Cedar City Airport, about 30 mi to the north, was used for this correction.

As mentioned above, only the recovery data from the aquifer test was analyzed. Because water levels in the affected observation wells did not reach a pumping equilibrium before the pump was shut off, the recovery data were affected by residual drawdown and trend corrections to the recovery data were necessary. Straight-line fits to semilogarithmic plots of the water levels in the observation wells during drawdown were used for determining the prerecovery trend. This prerecovery

Table A-1. Construction data for the wells used in the Hurricane Bench aquifer test, Washington County, Utah

[N/A, not applicable]

Well number	Radial distance (feet)	Casing diameter (inches to feet)	Open interval (feet below land surface)	Opening type
(C-42-14)12dbb-2	N/A	12 to 560	62 - 560	Screen
(C-42-14)12dba-2	34	12 to 510	120 - 510	Perforations
(C-42-14)12dbb-3	106	12 to 510	58 - 510	Screen
(C-42-14)12dbb-1	475	12 to 23	23 - 140	Open hole
(C-42-14)12dbc-1	590	10 to 100	100 - 270	Open hole
(C-42-14)12dda-1	1,665	12 to 40	40 - 425	Open hole
(C-42-14)12ada-1	2,500	12 to 300	101 - 300	Open hole

trend was extended through the recovery part of the aquifer test to correct for this trend.

Recovery data for the observation wells were initially plotted together by dividing time in elapsed minutes by the observation well's radial distance squared. However, recovery data from the closest observation well, (C-42-14)12dba-2, were eliminated from the analysis because its initially steep response is assumed to be affected by well-bore storage because its proximity to the pumping well (34 ft) and its large borehole size (12-in. diameter). Also, the maximum drawdown and recovery at this observation well were a substantial part of the saturated thickness of the aquifer and would cause the transmissivity to change during the aquifer test. Recovery data from observation well (C-42-14)12dda-1 were also eliminated because the barometric pressure and prerecovery-trend corrections were a substantial part of the recovery (as much as 0.5 ft of the total 1.6 ft of recovery) and could have introduced error into the analysis. Therefore, only recovery data from observation wells (C-42-14)12dbb-3, (C-42-14)12dbb-1, and (C-42-14)12dbc-1, were analyzed. Because the maximum 50-ft drawdown and recovery measured at the closest of the three wells, (C-42-14)12dbb-3, was less than 4 percent of the saturated thickness, changes in transmissivity with change in the saturated thickness of the aquifer were not substantial at these three observation wells. Because these three observation wells are all at a similar radial orientation with respect to the pumping well, the degree of horizontal anisotropy resulting from fractures within the sandstone could not be evaluated.

The Theis solution (1935) for confined aquifers was first chosen for the analysis. The aquifer is assumed to act as confined, as indicated by (1) the high barometric efficiency observed at well (C-42-14)12dba-2, and (2) drillers' logs for wells (C-42-14)12dbb-1 and (C-42-14)12dda-1, drilled with a cable-tool rig, both indicate that water was initially encountered deeper (12 ft and 6 ft, respectively) than the static water levels later measured in the wells. The Theis method assumes that water is released instantaneously from storage with a decline of hydraulic head. However, scatter in the composite plot of recovery versus time for these three observation wells indicated that well responses varied substantially from the Theis-type response. Calculations of transmissivity and storage values for the individual observation wells were also determined from separate time-recovery plots for each well, either using the Cooper-Jacob solution (Cooper and Jacob, 1946) or the Theis solution. These calculations show generally

higher values of transmissivity with increased distance from the pumped well. Assuming that the Navajo aquifer in this region is fairly homogeneous, this apparent increase in transmissivity with radial distance may indicate the effects of leakage or delayed yield. Also, the confined-type response to barometric pressure changes may only indicate the aquifer's confined response to small stresses; larger stresses may result in dewatering and a conversion to an unconfined aquifer response at closer observation wells.

Therefore, the recovery data were reanalyzed with the modified Hantush solution (Lohman, 1972, p. 32-34) for leaky confined aquifers with vertical movement. This solution provided the best fit to the composite plot of recovery data from the three observation wells (fig. A-3). This method was chosen because of the possibility that the underlying Kayenta Formation may act as a low-permeability layer and release a relatively large amount of water from storage as a result of pumping in the overlying Navajo aquifer. Hydraulic conductivity can be calculated by dividing transmissivity either by saturated thickness of the aquifer by the saturated thickness of the perforated interval of the production well. Transmissivity and storage-coefficient values calculated with this method are $1,075 \text{ ft}^2/\text{d}$ and 0.002, respectively. Assuming an average saturated aquifer thickness of 1,350 ft, the calculated hydraulic conductivity is 0.8 ft/day. This hydraulic conductivity value of 0.8 ft/d is smaller than the average value of 2.1 ft/day determined from laboratory analyses of outcrop samples of the Navajo Sandstone (Cordova, 1978). However, dividing the transmissivity by the 500-ft perforated interval of the production well results in a hydraulic conductivity of 2.2 ft/day, which is similar to the average value. This larger value is preferred because it is likely that small bedding plane features, such as thin, finer-grained layers formed during sand-dune deposition, reduce vertical hydraulic conductivity and vertical flow to the well from the deeper, unpenetrated part of the aquifer.

Anderson Junction Aquifer Test

The purpose of the Anderson Junction aquifer test was to determine the transmissivity and storage properties of the Navajo aquifer near Anderson Junction in Washington County, Utah (fig. A-4). The aquifer test was conducted in March and April 1996 by the USGS in coordination with the Washington County Water Conservancy District. The multiple-well aquifer

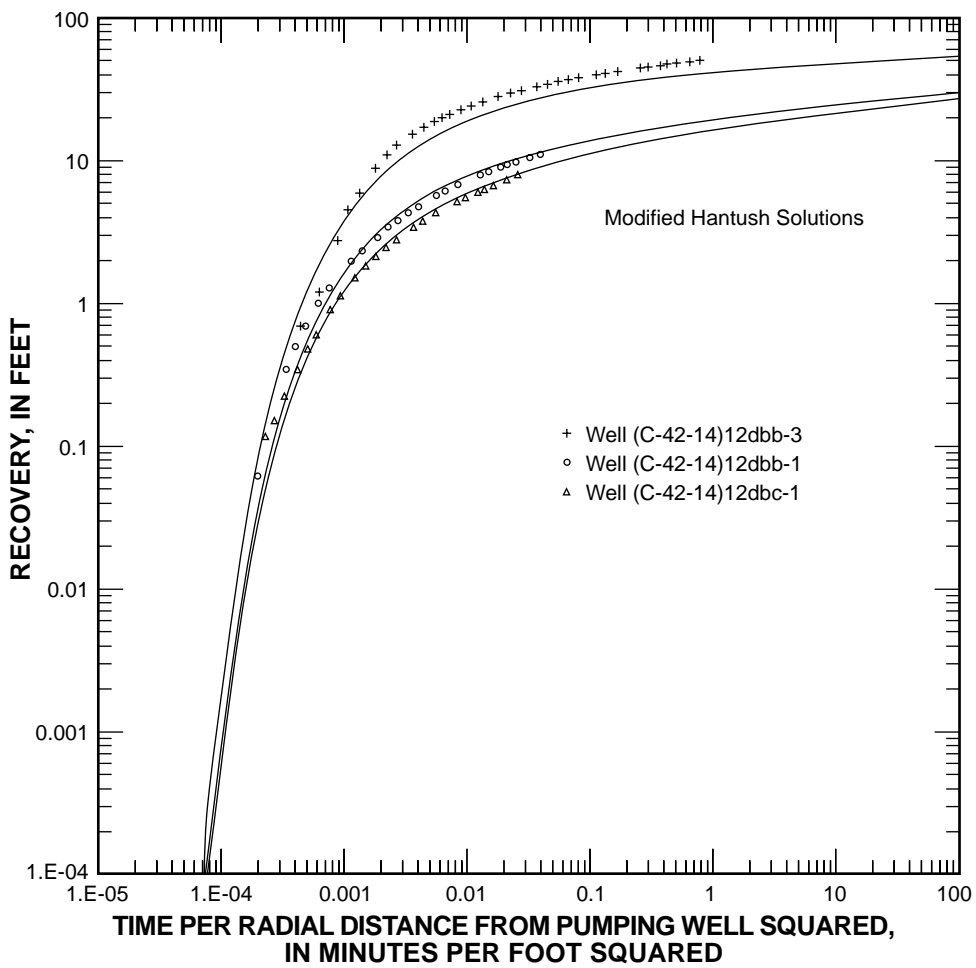


Figure A-3. Recovery data from wells during the Hurricane Bench aquifer test, Washington County, Utah, January and February 1996 (modified Hantush solution (Lohman, 1972)).

test involved pumping at well (C-40-13)28dcb-2 for about 4 days at an average rate of 1,100 gal/min. Discharge was measured with a pito tube, v-notch weir, and pygmy meter. The discharge from the production well was diverted into a 15-in. diameter ABS drain pipe, which transported the water 500 ft away from the well to a natural dry wash heading southeast under Highway I-15. Water levels were measured in three observation wells and the production well, (C-40-13)28dcb-2, for 4 days prior to the test, during the 4 days of pumping, and for as many as 20 days after the pump was shut off.

The aquifer-test site is in a highly fractured region of the Navajo Sandstone outcrop that has two predominant clusters of fracturing at orientations of 180 to 210 degrees and 90 to 130 degrees (Hurlow, 1998). On the basis of the Utah Geological Survey's fracture study, two observation wells were drilled spe-

cifically for the aquifer test at approximately the same radial distance from the pumped well, but at perpendicular orientations. Well (C-40-13)28dca-1, herein referred to as well A, is located 383 ft east-southeast of the production well along a 110-degree orientation (parallel to the 90 to 130 azimuthal cluster of fractures). Well (C-40-13)28dcc-1, herein referred to as well B, is located 376 ft south-southwest of the production well along a 200-degree orientation (parallel to the 180 to 210 degree azimuthal cluster of fractures). Well (C-40-13)28dcb-1, herein referred to as the original well, is located 10 ft due east of the pumped well. Data for the pumped well and observation wells are recorded in table A-2.

According to conversations with the driller and information from the drillers' logs, the Navajo Sandstone aquifer. Because wells A and B were both drilled by using the reverse rotary method with air, the driller

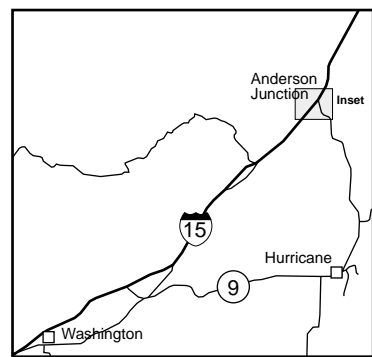
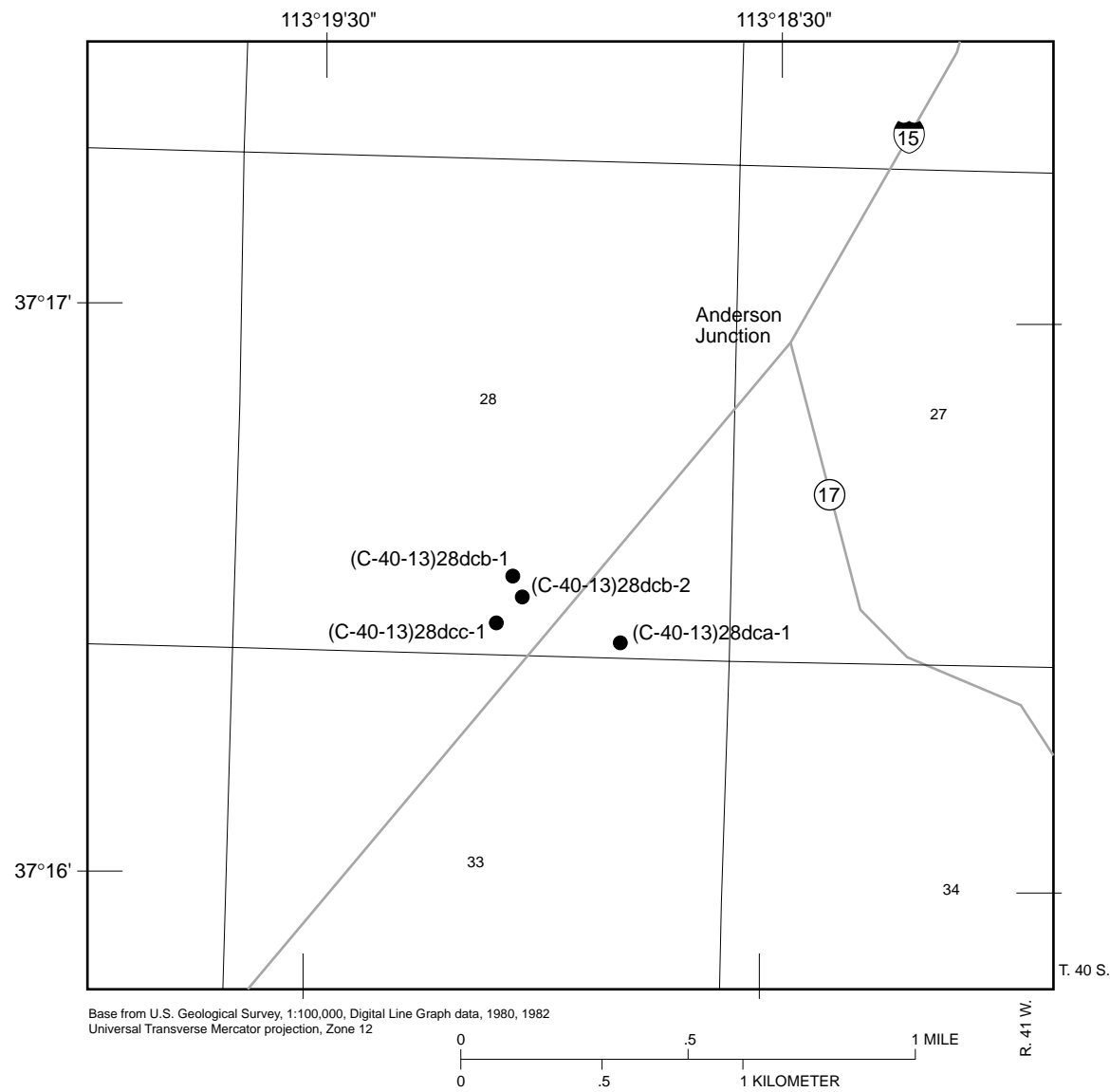


Figure A-4. Location of wells in the Anderson Junction aquifer test, Washington County, Utah, March and April 1996.

Table A-2. Construction data for the wells used in the Anderson Junction aquifer test, Washington County, Utah

Well name	Well number	Radial distance (feet)	Casing diameter (inches to feet)	Open interval (feet below land surface)	Opening type
Pumped well	(C-40-13)28dcb-2	0	16 to 500	110 - 470	Screen
Original well	(C-40-13)28dcb-1	10	6 to 225	160 - 225	Perforations
Well B	(C-40-13)28dcc-1	376	5 to 400	160 - 380	Perforations
Well A	(C-40-13)28dca-1	383	5 to 400	160 - 380	Perforations

could readily identify when the water table was reached (the pumped well was drilled with water, so such a determination could not be made). According to the driller, water was found in well B at a depth of 190 ft and afterwards rose in the casing to a depth of 31 ft. In well A, water was found at a depth of 56 ft and rose in the casing to a depth of 21 ft. The potentiometric surface is nearly flat between the two wells. According to the drillers' logs, the lithology causing the confined conditions is different at two of the observation wells. At well B, vertical anisotropy within the Navajo Sandstone (possibly as a result of grain alignment, cementation, or finer sediments) appears to cause the confined conditions. At well A, the confined conditions are probably caused by a poorly permeable layer of clays, silts, and sands in the unconsolidated alluvium overlying the Navajo Sandstone.

Measured water levels at the observation wells were not corrected for barometric changes because the magnitude of drawdown and recovery at all of the wells was much larger (19 to 80 ft) than the effects of barometric changes (generally less than 1 ft). Prepumping trend corrections were applied to all of the observation-well drawdown data because of a rise in water levels resulting from recovery after the development of the production well shortly before the aquifer test. Prerecovery trend corrections were applied to the observation-well recovery data because water levels did not reach a pumping equilibrium before the pumping well was shut off on March 22, 1996.

The drawdown and recovery data for the three observation wells were initially plotted together on log-log scale by dividing time by the observation well's radial distance squared. The drawdown and recovery data from the closest observation well (original well) were eliminated from the analysis because of delayed response in early time data caused by well-bore storage effects resulting from proximity to the pumped well and

large borehole size. Also, the maximum drawdown and recovery at this observation well (as much as 80 ft) made up a substantial part of the saturated thickness of the aquifer and would result in a substantial change in transmissivity during the aquifer test.

The data sets from the remaining two observation wells (wells A and B) were analyzed with three curve-matching solutions: (1) the Theis solution (1935) for confined aquifers, (2) the modified Hantush solution (Lohman, 1972, p. 32-34) for leaky confined aquifers with vertical movement, and (3) the Neuman solution (1974) for unconfined aquifers with delayed yield. None of these type curves fit both sets of data, indicating that the previously mentioned methods might not be applicable. In particular, the assumption of isotropy in the three methods is questionable. The presence of anisotropy at the Anderson Junction test site is indicated by the large difference in observed drawdown at the two observation wells: 33 feet at well A aligned with the 110-degree fracture orientation, and 19 ft at well B aligned with the 200-degree fracture orientation. These observations are consistent with a fractured anisotropic aquifer.

Therefore, a modified (simplified) version of a method presented by Papadopoulos (1965) for data analysis from a homogeneous and anisotropic aquifer was used. The Papadopoulos method assumes that the orientations of the principal axes directions for the transmissivity tensor are unknown. For the Anderson Junction aquifer test, the assumption is made that the two observation wells in the 110-degree and 200-degree orientations are parallel to the two principal axes.

Theory

The modification to the Papadopoulos method was developed by Dr. Paul Hsieh of the USGS (written commun., 1997). Assuming that observation wells A

and B are located along the maximum and minimum principal axes directions in an orthogonal orientation with respect to each other and the pumping well (fig. A-5), the drawdown in the observation wells are given by Papadopoulos (1965, eq. 15 and 16):

$$s(x, y, t) = \frac{Q}{4\pi\sqrt{T_{xx}T_{yy}}} \cdot W(u_{xy}) \quad (\text{A6})$$

with

$$u_{xy} = \frac{S}{4t} \cdot \left(\frac{T_{xx}y^2 + T_{yy}x^2}{T_{xx}T_{yy}} \right) \quad (\text{A7})$$

where s is drawdown,

Q is pumping rate,

T_{xx} and T_{yy} are the transmissivities along principal axes,

S is aquifer storage,

t is time, and

$W(u_{xy})$ is the well function of u_{xy} .

Note that x and y here stand for ξ and η as described by Papadopoulos (1965).

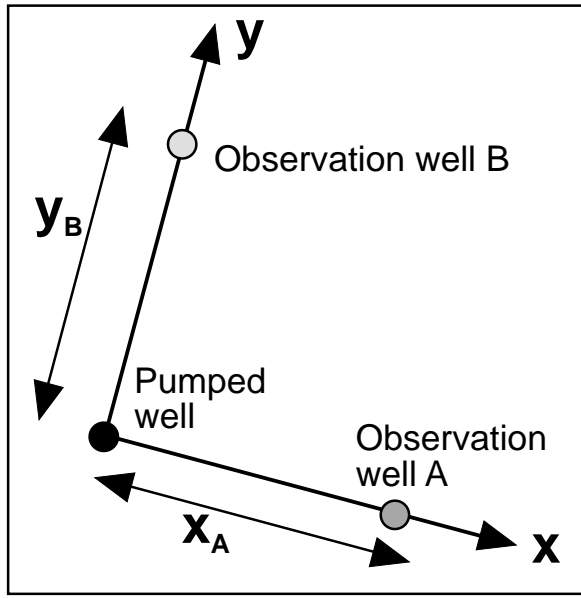


Figure A-5. Well-location geometry needed for applying modified version of Papadopoulos solution (1965).

Applying the preceding solution to observation well A, which is located at $x = x_A$, $y = 0$ yields:

$$s(x_A, 0, t) = \frac{Q}{4\pi\sqrt{T_{xx}T_{yy}}} \cdot W\left(\frac{Sx_A^2}{4T_{xx}t}\right) \quad (\text{A8})$$

In comparing this equation to the Theis solution:

$$s(r, t) = \frac{Q}{4\pi T} \cdot W\left(\frac{Sr^2}{4Tt}\right) \quad (\text{A9})$$

the analogies are: T of the Theis equation is substituted with $\sqrt{T_{xx}T_{yy}}$, S/T of the Theis solution is substituted with S/T_{xx} , and r of the Theis equation is substituted with x_A . This analogy can be extended to the Cooper-Jacob straight-line method (Cooper and Jacob, 1946), which also can be modified for anisotropic conditions. Under ideal conditions in an anisotropic aquifer, Papadopoulos shows that the straight-line parts of all observation well data on a semilog plot should have the same slope under ideal homogeneous conditions, so that the intercepts would yield T_{xx} greater than T_{yy} (fig. A-6). In the Cooper-Jacob method, the slope of the late time (straight-line part) data yields transmissivity from the determination of the change in drawdown per log cycle (Δs), and the intercept gives S/T , and thus S . Substituting $\sqrt{T_{xx}T_{yy}}$ for T yields the following equation modified from the Cooper-Jacob method, equations 5 and 6:

$$\sqrt{T_{xx}T_{yy}} = \frac{264(Q)}{(\Delta s)(7.48)} \quad (\text{A10})$$

for T in ft^2/d , Q in gallons per minute, and Δs in feet. Likewise, substituting T_{xx}/S for T/S yields the following equation modified from the Cooper-Jacob method:

$$\frac{S}{T_{xx}} = \frac{2.25t_{0a}}{[r_a]^2} \quad (\text{A11})$$

where t_{0a} is the x-intercept (time) for well A, and r_a is the radial distance to well A.

Next, applying the anisotropic solution to observation well B, which is located at $x = 0$, $y = y_B$, yields:

$$s(0, y_B, t) = \frac{Q}{4\pi\sqrt{T_{xx}T_{yy}}} \cdot W\left[\frac{Sy_B^2}{4T_{yy}t}\right] \quad (\text{A12})$$

where $\sqrt{T_{xx}T_{yy}}$ is like T of Theis, S/T_{yy} is like S/T of Theis, and y_B is like r of Theis. After plotting the data from observation well B on semilog paper, the straight-line parts fitted to the data must have the same slope (and Δs) as the observation well A data set. This ensures that $T_{xx}T_{yy}$ computed from observation well B

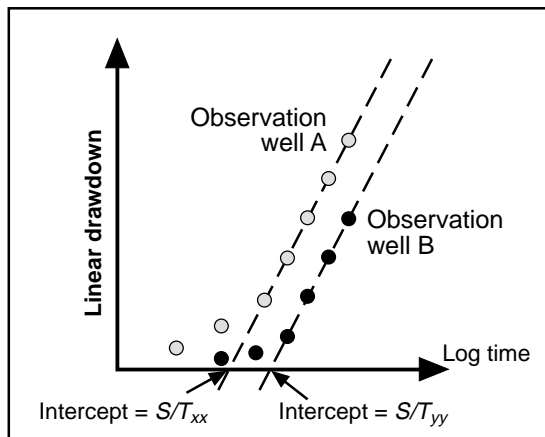


Figure A-6. Idealized data set for an anisotropic and homogeneous aquifer.

data is equal to $T_{xx}T_{yy}$ computed from observation well A data. By the same reasoning as above, substituting T_{yy}/S for T/S yields the following equation modified from the Cooper-Jacob method (Cooper and Jacob, 1946, eq. 8):

$$\frac{S}{T_{yy}} = \frac{2.25t_{0b}}{[r_b]^2} \quad (\text{A13})$$

where t_{0b} is the x-intercept (time) for well B, and r_b is the radial distance to well B.

In summary, the above straight-line fits to the observation well A and B data sets on a semilog graph should yield $\sqrt{T_{xx}T_{yy}}$ (the value from each of the data sets should be the same), S/T_{xx} , and S/T_{yy} . The following procedure can be used to determine T_{xx} , T_{yy} , and S separately:

1. Square the $\sqrt{T_{xx}T_{yy}}$ to obtain $T_{xx}T_{yy}$
2. Multiply S/T_{xx} and S/T_{yy} to obtain $S^2/(T_{xx}T_{yy})$
3. Multiply the result from steps 1 and 2 above to get S .
4. Divide the S obtained from Step 3 by S/T_{xx} to get T_{xx} .
5. Divide the S obtained from Step 3 by S/T_{yy} to get T_{yy} .

T_{xx} is known as the “principal transmissivity in the direction of the x axis.” T_{yy} is known as the “principal transmissivity in the direction of the y axis.” If T_{xx} is greater than T_{yy} , then the x axis points along the major principal direction, and the y axis points along the minor principal direction. If T_{yy} is greater than T_{xx} , then the y axis points along the major principal direction, and the x axis points along the minor principal

direction. Therefore, it is not necessary (nor warranted) to assume which is the major and which is the minor principal direction at the start of the analysis.

Application

With this modified version of the Papadopoulos method, the corrected recovery data for both the south and east observation wells are plotted on a semilog graph. In an ideal homogeneous anisotropic aquifer, the slopes of observation-well data sets should be the same. However, unlike the ideal case, the slopes of the straight-line parts of the two observation-well data sets for this aquifer test are not identical (fig. A-7). With these two unequal slopes, the square root of $T_{xx}T_{yy}$ computed from well A does not equal that computed from well B. This indicates that the aquifer is not completely homogeneous at this site. Nonetheless, because the late-time data of each plot are similar and approach straight lines, the same slope was fitted to each data set. By forcing both lines to have the same slope the product of $T_{xx}T_{yy}$ from both wells is the same and the data can be interpreted using a homogeneous anisotropic aquifer model.

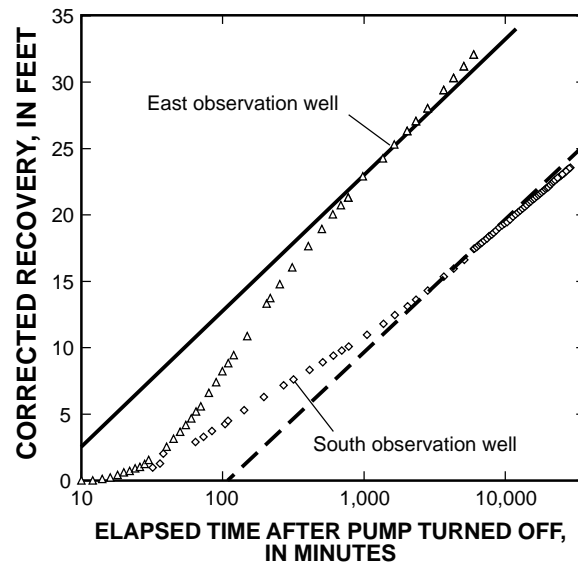


Figure A-7. Recovery data from wells during the Anderson Junction aquifer test, Washington County, Utah, March and April 1996.

The two fitted lines in figure A-7 have equal slopes (Δs) of 10 ft of drawdown per log cycle of time. Substituting these values into the Cooper-Jacob equation (5) where $Q = 1,100$ gal/min yields the relation:

$$\sqrt{T_{xx}T_{yy}} = 3,880 \left(\frac{ft^2}{d} \right) \quad (A14)$$

Also from figure A-7, the x-intercept on the semi-log plot for the well A recovery data is 5.5 minutes (0.0038 days); the x-intercept on the semi-log plot for the well B recovery data is 110.0 minutes (0.0764 days). Substituting the radial distance (r_a) to well A is 383 ft, and the radial distance (r_b) to well B is 376 ft into equations (6) and (8) yields:

$$\frac{S}{T_{xx}} = 5.829 \times 10^{-8} \quad \frac{S}{T_{yy}} = 1.216 \times 10^{-6} \quad (A15)$$

Solving these three relation simultaneously yields $T_{xx} \approx 18,000 \text{ ft}^2/\text{d}$, $T_{yy} \approx 900 \text{ ft}^2/\text{d}$, and $S \approx 0.001$.

However, because heterogeneities within the Navajo aquifer at Anderson Junction do not permit a unique equal-slope fit to the semilog plot of observation-well data from wells A and B, an analysis of the possible range of values is necessary. To determine the maximum amount of interpretative error that may introduced by "forcing" lines of equal slope to both observation-well data sets, the steepest and shallowest possible fitted slopes are shown in figure A-8. The steepest possible slope for the two data sets corresponds to the best fit for the well A data set. The shallowest possible slope for the two data sets corresponds to the best fit for the well B data set. On the basis of these alternative slopes and x-intercepts, the range of values for T_{xx} ranges from 15,000 to 22,500 ft^2/d , T_{yy} from 650 to 900 ft^2/d , and S from 0.0007 to 0.0025. Therefore, the average of the maximum and minimum possible values for the transmissivity and storage from the Anderson Junction aquifer test, including error brackets, is $T_{xx} \approx 19,000 \text{ ft}^2/\text{d} \pm 21\%$, $T_{yy} \approx 800 \text{ ft}^2/\text{d} \pm 19\%$, and $S \approx 0.0013 \pm 1/4 \log$ cycle. This indicates that the ratio of transmissivity (anisotropy factor) in the 110-degree and 200-degree orientations is about 24:1, but could range from 23:1 to 25:1, depending on the fitted slope. With an assumed aquifer thickness of 600 ft, horizontal hydraulic conductivity ranges from about 32 ft/d in the 110-degree orientation to 1.3 ft/d in the 200-degree orientation.

The range of hydraulic-conductivity values determined from this aquifer-test analysis is generally larger than Cordova's (1978, p. 26) laboratory determination of horizontal hydraulic-conductivity values that ranged from 0.36 to 5.0 ft/d . However, the laboratory-determined values do not include the effects of open fractures or other secondary openings that would increase the actual in-situ hydraulic conductivity.

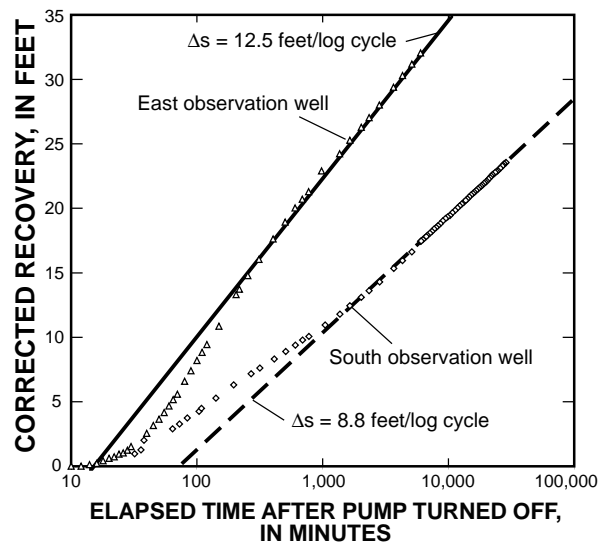


Figure A-8. Recovery data for wells during the Anderson Junction aquifer test showing range of possible slope, Washington County, Utah, March and April 1996.

Therefore, the Anderson Junction aquifer-test data may indicate that along the minor principal direction (200-degree orientation), the hydraulic-conductivity value of 1.3 ft/d is characteristic of unfractured rock and that the fractures along this orientation might be closed or unconnected. In the major principal direction (110-degree orientation), the hydraulic-conductivity value of 32 ft/d is about one order of magnitude higher than the range of laboratory values, indicating that fractures along this orientation might be open and more hydraulically connected.

Gunlock Well Field Aquifer Test

The purpose of the Gunlock Well Field aquifer test was to determine the transmissivity and storage properties of the Navajo aquifer downstream from the Gunlock Reservoir in Washington County, Utah (fig. A-9). The aquifer test was conducted in February 1996 by the USGS in coordination with the St. George Water and Power Department. The multiple-well aquifer test involved pumping at Gunlock well 7 for about 6 days at an average rate of 845 gal/min. Discharge was measured with an in-line flow meter. The discharge from the production well was diverted into a culinary supply line and removed from the aquifer-test site.

Water levels were measured in seven observation wells and the pumped well for about 18 days prior to

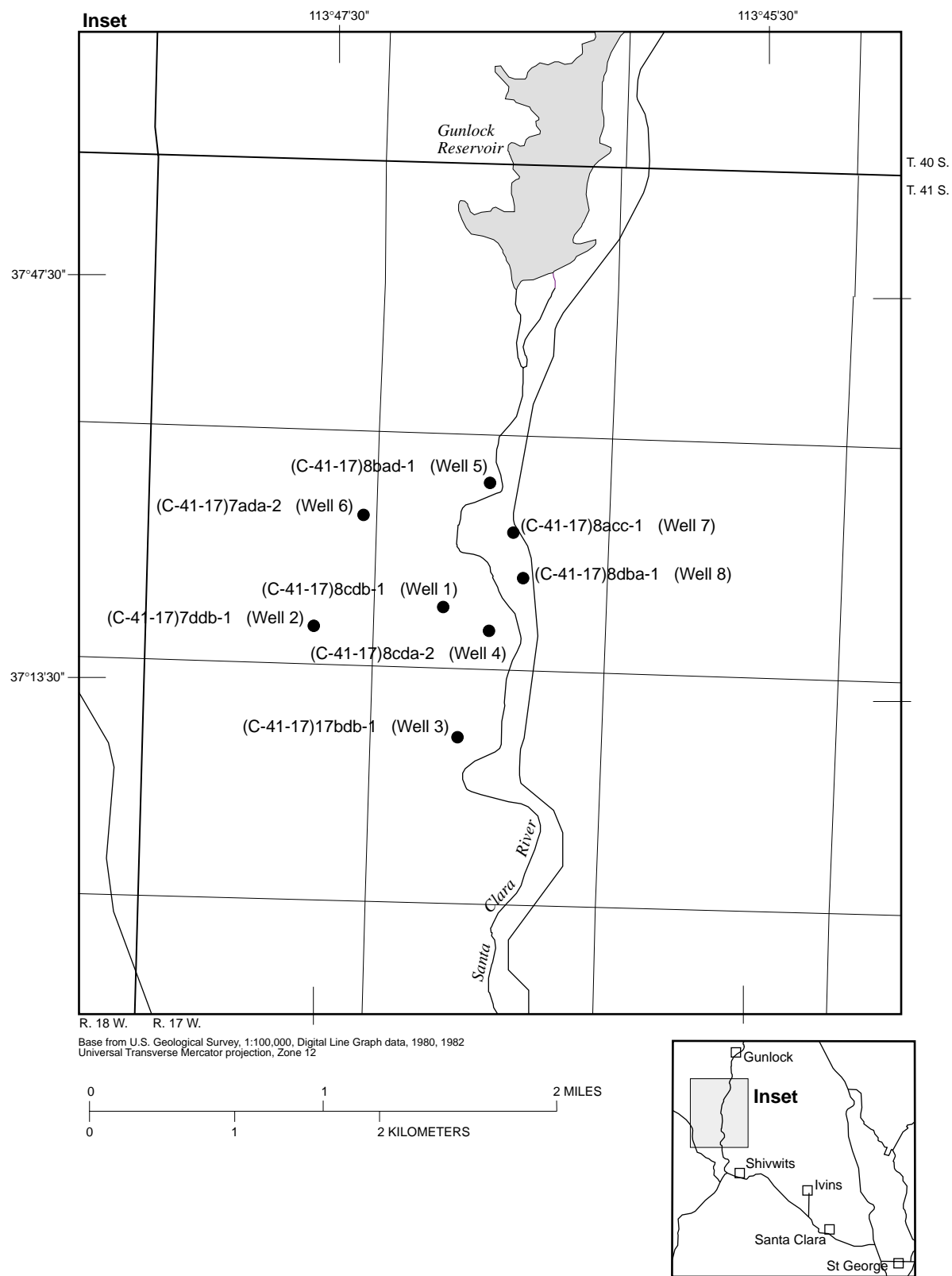


Figure A-9. Location of wells in the Gunlock aquifer test, Washington County, Utah, February 1996.

the test, during the 6 days of pumping, and for about 7 days after the pump was shut off. The pumped well and all of the observation wells are finished in the Navajo aquifer. Data for the pumped well and observation wells is reported in table A-3. Five of the observation wells (Gunlock wells 1, 4, 5, 6, 8) are production wells that had not been pumped for at least 19 days prior to the aquifer test. The two farthest observation wells are production wells that maintained a constant pumping rate both before and during the aquifer test. Gunlock well 3 (radial distance = 4,400 ft) was pumping at about 840 gal/min and Gunlock well 2 (radial distance = 4,855 ft) was pumping at about 570 gal/min.

Geology

At the aquifer-test site south of Gunlock Reservoir, the Navajo Sandstone is exposed at the surface and, because of erosion, is about 1,100 ft thick. As the Navajo Sandstone dips to the north-northeast, its thickness increases to a maximum of 3,000 ft at the contact with the overlying Carmel Formation about 1.5 mi north of the pumped well (Gunlock well 7). The Navajo Sandstone thins toward the southwest as a result of erosion until the geologic contact with the underlying Kayenta Formation is exposed about 2 mi southwest of the pumped well. The Navajo Sandstone is continuous for about 6 mi toward the northwest, beyond which it is offset completely by faulting. Similarly, the Navajo Sandstone is completely offset by the Gunlock Fault about 1 mi to the east of the pumped well. A generalized geo-

logic cross section in the vicinity of the pumped well is shown in figure A-10.

Surface-fracture studies of outcrop sites near the pumped well and lineament studies of areal photographs indicate that the sandstone is highly fractured in this region (Hurlow, 1998). Rose diagrams of these fracture and lineament orientations indicate that the principal direction of fracturing ranges from due north to northwest. Field observations show a predominant fracture trend in the due north-south direction. The Santa Clara River follows this fracture trend from just downstream from the Gunlock Reservoir to a bend in the river by Gunlock well 5. The river then bends to the west until it turns south again and follows another parallel fracture set to a location adjacent to the pumped well (Gunlock well 7). These north-south fracture sets were observed to be much more continuous and have wider apertures compared to other fractures exposed along the outcrop. On the basis of this surface fracturing, it is assumed that the aquifer is anisotropic and hydraulic conductivity is higher in this direction.

In addition to the Navajo Sandstone, fluvial unconsolidated deposits are along the Santa Clara River valley. The width of these fluvial sediments generally is less than a few hundred feet at the aquifer-test site. The depth of these sediments is unknown.

Hydrology

The Santa Clara River flows within 600 ft of the pumped well. The amount of water in the river along the reach near the pumped well depends on the

Table A-3. Construction data for wells used in the Gunlock aquifer test, Washington County, Utah, February 1996

Gunlock well number	Well number	Radial distance (feet)	Casing diameter (inches to feet)	Open interval (feet below land surface)	Opening type
7	(C-41-17)8acc-1	0	16 to 800	200 - 800	Screen
8	(C-41-17)8dba-1	710	16 to 800	200 - 800	Screen
5	(C-41-17)8bad-1	1,650	16 to 384	100 - 384	Perforations
4	(C-41-17)8cda-2	2,000	16 to 573	123 - 573	Screen
1	(C-41-17)8cdb-1	2,100	16 to 283	100 - 200	Perforations
6	(C-41-17)7ada-2	3,530	16 to 573	123 - 573	Screen
3	(C-41-17)17bdb-1	4,400	16 to 9	9 - 626	Open hole
2	(C-41-17)16bbd-1	4,850	16 to 288; 10 to 466	176 - 466	Perforations

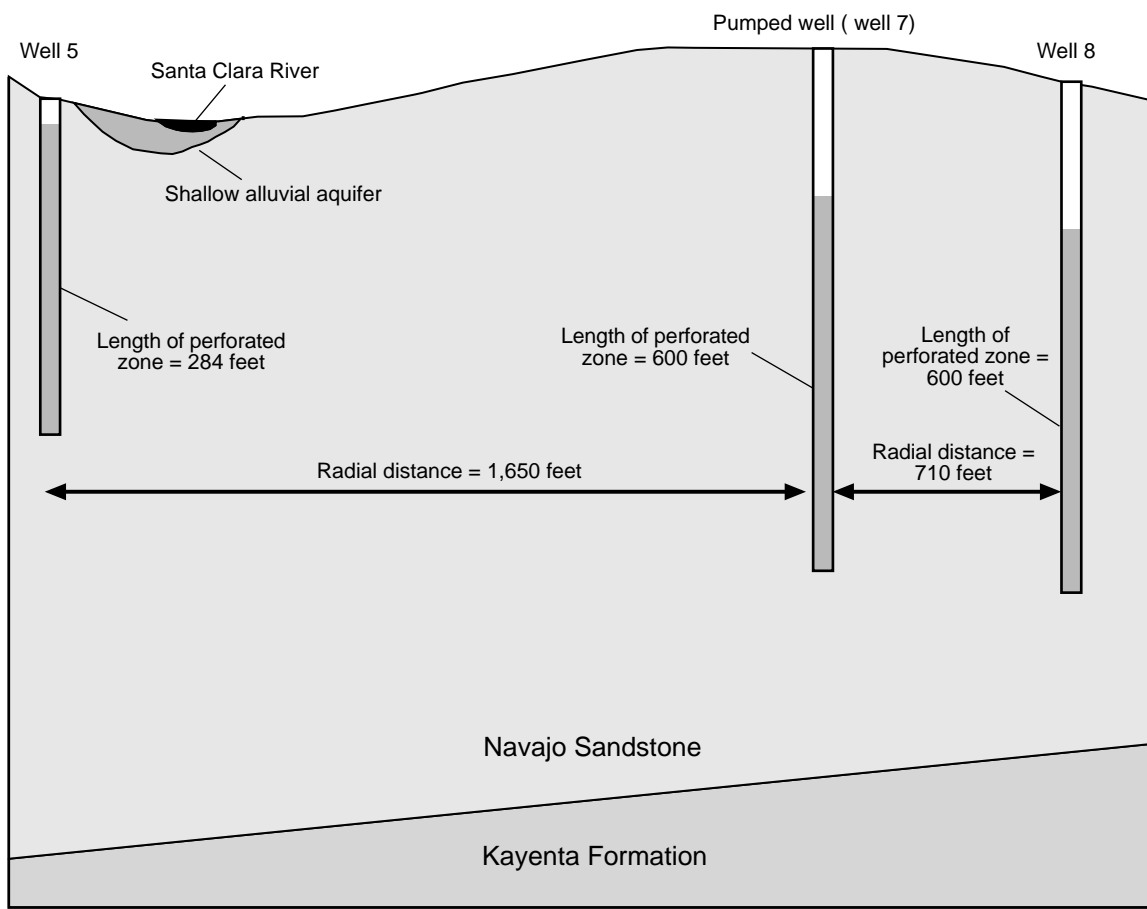


Figure A-10. Generalized geologic cross section in the vicinity of the pumped well in the Gunlock aquifer test, Washington County, Utah, February 1996.

upstream releases from Gunlock Reservoir. The valve controlling reservoir releases was closed more than a month before the aquifer test and was not opened until completion of the recovery part of the test. However, about $0.8 \text{ ft}^3/\text{s}$ was leaking from the base of the reservoir before and throughout the aquifer test. Flow in the river gradually decreased southward to a point about 4,000 ft south of the pumped well where the river bed was dry prior to the start of the aquifer test.

Prior to the aquifer test, a staff gauge was installed in the river adjacent to well 5 (about 1,500 ft north of the pumped well), a 6-in. Parshall flume was installed in the river adjacent to well 7, and a 3-in. Parshall flume was installed in the river south of well 8 (fig. A-9). Staff-gauge measurements adjacent to well 5 indicate that flow upstream from the pumped well was constant during both the pumping and recovery parts of the aquifer test. However, discharge measurements at both flumes indicated that a minimum of about 110 gal/min ($0.24 \text{ ft}^3/\text{s}$) was induced from the river into the shallow fluvial aquifer by the decrease in head in the

underlying Navajo aquifer during the pumping part of the aquifer test. Because decreases in discharge downstream from the lower flume could not be measured (but are assumed to have occurred, as evidenced by the drying up of that river reach), the total amount of water lost from the river as a result of pumping was probably larger.

Although no observation wells are located in the shallow fluvial aquifer, head decreases in the Navajo aquifer caused by pumping were assumed to induce additional water from the fluvial aquifer into the Navajo aquifer. For a hypothetical calculation, the following assumptions were made: (1) the average thickness of the fluvial aquifer is 20 ft; (2) the average width of the fluvial aquifer is 100 ft; (3) the effective porosity of the fluvial sediments is 20 percent; and (4) head in the fluvial aquifer decreased an average of 0.5 ft along the 5,500-ft reach, which showed a decrease in discharge during the aquifer test. The volume of water released by this 0.5 ft drop in water level in the fluvial aquifer would be about 8 million gal—about the same total vol-

ume of water pumped during the entire aquifer test. Although some part of the pumped water came from storage within the Navajo aquifer, most of the water moving toward the pumped well during the aquifer test was assumed to be induced flow from the shallow fluvial aquifer and the Santa Clara River.

The saturated thickness of the Navajo aquifer is estimated to range from about 600 ft at well 3 to about 1,100 ft at well 5. The saturated thickness at well 7 (the pumped well) is about 1,050 ft when not pumped. After pumping equilibrium has been established, the saturated thickness decreases to about 800 ft. The pumped well is perforated for a 600-ft interval during static conditions and for a 550-ft interval during pumping conditions. Therefore, the perforated interval during pumping at well 7 is more than $\frac{2}{3}$ of the total saturated thickness at the well site. The observation wells are generally perforated in the same upper part of the Navajo aquifer. The closest observation well (Gunlock well 8, radial distance = 710 ft, total drawdown of 21.5 ft) has a nearly identical perforated interval. The other observation well that had substantial drawdown (Gunlock well 5, radial distance = 1,650 ft, total drawdown of 1.2 ft) is perforated in the uppermost 280 ft of the aquifer (fig. A-10). However, because its radial distance is three times the vertical perforated interval (550 ft during pumping) of the pumped well, partial penetration effects should be negligible.

Data Reduction and Analysis

Measured water levels at the observation wells were not corrected for barometric changes. The magnitude of drawdown and recovery at the nearest observation well (well 8) was much larger than effects resulting from barometric changes (generally less than 1 ft). A comparison between barometric pressure and prepumping water levels at Gunlock well 5 did not show any correlation. Therefore, no corrections for barometric pressure variations were attempted at this well and the more distant observation wells (Gunlock wells 1, 4, and 6). Water-level increases of from 7 to 9 ft were measured at Gunlock wells 1, 4, and 6 throughout the prepumping and recovery parts of the aquifer test. After linear trend corrections were applied to the water-level data from these wells, the recovery data indicate that these wells were only affected slightly by pumping at well 7 (about 0.3 ft at each well), not enough to produce drawdown curves of sufficient quality for curve fitting.

Because of small variations in the pumping rate throughout the pumping part of the aquifer test, the observation-well recovery data were used for wells 5 and 8. The only corrections made to the recovery data for these two wells were to subtract the prerecovery trend. To determine the prerecovery trend at wells 5 and 8, a straight line was fitted to the latter part of a semilog plot of the prerecovery data. This trend was then extended for the recovery part of the test and added to uncorrected recovery. The drawdown and recovery data for these two observation wells were then plotted out together on a log-log scale by dividing the elapsed time by the observation well's radial distance squared.

Initial attempts to match the observed recovery curves for the two wells with the Theis solution (1935) for confined aquifers did not provide a satisfactory match; the Theis curve matches early time recovery data from well, but then deviates at later time (fig. A-11). The later-time observed drawdown is less than predicted by the type curve, which may indicate additional sources of water besides release of water from confined storage. No confining layer is present at the aquifer-test site, but early time responses at more distant observation wells initially appear to reflect confined conditions. Therefore, curve-fitting with the Neuman (1974) unconfined solution with delayed yield was attempted. Although the delayed-yield curve (the lower of curve in fig. A-12) provided a better individual match to the data from well 5, a single simultaneous solution for transmissivity and storage was not possible for both wells. The modified Hantush solution (Lohman, 1972, p. 32-34) for leaky confined aquifers also was attempted with the assumption that leakage from the overlying fluvial sediments would be similar to an overlying leaky layer, but an acceptable single-value solution could not be achieved. It is assumed that the large difference between the two well data sets may be a result, in part, of anisotropic conditions. Homogeneous and anisotropic conditions are indicated if the recovery data sets have offset but parallel late-time slopes, as shown earlier by applying a modified form of the Papadopoulos solution (1965) to the Anderson Junction aquifer test. However, later-time data on a semilog plot of recovery from the two Gunlock observation wells do not have similar slopes (fig. A-13). Therefore, the response at the two observation wells is assumed to be a combination of (1) anisotropic conditions that resulted from fracturing, and (2) leakage from the overlying river and fluvial aquifer (a partially penetrating boundary). There is no analytical method that can be used for this complex hydrologic setting.

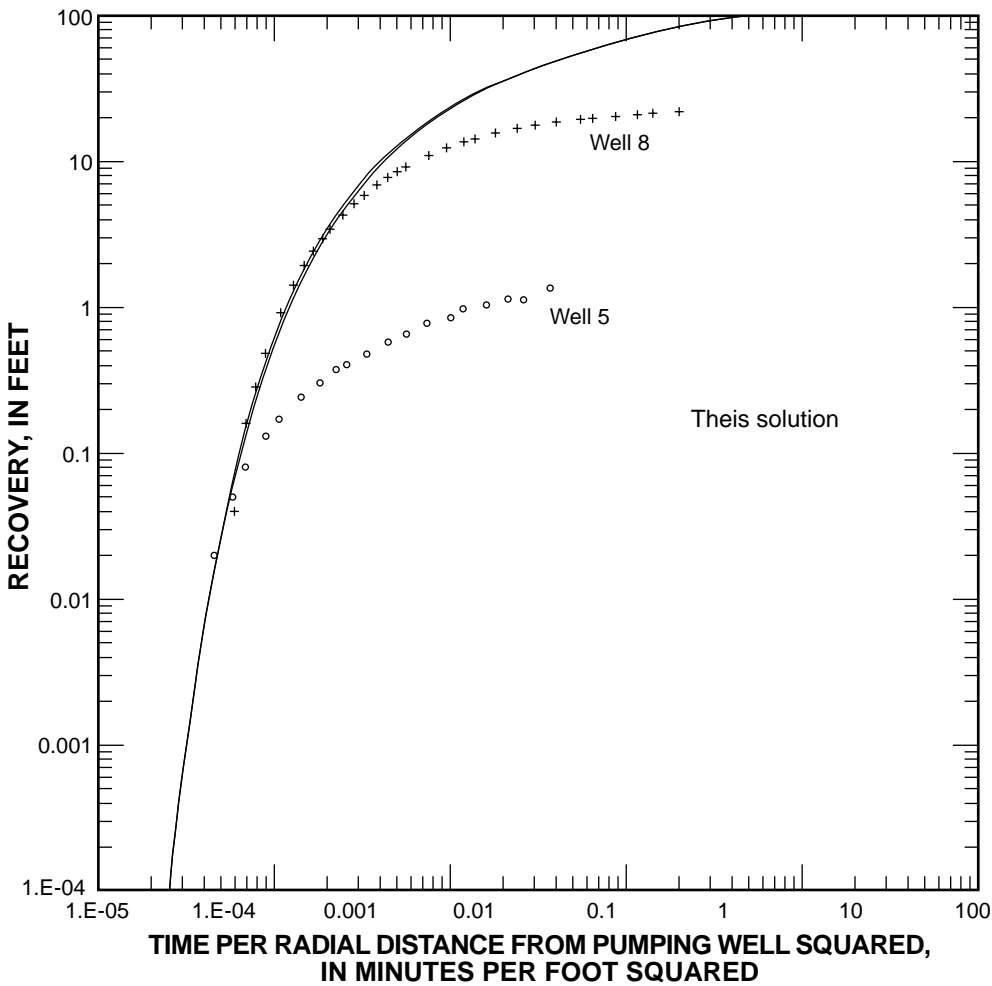


Figure A-11. Recovery data from two observation wells during the Gunlock aquifer test, Washington County, Utah, February 1996 (Theis solution, 1935).

Ground-Water Flow Model

To analyze the observation-well data from the Gunlock aquifer test, a three-dimensional ground-water flow model was constructed and calibrated using Modflow 96 (Harbaugh and McDonald, 1996). The ground-water flow model was developed as a tool for aquifer-test analysis and therefore uses the principles of superposition to simulate the change in heads and flows that resulted from pumping at well 7. As stated by Reilly and others (1987, p. 2), “The principle of superposition means that for linear systems, the solution to a problem involving multiple stresses is equal to the sum of the solutions to a set of simpler individual problems that form the composite problem.” In general, the principle of superposition can only be applied to a confined aquifer. However, Reilly stated that the principle of superposition can be applied to mildly nonlinear systems

such as an unconfined aquifer if the regional drawdown that results from pumping is less than 10 percent of the full saturated thickness of the aquifer. This is the case at the Gunlock aquifer-test site. The regional dewatering of the aquifer by pumping from well 7 represented only a very small percentage of the prepumping saturated thickness. By using the principle of superposition, only the changes in simulated heads and flows from pumping need to be analyzed. To isolate these changes, absolute elevation data were converted to relative elevation data such that prior to pumping, the water table everywhere in the model was at 0 ft. The initial conditions, rather than being specified in absolute terms (actual head values in ft above sea level), are specified relative to the heads and flows that existed prior to pumping at well 7.

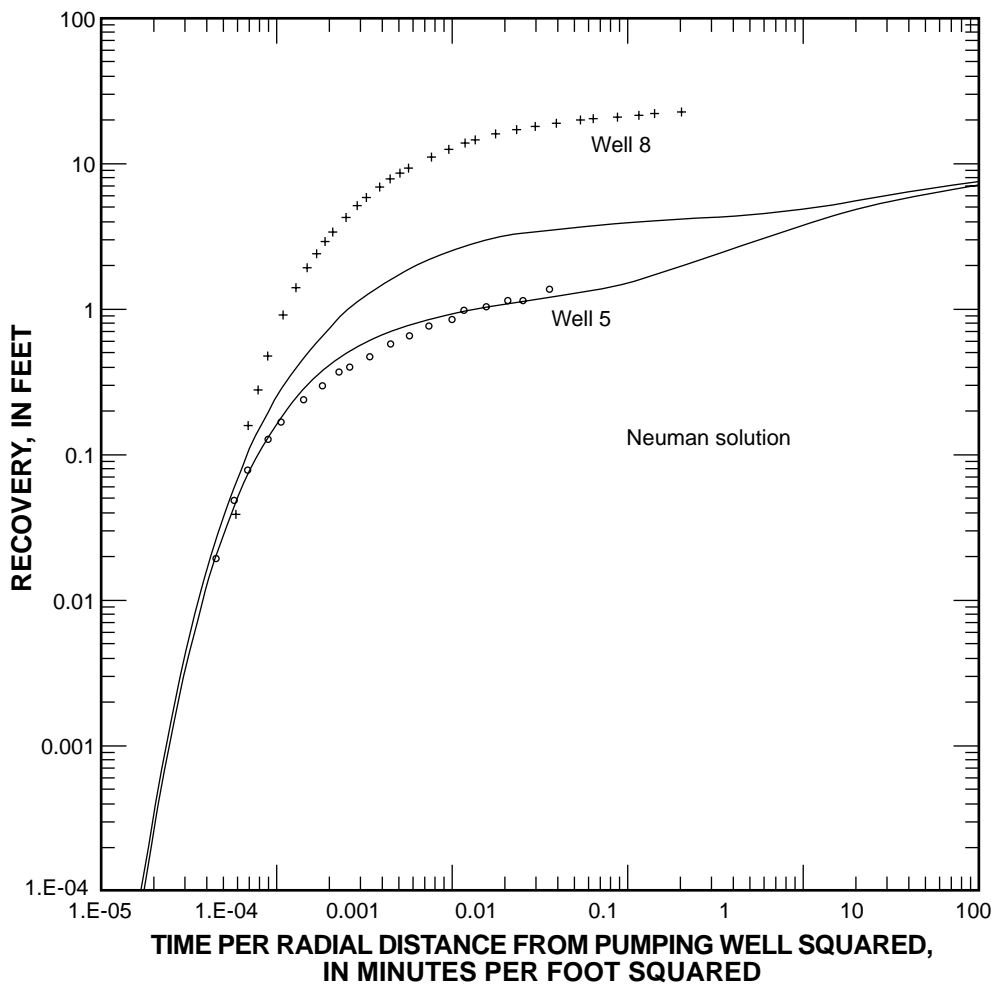


Figure A-12. Recovery data from wells during the Gunlock aquifer test, Washington County, Utah, February 1996 (Neuman solution, 1974).

The location of the model boundary with respect to the Gunlock part of the Navajo aquifer is shown in figure A-14a. The model was discretized into 163 rows by 149 columns. The cell size at the center of the model is about 10 ft by 10 ft (fig. A-14c) and increases with radial distance from the pumped well to a maximum cell size of about 400 ft by 400 ft along the perimeter of the model using a multiplier of approximately 1.5 (fig. A-14b). The active area of the model is surrounded by a no-flow boundary. The base of the model (bottom of layer 1) is also a no-flow boundary because published hydraulic-conductivity values for the Kayenta Formation determined from laboratory analyses are generally lower than values for the Navajo Sandstone (Weigel, 1987).

Because the model has only one layer that represents the Navajo aquifer, the combined effects of seepage from the river and shallow fluvial aquifer were

simulated by using the River Package. The fluvial aquifer is not simulated as a separate layer because there is no available data on its geometry, aquifer properties, or water levels. Conductance values of river cells were varied during model calibration to match measured losses along the Santa Clara River. The stage of the river was specified at 0 ft everywhere, the same elevation as the top of the aquifer and the defined initial head value. Thus, until the stress from pumping propagated out to the nearest river cells, no seepage from the river would be simulated. In this manner, the changes in stream seepage rates as a result of pumping at well 7 could be isolated and evaluated.

The Well Package is used to simulate pumping at well 7. The specified pumping rate was 845 gal/min for the stress period representing the pumping part of the aquifer test. Because Gunlock Wells 2 and 3 were also pumping both before and throughout the aquifer test,

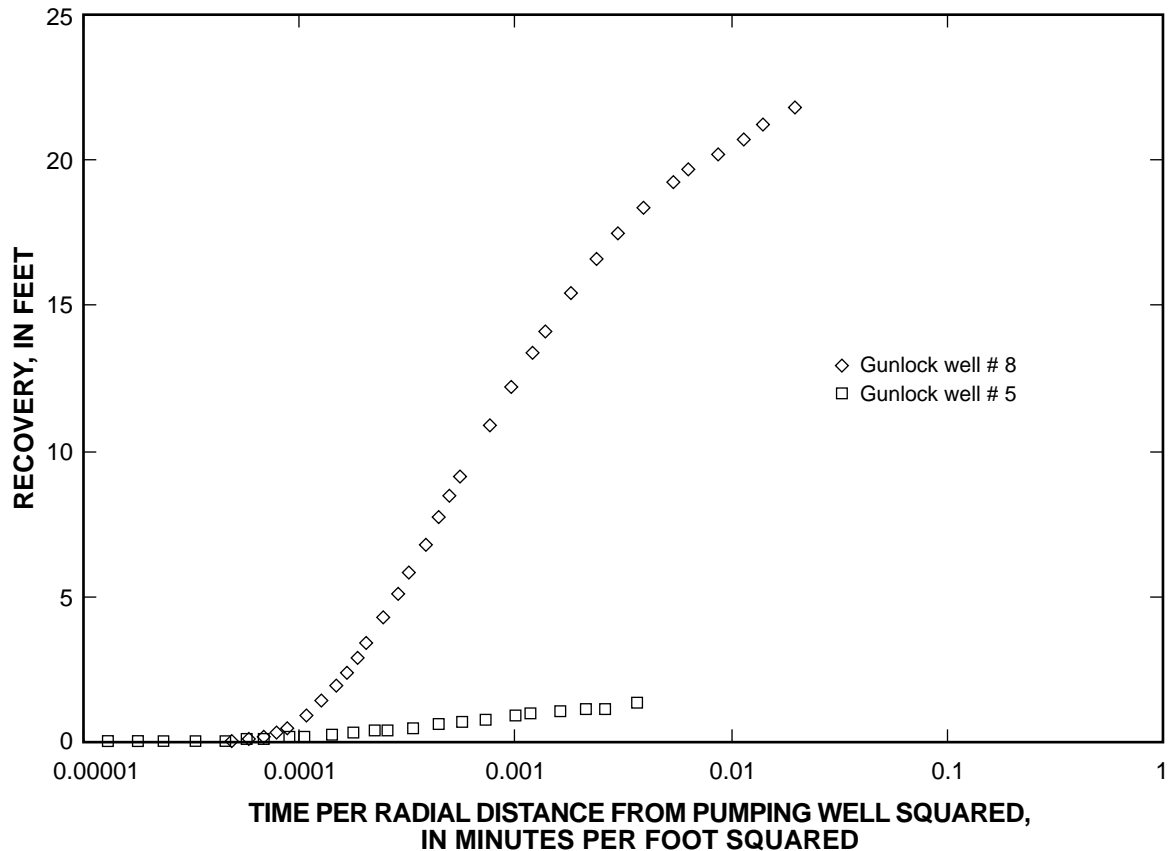


Figure A-13. Recovery data showing different late-time slopes for wells during the Gunlock aquifer test, Washington County, Utah, February 1996.

these were not simulated as additional stresses; the model was constructed to evaluate only changes resulting from pumping at well 7.

Model Calibration

The parameters used to calibrate the ground-water flow model are (1) drawdown curves at the nearest two observation wells (wells 5 and 8), (2) total drawdown at well 7 and at more-distant observation wells, (3) ground-water budget parameters, (4) anisotropy resulting from fracturing, and (5) known aquifer boundaries.

Matching measured drawdown/recovery curves at wells 5 and 8 was the most important calibration point of the model. The final match of computed drawdown to measured recovery is shown in figure A-15. Generally, the computed drawdown matches the measured drawdown at both observation wells at early and late time. At “middle” time, the computed drawdown values are slightly less than measured values. The lack of a perfect match is probably because of the simplify-

ing assumptions, such as homogeneity in aquifer properties, uniform anisotropy in the north-south direction, and the assumption of horizontal flow in a single-layer model.

Matching total drawdown at the pumped well and distant observation wells was not as high a priority as matching drawdown curves at the nearby observation wells. Nevertheless, this was considered important information for the calibration. The total computed drawdown of 303 ft at the pumped well was more than the 257 ft of measured drawdown. However, matching drawdown at the pumped well is complicated by finite-difference limitations and the poor-quality data associated with pumped well measurements. Wells 1, 4, and 6 had similar computed-versus-measured total drawdown values. As mentioned earlier, because these wells were undergoing substantial recovery during the aquifer test, the corrected drawdown values computed from water-level measurements may contain some error. Well 3 displayed no measurable drawdown during the pumping part of the aquifer test. However, both this well and well 2 (outside the active model boundary) were pumping

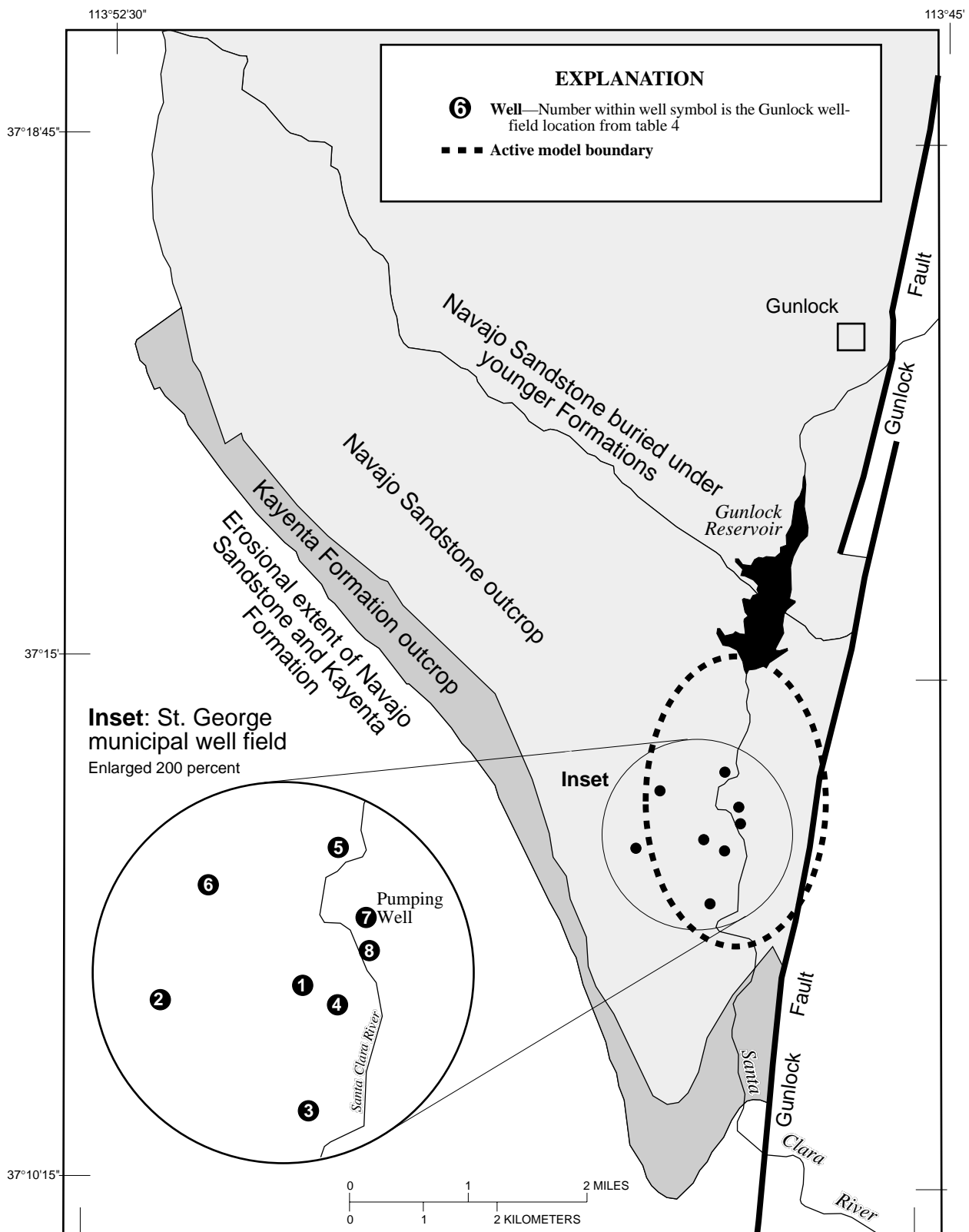


Figure A-14. (a) Boundary, (b) finite-difference grid, and (c) detail of finite-difference grid for the ground-water flow model of the Gunlock aquifer test, Washington County, Utah, February 1996.

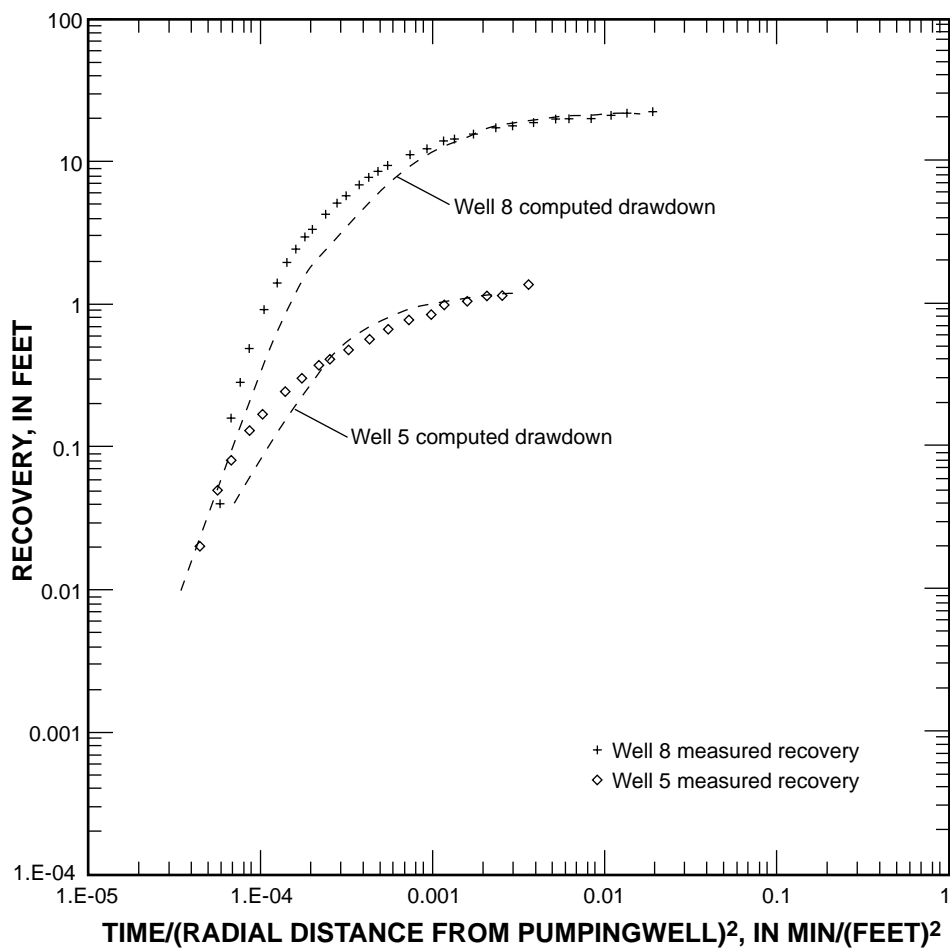


Figure A-15. Measured recovery and computed drawdown for wells during the Gunlock aquifer test, Washington County, Utah, February 1996.

during the test, so it was not possible to determine if there were very small effects at these wells.

In the ground-water flow model, more than 90 percent, or 760 gal/min, of water discharging from the aquifer at the pumped well came from the River Package (simulating both the Santa Clara River and shallow fluvial aquifer) at the end of the 6-day pumping period. This is much more than the measured 110 gal/min loss from the Santa Clara River but also includes the dewatering of the shallow fluvial sediments that was not measured during the aquifer test. The other 10 percent, or 80 gal/min, came from aquifer storage.

As discussed above, the predominant orientation of surface fracturing on the exposed Navajo Sandstone outcrop near the pumped well is north-south. Although the orientation of preferential flow as a result of fracturing was a constraint in developing the ground-water flow model, there was no prior information regarding the relative degree of anisotropy. Therefore, anisotropy

factors for $K_{\text{north-south}}: K_{\text{east-west}}$ from 1:1 to 10:1 were tried during the calibration process. The final calibrated model uses an anisotropy factor for $K_{\text{north-south}}: K_{\text{east-west}}$ of 3:1.

As discussed earlier, the Gunlock part of the Navajo aquifer has a limited extent as a result of faulting and erosional boundaries to the east, south, and west. However, water-level measurements during the aquifer test indicated that the drawdown cone had not reached any of these boundaries. Similarly, after 6 days of simulated pumping, the ground-water flow model did not produce substantial drawdown at these boundaries. Simulated drawdown at the nearest boundary, the Gunlock Fault to the east, was less than 0.5 ft. It is possible, however, that long-term pumping at well 7 may result in noticeable boundary effects at the observation wells, such as increased rate of drawdown with time.

Generally, the model was more sensitive to changes in hydraulic conductivity and anisotropy ratios

and less sensitive to changes in storage and riverbed conductance. However, any general statements regarding relative sensitivity may oversimplify a more complex situation. For example, although order-of-magnitude changes in storage may not affect total drawdown substantially at the pumped well and nearby observation wells, they strongly affect total drawdown and the shape of the drawdown cone at greater radial distances, as well as the water-budget components. Similarly, although order-of-magnitude changes in riverbed conductance may not cause substantial changes to the water-budget components and the extent of the drawdown cone, such changes strongly affect drawdown at observation wells.

There are two important limitations to the calibrated ground-water flow model and its use as a tool for analysis of aquifer-test data from the Gunlock site. First, a single-layer model does not simulate flow in the shallow fluvial sediments along the Santa Clara River, nor allow for the simulation of vertical ground-water flow and determination of vertical anisotropy. If another aquifer test is to be conducted at this site, it would be helpful to drill a few shallow observation wells into the fluvial aquifer to determine hydrologic properties of these sediments, thickness of the fluvial aquifer, and drawdown caused by pumping from the Navajo aquifer. These data could be used to construct an additional model layer representing the shallow fluvial aquifer. Second, anisotropic conditions are assumed to be consistent throughout the modeled area. Differences in fracture density and orientation at the aquifer-test site may result in a varying degrees of anisotropy. Because detailed data about the variation in fracturing both laterally and vertically are not available for the site, aquifer properties were assumed to be uniform throughout the simulated area. Additional surface- and borehole-fracture data at the site may help to identify the variability in anisotropy due to fracturing.

Summary

The values determined from model calibration are 0.33 ft/d for horizontal hydraulic conductivity in the east-west orientation and 1.0 ft/d for horizontal hydraulic conductivity in the north-south orientation. Multiplying these values by the aquifer thickness of 1,100 ft at the pumped well results in transmissivity values of about 360 to 1,100 ft²/d.

The range of hydraulic-conductivity values determined from this aquifer test are similar to Cordova's (1978, p. 26) laboratory determination of hori-

zontal hydraulic-conductivity values that ranged from 0.36 to 5.0 ft/d for samples from the Navajo aquifer at various locations within Washington County. They are also similar to the horizontal hydraulic-conductivity value of 0.8 ft/d determined from the Hurricane Bench aquifer test. However, the values are lower than the range of horizontal hydraulic-conductivity values of 1.3 to 32 ft/d determined from the Anderson Junction aquifer test. Because the Navajo Sandstone is composed of well-sorted very fine sand and varies little throughout southwestern Utah, the higher values of horizontal hydraulic conductivity determined from the Anderson Junction aquifer test are probably because of a higher degree of fracturing (higher fracture density and larger average aperture).

The value for storage coefficient determined from model calibration is 0.001. This value is the same order-of-magnitude as the value of 0.002 determined from the Hurricane Bench aquifer test and the value of 0.0013 determined from the Anderson Junction aquifer test.

Grapevine Pass Aquifer Test

The purpose of the Grapevine Pass aquifer test was to determine the transmissivity of the Navajo aquifer near Grapevine Pass, about 7 mi northeast of St. George in Washington County, Utah (fig. A-16). The aquifer test was conducted in February 1996 by the USGS in coordination with the Water Department of Washington, Utah. Unlike the other aquifer tests, this was a single-well aquifer test with drawdown and recovery measured only in the pumped well. Water levels were measured in well (C-41-15)28dcb-2 during the 24 hours prior to the test, during the 24 hours of pumping, and during the 24 hours after the pump was shut off. Water from the pumped well was diverted into nearby Grapevine Pass Wash and removed from the aquifer-test site. Discharge was estimated to average 180 gal/min and was measured with both a v-notch weir and a pitot tube attached to the discharge pipe.

According to field observations, geologic maps, and surface-fracture surveys, the Navajo Sandstone outcrop in the immediate vicinity of the aquifer test site has no prominent surface fracturing (Hurlow, 1998). It was noted, however, that surface fractures are present within about 1 mi of the site, both up- and down-canyon. According to the drillers' log, the Navajo Sandstone is about 915 ft thick at the site and is interbedded with layers of siltstone and mudstone. The drillers' log

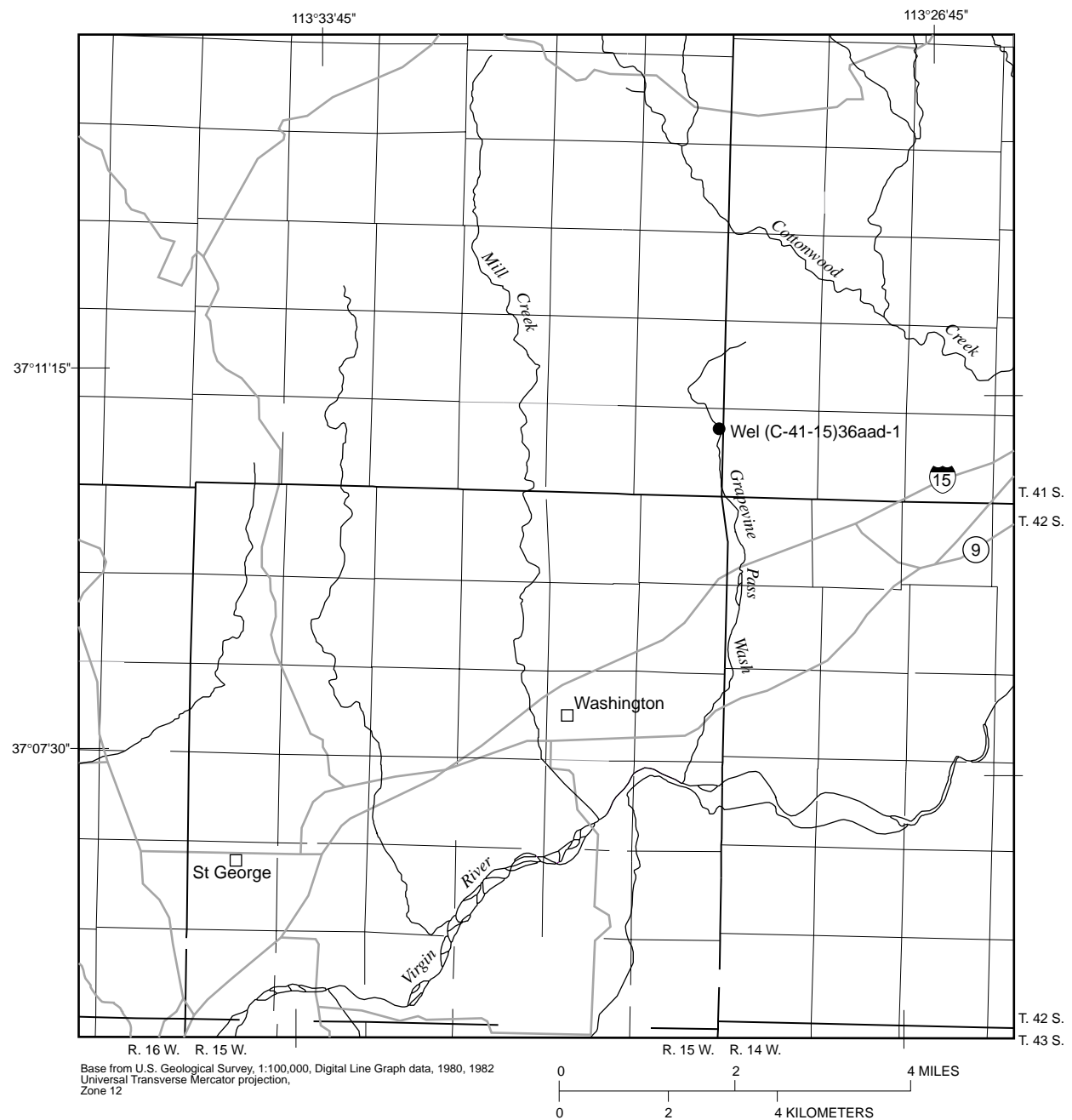


Figure A-16. Location of well in the Grapevine Pass aquifer test, Washington County, Utah, February 1996.

notes that the Navajo Sandstone has a much smaller grain size there than at other wells completed in the Navajo Sandstone. The Kayenta Formation, made up of siltstone with intermixed clays and sands, is present from a depth of 920 ft to the bottom of the drillhole at 950 ft. The Utah Geological Survey also analyzed bore-hole cuttings from three wells drilled in the Navajo Sandstone in Washington County: the Grapevine Pass production well, the Anderson Junction production well about 20 mi northeast of St. George, and a production well in the Winchester Hills subdivision about 7 mi north of St. George. When compared with lithologic analyses from the two other wells, the Grapevine Pass site had much more interbedding with finer siltstone and mudstone layers (J. Wallace, Utah Geological Survey, written commun., 1996). Therefore, the fine-grained material at this site and the lack of surface fracturing may indicate lower hydraulic conductivity in this area. After the well was completed, the static water level was about 350 ft below land surface, which indicated a saturated thickness of about 570 ft for the Navajo aquifer.

The Cooper-Jacob straight-line method was chosen for analysis of the data. The semilog plot of recovery versus time used for the analysis is shown in figure A-17. The early time recovery data apparently are affected by well-bore storage effects, as a result of a combination of the large diameter well casing (12 in.) and the very small perforations necessary to keep the fine grained sand matrix of the aquifer from entering the casing. A method outlined in "Groundwater and Wells" (Driscoll, 1986, p. 232 -235) shows an interpretive technique for determining the critical time when the borehole-storage effect becomes negligible when using the following equation (eq. 9.9, p. 233):

$$t_c = \frac{0.6([d_c]^2 - [d_p]^2)}{Q/s} \quad (\text{A16})$$

where

t_c is the time in minutes when casing storage becomes negligible,

d_c is the inside diameter of the well casing in in.,

d_p is the outside diameter of the pump column pipe in in., and

Q/s is the specific capacity of the well in gal/min/ft of drawdown at t_c .

For the Grapevine Pass aquifer test, $d_c = 12$ in.; $d_p = 4.23$ in.; $Q = 180$ gal/min. Assuming an initial recovery (s) of 200 ft, the estimated initial iteration is:

$$t_c = \frac{0.6([12]^2 - [4.23]^2)}{180/200} = 84 \text{ minutes} \quad (\text{A17})$$

From the semilog recovery plot, at $t = 84$ minutes, the recovery is 362 ft. Solving for t_c with a recovery value of 362 ft yields $t_c = 152$ minutes for the second iteration. Working through this process for two more iterations yields a value for t_c of 158 minutes. This value correctly estimates the break in slope shown in figure A-17.

Thus, the Cooper-Jacob straight-line method (Cooper and Jacob, 1946) is used for time greater than 158 minutes. However, fitting a straight line to the recovery data beyond 158 minutes does not yield one unique fit. Two possible matches (lines T₁ and T₂) are shown in fig. A-17. The calculated transmissivity values from these lines are 160 ft²/d and 330 ft²/d, respectively. Because of this possible range of interpreted values, an order-of-magnitude value of 100 ft²/d will be reported for this aquifer test. Assuming the maximum possible saturated aquifer thickness of about 500 ft, the horizontal hydraulic conductivity is about 0.2 ft/d. This is about one order of magnitude less than horizontal hydraulic-conductivity values determined from laboratory analysis of outcrop samples (Cordova, 1978, p. 26) and from the results of the other multiple-well aquifer tests. This lower hydraulic conductivity is consistent with the presence of finer-grained material and the lack of surface fracturing at this location.

New Harmony Aquifer Test

The purpose of the New Harmony aquifer test was to determine the transmissivity and storage properties of the Tertiary Pine Valley quartz monzonite along Ash Creek near New Harmony in Washington County, Utah (fig. A-18). The aquifer test was conducted during October and November 1996 by the USGS in coordination with the Church of Latter Day Saints Property Division. The multiple-well aquifer test involved pumping at well (C-38-13)35aba-1 for 7 days. The discharge from the pumped well was diverted into a 12-in. diameter pipe that carried the water to sprinkler pivots more than 1 mi away. Discharge throughout the test was estimated to average 1,050 gal/min (2.34 ft³/s). Cumulative discharge was measured with an in-line flow meter. The average discharge rate was calculated by dividing the total number of gallons pumped by 7. Instantaneous discharge measurements were made with the in-line flow meter and a Clampatron meter through-

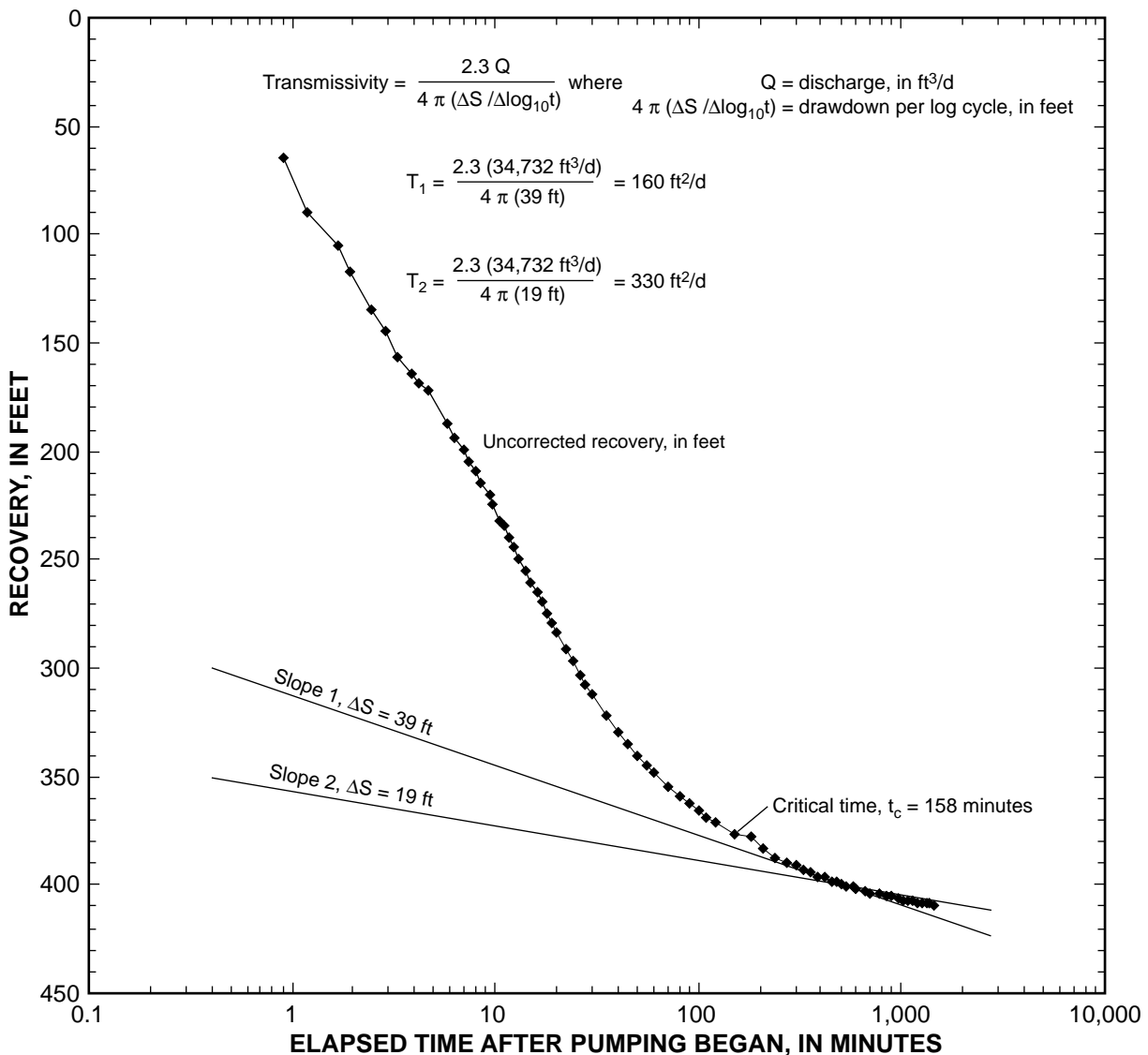


Figure A-17. Recovery data for the Grapevine Pass aquifer test using the Cooper-Jacob straight-line method, Washington County, Utah, February 1996 (Lohman, 1972).

out the test to ensure that the pumping rate did not fluctuate by more than 10 percent.

Water levels were measured manually in 10 observation wells and the pumping well beginning 18 days prior to the test, during 7 days of pumping, and for 7 days after the pump was shut off. Radial distances of the observation wells ranged from 825 to 7,950 ft. Data for the pumping well and observation wells are reported in table A-4. Observation well (C-38-13)35abb-1, referred to as the recorder well, was equipped with an automatic data recorder that continuously measured water levels beginning 18 days prior to the test, during the pumping part of the test, and for as much as 2

months after the pump was shut off. Because of the pumped well's proximity to Ash Creek, a flume was installed on the creek about 1 mi downstream of the well (and about 50 ft southwest of well (C-38-13)36cdd-1 to measure discharge. However, no decrease in flow was detected during pumping.

Hydrogeology

Based on drillers' logs and a geologic map by the Utah Geologic Survey (Hurlow, 1998), there is a 20- to 60-ft thick surficial layer of Quaternary fluvial material associated with Ash Creek at the aquifer-test site.

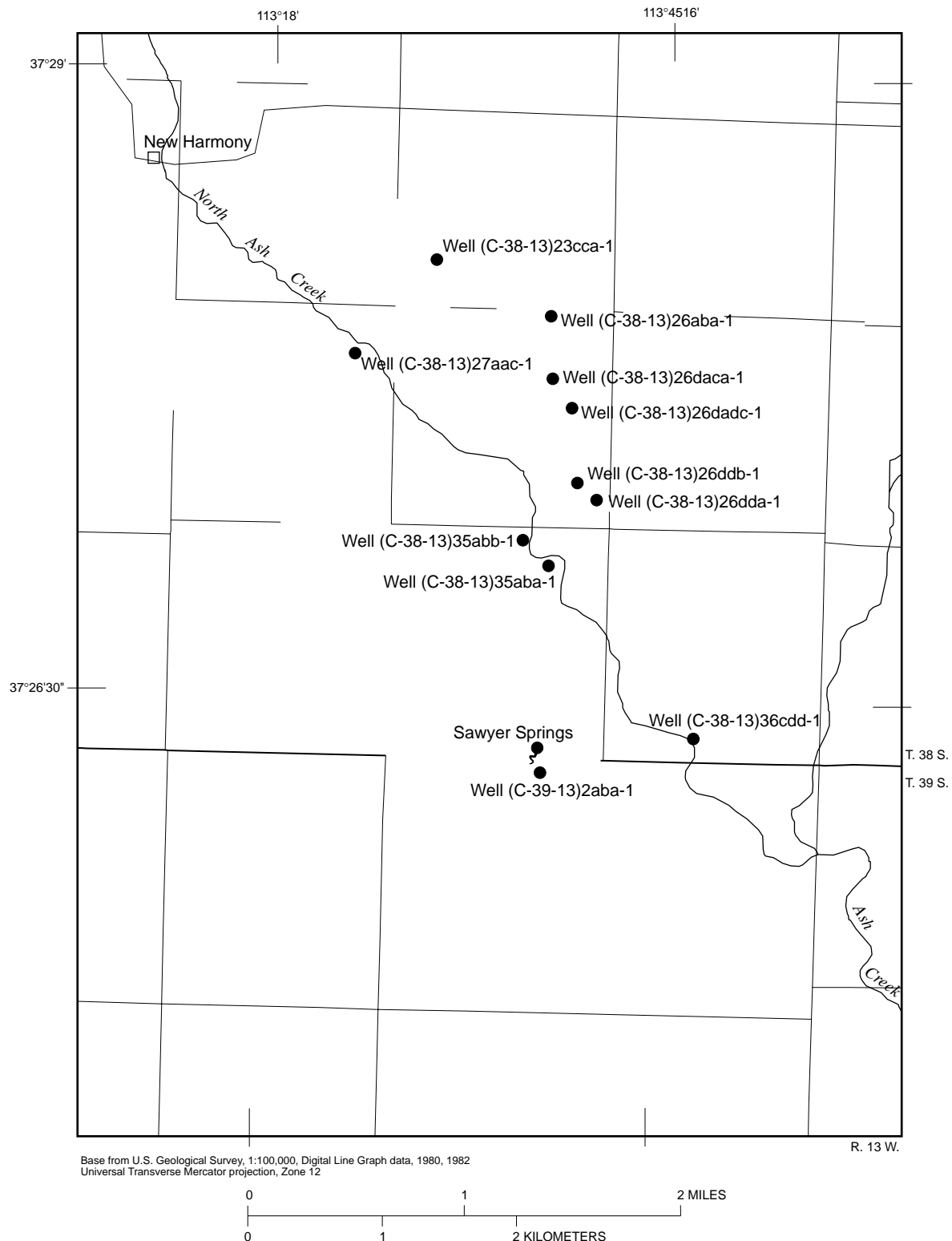


Figure A-18. Location of wells in the New Harmony aquifer test, Washington County, Utah, October and November 1996.

Table A-4. Construction data for wells observed during the New Harmony aquifer test, Washington County, Utah, October and November 1996
[NA, Not available]

Well number	Radial distance (feet)	Casing diameter and length (inches to feet)	Open interval (feet below land surface)	Opening type	Geologic formation ¹
(C-38-13)35aba-1	0	12 to 620	220 - 620	Perforations	Tvip
(C-38-13)35abb-1	825	6 to 370	180 - 370	Perforations	Tvip
(C-38-13)26dda-1	2,100	6 to 200	160 - 200	Perforations	Tvip
(C-38-13)26ddb-1	2,150	6 to unknown	NA NA		Tvip
(C-38-13)26adc-1	3,600	8 to 62; 6 to 199	40 - 199	Perforations	Tvip
(C-38-13)26aca-1	4,500	NA	NA NA		NA
(C-38-13)36ccdd-1	5,650	16 to 590	140 - 590	Perforations	Tvip
(C-39-13)2aba-1	5,800	16 to 400; 8 to 600	200 - 600	Perforations	Tvip
(C-38-13)26aba-1	6,050	6 to 177	150 - 175	Perforations	Tvip
(C-38-13)27aac-1	6,950	6 to 258	160 - 258	Perforations	Tvip
(C-38-13)23cca-1	7,900	12 to 130	36 - 122	Perforations	Qs

¹See pl. 1 for definitions of geologic formations.

Underlying these unconsolidated sediments is the Tertiary Pine Valley quartz monzonite (Tvip), which is estimated to be as much as 3,000 ft thick. A schematic cross section through some of the wells at the aquifer-test site is shown in figure A-19. Although this fine-grained crystalline rock has low primary porosity, it has highly fractured zones capable of transmitting a large amount of ground water. Cook (1957, p. 73-75) describes fracturing in the Pine Valley quartz monzonite as follows:

"The basal 'dark brown zone' has a pseudocolumnar structure due to intersecting vertical joint sets and it forms vertical cliffs above the weak Claron limestone...The basal zone grades upward into the slightly less resistant but much thicker 'brown zone,' also greatly fractured by vertical joints...The purple zone rock has a pale reddish-purple groundmass and is much less jointed than the two lowermost zones. However, incipient jointing is often seen, marked by aligned, elongate weathering depressions."

A driller's log from the nearest observation well (C-38-13)35abb-1 indicates that there was a highly permeable fracture zone from 243 to 340 ft depth. Because there is no poorly permeable lithologic layer overlying the quartz monzonite, it is assumed that the aquifer is unconfined. It is possible, however, that areas with low

fracture interconnectivity within the quartz monzonite may act as poorly permeable confining zones for underlying highly fractured zones.

Data Reduction and Analysis

During the aquifer test, only the recorder well (radial distance of 825 ft) showed substantial drawdown due to pumping. Measured water levels at this well were not corrected for barometric changes. The total change in water level at this well due to pumping was about 5.5 ft. The maximum possible change in water level due to fluctuating barometric pressure, assuming 100-percent efficiency, is only 0.2 ft, or 3.6 percent of the total change, and is therefore considered negligible.

The 5.5 ft of total drawdown at the recorder well was similar in order of magnitude to the 17 ft of total drawdown at the pumped well. The recorder well shares only 60 ft of the 400-ft open interval of the pumped well (fig. A-19); larger total drawdown at the recorder well would be expected if the open intervals of the two wells were the same. A plot of log-drawdown versus log-time data from the recorder well does not fit a Theis curve (fig. A-20). The Theis-curve solution shown in this figure was calculated with a storage value of 0.001 and a

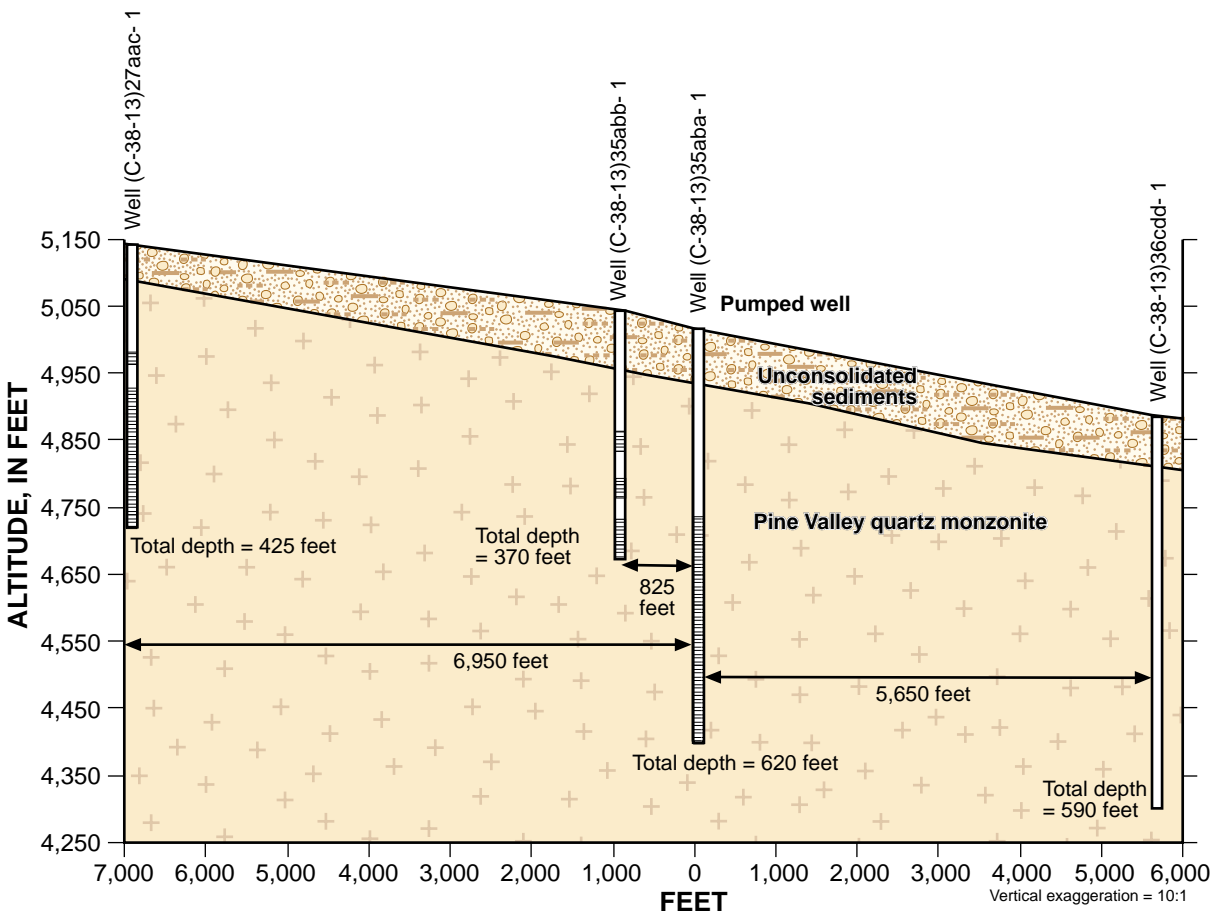


Figure A-19. Schematic cross section of selected wells and lithology of the New Harmony aquifer-test site, Washington County, Utah, October and November 1996.

transmissivity value of $9 \text{ ft}^2/\text{min}$ (from specific capacity data from the pumped well), but other values of transmissivity and storage did not improve the match.

The drawdown data at the recorder well, however, plots as a straight line with the square root of time as the horizontal axis (fig. A-21). This indicates that the recorder well and the pumped well may be connected by a highly transmissive fracture, which indicates linear rather than radial flow conditions. Jenkins and Prentice (1982) describe: "...an extreme condition where a homogenous aquifer is bisected by a single fracture having a permeability sufficiently large that the ratio of the fracture permeability to the aquifer permeability approaches infinity...Under this extreme condition, flow in the aquifer is linear toward the fracture rather than radial toward the well. (figure A-22) shows a conceptual model of a linear flow system. A homogenous aquifer is bisected by a highly permeable fracture which has been penetrated by a well. When the well is

pumped, the water level in the fracture declines, inducing flow into the fracture from the aquifer. The open fracture is a planar production surface that is an extension of the well itself. The well and its hydraulically connected production surface are here called an extended well... The flow lines in the aquifer are parallel; thus, flow in the aquifer is linear and laminar toward the extended well...Drawdown is a function of the perpendicular distance from the extended well, not a function of the radius from the pumped well. Thus, radial flow equations cannot adequately describe aquifer test data from a linear system."

Jenkins and Prentice (1982) also discuss the special case where the observation wells penetrate the production surface of the extended well:

"The drawdown in an observation well which penetrates the production surface of the extended well will be the same as the drawdown in the pumped well, if the pumped well data are corrected for entrance

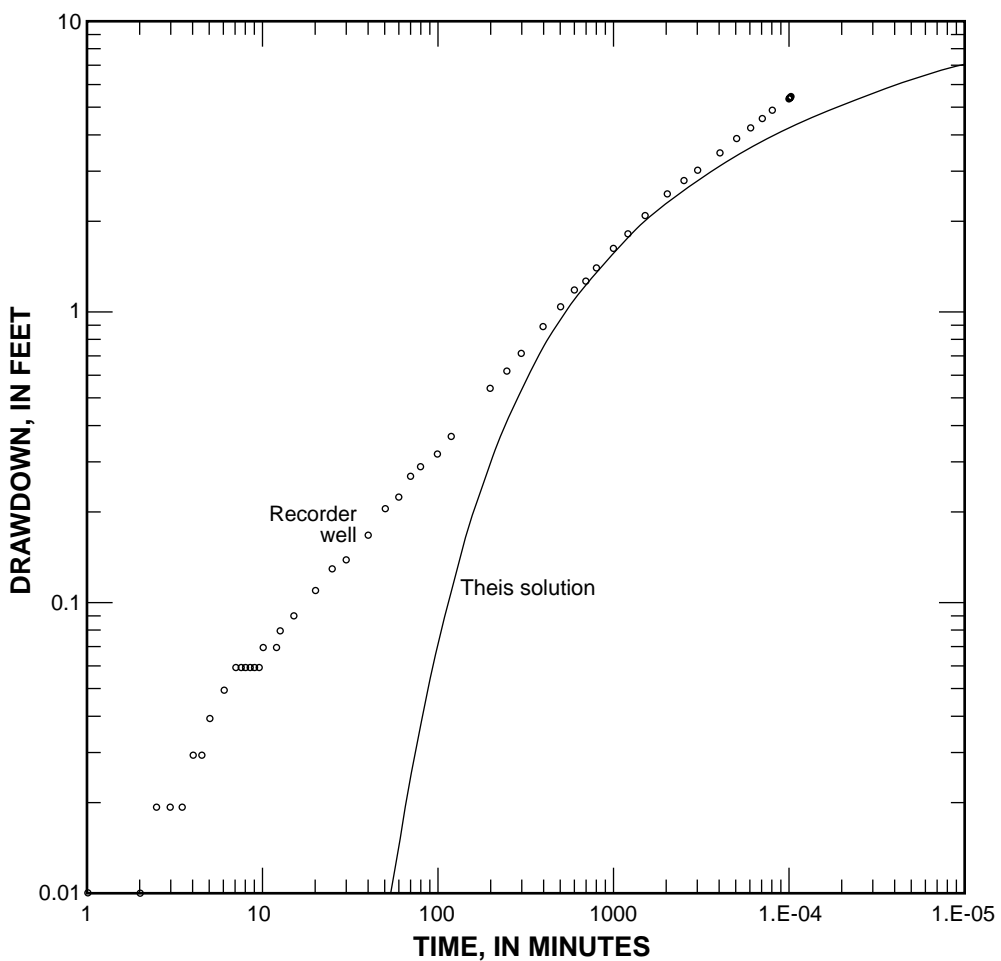


Figure A-20. Drawdown data from the recorder well during the New Harmony aquifer test, Washington County, Utah, October and November 1996 (Unconfined Theis solution).

losses and turbulent flow in the fracture near the well bore. Because the observation well lies along the axis of the trough of depression where water-level declines are greatest...a unique value for T (transmissivity) cannot be determined unless L (fracture length) is known and S (storage) can be reasonably estimated."

Jenkins and Prentice (1982) suggest that flow near the well may be linear if a straight line can be fitted to a plot of drawdown versus the square root of time. Based on this finding, Paul Hsieh (U.S. Geological Survey, written commun., 1997) suggested analyzing the drawdown data of the recorder well using equation 19 of the Jenkins and Prentice paper:

$$s = \left(\frac{Q}{L\sqrt{\pi TS}} \right) \sqrt{t} \quad (\text{A18})$$

where s = drawdown,

Q = pumping rate,

L = fracture length,
 T = transmissivity,
 S = storage, and
 t = time.

Equation A-18 is in the form of a linear equation, $y=mx+b$ where the Y axis is drawdown and the X axis is the square root of time. Therefore, the slope of the straight line fitted to the data of figure A-21 is 0.056 and is equal to the expression $\left(\frac{Q}{L\sqrt{\pi TS}} \right)$. Moving the pumping rate (Q) and $\pi^{-1/2}$ to the left side of the expression yields the relation:

$L\sqrt{TS} = 23.6ft^2/(\sqrt{t})$. Because no other information is available to uniquely define storage or transmissivity for the New Harmony aquifer test, this is the quantity reported. Jenkins and Prentice (1982) stated that: "Where L is unknown and the fracture appears to be infinite during an aquifer test, a unique value for T

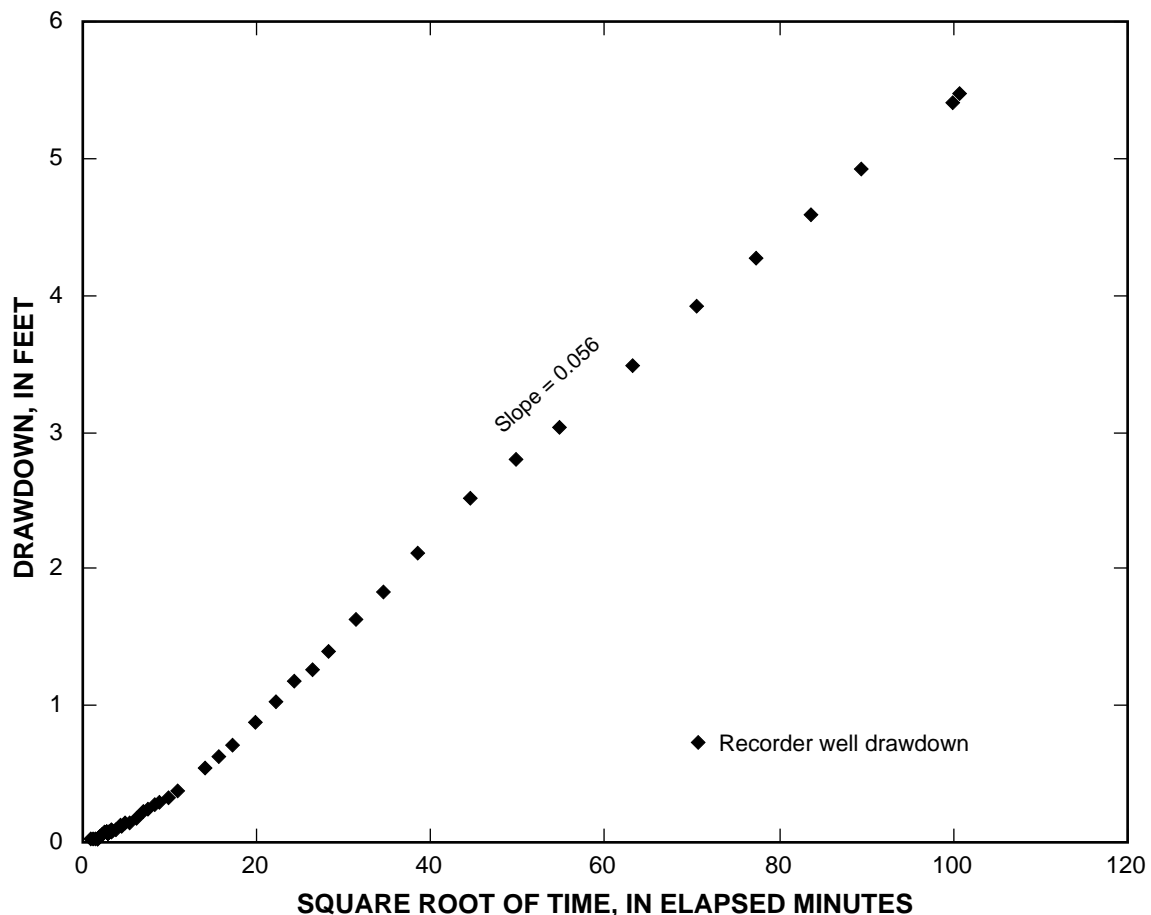


Figure A-21. Drawdown data from the recorder well during the New Harmony aquifer test, Washington County, Utah, October and November 1996 (Jenkins and Prentice solution).

cannot be determined..... Because the length of fractures varies from a few feet to thousands of feet, values of T determined using estimated L and S values should be used with caution.” However, if we assume that the fracture length is at least the 825 ft distance between the pumped well and the recorder well, then the product of T and S would be

less than or equal to $8.1 \times 10^{-4} \text{ ft}^2/\text{s}$.

It should be noted that the aquifer test was only of short duration. Longer-term pumping will result in more drawdown at the pumped well. As stated by Gringarten (1982), the long-term drawdown at the production well can be estimated using the Theis solution with a radial distance half the fracture length. Paul Hsieh (U.S. Geological Survey, written commun., 1997) suggested that “this method of estimating long-term drawdown strongly depends on the estimated fracture

length... (Similar to the radial flow case), the drawdown will not stabilize, but is ever increasing, although at a slower and slower rate.”

SUMMARY

Of the 10 observation wells measured during the New Harmony aquifer test, only the recorder well (radial distance of 825 ft) showed substantial drawdown due to pumping. A plot of drawdown data from this well versus the square root of time shows that flow near the well may be linear rather than radial. In a situation where the only affected observation well may intersect the same fracture (or extended well) as the pumped well, a unique value for transmissivity cannot be determined because both the fracture length and storage are unknown. Therefore, the product of fracture length and the square root of transmissivity times storage, $L\sqrt{TS}$, will be reported as about $24 \text{ ft}^{2}/\text{s}^{1/2}$.

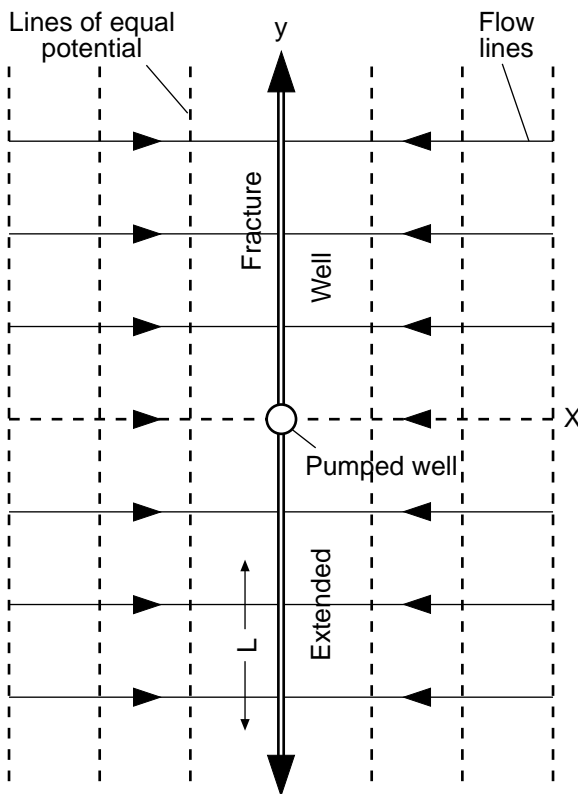


Figure A-22. Conceptual model of a homogeneous aquifer bisected by a single fracture (Jenkins and Prentice, 1982).

REFERENCES

- Cook, E.F., 1957, Geology of the Pine Valley Mountains, Utah: Utah Geological and Mineralogical Survey Bulletin No. 58, 111 p.
- Cooper, H.H., Jr., and Jacob, C.E., 1946, A generalized graphical method for evaluating formation constants and summarizing well-field history: Transactions, American Geophysical Union, v. 27, p. 526-534.
- Cordova, R.M., 1978, Ground-water conditions in the Navajo Sandstone in the central Virgin River basin, Utah, State of Utah Department of Natural Resources Technical Publication No. 61, 66 p.
- Driscoll, F. G., 1986, Groundwater and wells, Second Edition: Johnson Division, St. Paul, Minn., 1089 p.
- Gringarten, A.C., 1982, Flow-test evaluation of fractured reservoirs, Geological Society of America Special Paper 189, p. 237-263.
- Harbaugh, A.W. and McDonald, M.G., 1996, User's documentation for MODFLOW-96, an update to the U.S. Geological Survey Modular Finite-Difference Ground-Water Flow Model, U.S. Geological Survey Open-File Report 96-485, 56 p.
- Hurlow, H.A., 1998, The geology of the central Virgin River basin, southwestern Utah, and its relation to ground-water conditions, Utah Geological Survey Water-Resources Bulletin 26, 53 p.
- Jenkins, D.N., and Prentice, J.K., 1982, Theory for aquifer test analysis in fractured rocks under linear (nonradial) flow conditions, *Ground Water*, v. 20, no. 1, p. 12-21.
- Lohman, S.W., 1972, Ground-water hydraulics: U.S. Geological Survey Professional Paper 708, 70 p.
- Neuman, S.P., 1974, Analysis of pumping test data from anisotropic unconfined aquifers considering delayed gravity response, *Water Resources Research*, v. 11, no. 2, p. 329-342.
- Papadopoulos, I.S., 1965, Nonsteady flow to a well in an infinite anisotropic aquifer, in *Proceedings of the Dubrovnik Symposium on Hydrology of Fractured Rocks*, International Association of Scientific Hydrology, Dubrovnik, Yugoslavia, p. 21-31.
- Reilly, T.E., Franke, O.L., and Bennett, G.D., 1987, The principle of superposition and its application in ground-water hydraulics, U.S. Geological Survey Techniques of Water-Resources Investigation Book 3 chap. B6, 28 p.
- Theis, C.V., 1935, The relation between the lowering of the piezometric surface and the rate and duration of discharge of a well using groundwater storage, *American Geophysical Union Transactions*, vol. 16, p. 519-524.
- Weigel, J.F., 1987, Selected hydrologic and physical properties of Mesozoic formations in the Upper Colorado River Basin in Arizona, Colorado, Utah, and Wyoming—excluding the San Juan Basin, U.S. Geological Survey Water-Resources Investigations Report 86-4170.

Appendix B

Model Sensitivity Analyses

B1—SENSITIVITY ANALYSIS FOR MODEL SIMULATING THE UPPER ASH CREEK DRAINAGE BASIN AQUIFERS

The baseline model for the upper Ash Creek drainage basin was tested to determine how sensitive simulation results were when selected properties and fluxes were varied within what was deemed a reasonable range. The properties varied were (1) hydraulic-conductivity values for each of the simulated aquifers (the basin fill, the alluvial fan, and the Pine Valley monzonite); (2) the conductance values between each of the aquifers (basin fill to alluvial fan and alluvial fan to monzonite); (3) the vertical conductance of the river cells used to represent Ash, Sawyer, and Kanarra Creeks; (4) the depth at which evapotranspiration by riparian vegetation ceases; and (5) the maximum evapotranspiration rate for cottonwoods and pasture grasses. Fluxes that were varied were (1) areal recharge from precipitation; (2) recharge from unconsumed irrigation water; and (3) recharge from infiltration along ephemeral streams.

The graphs shown indicate the magnitude of variation from the baseline simulation. Figures B1-1, 2, and 3 show how baseline heads in each layer reacted to variations in hydraulic conductivity of the three layers. Variations in hydraulic conductivity of the basin-fill and Pine valley monzonite aquifers affected calculated water levels more substantially (greater than 100 ft) than variations in hydraulic conductivity of the alluvial-fan aquifer (less than 100 ft). The same variations in hydraulic conductivity in each layer affected only

spring discharge substantially. Other discharge fluxes were affected minimally (figs. B1-4, 5, and 6).

Calculated water levels in the baseline model were moderately sensitive to variations in the vertical leakance between the basin-fill and alluvial-fan aquifers, especially in layers 2 and 3, and insensitive to variations in the vertical leakance between the alluvial-fan and Pine Valley monzonite aquifers (figs. B1-7 and 8). Simulated discharge amounts were largely insensitive to the variations in vertical leakance, except for spring discharge, which is linked to head change occurring in layer 3 (Pine Valley monzonite aquifer) (figs. B1-9 and 10).

Simulated water levels in all layers respond slightly to variations in riverbed conductance, but simulated river gains and evapotranspiration are more sensitive to these variations because much of this discharge occurs near the perennial reaches that are simulated in the stream package. Discharge components that occur away from the river corridor were not substantially affected by the variations (figs. B1-11 and 12).

Simulated water levels were largely insensitive to reasonable variations in the depth at which evapotranspiration ceases and in the maximum evapotranspiration rate (5 ft or less in all layers) (figs. B1-13, 14, 15, and 16). Discharge boundaries were not appreciably affected by variations in the depth at which evapotranspiration ceases or in the maximum evapotranspiration rate. Discharge to Ash Creek increased by only about 18 percent when extinction depths were decreased to 60 percent of baseline values. All other discharge amounts were minimally affected.

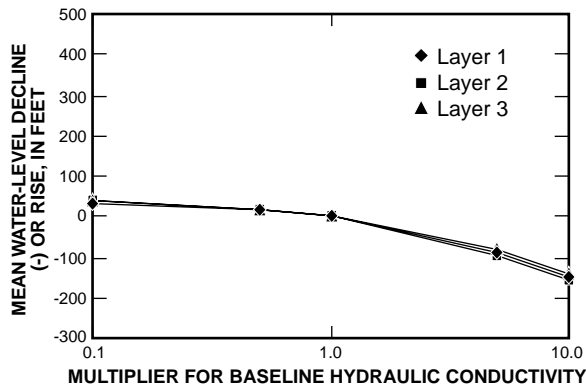


Figure B1-1. Sensitivity of water level to variations in horizontal hydraulic conductivity of the basin-fill aquifer in the ground-water flow model of the upper Ash Creek drainage basin, Utah.

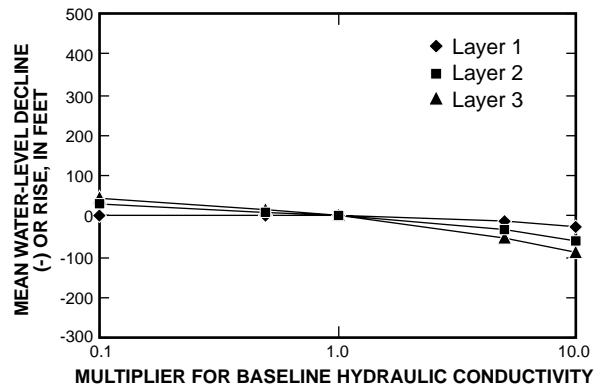


Figure B1-2. Sensitivity of water level to variations in horizontal hydraulic conductivity of the alluvial-fan aquifer in the ground-water flow model of the upper Ash Creek drainage basin, Utah.

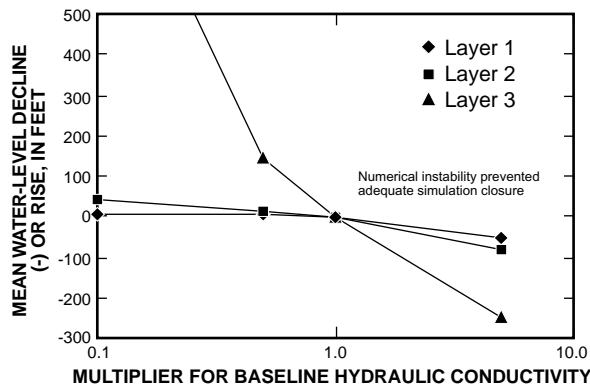


Figure B1-3. Sensitivity of water level to variations in horizontal hydraulic conductivity of the Pine Valley monzonite aquifer in the ground-water flow model of the upper Ash Creek drainage basin, Utah.

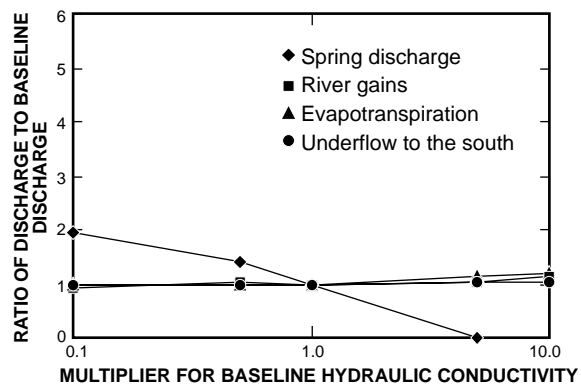


Figure B1-4. Sensitivity of discharge boundaries to variations in horizontal hydraulic conductivity of the basin-fill aquifer in the ground-water flow model of the upper Ash Creek drainage basin, Utah.

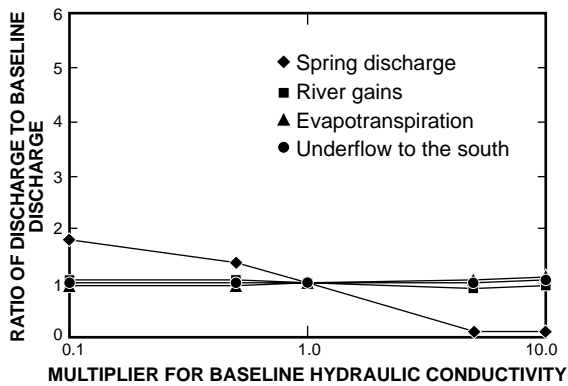


Figure B1-5. Sensitivity of discharge boundaries to variations in horizontal hydraulic conductivity of the alluvial-fan aquifer in the ground-water flow model of the upper Ash Creek drainage basin, Utah.

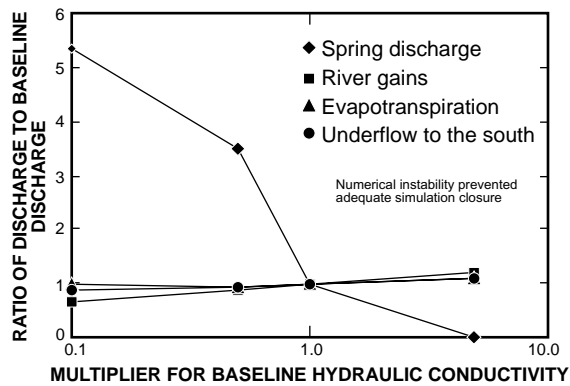


Figure B1-6. Sensitivity of discharge boundaries to variations in horizontal hydraulic conductivity of the Pine Valley monzonite aquifer in the ground-water flow model of the upper Ash Creek drainage basin, Utah.

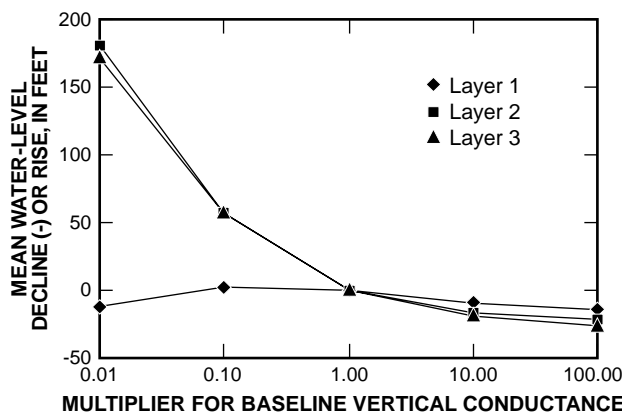


Figure B1-7. Sensitivity of water level to variations in vertical conductance between the basin-fill and alluvial-fan aquifers in the ground-water flow model of the upper Ash Creek drainage basin, Utah.

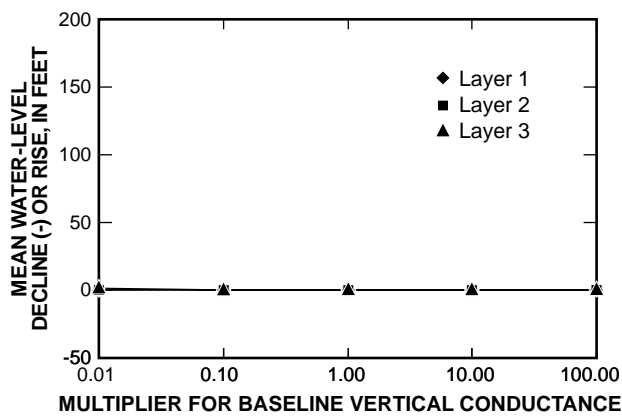


Figure B1-8. Sensitivity of water level to variations in vertical conductance between the alluvial-fan and Pine Valley monzonite aquifers in the ground-water flow model of the upper Ash Creek drainage basin, Utah.

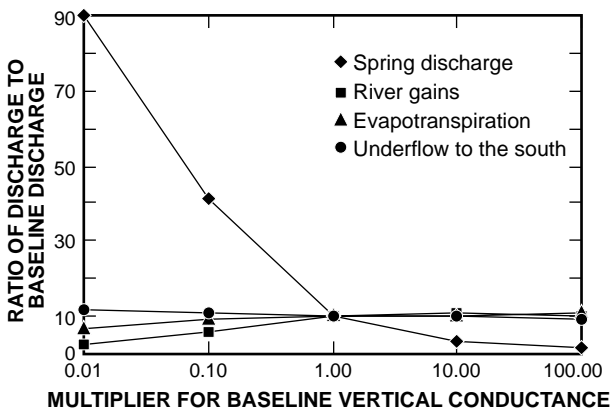


Figure B1-9. Sensitivity of discharge boundaries to variations in vertical conductance between the basin-fill and alluvial-fan aquifers in the ground-water flow model of the upper Ash Creek drainage basin, Utah.

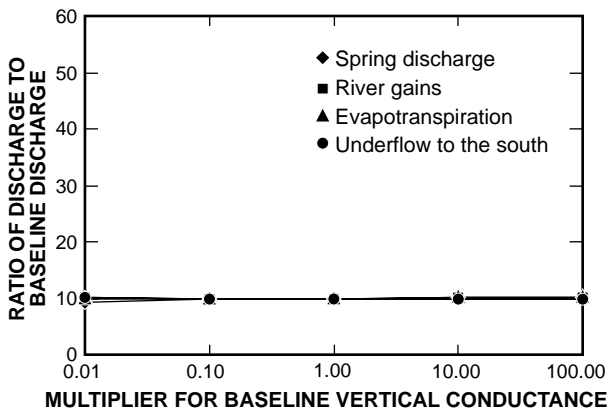


Figure B1-10. Sensitivity of discharge boundaries to variations in vertical conductance between the alluvial-fan and Pine Valley monzonite aquifers in the ground-water flow model of the upper Ash Creek drainage basin, Utah.

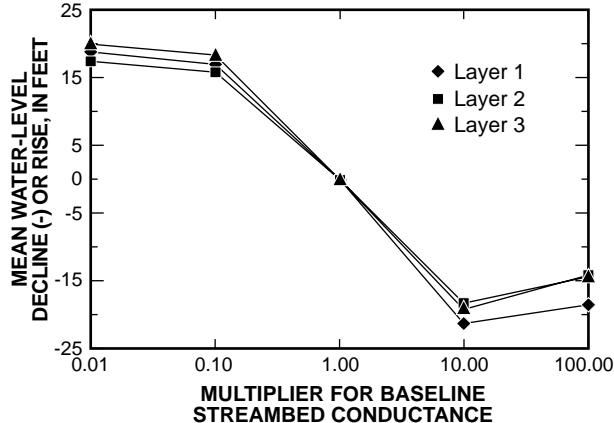


Figure B1-11. Sensitivity of water level to variations in streambed conductance in the ground-water flow model of the upper Ash Creek drainage basin, Utah.

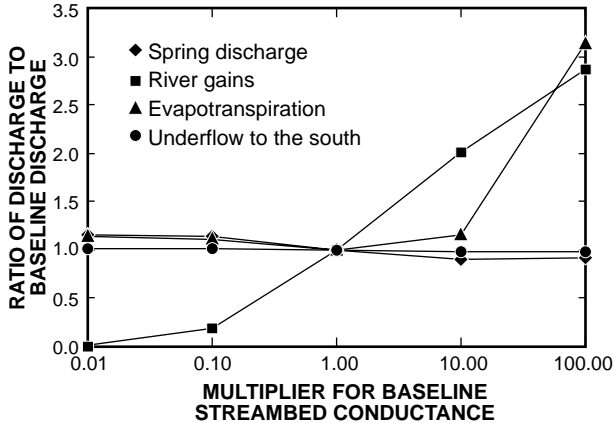


Figure B1-12. Sensitivity of discharge boundaries to variations in streambed conductance in the ground-water flow model of the upper Ash Creek drainage basin, Utah.

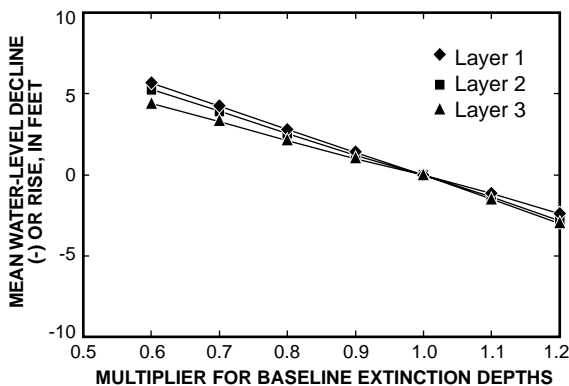


Figure B1-13. Sensitivity of water level to variations in the depth at which evapotranspiration ceases in the ground-water flow model of the upper Ash Creek drainage basin, Utah.

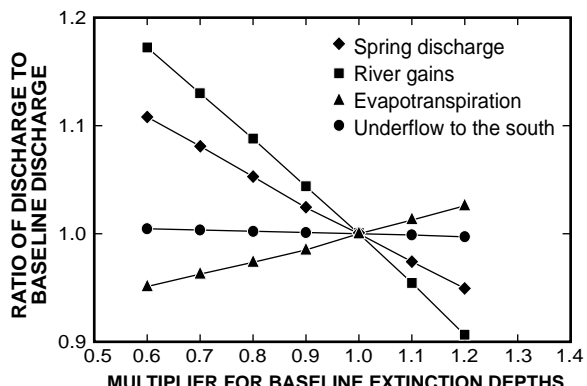


Figure B1-14. Sensitivity of discharge boundaries to variations in the depth at which evapotranspiration ceases in the ground-water flow model of the upper Ash Creek drainage basin, Utah.

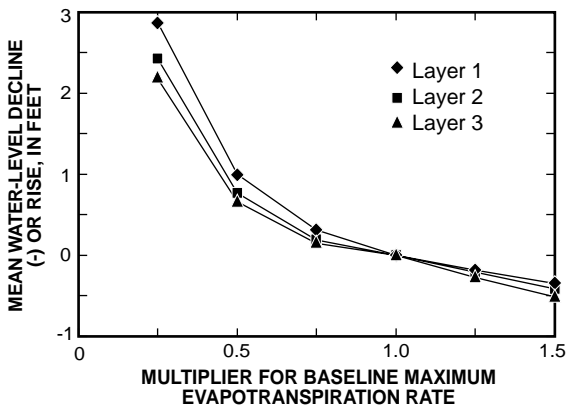


Figure B1-16. Sensitivity of discharge boundaries to variations in the maximum evapotranspiration rate in the ground-water flow model of the upper Ash Creek drainage basin, Utah.

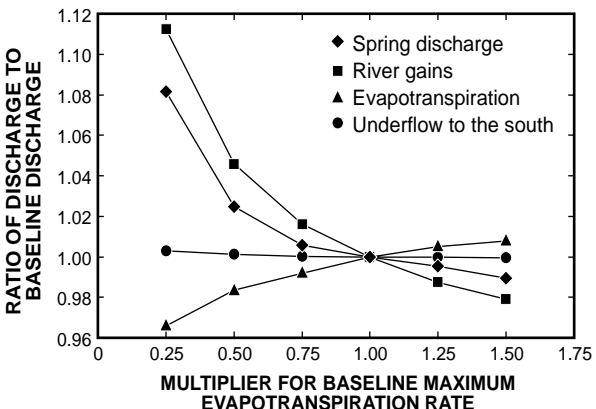


Figure B1-15. Sensitivity of water level to variations in maximum evapotranspiration rate in the ground-water flow model of the upper Ash Creek drainage basin, Utah.

B-2—SENSITIVITY ANALYSIS FOR MODEL SIMULATING THE MAIN NAVAJO AND KAYENTA AQUIFERS

The baseline model for the main part of the Navajo and Kayenta aquifers was tested to determine sensitivity of simulation results to variation in properties and fluxes within what is considered a reasonable range. The parameters varied were (1) hydraulic-conductivity values for each of the simulated aquifers (the basin fill, the alluvial fan, and the Pine Valley monzonite); (2) the vertical leakance between the two aquifers; (3) the streambed conductance of river cells; (4) the conductance of general-head boundaries representing subsurface inflow; (5) the drain conductance of springs, as well as drains simulating seepage to underlying formations; and (6) the amount of areal recharge.

The graphs indicate how much simulation results changed from the baseline simulation. How baseline water levels in each layer and head-dependent fluxes responded to variations over two orders of magnitude in hydraulic conductivity of both model layers are shown in figures B-2 through 4. Variations in hydraulic conductivity of the Navajo aquifer affected calculated water levels more substantially (as much as ± 300 ft) than variations in hydraulic conductivity of the Kayenta aquifer (+100 to -250 ft). The same variations in hydraulic conductivity in each layer moderately affected net general-head boundary recharge (subsurface inflow) and discharge to rivers. Other recharge and

discharge fluxes were affected minimally. Water levels and fluxes in the baseline model were insensitive to variations in the vertical leakance between the Navajo and Kayenta aquifers (figs. B2-5, B2-6).

Simulated water levels and seepage fluxes from and to rivers were very sensitive to variations over two orders of magnitude in riverbed conductance (figs. B2-7, B2-8). However, simulated spring discharge and net general-head boundary-recharge (subsurface inflow) fluxes were less sensitive to these variations because these recharge and discharge components are not located along the river corridors. Simulated water levels and fluxes were largely insensitive to variations over four orders of magnitude in general-head boundary conductance (subsurface inflow). However, recharge at general-head boundary cells was quite sensitive to these variations (figs. B2-9, B2-10). Simulated water levels and fluxes were not sensitive to variations over four orders of magnitude in drain conductance, including spring discharge, which would be directly affected by this parameter (figs. B2-11, B2-12). This may indicate that even at one-hundredth of the baseline simulation, these conductance values are still too high to impede this source of discharge.

Simulated water levels were very sensitive to variations in areal recharge. Variations in recharge by a factor of 2 caused average water-level changes of more than 160 ft in both model layers (fig. B2-13). This increase in areal recharge produced large increases in discharge to rivers, spring discharge, and general-head boundary recharge, whereas recharge from rivers was largely unaffected (fig. B2-14).

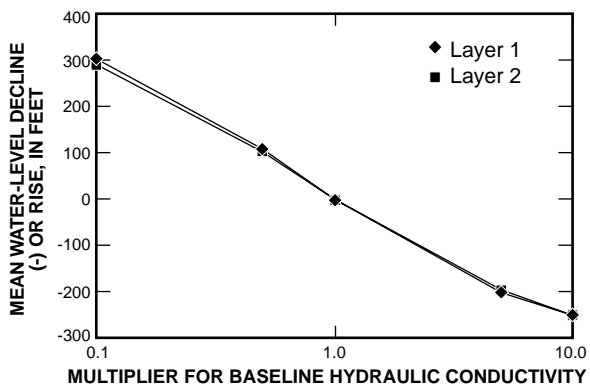


Figure B2-1. Sensitivity of water level to variations in horizontal hydraulic conductivity of the Navajo aquifer in the ground-water flow model of the main part of the Navajo and Kayenta aquifers within the central Virgin River basin study area, Utah.

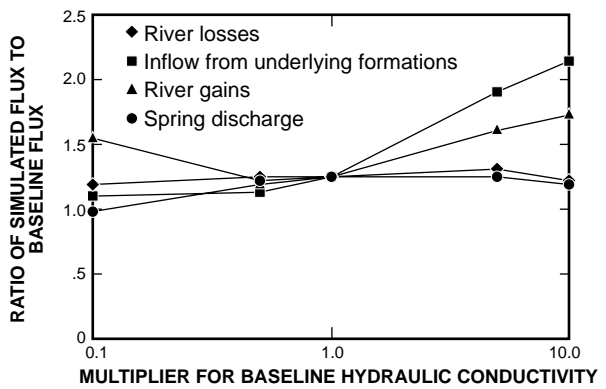


Figure B2-2. Sensitivity of simulated flux to variations in horizontal hydraulic conductivity of the Navajo aquifer in the ground-water flow model of the main part of the Navajo and Kayenta aquifers within the central Virgin River basin study area, Utah.

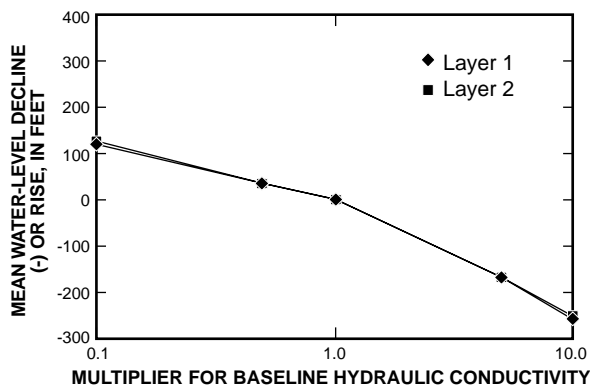


Figure B2-3. Sensitivity of water level to variations in horizontal hydraulic conductivity of the Kayenta aquifer in the ground-water flow model of the main part of the Navajo and Kayenta aquifers within the central Virgin River basin study area, Utah.

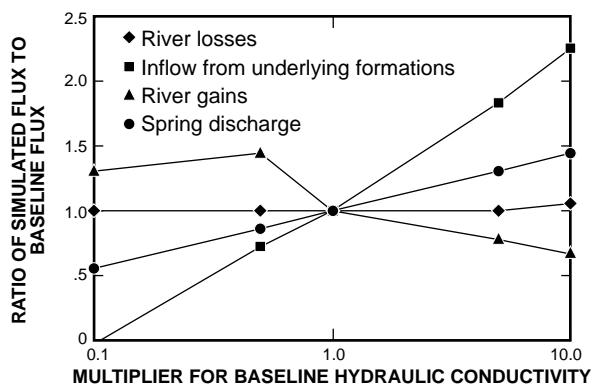


Figure B2-4. Sensitivity of simulated flux to variations in horizontal hydraulic conductivity of the Kayenta aquifer in the ground-water flow model of the main part of the Navajo and Kayenta aquifers within the central Virgin River basin study area, Utah.

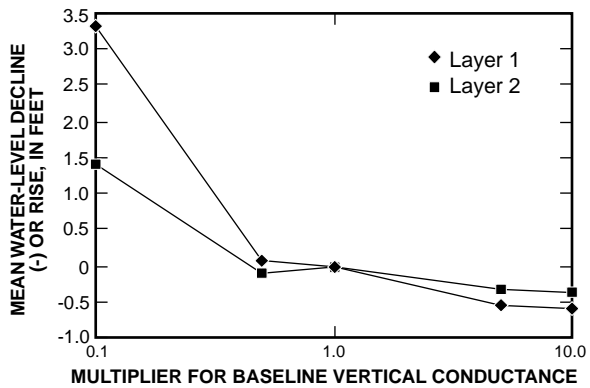


Figure B2-5. Sensitivity of water level to variations in vertical conductance between the Navajo and Kayenta aquifers in the ground-water flow model of the main part of the Navajo and Kayenta aquifers within the central Virgin River basin study area, Utah.

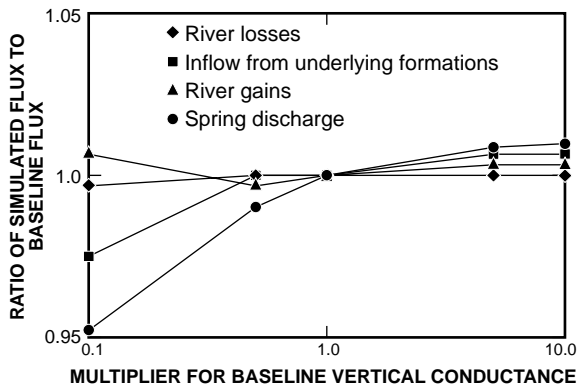


Figure B2-6. Sensitivity of simulated flux to variations in vertical conductance between the Navajo and Kayenta aquifers in the ground-water flow model of the main part of the Navajo and Kayenta aquifers within the central Virgin River basin study area, Utah.

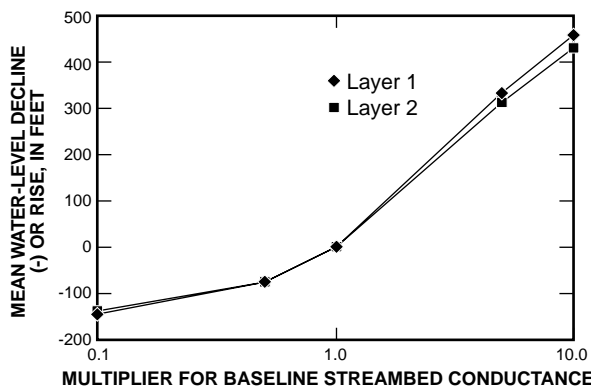


Figure B2-7. Sensitivity of water level to variations in streambed conductance in the ground-water flow model of the main part of the Navajo and Kayenta aquifers within the central Virgin River basin study area, Utah.

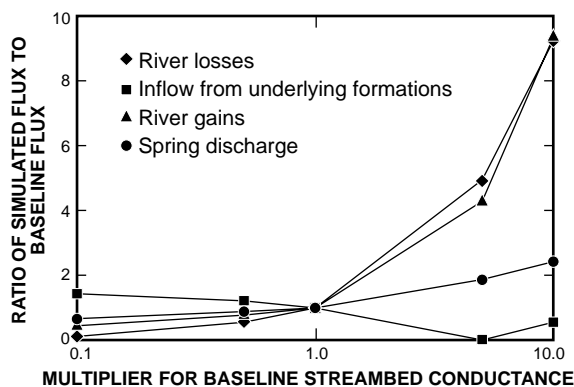


Figure B2-8. Sensitivity of simulated flux to variations in streambed conductance in the ground-water flow model of the main part of the Navajo and Kayenta aquifers within the central Virgin River basin study area, Utah.

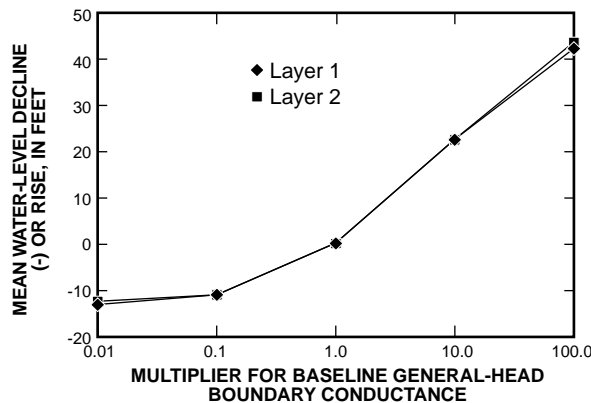


Figure B2-9. Sensitivity of water level to variations in general-head boundary conductance, representing inflow from underlying formations, in the ground-water flow model of the main part of the Navajo and Kayenta aquifers within the central Virgin River basin study area, Utah.

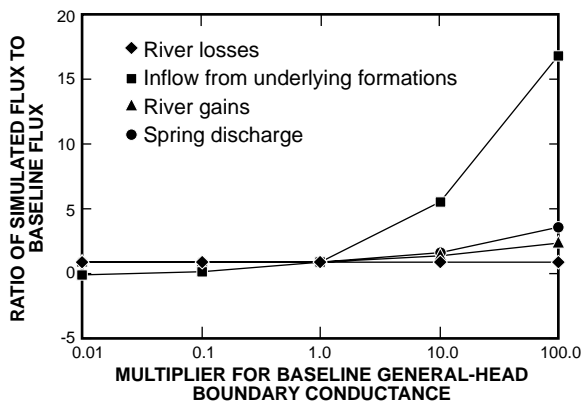


Figure B2-10. Sensitivity of simulated flux to variations in general-head boundary conductance, representing inflow from underlying formations, in the ground-water flow model of the main part of the Navajo and Kayenta aquifers within the central Virgin River basin study area, Utah.

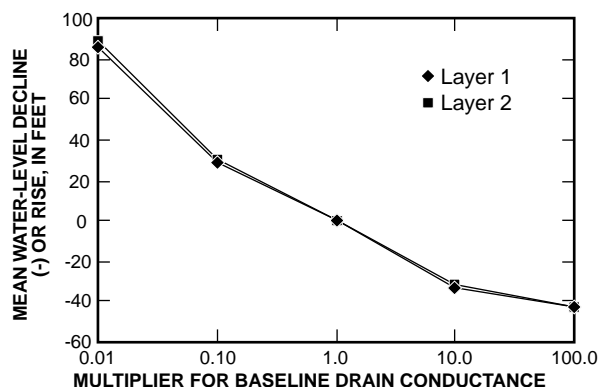


Figure B2-11. Sensitivity of water level to variations in drain conductance, representing spring discharge, in the ground-water flow model of the main part of the Navajo and Kayenta aquifers within the central Virgin River basin study area, Utah.

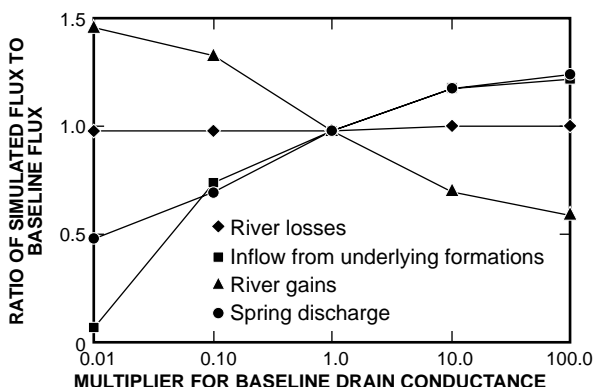


Figure B2-12. Sensitivity of water-budget flux to variations in drain conductance, representing spring discharge, in the ground-water flow model of the main part of the Navajo and Kayenta aquifers within the central Virgin River basin study area, Utah.

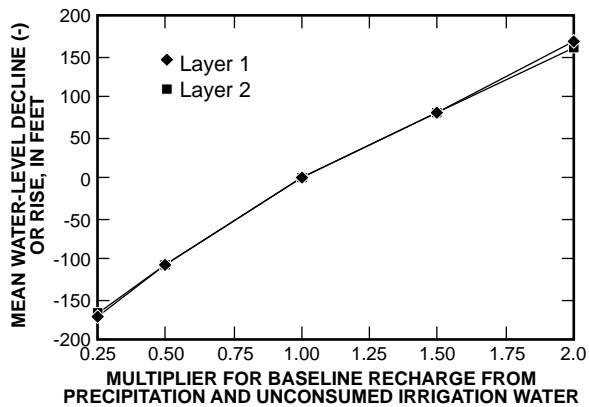


Figure B2-13. Sensitivity of water level to variations in recharge from precipitation and unconsumed irrigation water in the ground-water flow model of the main part of the Navajo and Kayenta aquifers within the central Virgin River basin study area, Utah.

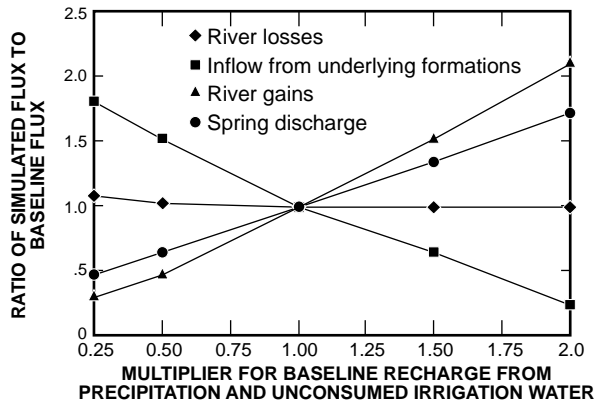


Figure B2-14. Sensitivity of simulated flux to variations in recharge from precipitation and unconsumed irrigation water in the ground-water flow model of the main part of the Navajo and Kayenta aquifers within the central Virgin River basin study area, Utah.

B-3—Sensitivity Analysis for Model Simulating the Gunlock Part of the Navajo Aquifer

The baseline model for the Gunlock part of the Navajo and Kayenta aquifers was tested to determine sensitivity of simulation results to variation in properties and fluxes within what is considered a reasonable range. The parameters varied were (1) hydraulic-conductivity values for each of the simulated aquifers (the Navajo and Kayenta aquifers); (2) vertical hydraulic-conductance values between the two aquifers; (3) streambed conductivity of model cells simulating the Santa Clara River; (4) anisotropy; (5) amount of areal recharge as infiltration of precipitation, and (6) infiltration of water from Gunlock Reservoir.

Simulated water levels in the model domain are sensitive to changes in horizontal hydraulic-conductivity values of both the Navajo and Kayenta aquifers. Decreasing the hydraulic conductivity of the Navajo aquifer by 0.5 caused calculated water levels to rise an average of almost 50 ft in both the Navajo and Kayenta aquifers (fig. B3-1). The same decrease in the conductivity of the Kayenta aquifer caused average water-level rises of about 25 ft (fig. B3-3). Increases in hydraulic-conductivity values caused an average water-level decline of as much as 100 ft. These effects are not the same near St. George city municipal well field., where decreasing hydraulic-conductivity values caused a general decline in water levels, and increased hydraulic-conductivity values caused water-level rises. This is a localized effect caused by the simulated ground-water withdrawals. When the hydraulic-conductivity value of the Navajo aquifer was reduced to 0.1 of the baseline value, the model simulated complete dewatering at several cells where withdrawals are simulated. The head-dependent flux into and out of the ground-water system from the Santa Clara River was moderately sensitive to increases in hydraulic conductivity (figs. B3-2 and 4). The Santa Clara River is the only head-dependent boundary in the simulation, and mass balance within the model domain is maintained by flux across this boundary. Therefore, when simulated inflow to the ground-water system increases, a corresponding increase in outflow also will be simulated. Simulated water levels and fluxes were largely insensitive to

changes in the vertical conductance between the Navajo and Kayenta aquifers (figs. B3-5 and 6).

Decreasing the hydraulic conductivity of the Santa Clara River streambed by one order of magnitude caused calculated water levels to decline substantially from baseline levels (fig. B3-7). As discussed previously, mass balance in the model domain is maintained by flux across the mathematical boundary that simulate the river. The minimum inflow that must be simulated from the Santa Clara River is equal to the difference between the amount of recharge specified from precipitation and from Gunlock Reservoir, and the average discharge simulated at the St. George city municipal well field. When streambed conductivity was reduced, large calculated water-level declines were required to maintain that minimum inflow. Simulated water levels were largely insensitive to increases in streambed hydraulic conductivity. Simulated fluxes to and from the Santa Clara River were sensitive to changes in streambed conductivity (fig. B3-8). Inflow in the model that exceeds the minimum is recirculated back to the lower reaches of the Santa Clara River.

Simulated water-levels were quite sensitive to changes in anisotropy; simulated fluxes varied only slightly (figs. B3-9 and 10). Removing the effects of anisotropy (anisotropy equals 1) caused calculated heads to increase an average of about 100 feet; at the St. George city municipal well field, however, calculated water levels declined. When effective conductivity of the model domain is reduced, the hydraulic gradient and saturated thickness of the Navajo aquifer needs to be increased to simulate the same amount of ground-water flow through the system. A similar effect is seen when specified recharge from precipitation or from Gunlock Reservoir is changed (figs. B3-11, and 13). When recharge amounts decrease, water levels decline and the resulting hydraulic gradient is decreased. When recharge is increased, gradients and the saturated thickness of the Navajo aquifer increase to compensate the additional flow of ground water from recharge areas to the St. George municipal well field and the Santa Clara River. Net flux to the Santa Clara River equates directly to the amount of change in the specified flux from precipitation and from Gunlock Reservoir (figs. B3-12 and 14).

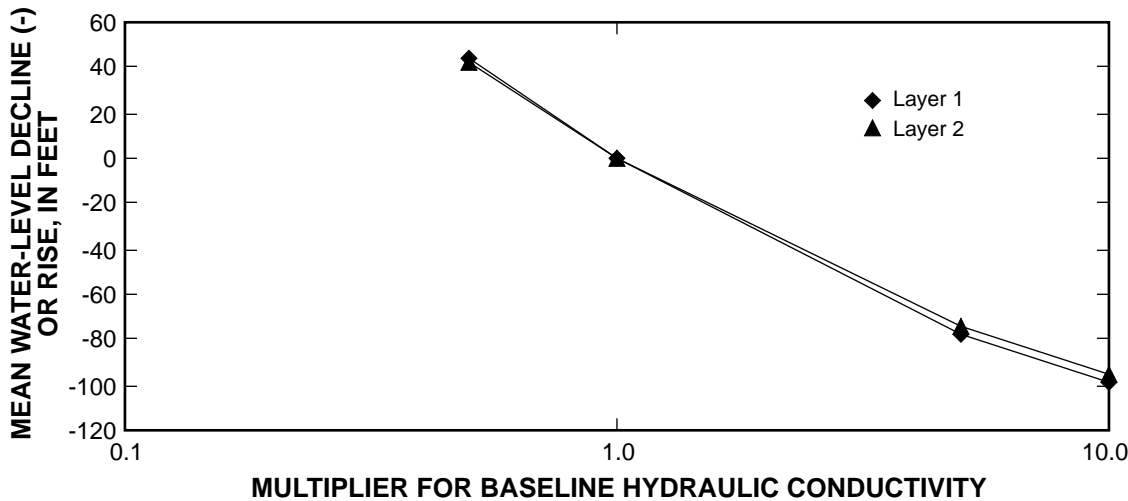


Figure B3-1. Sensitivity of water level to variations in the horizontal hydraulic conductivity of the Navajo aquifer in the ground-water flow model of the Gunlock part of the Navajo and Kayenta aquifers within the central Virgin River basin study area, Utah.

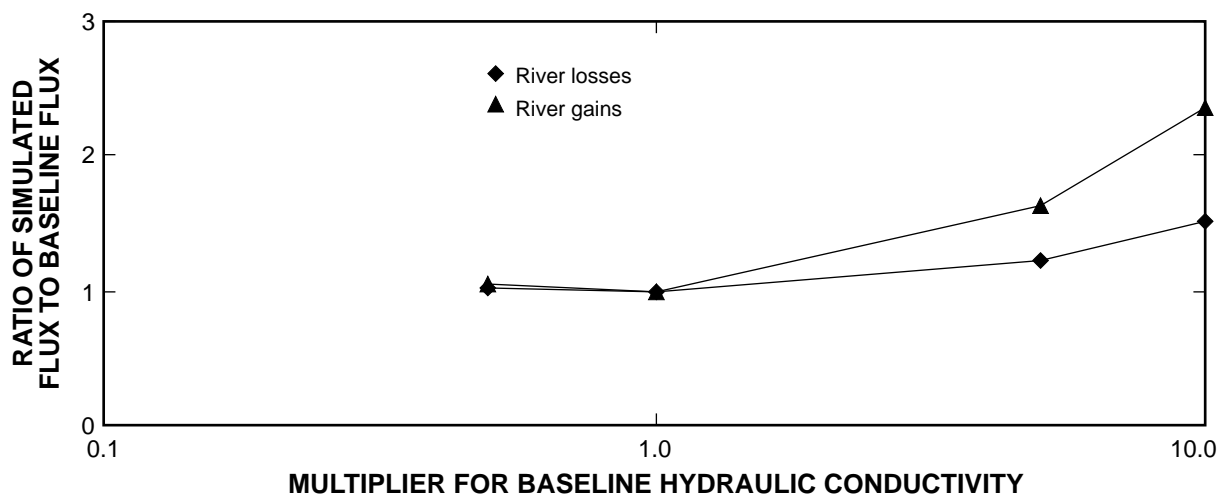


Figure B3-2. Sensitivity of simulated flux to and from the Santa Clara River to variations in horizontal hydraulic conductivity of the Navajo Sandstone aquifer in the ground-water flow model of the Gunlock part of the Navajo and Kayenta aquifers within the central Virgin River basin study area, Utah.

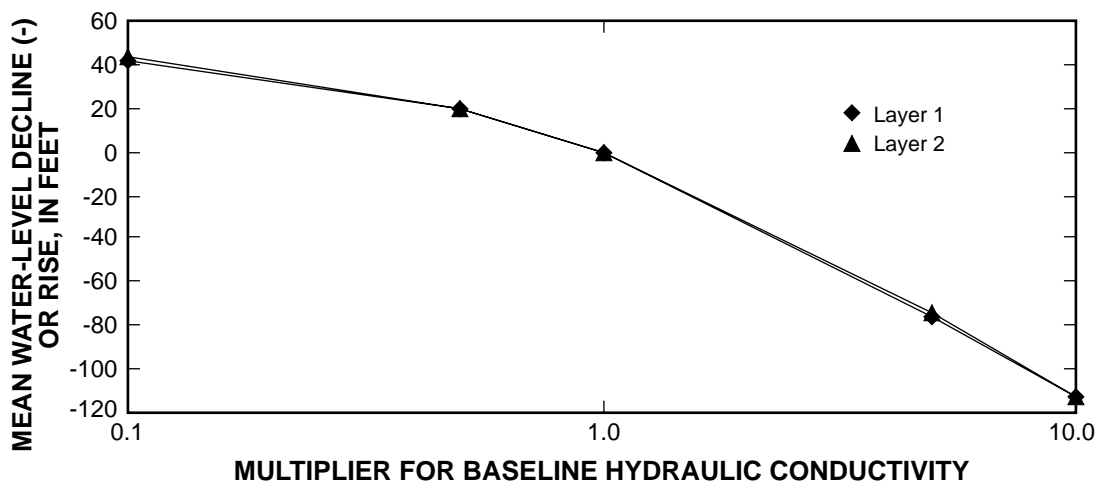


Figure B3-3. Sensitivity of water level to variations in the horizontal hydraulic conductivity of the Kayenta aquifer in the ground-water flow model of the Gunlock part of the Navajo and Kayenta aquifers within the central Virgin River basin study area, Utah.

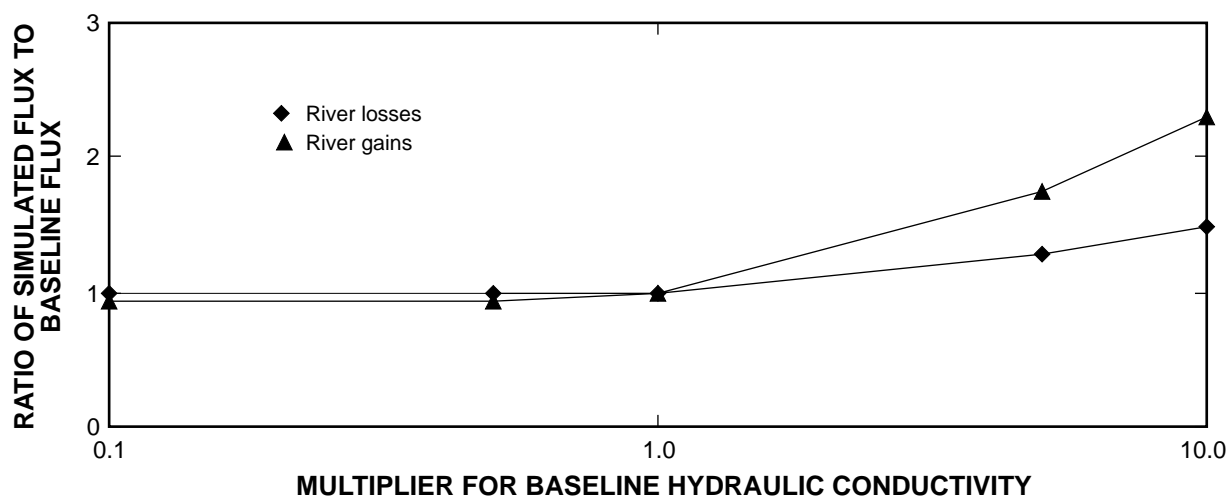


Figure B3-4. Sensitivity of simulated flux to and from the Santa Clara River to variations in horizontal hydraulic conductivity of the Kayenta aquifer in the ground-water flow model of the Gunlock part of the Navajo and Kayenta aquifers within the central Virgin River basin study area, Utah.

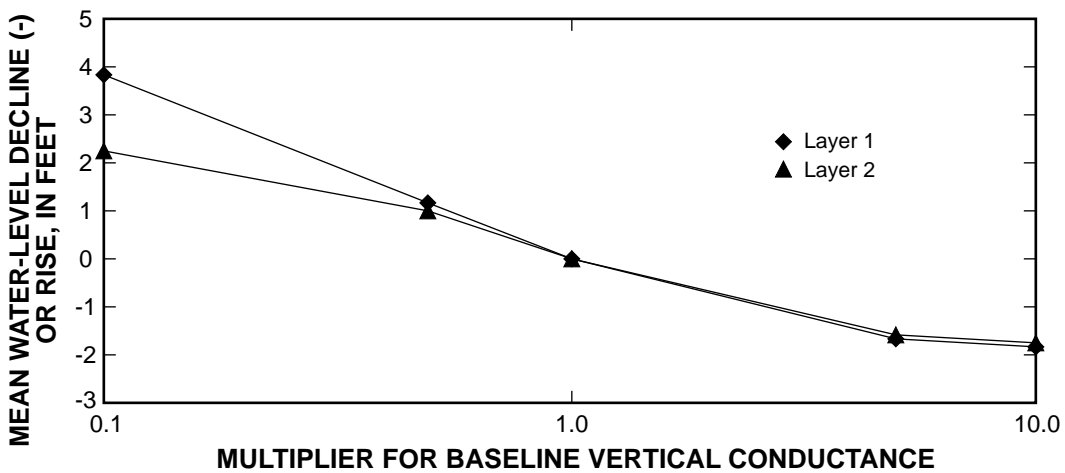


Figure B3-5. Sensitivity of water level to variations in the vertical conductance between the Navajo and Kayenta aquifers in the ground-water flow model of the Gunlock part of the Navajo and Kayenta aquifers within the central Virgin River basin study area, Utah.

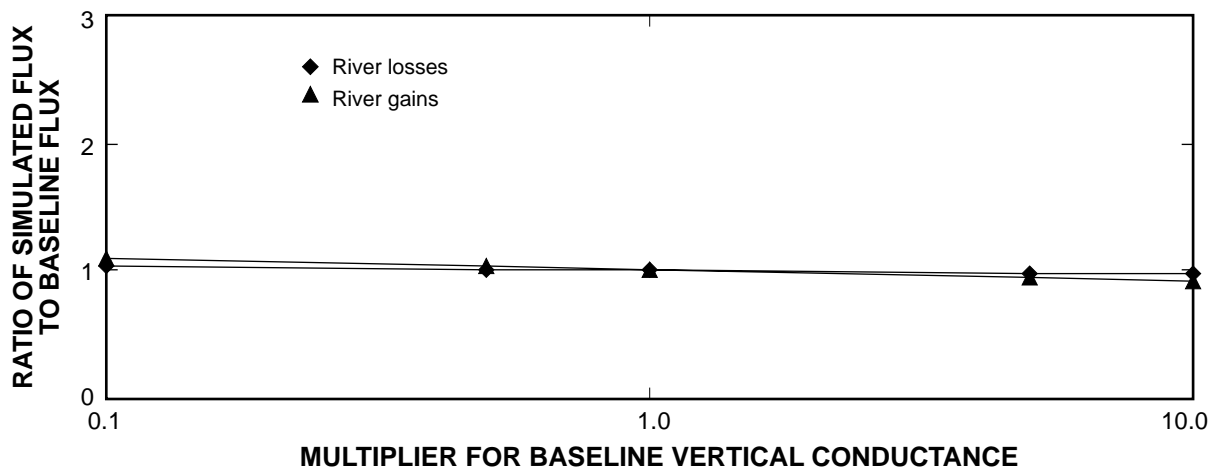


Figure B3-6. Sensitivity of simulated flux to and from the Santa Clara River to variations in vertical conductance between the Navajo and Kayenta aquifers in the ground-water flow model of the Gunlock part of the Navajo and Kayenta aquifers within the central Virgin River basin study area, Utah.

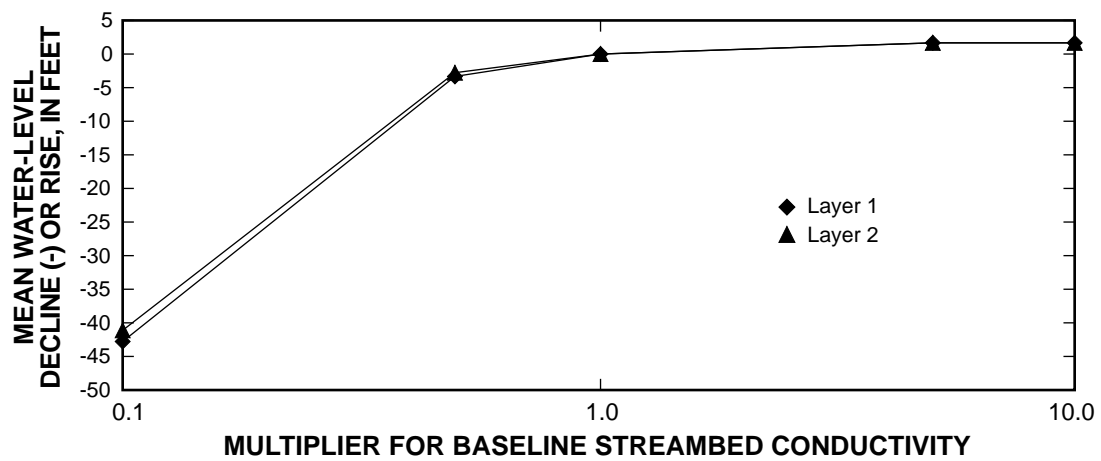


Figure B3-7. Sensitivity of water level to variations in streambed conductance in the ground-water flow model of the Gunlock part of the Navajo and Kayenta aquifers within the central Virgin River basin study area, Utah.

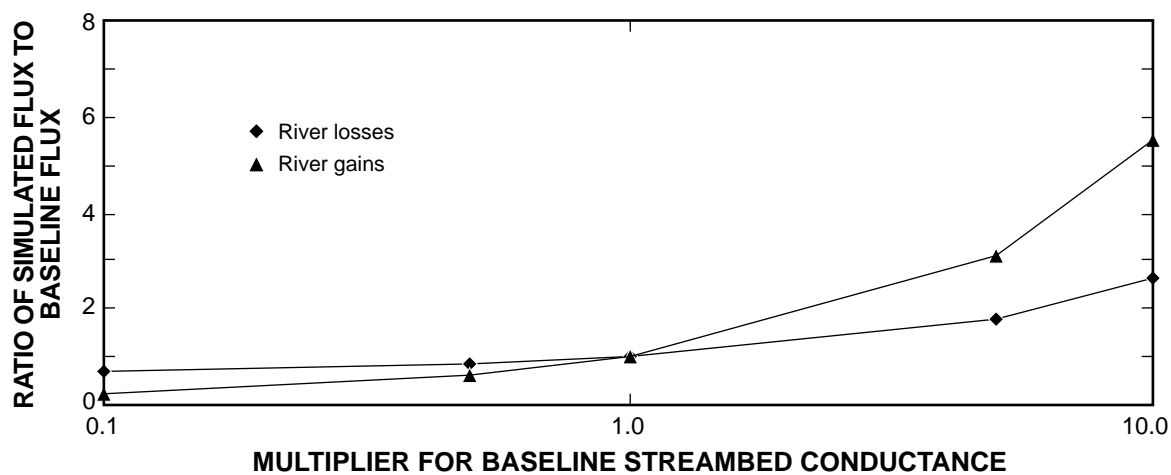


Figure B3-8. Sensitivity of simulated flux to and from the Santa Clara River to variations in streambed conductance in the ground-water flow model of the Gunlock part of the Navajo and Kayenta aquifers within the central Virgin River basin study area, Utah.

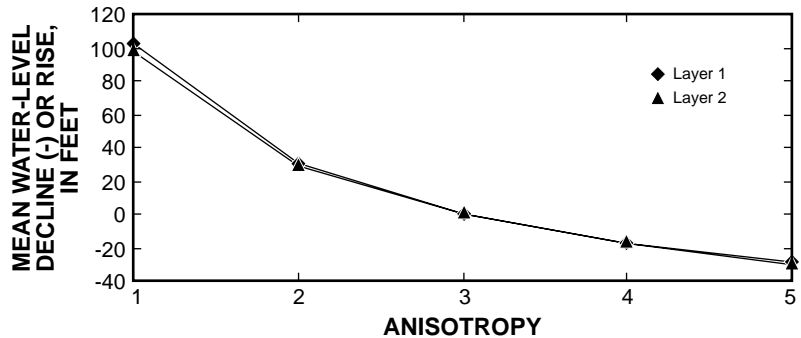


Figure B3-9. Sensitivity of water level to variations in anisotropy in the ground-water flow model of the Gunlock part of the Navajo and Kayenta aquifers within the central Virgin River basin study area, Utah.

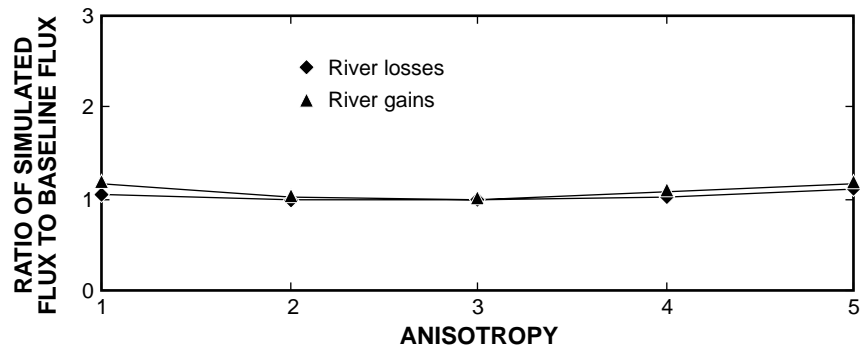


Figure B3-10. Sensitivity of simulated flux to and from the Santa Clara River to variations in anisotropy in the ground-water flow model of the Gunlock part of the Navajo and Kayenta aquifers within the central Virgin River basin study area, Utah.

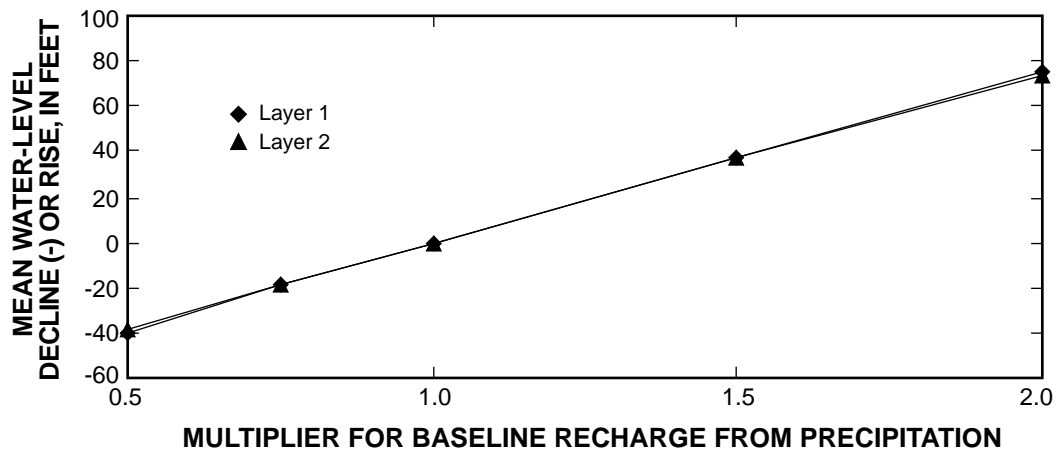


Figure B3-11. Sensitivity of water level to variations in recharge from precipitation in the ground-water flow model of the Gunlock part of the Navajo and Kayenta aquifers within the central Virgin River basin area, Utah.

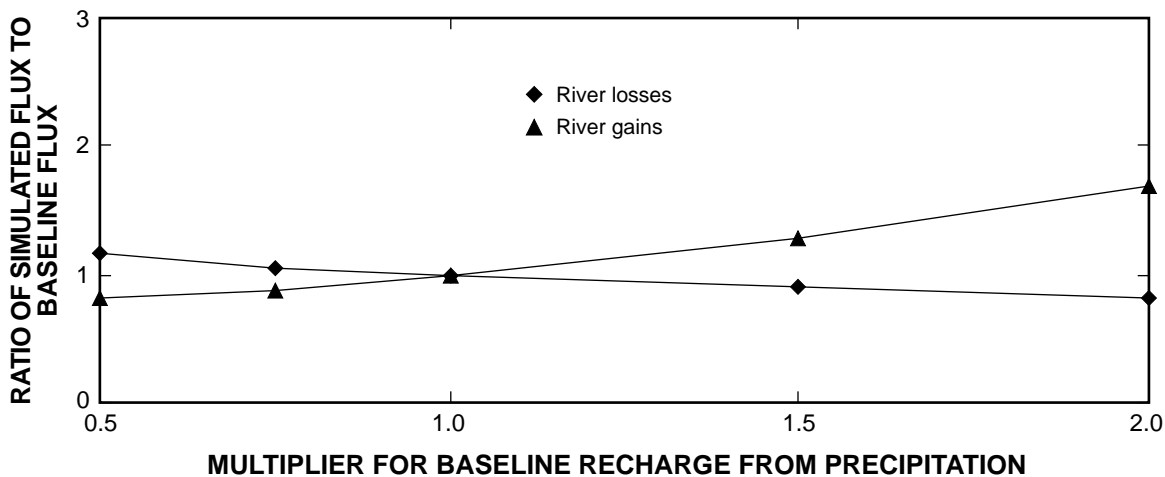


Figure B3-12. Sensitivity of simulated flux to and from the Santa Clara River to variations in recharge from precipitation in the ground-water flow model of the Gunlock part of the Navajo and Kayenta aquifers within the central Virgin River basin study area, Utah.

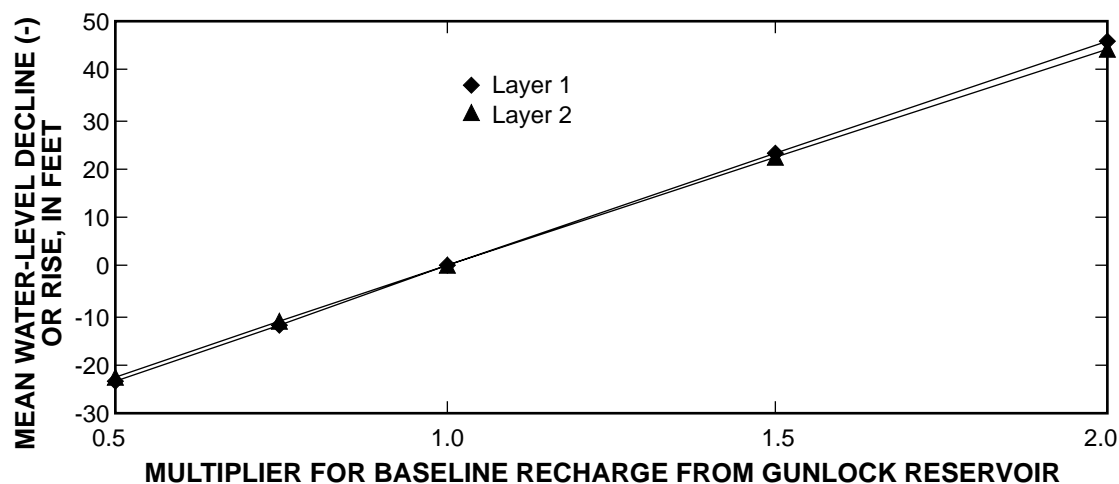


Figure B3-13. Sensitivity of water level to variations in recharge from the Gunlock Reservoir in the ground-water flow model of the Gunlock part of the Navajo and Kayenta aquifers within the central Virgin River basin study area, Utah.

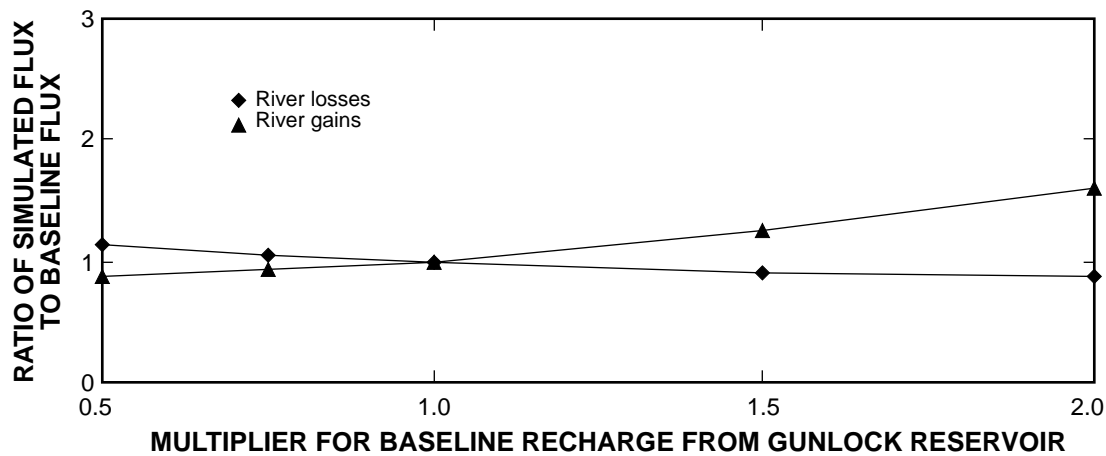


Figure B3-14. Sensitivity of simulated flux to and from the Santa Clara River to variations in recharge from the Gunlock Reservoir in the ground-water flow model of the Gunlock part of the Navajo and Kayenta aquifers within the central Virgin River basin study area, Utah.



The Utah Department of Natural Resources receives federal aid and prohibits discrimination on the basis of race, color, sex, age, national origin or disability. For information or complaints regarding discrimination, contact the Executive Director, Utah Department of Natural Resources, 1636 West North Temple #316, Salt Lake City, UT 84116-3193 or Office of Equal Opportunity, US Department of the Interior, Washington, DC 20240.

Technical Publication No. 116, Utah Department of Natural Resources, 2000